Generalized Spatio-Temporal Model for the Optimal Sizing, Operation, and Location of Energy System Assets

Aniq Ahsan
St Cross College
University of Oxford

A thesis submitted for the degree of
Doctor of Philosophy in Engineering Science

Michaelmas 2022

Acknowledgements

I want to thank everyone who has helped me get through this chaotic roller-coaster of a DPhil.

I want to first thank my supervisor, Malcolm McCulloch, for his guidance and support. You have pushed me when I needed it and patiently helped me up when I have stumbled. I am truly grateful to have a supervisor who cares more about me than my work. I hope to pay this forward to the next generation of academics.

I want to thank, Scot, for plowing through details of my work with me throughout my DPhil. I should have listened to you earlier. Always listen to Scot.

I want to thank the many people in the energy and power group (EPG) in Oxford who have read various chapters of my thesis and given me comments. Thank you Alycia, Claire, Flora, Jesus, Nicole, Monica, Scot, and the rest who have read various parts of my thesis at various stages. This thesis would not be nearly as polished without you. I also want to thank the EPG Pomodoro gang and my twitch followers for motivating me by working with me through the final stages of the DPhil. Thank you Miriam for starting and walking through this crazy DPhil journey alongside me.

I want to thank my closest friends; I genuinely would not be the human I am without my interactions with you. I want to thank my flatmates and some of my closest friends, Laurence, Sean, Alexander, and Jay for dealing with my quirkiness and the amazing deep conversations. Thank you Holly for being there with me during the craziest of my times, you have seen me though the worst of my states. Thank you Blaine for strategizing with me though various difficult decisions and conversations. Thank you Alycia for all the deep philosophical conversations and plots to topple the existing corrupt systems. Thank you Zheng Hao, Chia Chang and Yu Hang back in Singapore for helping me through various crazy stages, especially due to COVID. We

tried, most of you all have now met each other. My one dream now is to tear the fabric of spacetime by having you all at one place and time.

Thank you to the Jiujitsu gang, the weekly sessions have been a source of stability in the chaos. Ed, Tom, Jake, Elena, Blaine, Alex, the airtime you have given me. Thank you Cameron, Jason, Yuki, Cathy and the rest of the virtual board games gang. Thank you to Dungeons and Dragons groups run by Alexander, Holly, and Alycia. I genuinely needed the occasional escape from reality.

Thank you Alicia Ng for inspiring me during high school to pursue my love for physics. Thank you Chin Jia Min for mentoring me after high school and really pushing me to learn how to plan and conduct research, and manage "minions". Thank you Alfred Huan for believing in me and helping me navigate the A*STAR system to find my DPhil topic. You three have been pivotal in setting me on the course to pursue this DPhil.

Last but certainly not least, I want to thank my family for their uncompromising love and support. Aiman, and Eatsham, I don't know what I have done without you. Thank you mom and dad for raising me and all the hard work you have gone through to get me here. You have made so many sacrifices I do not know where or even how to begin.

And of course I want to thank Allah (God) for giving me the opportunity, strength, and guidance to make an impact on the world. May you keep me on the right path so that I may do more to appreciate the beauty of your creation, do my part to help the world, and attain success in this life and the hereafter.

Contents

Abstract

Future energy systems will contain large amounts of distributed energy resources (DER). In DER-based energy systems asset related to energy demand, supply, transport, storage, conversion, and demand response will be deeply coupled. This thesis develops the Space-Time Energy Vector Flow Networks (STEVFNs; pronounced "Steven") unified asset model-generator, system design model-generator, and tool for the optimal design of DER-based energy systems. This thesis is the first to develop a generalized spatio-temporal asset model-generator that unifies energy demand, energy supply, energy transport, energy storage, energy conversion, and demand response assets. STEVFNs enables energy system design by co-optimizing the sizing, operation, and location of energy system assets. It utilizes modern advancements in convex programming and is the first to enable the optimization of energy system design with rapid scenario assessment. It is demonstrated using a case study of designing an energy system to satisfy Singapore's hourly electricity and high temperature heating demand using intercontinental solar and wind farms, distributed batteries, HVDC lines, distributed ammonia storage, ammonia transport, and various conversion technologies. STEVFNs is available as an open-source tool on GitHub [1] for the co-optimization, with rapid scenario assessment, of the sizing, operation, and location of energy system assets that can provide energy demand, supply, transport, storage, conversion, and demand response.

Nomenclature

Acronyms

ACOPF Alternating Current Optimal Power Flow

AMD Advanced Micro Divices

BAU Business As Usual

BESS Battery Energy Storage System

CLEWs Climate, Land (Food), Energy, and Water strategies

CPT Charge Parity Time reversal

CPU Central Processing Unit

CUDA Compute Unified Device Architecture

DC Direct Current Optimal Power Flow

DCP Disciplined Convex Programming

DER Distributed Energy Resource

DOD Depth of Discharge

DPP Disciplined Parametrized Programming

emf Electromotive Force

ESS Energy Storage System

FPGA Field-Programmable Gate Array

GHG Greenhouse Gas

GIS Geographic Information System

GPU Graphics Processing Unit

HTH High Temperature Heating

ISNs Industrial Symbiosis Networks

lat-lon Latitude and Longitude

LP Linear Program

LTH Low Temperature Heating

MAED Model for Analysis of Energy Demand

NP Non-deterministic Polynomial-time

RE Renewable Energy

ROCm Radeon Open Compute Platform

SCS Splitting Conic Solver

SOC State of Charge

STEVFNs Space Time Energy Vector Flow Networks; pronounced like the name "Steven"

UML Universal Modelling Language

Other Symbols

$\dot{x}$ A dot above a quantity means the rate of change of a quantity with time.

$\mathbf{P}$ The symbol $\mathbf{P}$ with any number of superscripts or subscripts indicate DCP optimization parameters in the optimization language. This is also the conversion function or cost function parameters in the asset modeller language.

$\vec{x}$ Symbols with an arrow above them are vector quantities.

Variables

Δt [h] Difference between the time of the source, and the time of the target node of edges of a component.

δt [h] Operational Time Difference. This is the difference in time of the source nodes of consecutive edges of a component.

η Efficiency

η_c ; η_d Charging and discharging efficiency

ψ "Conversion Function" of a component.

$\vec{\psi}_g$ Conversion function of generalized coordinates that are curtailed.

$\vec{\psi}_h$ Conversion function of generalized coordinates that are conserved.

$\vec{\mathbf{P}}_\psi$ Conversion function parameters.

$\vec{\mathbf{P}}_f$ Cost function parameters.

$\vec{x}_g$, $\vec{y}_g$ Generalized coordinates flowing into or out of a node that are curtailed at a node.

$\vec{x}_h$, $\vec{y}_h$ Generalized coordinates flowing into or out of a node that are conserved at a node.

$\vec{x}_{i,j}$ Generalized coordinates/quantities flowing out of the source node of edge with source node i, and target node j.

$\vec{y}_{i,j}$ Generalized coordinates/quantities flowing into the target node of edge with source node i, and target node j.

F Generalized Force acting on an object.

f_{asset} Total cost of an asset.

$f_{size,t}$ Cost of sizing an asset/component to meet the flow at timestep t.

f_{size} Total cost of sizing an asset/component to meet the flows for all timesteps.

$f_{use,t}$ Usage cost of operating an asset/component at timestep t.

f_{use} Total cost of using an asset/component over all timesteps.

g Inequality function of a node.

h Equality function of a node.

I [A] Current flowing into a battery.

P , P_{in} [W] Power supplied to a generalized object

P_c ; P_d [W] Charging and discharging Power

P_{out} [W] Power supplied by a generalized object

q Generalized coordinate or generalized quantity.

Q [Ah] Amount of electrical charge in a battery.

q_t Generalized coordinate/quantity at timestep t. This is also the generalized coordinate/quantity flowing from timestep t to timestep $t + 1$.

t_0 [h] The time the component is operated from. It is the first operational time.

t_1 [h] The time the component is operated until. It is the final operational time.

V [V] Voltage

x , q_{out} Flow of generalized coordinate/quantity out of the source node of an edge. This is also referred to as the flow of an edge.

y , q_{in} Flow of generalized coordinate/quantity into a target node of an edge. This is given by the conversion function of the edge.

Chapter 1

Introduction

This thesis addresses the core research question:

"*Can a generalized spatio-temporal asset model-generator be developed and utilized to optimize the sizing, operation, and location of energy system assets?*"

1.1 Context of Research Question

Combating climate change is one of the biggest challenges of our time [2]. To minimize the impact of climate change, society needs to limit its cumulative greenhouse gas (GHG) emissions until it reaches net zero GHG emissions [3]. According to 2022 CAIT database [4], energy end-use and services[1] accounted for 76% of global GHG emissions in 2019. The world is and will be reducing these energy related GHG emissions by using large amounts of renewable energy (RE) to satisfy its end-use energy service demands. Unlike fossil-based energy generation technologies, the most effective RE technologies produce electricity that is distributed, and intermittent [5, 6]. These RE technologies are thus also referred to as distributed energy resources (DER). The future energy system will thus be very different from the past and current fossil-based systems. New methods will therefore be needed to optimally size and operate assets that form these new energy systems. This thesis refers to the sizing, operation and location of assets that perform different functions of an energy systems as the "design" of an energy system.

[1]Energy end-use and services refer to the uses of energy such as for heating, cooling, transport, lighting, computing, etc. When the use of energy is a form of energy such as heat, then it is referred to as an "energy end-use". When the use of energy is not a form of energy such as passenger transport, it is referred to as an "energy service".

These new methods required for energy system design can be split into "models", "model-generators", "modelling principles" and "tools". In this thesis, a model refer to a mathematical representations of an entity such as a physical object, process, system, concept. Examples of a model include I^2R losses in a wire; the constraints and variables representing a battery with no losses; and the zero-order models of energy systems of countries in the OSeMOSYS starter kits [7]. A model-generator refers to a framework that can be applied to systematically generate a model. Examples of model-generators include OSeMOSYS[8], MARKAL/TIMES[9, 10], PyPSA[11], MAED[12], and MESSAGE[13]. A model-generator consists of multiple underlying modelling principles which determine the entities they can generate models for, the descriptive richness of the models they generate, and how the models they generate can be used. Modelling principles include Newton's Laws; Lagrangian or Hamiltonian Dynamics; Quantum Mechanics; Linear, the use of convex, or non-convex functions; and visualization, accounting, simulation, or optimization. A tool is an implementation of a model-generator as usable software and/or hardware; this provides a user interface (UI) and user experience (UX), even if very basic, with which to generate models. Examples of tools include the opensource OSeMOSYS code[14] and its interfaces: clicSAND[15], MoManI[16], and otoole[17]; and MARKAL/TIMES[18] and its interface VEDA[19].

1.1.1 Coupled Functions of an Energy System

Unlike the past and current fossil-based systems, the problems of energy demand, supply, transport, storage, conversion, and demand response are deeply coupled in the design of DER based energy systems.

Urbanization is causing global energy demand to become more spatially concentrated. However, global DER is spatially distributed [5, 6]. Thus, increasing DER penetration (i.e. the fraction of electricity produced from DER) will mean that future global energy supply will be distributed, unlike fossil-based power plants. The energy usage of a city grows approximately linearly with its population. However, because cities can and do spread vertically, the population (and thus energy usage) grows super-linearly with the area occupied by a city. However, the amount of DER

supply in a city is proportional to its area. Thus, as cities grow, their energy usage will outgrow their DER supply.

Furthermore, various cities also have geo-political boundaries that limit the maximum amount of DER resource they can extract from their surroundings. Prime examples of these are city-states such as Singapore, which can only supply 10-20% of its energy using DER even if they utilize all available area (including rooftops and water bodies) [20]. Thus, future cities will need to extract from DER that are located very long distances away, in other countries or even other continents. This thesis refers to DER that are located very long distances away as long-distance DER farms. Future energy systems will have significant amounts of long-distance DER farms. The future energy system thus needs to move energy in space, or equivalently, transport energy from one location to another location.

We cannot control when the wind blows or when the sun shines. This means that there will be a mismatch in time between when energy is demanded and supplied. The societal value of lost load, especially of electricity demand, is very high. The future energy system thus will require energy to move in time. This may be done by energy storage or demand response.

In 2020, electricity only accounted for 20.5% of global final energy consumption [21]. Thus, without any fuel switching, even if all electricity is produced from DER, most energy related emissions will still remain. This is because there is a mismatch in type between the form of energy that is generated and used. The future energy system thus needs to move energy in type, or equivalently, convert energy from one form to another form. This will allow the energy system to satisfy non-electrical end-use energy services using electricity generated from RE; this is also known as electrification.

The energy system performs a set of functions, such as generation, use, and movement in space (transport). Assets in an energy system can perform one or more of these functions, sometimes concurrently. There is a minimum and sufficient set of functions that can describe all functions of an energy system; this is referred to as the "basis functions" of an energy system. There may be multiple sets of basis functions of an energy system. However, given the way energy systems are evolving, it

is unclear which set is useful to describe assets of an energy system for the optimal sizing and operation of these assets.

The functions of fossil-based energy systems are sufficiently decoupled. The assets that perform these functions can thus be sized quasi-independently of each other. However, in DER-based energy system, these functions, and thus the problem of sizing and operating these assets, will become deeply coupled. The ideal size of one asset will affect the ideal size of other assets. Thus, the future energy system needs to be designed holistically by considering all functions and assets of an energy system, concurrently.

Existing energy system design models are specialized to handle a subset of the functions or assets of an energy system. To design future energy systems, models for all types of assets and functions are required to work together. Efforts have been made to patch existing bespoke models together. However, these "patchwork" models are either too computationally intensive (because they need to undo the assumptions that make them so efficient), or make overly simplistic assumptions. This thesis takes a few steps back to observe the problem with a wider prospective, and uses concepts from theoretical physics to build a unified, generalized spatio-temporal asset model that can describe all types of energy system assets and functions. This unified asset model will lay the basis about how and where to simply energy system design problems in a systematic and modular manor while ensuring the results are accurate enough to still be useful.

1.1.2 Co-optimization of Sizing, Operation, and Location

Compared to fossil-based energy systems, the deep coupling of the functions of DER based energy systems, create additional flexibility in the operation of their energy system assets. Thus, the way assets are operated affects their optimal sizing more strongly in DER based energy systems. Similarly, the sizing of the assets in a DER based energy system affects their optimal operation more strongly as well. Finally, the location of these assets affects their sizing and operation, and vice versa. Thus, to design DER based energy systems, it is even more important to co-optimize the sizing, operation, and location of the energy system assets.

1.1.3 Optimization for Scenario Assessment

When performing a "case study", the optimal energy system design depends on the efficiency and cost assumptions of its constituent assets, as well as the latitude and longitude of the location of these assets; these are referred to as "scenario assumptions". There are uncertainties in future scenarios. Thus, future energy system design requires assessing how the optimal energy system design is affected by scenario assumptions.

There are various ways to classify energy systems modelling in the literature such as accounting, simulation, optimization, and top-down and bottom-up models. One way of classifying these models is by their workflow for scenario assessment. There are two traditional types of workflows for scenario assessment: simulation and optimization. Simulation workflows use tools such as MAED-2 [12, 22], LEAP [23], which are quick and accurate. This allows the testing of a scenario every few minutes. However, simulation tools only simulate a specific size and operation of assets at each location. This may not be the optimal when the scenario is changed. Simulation workflows thus overestimate the true cost of the optimal energy system design for any given scenario.

Optimization workflows, used by tools such as OSeMOSYS [8] and MARKAL/TIMES [9], which can find the optimal design and operation given a specific scenario. However, these optimization tools take a much longer time to run by definition as they have to perform one or multiple "simulations" in each iteration, and multiple iterations before they find an optima. These optimization tools thus have to make assumptions to simply the problem and reduce the computational burden and thus time taken to solve. Even after these simplifications, for large systems, traditional optimization workflows can take hours or days to test one scenario. Often in the scenario assessment process, one scenario needs to be assessed to determine the next scenario to test. This makes traditional optimization workflows unsuitable for quickly testing a large number of scenarios.

There have been recent advancements in convex optimization that allow the re-optimization of problems with the same "structure" but different "parameters" in fractions of the time taken to run the original optimization problems. This is done by

defining convex optimization problems in a language called Disciplined Parametrized Programming (DPP) [24]. DPP is an extension to another language for describing convex optimization problems called Disciplined Convex Programming (DCP) [25, 26]. DCP and DPP have also been implemented as an open source convex optimization modelling package in the Python programming language called CVXPY [25]. DCP and DPP increase the time taken to perform a convex optimization problem the first run. They however reduce the time taken to perform the optimization again for different parameters by up to orders of magnitude. This opens up the possibility of making a model-generator and tool that can enable a new workflow that can combine the functionality of traditional optimization tools with the workflow of traditional simulation tools.

1.2 Scope

Functions and Assets of an Energy System

This thesis aims to elucidate the objective techo-economic functions of an energy system. This thesis does not aim to model or assess the socio-political functions of an energy system. Policy makers may utilize the techo-economic implications from this thesis and compare it with their own evaluations of the socio-political aspects of the energy system. This will allow for a systematic approach to whole systems thinking and assessment.

This thesis considers the following set of energy system assets:

1. Energy Demand Assets: These are assets that use energy to satisfy some end-use demand or service.

2. Energy Supply Assets: These are assets that generate, or extract energy from the surroundings.

3. Energy Transport Assets: These are assets that move energy from one location to another.

4. Energy Storage Assets: These are assets that store energy and thus move energy from one time to the next time.

5. Energy Conversion Assets: These are assets that convert energy from one form to another.

6. Demand Response Assets: These are assets that shift the demand, or use, of energy either to the future or the past.

This thesis considers the set of techo-economic functions of an energy system that can describe the functions of these six types of assets.

Optimal Sizing, Operation, and Location of Assets

In this thesis, energy system design refers to the sizing, and operation of assets at various locations in an energy system. The sizing of these assets at a specific location includes "zero sizing", i.e. not using the assets. This thesis considers the design of an energy system as a whole. It thus considers the combined optimal sizing, operation, and location of all the assets of an energy system, where each of these assets can affect the sizing, operation, and location of other assets. Even though the thesis considers the co-optimization of sizing, operation, and location of assets in an energy system, the optimal sizing of assets at various locations is the primary objective; the optimal operation is considered because it affects the optimal sizing of assets.

In this thesis, the optimal energy system is the energy system that minimizes the economic cost of the system, or equivalently maximizes the economic welfare of an energy system. It does not refer to hierarchical system assessments. It also does not refer to multi-criteria assessments. If a system does have multiple criteria, they can be considered by normalizing or internalizing them as an economic cost (or welfare).

Leonard [27] splits energy system design into three main stages: the preliminary stage, feasibility study, and the final design stage. The preliminary stage checks if a problem is worth trying to solve. The feasibility study finds the best way to solve the problem. The final design stage is used in the execution of the energy system design plan. This thesis focuses on the feasibility study stage of energy system design.

1.3 Thesis Structure

The core question the thesis addresses is:

"*Can a generalized spatio-temporal asset model-generator be developed and utilized to optimize the sizing, operation and location of energy system assets?*"

1.3.1 Thesis Subquestions

To address the core thesis question, the thesis sequentially answers the following sub-questions in their respective chapters:

1. What are the minimum and sufficient theoretical basis functions of all assets in an energy system, and can these functions be used to create a unified model-generator of assets? (Chapter 3)

2. Can a model-generator of energy system design problems be developed, that utilizes the unified model-generator of assets, to co-optimize the sizing, operation, and location of real assets? (Chapter 4)

3. How are models for real-world assets generated from traditional data using the model-generators? (Chapter 5)

4. Can the model-generators be implemented as an easily accessible tool? (Chapter 6)

5. How do these model-generators and tool yield insights into real world energy system problems? (Chapter 7)

1.3.2 Thesis Roadmap

The rest of the thesis addresses the core thesis question and is structured as follows: Before the core thesis question is addressed, the gaps in the literature that the model-generator for assets, model-generator for energy system design problems, and tool presented in this thesis need to be identified. To do this, Chapter 2 presents a portrait of the current energy system modelling methods classified by their purpose, complexity, and optimization problems they consider. The major motivation of the framework that the thesis presents can be viewed as the need to more effectively

translate the optimal design of energy system into a mathematical optimization problem. This is done by having an intermediary unified asset model-generator that can build models to represent the physics of any asset that can perform any combination of the basis functions of the energy system. Chapter 3 develops this intermediary model-generator as a generalized spatio-temporal asset model-generator. It uses theoretical physics concepts such as generalized coordinates and movement of quantities in time to unify all types of energy system assets. In doing so, it also elucidates a useful set of basis functions of an energy system. Chapter 4 then uses this asset model-generator to develop a model-generator for optimal energy system design. This system design model-generator consists of three "languages" and translations between these languages. It uses the asset model-generator as an intermediary "asset modeller language" to translate the description of an optimal energy system design problem in a simple "system designer language" to a description as a mathematical optimization problem in the "optimizer language". This theoretically proves that solutions exist for generating models for all energy system asset using the model-generators; however, it does not find these solutions. Chapter 5 finds some of these solutions by generating models for eleven classes of real world energy system assets in the framework. This generates models for these assets from traditional data. Chapter 6 implements the model-generators into an open-source python tool that utilizes CVXPY. Chapter 7 finally demonstrates the tool by performing a hypothetical case study to design an energy system for Singapore. This demonstration provides a stress test to validate system dynamics of the energy system model generated by the model-generators and tool. The energy system in the case study satisfies Singapore's hourly electricity and industrial high temperature heating demand using intercontinental solar and wind DER farms at up to three locations around the world. The energy system moves energy in space, time, type using distributed batteries, ammonia storage, HVDC lines, ammonia transport, and various energy conversion technologies. Chapter 8 concludes the thesis by summarizing the contributions the thesis makes to knowledge. It finally charts out future research questions that researchers can try to tackle using the instruments that this thesis provides.

Chapter 2

Literature Review

Authors in the literature have classified energy system model-generators and models based on various aspects such as purpose and technology types included [28]. This chapter introduces a new classification that links the models in the literature based on their purpose, modelling complexity, and the underlying mathematical optimization problem they solve. This classification is shown in figure 2.1. This new presentation of the literature identifies a gap in the literature for a system design model-generator for optimal sizing and operation of energy system assets for scenario assessment. It also highlights a unified asset model-generator for energy system assets as a path to filling that gap.

The purpose of energy systems models and their model-generators can be split into four types; these are discussed in Section 2.1. These model-generators have various degrees of modelling complexity breadth and depth; these are discussed in Section 2.2. The optimization problems that these model-generators involve can be categorized based on the type of optimizations problem, and the methods used to tackle them; these are discussed in Section 2.3. Finally, Section 2.4, presents the gaps in the literature that this thesis fills.

2.1 Purpose

Energy system models are built to fulfil various purposes. Figure 2.2 shows how energy systems model generators can be categorized based on the purpose of the models that they generate. These can be split into four main types The first type is visualization and accounting. The second type is the simulation. The third type

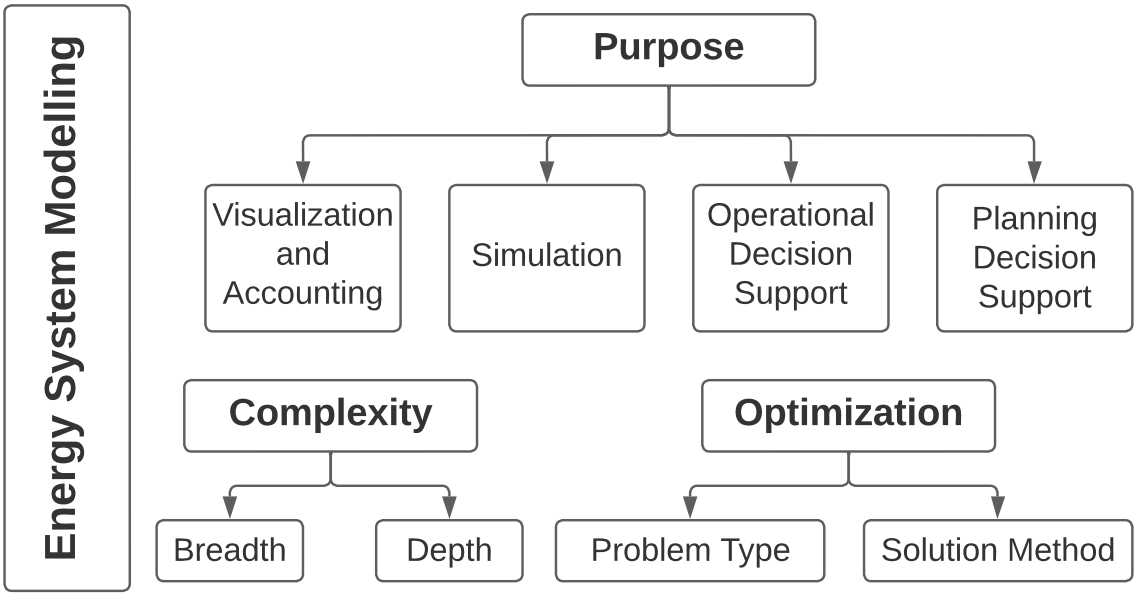

Figure 2.1: Classification of energy system model generators. Energy systems model generators can be split based on their purpose and the modelling complexity of their assets. They can also be split based of the type of optimization problems and solution methods they employ.

is operational decision support. The final type is planning or investment decision support. Some model-generators may have multiple purposes, but they generally have one main purpose.

2.1.1 Visualization and Accounting

One main purpose of energy system modelling is to visualize and account for various aspects such as energy, fuel, cost, emissions etc. Other than the generic graphs and bar-charts, there are two main models for energy visualization and accounting: Sankey diagrams, and energy balance tables. Sankey diagrams are useful for visualizing flows of quantities by representing the quantity of flow as the thickness of arrows. Sankey diagrams were first used by Sankey (after which the diagrams were named) to visualize the efficiency of steam engines [29]. Sankey diagrams are used by the IEA [21] to visualize flows of energy. Sankey diagrams are also widely used in to represent various quantities such as energy, emissions, costs, and materials in industrial ecology [30]. Energy balance tables are useful for accounting for fuel conversions and usage by various energy sectors. The IEA [31], IPCC [3] and various countries such as Singapore [32], currently use energy balance tables to account for fuel usage and thus

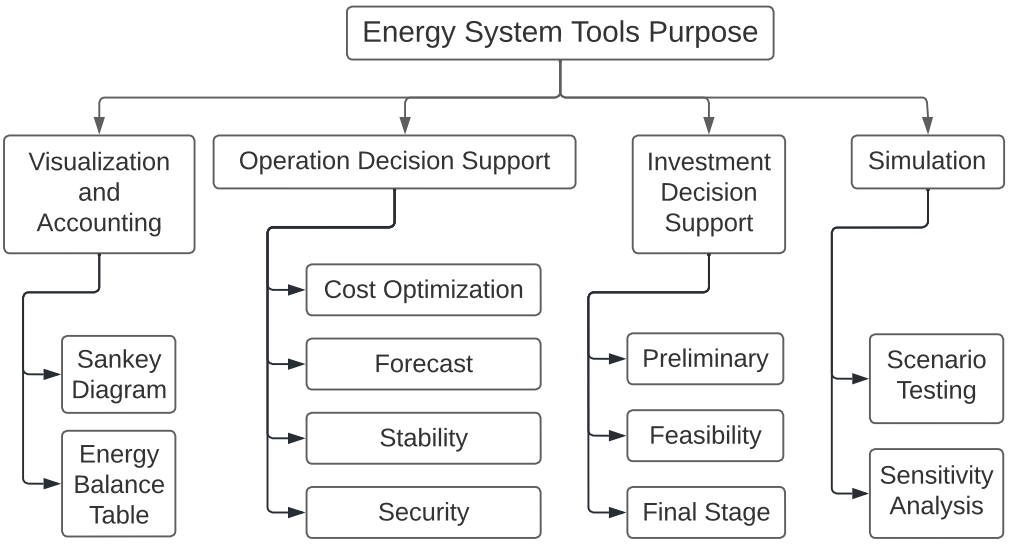

Figure 2.2: Classification of energy system model-generators based on their purpose. This thesis deals with the feasibility study in investment decision support with scenario testing, measured using cost optimization.

carbon emissions. Visualization tools are useful for studying and presenting results and are thus used as aids alongside other energy system tools.

2.1.2 Simulation

A multitude of energy system model-generators perform some sort of simulation of future energy usage, cost, emissions, etc. These run very quickly and can be very complex. Some of these simulations are performed for scenario testing. They change policy decisions and simulate the economic, technical, or environmental impact of these policy decisions. Examples of model-generators that generate models to simulate future energy systems include AURORAxmp [33, 34], MAED-2 [12, 22], LEAP [23] and LOADMATCH [35]; a more comprehensive list is compiled by Ringkjøb et al. [28]. Bussar et al. [36] for example, perform multiple simulations with different future assumptions to perform a sensitivity analysis on the impact of renewable energy integration on storage demand. Simulation tools are useful for understanding the robustness of the simulated impact to uncertainties in future predictions.

Various energy system model-generators that provide decision support also simulate energy systems. However, as their main purpose may not be simulation, they may not be able to use very complex asset models. For example, models that perform

optimization need to simulate energy systems multiple times, they thus need to be simpler to be able to be run in reasonable time. Energy systems models that are built for the main purpose of simulation do not have that restriction and can be a lot more complex.

2.1.3 Operational Decision Support

Various energy system model-generators build models for operational decision support. For example, Pereira et al, [37] and Monticelli et al. [38] perform optimal control of energy systems to increase the security and reliability of the grid, minimizing the risk of grid instabilities. Soroudi et al. [39] optimize energy system operation using Direct Current Optimal Power Flow (DCOPF) purely to minimize the cost of operation.

2.1.4 Planning Decision Support

Some energy system models and their model-generators support in planning or investment decisions. Leonard [27] splits energy system design and planning into three main stages: the preliminary stage, feasibility study, and the final design stage The preliminary stage is a very basic stage to see if a certain problem is even worth solving. The preliminary stage is usually performed by basic "back-of-the-envelope" calculations and rarely need specific energy system models. It checks if a problem is beneficial to solve and if tools exist to solve the problem.

The feasibility study is a much more complex study that assesses the various strategies to solve an energy systems problem. This could include the types of various assets needed to tackle an energy system problem. These include simulation tools such as MAED [22, 12] and LEAP [23], and optimization tools such as OSeMOSYS [8] and MARKAL/TIMES [10, 9]. This thesis mainly focuses on energy models intended for feasibility studies.

Once the strategy is finalized in the feasibility stage, the final design stage irons out the details of how to execute the strategy. AutoCAD [40] and Revit [41] provide a

deep technical plan of the exact size and brand of assets. Monday.com [42] and BambooHR [43] provide timeline and manpower management for building the projects. Powerfactory [44] can be used for accurate power systems analysis of grid designs.

2.2 Complexity

Energy system models and their model-generators in the literature can be categorized based on their modelling complexity. Figure 2.3 shows how energy systems models in the literature can be categorized based on their model complexity. The complexity consists of their breadth (fidelity) and depth (accuracy). The modelling breadth or fidelity of a model is the range of effects or processes that a model considers. The modelling depth is the accuracy of the various effects that a model accounts for.

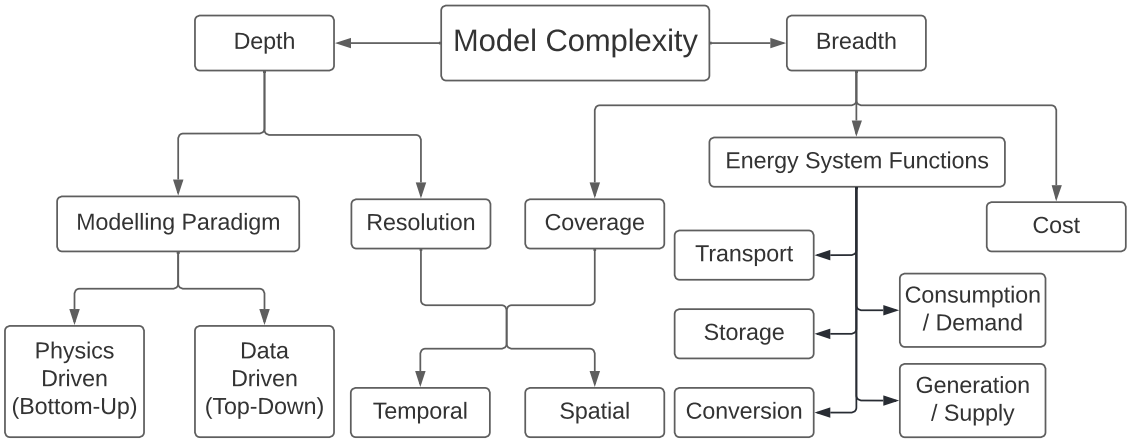

Figure 2.3: Classification of model complexity of asset models in the literature.

2.2.1 Breadth of Modelling Complexity

In the context of an energy system, the breadth of modelling complexity includes the types of energy system assets: usage/demand, generation/supply, transport, storage, conversion, and demand response. The breadth of modelling complexity also includes the types of potential costs and the spatio-temporal coverage.

Energy System Asset Types

Figure 2.3 shows the classification of energy system asset types considered in the literature. There are six main energy system assets. The first type of an energy

assets are energy usage or energy demand assets. This demand is met by the second type energy system assets: energy generation or energy supply assets; these extract energy from the surrounding. However, as energy may not be produced at the same time as it is demanded, it needs to be stored; this is done by energy storage assets, the third type of energy system assets. The energy may also be produced at a different place than where it needs to be consumed. It thus needs to be transported from one place to another; this is done by the fourth type of energy system assets, transport assets. There may also be a mismatch between the type of energy supply and demand. The energy thus needs to be converted from one form to another; this is the fifth type of energy system assets, energy conversion assets. The sixth and final type of energy system asset is demand response assets. Energy systems models in the literature account for a combination of these types of energy system assets. These are treated as different problems, and thus, not all energy system model and model-generators account for all types of energy system assets.

Figure 2.4 shows the classification of usage assets modelled in the literature. The types of usage assets modelled in the literature can be categorized based on the demand sectors they account for, the end-use energy and services they simulate, and the types of market they consider. The IEA energy balance tables [31] and Sankey diagrams [21] split demand into different sectors such as industrial, transport, commercial and residential. These are particularly useful for models whose main aim is accounting and visualization. However, the sector does not affect the physics of assets. The same sector can have different types of assets, and different sectors can have the same type of asset.

End-use energy and services are the type of energy or service that is ultimately consumed by consumers. These can be split in various ways in the literature. This thesis uses the categorization used in the MAED methodology with some changes. [22, 12]. End-use energy and services are split into electricity, cooling, low-temperature heating, high-temperature heating, passenger transport, and goods transport. The MAED methodology splits end-use heating into low, medium and high temperature heating; this is based on the technologies required for those end-use services. This thesis splits heating into low and high temperature heating because low temperature

heating can be provided by heat pumps, while high temperature heating cannot. This means that the coefficient of performance (COP) of high temperature heating is close to one, and the COP of low temperature heating is much higher (3-5) [45, 46, 47].

The types of markets considered in the literature can be split based on their complexity. The simplest models have no markets [28], i.e. they have fixed demands. These are sometimes referred to as perfectly inelastic demand, or sometimes just inelastic demand [48, 49, 50, 51]. Some model-generators can generate models that consider the effects of the invisible hand and market equilibrium, but treat markets separately, i.e. they consider the state of other markets as constant while finding the equilibrium of the current market. These are called partial equilibrium models [9, 10]. MARKAL/TIMES is an example of partial equilibrium model-generator [9]. More complicated economic models consider the effects of one market equilibrium on other markets, simultaneously. These are called computable general equilibrium models [52, 53, 54, 55]. Attempts have been made to link multiple model-generators together to account for nonlinear effects such MARKAL-MACRO [56]. MACRO is a non-linear, top-down optimization model-generator to simulate aggregated economic activity, while MARKAL is a linear bottom-up optimization model-generator for long term energy system design at least cost. However, as models built by both model-generators perform optimization with different assumptions, this leads to inefficient optimization and thus a dramatically increased optimization time. The linking also make it difficult to study the computational complexity to find ways to increase optimization efficiency or make good approximations or reduce computational time.[57] Some energy system models in the literature go one step further and propose novel markets such as reserve, merit order, or distributed price signalling markets [58, 59, 60].

Figure 2.5 shows the classification of energy generation assets considered in the literature. Energy cannot be created or destroyed, thus generation assets do not create energy. Generation assets instead can be viewed as assets that extract energy from the surrounding. The types of generation or supply assets considered in the literature can be split based on the technology and the approach to simulating that technology. The technologies considered in the literature are either conventional generation technologies (such as power plants) or renewable generation technologies (such

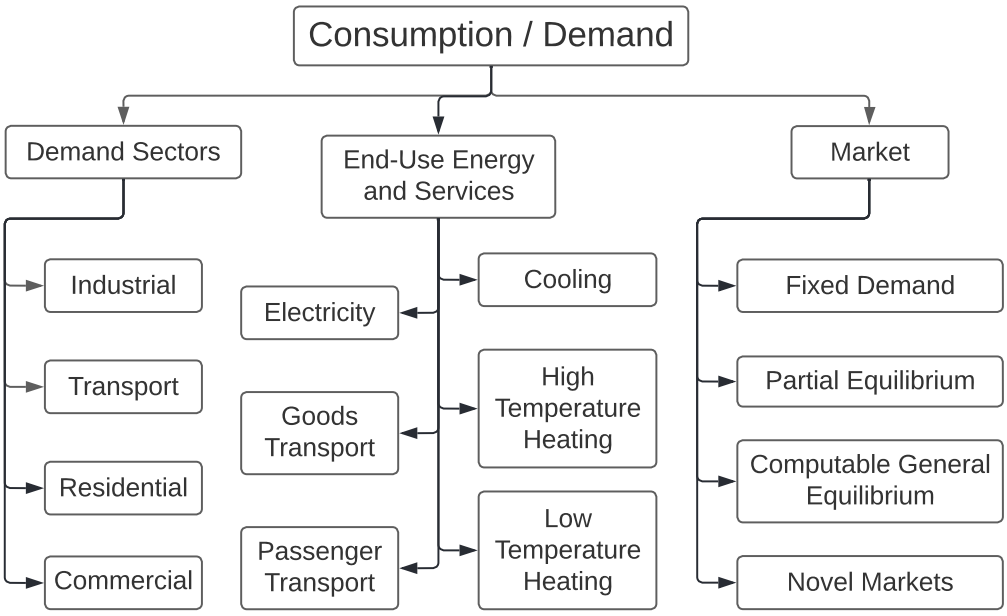

Figure 2.4: Classification of usage or demand assets in the literature.

as solar, wind, and water). While almost all energy system models in the literature model conventional generation [28], some model-generators such as LOADMATCH [61] explicitly only model renewable generation technologies as they are designed to model energy systems with 100% renewable energy. There are two main approaches to modelling these generation assets, the first is to model single assets, while ignoring the processes and materials used to build, extract or retire the assets. The second approach is the use whole system modelling or lifecycle assessment (LCA) [62]. In this, the whole lifecycle of a process, and the material flows surrounding an asset are considered, i.e. from "cradle to grave" of an asset. In the context of energy systems, LCA models would, for example, include the extraction of materials used to build the power plant, the extraction of fuel used in the power plant, and even the fuel and materials used to retire the power plant, including recycling, waste management, etc [63, 64, 65, 66, 67].

Figure 2.6 shows the classification of energy energy storage assets considered in the literature. These may be divided based on the type of energy they store, i.e. into chemical, thermal, mechanical, electrical, and gravitational energy storage systems. Chemical energy storage systems include conventional batteries [68, 69, 70, 71], flow batteries [72], or chemical energy vectors such as hydrogen and ammonia [73]. Me-

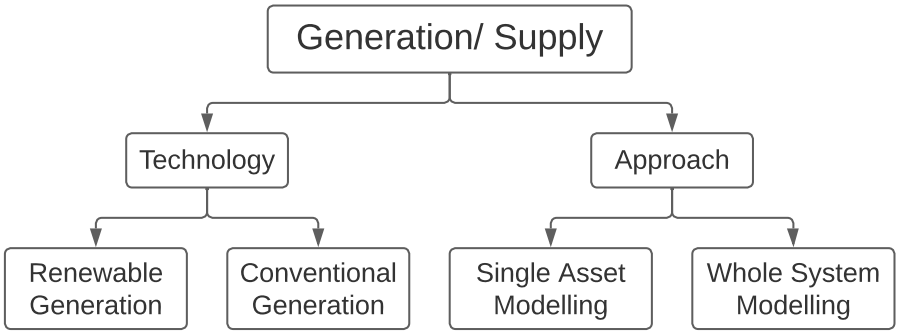

Figure 2.5: Classification of generation or supply assets in the literature.

chanical energy storage systems include compressed air energy storage systems [74] and flywheels [75, 76]. Electrical energy storage systems include capacitors [77] and inductors [78]. Capacitors, inductors and flywheels usually store very little energy and charge and discharge completely in very little time; they are thus traditionally used for frequency response or frequency balancing [79]. However, there are special types of flywheels [80], super-capacitors [81], and superconductive inductors [82] that work at longer timescales and store more energy. The last, but certainly not the least, is gravitational energy storage systems. The most prominent type of gravitational energy storage system is pumped hydro [83]; they make up 42% of currently installed energy storage systems around the world (by energy capacity) [84].

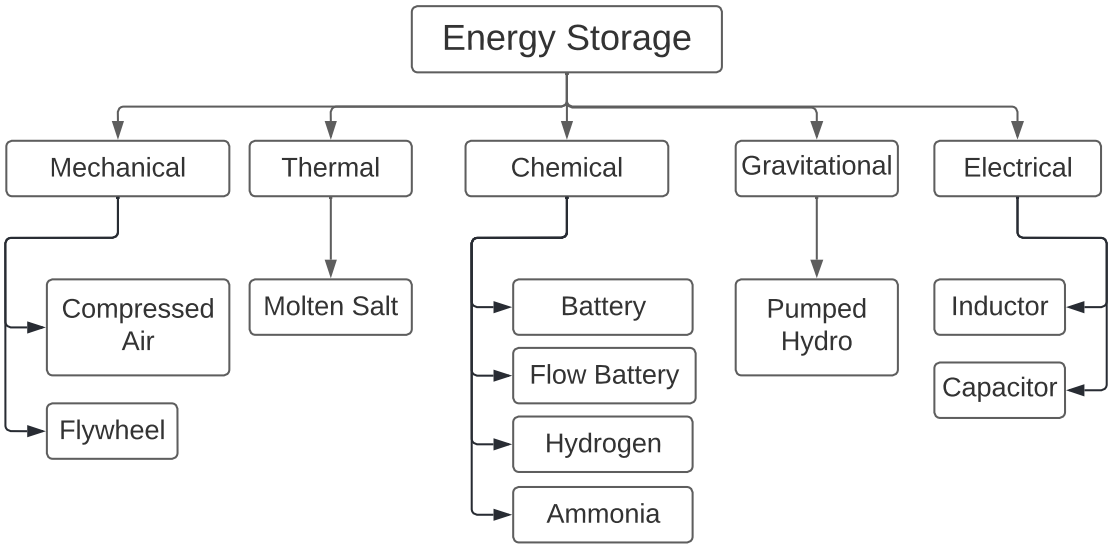

Figure 2.6: Classification of energy storage assets in the literature.

Some models in the literature also account for demand side management, or de-

mand response models [85, 86, 87, 88]. Figure 2.7 shows the classification of demand side management assets considered in the literature. Some of these demand responses delay usage of energy when energy is not available [89, 90]. Some use earlier usage such as when there is a surplus in supply, or when supply is cheaper [28]. Some of the literature consider indirect forms of demand response such as by flexible space or water heating or cooling [91, 92].

Various authors in the literature try to make links between demand response and energy storage. Some treat them separately and discuss the similarities and differences between them [93, 28, 94, 95]. Huang et al. also classify energy storage and demand response of various energy types together as "integrated demand response" [96]. Some have started to describe demand response and energy storage as movement of energy in time [28]. However, to the best of our knowledge, demand response and energy storage has not been mathematically formalized in the literature of energy systems modelling. Some authors have even tried to make links between energy storage and geospatial demand shifting, particularly in the context of data centres [97]. In this thesis, we shall formalize the idea of movement of energy in time to elucidate the equivalence of all these demand responses, and unify them as just movements of energy in space, time and type.

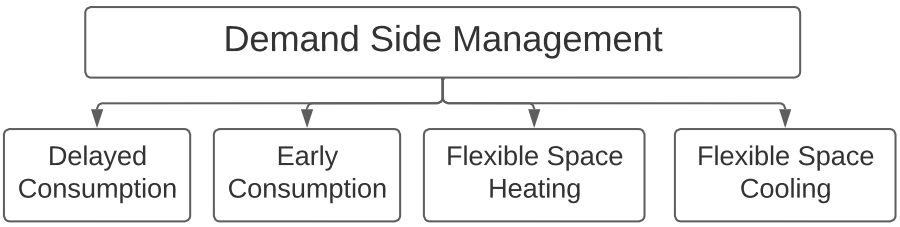

Figure 2.7: Classification of demand side management assets in the literature.

Figure 2.8 shows the classification of energy transport models considered in the literature. The types of energy transport models considered in the literature can be split into electrical and non-electrical energy vectors. These can further be split into the types of vectors, and the methods used to simulate them. Types of electrical energy transport in the literature include AC distribution or transmission grids, and high voltage DC (HVDC) interconnectors. Electrical transport models range from

complex full three phase AC models such as with ACOPF [98, 99, 100]. Some make linear approximations such as DCOPF [101, 102] and variations of it that try to account for losses [103, 104]. Some models consider individual edges and model zonal transport [105, 106, 107]. The simplest models, sometimes referred to as copper plate models, assume instantaneous transport, with no limits or losses [108].

The types of non-electrical energy vectors modelled in the literature include hydrogen [109], ammonia [110], and even conventional fossil fuels [111]. These are usually transported via freight (land, sea, or air) or via pipelines (if they are liquid). Some models in the literature consider existing routes such as shipping routes, roads, etc [110]. Some models in the literature also consider new potential routes, [73]. These new routes are sometimes modelled using simple methods such as by assuming straight lines, or "as the bird flies", or via more complex shortest path algorithms that optimize the cost and efficiency of going through different terrain [112].

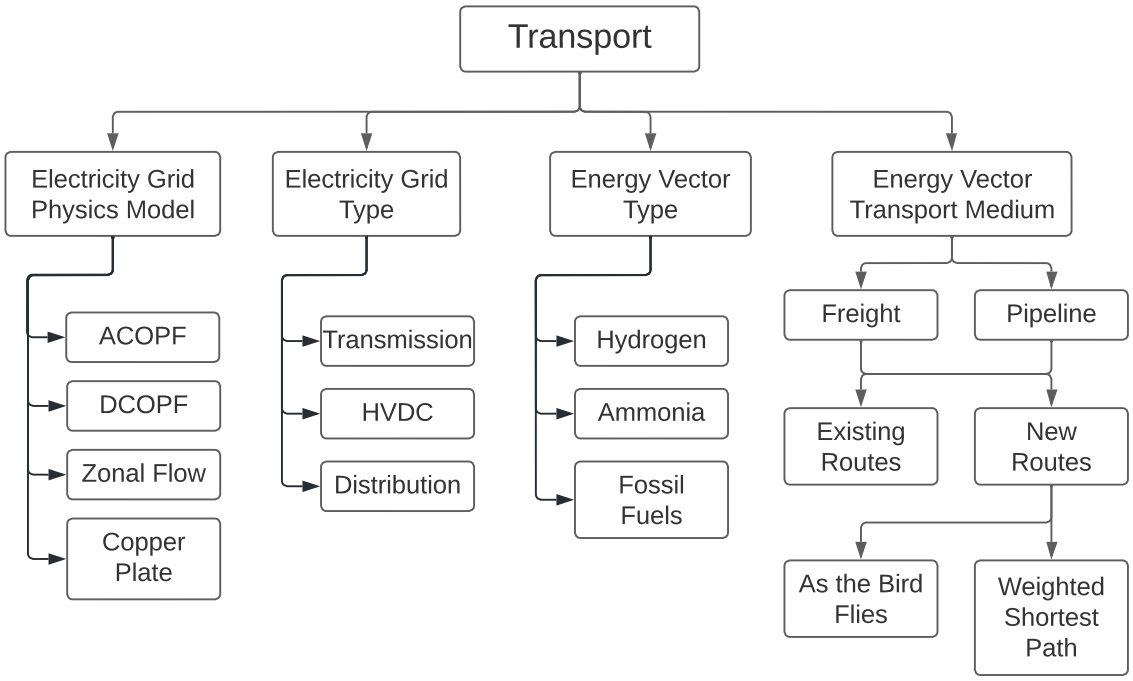

Figure 2.8: Classification of energy transport assets in the literature.

Energy conversion assets convert energy or fuel from one form to another. Figure 2.9 shows the classification of energy conversion models considered in the literature Energy conversion models used in the literature can be categorized based on the types of energy or fuel they consider, and methods used to model them. The types

of energy that is considered can be split into primary energy supply, intermediate energy vectors, and end-use energy and service demand [28, 22, 13]. Some models in the literature split them based on energy sector instead of type of energy; but in general you can do both [28, 113, 114]. Splitting them based on sector is more useful for accounting, while splitting them based on energy type is useful for studying their physics modelling.

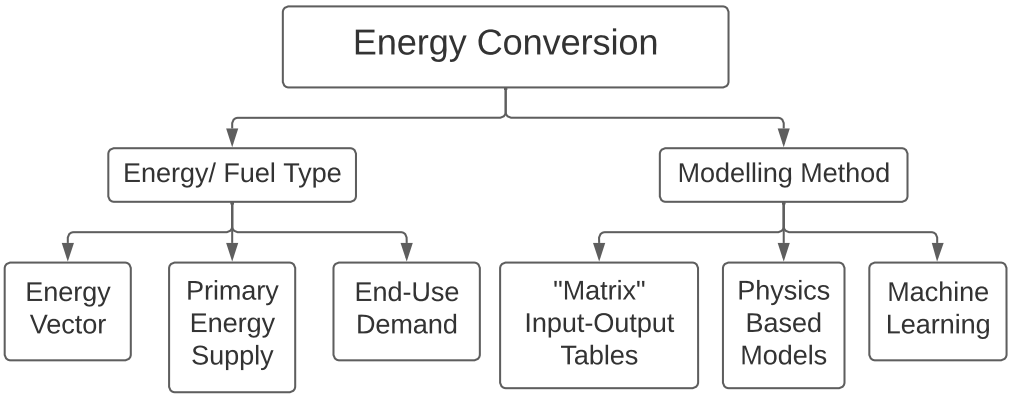

Figure 2.9: Classification of energy conversion assets in the literature.

Cost

Figure 2.10 shows the classification of costs considered in energy system models in the literature. Costs can be categorized based on the type of cost, and the method used to calculate them. Almost all energy system models that model costs account for the two private costs: capital cost, and operational and maintenance costs. Some models also consider the tax on different energy system assets, e.g. carbon tax [115, 116]. However, there may be externalities of producing and using the energy system. This includes impact on climate, pollution and health hazards. According to some authors such as Jacobson et. al, these externalities may be a few times larger than the private capital and operational costs of assets [117]. However, the value of these externalities can vary by a few times as they can be defined or interpreted in various ways. E.g. calculations for health impact of non-RE energy sources can be calculated by multiplying the estimated deaths from pollution with the value of statistical life [118]. However, the value of statistical life may depend on the willingness and ability of individuals to "'pay" for their life. This objectifies human life and manifests itself

as an income elasticity of value of statistical life; i.e. the lives of richer people are valued higher [119]. This creates a multitude of ethical conundrums, and thus these externalites need to be carefully considered before they are internalized and combined with private economic costs.

Some models calculate the various types of costs separately and present them using multi-criteria decision methods [120, 121]. Some models normalize all types of costs to a generalized numerical cost, usually in terms of economic cost [117]. Some models use hierarchical structures for visualization and decision making where certain types of costs are strictly more important than other types of costs; thus, some types of costs are minimized before others. These hierarchical costs are usually used for Geographic Information System (GIS) analysis [122] or to avoid the ethical issues of internalizing health costs as externalities described in the previous paragraph.

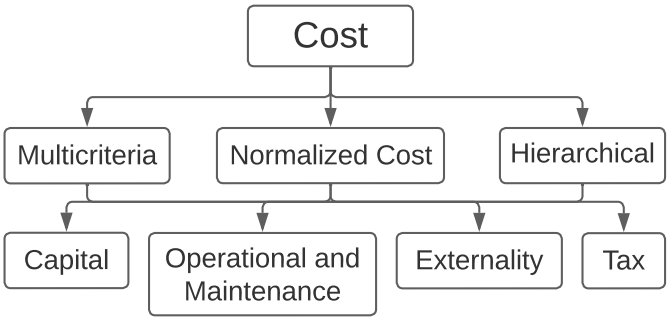

Figure 2.10: Classification of objective functions or costs used by energy system models in the literature.

Spatio-Temporal Coverage

As shown in figure 2.3, energy system models in the literature can also be classified based on the spatio-temporal range that they cover; this is a type of modelling complexity depth. The temporal coverage of models in the literature spread across multiple orders of magnitude [28]. Temporal coverage start from subseconds and seconds, usually found in models used for multiphysics asset design or electrical grid stability analysis [123, 124]. Some energy system models in the literature cover minutes, hours or even days. Examples include optimal dispatch operational models [108, 125, 126, 127]. Finally, system design, planning and investment models cover

years or even decades of time [53, 128]. Some models in the literature are generalized and allow the users to define custom spatio-temporal coverage [44, 8, 7].

The spatial coverage of energy system models in the literature also varies over orders of magnitude [28]. Some models are build to study individual assets and thus only cover individual components or even materials of devices using complex multi-physics models [124, 129]. Other energy systems also cover local, regional, national, continental or even global scales [130]. There is a trade-off between spatio-temporal resolution and coverage. Increasing either increases the computational requirements and places limits on the resolution of models that cover a large geographical area. This is why most models that cover the world are either top-down or a hybrid between top-down and bottom-up models [28]. Top-down and bottom up models can be defined in different ways in the literature, one way to define them is the following classification used by Ringkjøb et. al [28]. Bottom-up models are often also referred to as engineering models and are based on technological descriptions of the energy system. Top-down models are often also referred to as economic models and are based on macroeconomic relationships and long-term changes. Furthermore, these are usually economic or market models with very simple technological assumptions [53]. Finally, some models are background independent and thus allow users to define the spatio-temporal coverage [131]. These models are more flexible, but are also more difficult to use. Even though they theoretically allow us for the modelling of broad spatio-temporal coverage, their resolution is limited by computational complexity: i.e. the computational complexity of these models become too high to use at high combined spatio-temporal coverage.

2.2.2 Depth of Modelling Complexity

The modelling depth is the accuracy of the various effects that a model accounts for. In the context of an energy system, these are the spatio-temporal resolution of energy system models. It also includes the modelling paradigm, i.e. if a model is predominantly bottom-up physics-driven, or if it is top-down data-driven.

Modelling Paradigm

Energy system models in the literature can be classified based on their modelling paradigm. Energy systems can model individual assets using physics-driven bottom-up models, or using using data-driven top-down models [28]. The former and latter are also referred to as white-box and black-box models, respectively. However, these philosophically also map to scientific deduction and induction, respectively. Scientific theories, in general, are a combination of both. Thus, all models will, in general, have some elements of both. Models that are not predominantly either, or are a combination of both, are referred to as gray-box or hybrid models.

Spatio-Temporal Resolution

Energy system models can also be classified based on their spatio-temporal resolution. Temporal resolutions of models, just like coverage, can range from subseconds, to seconds, minutes, hours, days, years, and even decades [28]. Similarly, the spatial resolution of models can range from meters or kilometers used in geographic information system (GIS) models [132], to local, regional, national, continental [133], and even global resolutions [130]. When the resolution and coverage of a model is equivalent, it means that the model only considers the total, or average over that period of time or space. An example of models with equal spatial resolution and coverage include "copper plate" models [108]. An example of models with equal temporal resolution and coverage are GIS models [134]. Finally, just like with spatio-temporal coverage, some models are background independent and thus allow users to define custom spatio-temporal resolutions.

2.3 Optimization

Energy system models and their model-generators in general deal with some sort of optimization. Even some simulation models include some intermediate optimization. In the most trivial of cases, especially for models used for visualization and accounting, energy system models could have "no optimization". For all non-trivial cases, figure 2.11 classifies the types of optimization problems tackled by energy system models in the literature and the methods used to solve them.

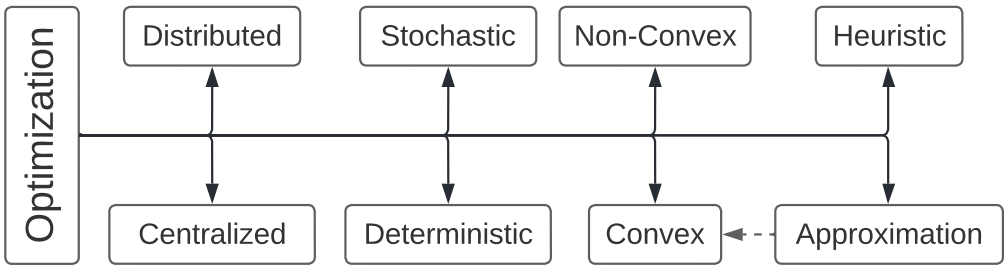

Figure 2.11: Classification of classes of optimization problems and strategies to deal with them.

2.3.1 Uncertainty

Optimization problems considered in the literature can firstly be split based on if they consider uncertainty. Some models assume perfect foresight and are deterministic [8, 7]. Other models, especially those used for real-time operational decision making, are stochastic. When problems are stochastic, optimization can have various goals such as minimizing the average cost, to minimizing the worst case scenario, or even requiring the satisfaction of demand in above a certain fraction of time [135, 136].

2.3.2 Control Scheme

Optimization problems are global problems and are traditionally solved using centralized algorithms that have information about and can control all decisions in a system [59]. However, for very large problems, the flow of information may not be feasible or secure; and centralized control may not be desirable due to ethical or privacy reasons. To deal with this, some energy systems models restrict the flow of information and/or the control of variables to a subset of entities, such as for agent-based modelling [137]. These can be broadly considered distributed optimization problems, or problems that use distributed algorithms.

2.3.3 Convexity

Regardless of whether an optimization problem considers uncertainty or if it uses centralized algorithms to solve it, it can eventually be classified as either a convex or non-convex problem. In a convex problem, a local optimum (or solution) of a problem is also the global optimum of the problem. This means that it is easy to test

if a (local) solution is a true (global) solution to a problem. It also usually means that algorithms exist to find the solution in reasonable time. Convex problems can be divided into a hierarchy of problems based on complexity. The simplest problems are linear programs (LP), there are multitude of sequential and parallel algorithms available to solve these "simple" problems [138, 139]. Most energy system tools used outside of academia only consider LP [8, 10]. More complicated convex problems, in order of complexity, include quadratic programs (QP), second-order cone programs (SOCP), semidefinite programs (SDP), and cone programs (CP) [139].

Convex problems higher up in the hierarchy of complexity are more difficult to solve. However, it is still easy to solve them, or at least test their solutions, compared to non-convex problems. Non-convex problems are problems with multiple local optima of different values. Thus, a local optimum of a non-convex problem is not a global optimum, or true solution of the problem [139]. This means that it is, in general, very hard to test the solution of non-convex problems, let alone find solutions. I.e. non-convex problems are in general NP (nondeterministic polynomial time) hard [140]. We can solve some specific cases, if information about the problem structure is known [141]. However, no general algorithm exists to find, or even test, solutions for non-convex problems easily.

2.3.4 Approximation vs Heuristic

No general algorithm exists to find, or even test, solutions for non-convex problems. Thus, non-convex problems are usually tackled by finding reasonable solutions, rather than the optimum solution. To deal with non-convex problems, we either use heuristic algorithms, or make approximations to the problem that transform it to a convex problem that can then be solved more easily. Heuristic algorithms cannot guarantee the optimum solution, but can be useful for finding reasonably good solutions, especially for "real" systems or data. These "real" systems are usually represented in the literature using standardized datasets specific to the field; these are used for comparing and benchmarking algorithms [142]. Common heuristic algorithms for global optimization include machine learning [143, 59, 100], particle swarm, genetic evolution, basin hopping, shuffled frog leaping, or annealing algorithms [144].

Some authors in the literature use approximations instead of heuristics when dealing with non-convex problems. When approximating non-convex problems, we can either approximate the cost function (which would lead to sub-optimal solutions), or approximate constraints (which lead to violations in the original problem). Under special conditions, it is possible to find "convex relaxations" to a problem [145]. Convex relaxations are approximations to original problems that still give the solution to the original problem. However, it is not always possible to find convex relaxations. Furthermore, it is difficult to find good approximations that still give reasonable results. If the approximation is too simple, then it looses too much of the physics and the solution is no longer useful. If the approximation is too complicated, then the problem may still be difficult to solve, or perhaps still non-convex. In general, each energy system optimization problem needs to be treated individually to find good approximations. There are currently no general methods for finding good approximations for energy systems optimization problems. This is why most of the literature default to the simplest linear approximations when a problem is too complicated to solve [28]. However, these linear approximation may loose a lot of the essential physics of the energy system and more accurate approximations may exist that can still preserve the essential emergent physics of the system. Piece-wise linear and integer programming does allow tools such as MARKAL, TIMES, MESSAGE, and OSeMOSYS to capture more of the essential physics; however, these come with computational penalties.

2.4 Gap Analysis

Chapter 1 highlights the need for methods for the optimal sizing, operation and location of energy system assets, that can perform any function of an energy system, with scenario assessment. This chapter maps out the existing literature on energy system design, asset modelling, and optimization. There are gaps in the literature in these three areas summarized in Figure 2.12. The first gap in the literature is the lack of energy system design model-generators that generate models that optimize the sizing, operation and location of energy systems assets at the same time. Existing model-generators in this space are lacking due to the other two gaps in the

literature. The second gap is the lack of a unified asset model-generators that can generate models to represent any type of energy system asset that can fulfil any function of an energy system. This prevents the study of the trade off between asset modelling breadth and depth on the accuracy and computational complexity of the corresponding optimization problem. The last gap in the literature is the lack of a model-generator to generate models for energy system design optimization with rapid scenario assessment.

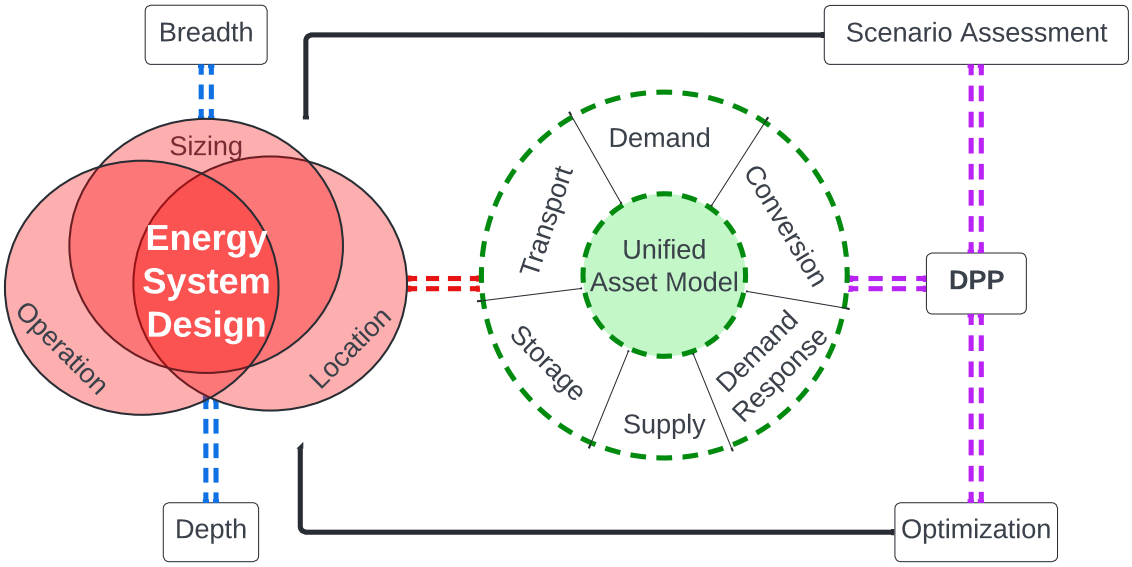

Figure 2.12: Gap analysis of energy system design literature. The gaps in the literature are dotted lines. This thesis fills these gaps by building a unified asset model that combines all types of energy system assets. This is combined with DPP to formulate a framework for optimization with scenario assessment. This allows the study of the trade offs between model breadth and depth. This ultimately enables the optimal energy system design: the optimal sizing, operation, and location of assets in an energy system.

2.4.1 Sizing, Operation, and Location

The first gap in the literature is the lack of a system design model-generator that generates models to optimize the sizing, operation and location of energy system assets. This is for the purpose of feasibility studies in the design process of an energy system. Most model-generators in the literature are designed to build models to perform a subset of the three: sizing, operation and location of assets. The optimal

design of future energy systems requires performing all three, concurrently. This thesis focuses on improving the model-generators in this intersection.

Some model-generators in the literature only build models to perform one of optimal sizing, operation, or location of assets. Some work in the literature primarily focus on the cost optimal operation of assets of a given size. These use very accurate non-linear models of assets such as the battery model by Ahsan et al. [108] that consider the non-linear dependence of battery efficiency and degradation on the state of charge and current. However, this forces the optimization problems of such models to become too computationally difficult to solve for large number of timesteps. Konneh et al. [146] deal with this using the traditional method of model predictive control, which only optimizes for a small time horizon. Dashtdar et al. [147] instead overcome this by using heuristic genetic algorithm, while Zhu et al. [148] utilize deep reinforcement learning to harness the power of modern GPUs. Research in this area is also moving towards more complicated sub-problems such as operations under uncertainty in the work of Mobasseri et al. [149], or with robustness in the work of Yang et al. [150]. These models are designed to be utilized for real-time dispatch, and excel at it. However, the computational complexity of these models make them unsuitable for the sizing of these assets, and thus for the design of energy systems.

Some model-generators in the literature focus on the sizing of assets in an energy system. Because of this, model-generators such as MAED [12, 22], and LEAP [23] ignore the operation of assets and purely focus on the sizing of various assets. These lean into their simplicity and act as simulation tools allowing for quick assessment of different scenarios. However, while these tools are quick enough to be used for scenario assessment, they do not optimize the sizing of assets for a given scenario. LEAP has been integrated with optimization models such as NEMO [151]. However, as the initial versions of NEMO were informed by OSeMOSYS, NEMO also suffers from similar limitations as OSeMOSYS. Lee et al. [152] uses multi-agent based models to simulate specific operational strategies while optimizing the size of assets. However, this does not optimize the operational strategy given a sizing. Ma et al. [153] overcome this using the traditional approach of bi-level optimization. The lower level optimizes the operation of assets given the constraint of asset sizes. The upper level then

optimizes the size of assets. These bi-level optimization models utilize models that only perform optimal operation for the lower level optimization. This allows them to utilize advances in that field. However, this makes these bi-level optimizations strictly harder to solve, and the computational complexity increases rapidly making these models only suitable for small number of assets that need to be sized.

Some models focus on the location of assets in an energy system. These use GIS tools to find optimal locations for RE such as PV or Wind. They typically employ hierarchical methods such as those employed Settou et al. [154] or multi-criteria decision-making (MCDM) methods such as the analytic hierarchy process (AHP) method developed by Saaty et al. [155]. These methods are useful for identifying potential locations for assets at very high spatial resolutions. For example, Ouchani et al. [156] perform GIS mapping of PV and irrigation in Morocco to determine the potential capacity of available DER resources in a region. However, the high spatial resolution of these models makes it difficult to use them for optimal system design. Using them directly will either be equivalent to performing brute force optimization over millions of locations at best (if selecting just one location), and will make the problem computationally intractable at worst (if selecting multiple possible locations).

Some model-generators are designed for optimal operation and sizing of assets. For example, tools such as OSeMOSYS [8] and MARKAL/TIMES [10, 9] are designed for optimal sizing and operation of energy system assets. However, as these model-generators aim to include as many types of assets as possible, and due to computational limitations, they make very simplistic linear assumptions. OSeMOSYS is only able to account for perfectly inelastic demand of energy. There are attempts to introduce elasticity into OSeMOSYS such as by Lavigne [157] using a convenient easy-to-use method, and using terms that are naturally used in economics. However, as OSeMOSYS uses linear programming, Lavigne's work was only able to approximately represent elastic demand using step functions which will lead to solution stability issues, especially for large problems [157]. MARKAL/TIMES models markets by using linear energy markets with linear demand and supply curves. However, as MARKAL/TIMES is still a linear model-generator overall, it is not able to model the influence on markets on each other; thus, it is only a partial equilibrium model

instead of a computable general equilibrium model. These model-generators were developed for a specific location and thus do not consider the transport of energy in space naturally. Extensions to these will be discussed later.

Some model-generators are designed to perform optimal operation of assets at different locations. Model-generators such as pandapower [158], optimize the operation of various assets on a grid using DCOPF or ACOPF approximations. The OPEN tool [101] extends this by adding different markets and assets in a modular way. Baker [159] uses machine learning to emulate ACOPF solvers allowing the grid structure to be learnt for real-time dispatch. However, this needs to be re-learnt when the energy system structure changes. While these tools are efficient for operational dispatch of assets at different locations, they are not suitable for sizing assets.

Some model-generators are designed for optimal sizing and location of assets. For example, OnSSET [160] integrates GIS tools to find optimal electricity access strategies. However, this assumes very simple assumptions of grid operation. Salmon et al. [161] perform geospatial analysis to find optimal locations for green ammonia production. However, they do not integrate the optimal operation or sizing of assets that consume the ammonia.

This thesis focuses on tools that perform optimal sizing, operation and location of assets, concurrently. Barnes et al. [162] extend OSeMOSYS to handle transport of energy between different countries in OSeMOSYS Global. While OSeMOSYS Global does extend OSeMOSYS to be able to do optimal sizing, operation and location of assets, it still suffers from the same limitations of linear model assumptions as it is built on OSeMOSYS. PyPSA [11] has been extended to account for different countries in Europe as PyPSA-Eur [163]. PyPSA-Eur however, only focuses on electrical assets. PyPSA-Eur has thus been extended further to include different sectors as PyPSA-Eur-Sec [164]. Ramos et al. [165] perform a similar extension to OSeMOSYS as a climate, land, energy, and water systems (CLEWs) model. However, as PyPSA-Eur and PyPSA-Eur-Sec are based on PyPSA, they treat the power system as the core and the rest of the energy system as add-ons. Similarly, the CLEWs implementation of OSeMOSYS is based on OSeMOSYS that uses the energy system as the core. This makes the conceptual modelling of whole energy systems more complex. This

asymmetry also makes it difficult to study the trade-offs between the model accuracy of various assets on the overall system design. For example, the CLEWs extension of OSeMOSYS currently only uses the climate, land, and water sectors as constraints, and do not optimize the assets that utilize these other resources.

Note that most of the approaches in the literature to build models to perform optimal sizing, operation, and location of assets involve "patching" together existing bespoke models that perform a subset of the three problems. These "patchwork" models make it difficult to model and study whole energy system problems. They are also make assumptions that need to be undone when communicating with other bespoke models. This motivates the design of a framework from ground-up for the combined optimal sizing, operation and location of assets in an energy system.

2.4.2 Disciplined Parametrized Programming

In this thesis performing a "case study" is defined as the optimal sizing and operation of assets at various locations, i.e. the energy system design problem. The optimal energy system design in a case study depends on the efficiency and cost assumptions of its constituent assets, and the lat-lon of the locations; these are referred to as "scenario assumptions". There are uncertainties in future scenarios. Thus, future energy system design requires assessing how the ideal energy system design is affected by scenario assumptions.

A generic process for performing a case study with different scenarios is shown in Figure 2.13(a). The first step is to define the case study. This is the set of assets that can be built and operated at various locations. The second step is to select a set of scenario assumptions. These are the efficiency and cost assumptions of the constituent assets, and the latitude and longitude (lat-lon) of the locations of these assets. Once a specific scenario is selected, the optimal system design is found for the given scenario. This is the optimal sizing and operation of each asset at different locations. The results are then analyzed; this process usually takes a few minutes. The insights from the results are used to determine a new set of scenarios to be tested. The process is then repeated until a good understanding of the case study is achieved.

The case study is concluded by describing the optimal system design and how it is affected by scenario assumptions.

In this case study design process, finding the optimal energy system design for a given scenario is the dotted task in the flowchart in Figure 2.13(a). There are two traditional frameworks for finding the optimal system design: simulation and optimization; these are shown in Figures 2.13(b) and 2.13(c), respectively. Simulation frameworks are used by model-generators such as MAED-2 [12, 22], LEAP [23]. These are quick and take the orders of seconds to run. They enable a workflow in which multiple scenarios can be tested per hour. However, simulation frameworks only simulate a specific size, operation and location of assets. This may not be the optimal design assets for a specific scenario. Simulation frameworks thus overestimate the true cost of the optimal energy system design given a scenario. To better estimate the optimal design, the size and operation of assets are manually changed and the simulation is rerun for the same scenario. This however increases the time it takes to assess each scenario and requires a lot of work.

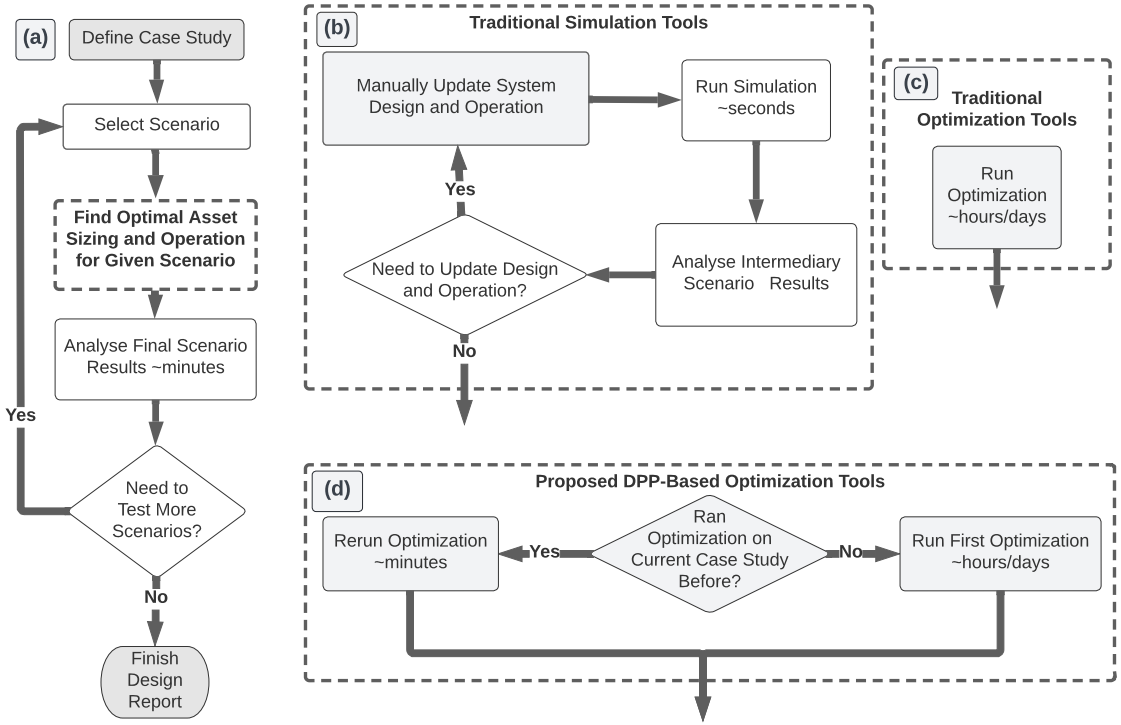

Figure 2.13: Energy System Design Case Study Process. (a): A typical energy system design case study process consists of defining a case study and finding the optimal design and operation for multiple scenarios. There are two traditional scenario analysis frameworks. (b): The first traditional framework consists of simulation tools that are quick. This framework allows scenarios to be analyzed every few minutes. However, simulations needs to be repeated manually to find the optimal design and operation for each scenario. (c): The second traditional framework consists of optimization tools. These automatic find a closer to optimal design and operation for each scenario. However, these are slow and only allow scenarios to be tested every few hours or days. (d): The proposed framework consists of DPP-based tools that can rerun optimizations for the same case study but different scenarios very quickly. This allows the accuracy of traditional optimization tools with the speed of simulation tools.

Optimization frameworks are used by model-generators such as OSeMOSYS [8] and MARKAL/ TIMES [9]. These are shown in Figure 2.13(c). These can find the optimal energy system design given a specific scenario. This makes traditional optimization frameworks more accurate than simulation frameworks. However, traditional optimization frameworks take much longer time to run than simulation frameworks. Traditional optimization frameworks can take hours or days to test each scenario. A scenario needs to be assessed to determine the next scenario to test. Thus, traditional optimization frameworks only allow workflow in which scenarios can only be properly be tested once every few hours or even days. This makes traditional optimization workflows unsuitable for quickly testing a large number of scenarios. There are methods of testing batches of scenarios in parallel such as using OSeMOSYS-PuLP [166]. However, these require the user to know before hand the scenarios that need to be tested; batch processing cannot help when a scenario needs to be analyzed to determine what the next scenario that needs to be tested is. Furthermore, such Monte Carlo methods scale linearly at best and become computationally too intensive for sensitivity analysis when the number of variables becomes very large [166].

There have been recent advancements in convex optimization that allow the re-optimization of problems with the same "structure" but different "parameters" in fractions of the time taken to run the original optimization problems. This is done by defining convex optimization problems in a language called Disciplined Parametrized Programming (DPP) [24]. DPP is an extension to another language for describing convex optimization problems called Disciplined Convex Programming (DCP) [25, 26]. DCP and DPP have also been implemented as an open source convex optimization modelling package in the Python programming language called CVXPY [25]. DCP and DPP increase the time taken to perform a convex optimization problem the first time. They however reduce the time taken to perform the optimization again for different parameters by up to orders of magnitude.

DCP, DPP, and their implementation in CVXPY enable a new type of framework shown in 2.13(d). This combines the speed and workflow of traditional simulation frameworks with the accuracy and functionality of automated optimization of traditional optimization frameworks. In this new framework, the first time an optimization

is performed takes slightly longer than traditional optimization workflows, but still on the order of hours or days. However, optimizations for subsequent scenarios can be performed in orders of seconds or minutes. This allows for the assessment of multiple scenarios per hour just like traditional simulation frameworks, but with the accurate automated optimization of each scenario like traditional optimization frameworks. DPP thus has the potential bridge the gap between optimization and scenario assessment in energy system design. DPP has not been exploited in energy system design tools yet.

2.4.3 Unified Asset Model

Existing energy system design model-generators only consider a subset of energy system assets that can only perform a subset of energy system functions. Increasing the type of assets dramatically increases the computational complexity of the problem. Thus, model-generators that include different assets make simplistic assumptions such as linear assumptions in OSeMOSYS [8] and MARKAL/TIMES [9] or only use CLEWs [165] as constraints instead of optimize their operation. The second major bottleneck to improving energy system design is the need to study the tradeoff between the breadth and depth complexity of asset models. This requires a model-generator of assets that unifies the various types of energy systems assets. Heussen et al. [167] combine various types of asset models into one as "power nodes". This allows all assets to perform any combination of functions of the constituent assets. However, this is a "subtractive" rather than an "additive" model-generator. Assets are first modelled as the sum of all sub-models, and unnecessary sub-models are removed from the asset model. This means that adding more types of assets to a case study increases the model complexity of all assets in the case study. This also does not elucidate the underlying link between the different asset models and simply patches together asset models similar to how optimization tools patch together various optimization tools. Energy hubs [168] use a very similar concept to power nodes but for all types of energy flows. These suffer from the same limitations as power nodes. Furthermore, energy hubs use matrices to model energy hubs similar to how processes are modelled in industrial symbiosis such as the work done by Kerdlap [169].

Modelling assets this way limits the model-generator to linear models and increasing the number of assets leads to increasingly large sparse matrices. These sparse matrices are used for both parameters of the problem, and the optimization variables. This makes it both computationally difficult to simulate and optimize these systems. This problem is shared by the many combined energy system capacity and operation optimization models including OSeMOSYS, MARKAL, PyPSA, and their derivatives such GeoOSeMOSYS, OSeMOSYS-Global, PyPSA-Earth, OSeMOSYS-PuLP.

There is thus a gap in the literature for a unified asset model-generator that is "additive" and that unifies all the six different types of energy system assets. This asset model-generator needs to be able to elucidate the trade offs between modelling depth and breadth complexity. The accuracy and computational complexity of a model can be studied with DCP and DPP. Thus, a unified asset model-generator that also harnesses the power of DPP may be a potential bridge to understanding this trade off.

This thesis fills the gaps in the literature represented by the dotted lines in Figure 2.12. Chapter 3 builds a unified asset model-generator that can generate models of all types of energy system assets that can perform any function of an energy system. Chapter 4 utilizes this unified asset model-generator and DPP to build a system design model-generator that allows the optimization of energy system design with scenario assessment. The use of DPP also allows the study of trade offs between modelling depth and breadth complexity. Chapter 5 models real assets using these new model-generators. Chapter 7 finally implements these model-generators as an open-source tool and demonstrates this tool using a case study of Singapore.

Chapter 3

Generalized Spatial-Temporal Asset Model-Generator

This chapter answers sub-question 1 of the thesis:

"What are the minimum and sufficient theoretical basis functions of all assets in an energy system, and can these functions be used to create a unified model-generator of assets?"

This chapter utilizes generalized coordinates and develops a mathematical formalism of the movement of these generalized coordinates in time to build a generalized spatio-temporal asset model-generator. This unified model-generator can generate models that can describe any asset that can perform any combination of functions of the six types energy system assets: energy generation, consumption, transportation, storage, conversion, and demand response assets.

As Chapter 2 identifies, there is a need for a system design model-generator to study how the optimal sizing, operation and location of assets of an energy system is affected by scenario assumption, or parameters. It also highlights a unified asset model-generator as a path towards that goal. Some spatio-temporal model-generators exist in the literature such as the work by Moksnes et. al [170], but these models make it difficult to understand the tradeoff between computational complexity, and modelling accuracy, and other limitations Chapter 2 discusses. This motivates the core question of the thesis "Can we utilize a generalized spatio-temporal asset model-generator to optimize the sizing, operation and location of energy system assets?" To answer this question, this thesis develops a framework that utilizes a generalized

spatio-temporal asset model-generator as an intermediary model-generator to translate energy system design problems to mathematical optimization problems. Such a framework is referred to as a "model-generator" for energy system models. Before this model-generator can be developed, the generalized spatio-temporal asset model-generator used in this thesis needs to be developed. This chapter thus develops this intermediary asset model-generator required for the system design model-generator. This is done by using three concepts, modelling principles. The first is using generalized coordinates to model interactions. The second is mathematically formalizing the movement of energy in time. This allows the modelling of interactions as flows. The final concept is to define all functions of an energy system as flows of generalized coordinates in a space-time energy vector network. This allows the definition of an asset as an object that fulfils a set of functions of an energy system.

To be useful as an intermediary asset model-generator for the system design model-generator, this asset model-generator must generate models that meet the following requirements:

1. It needs to be able to model all the functions of an energy system.
2. It needs to be able to model any asset that can perform any combination of the functions of an energy system.
3. It needs to account for state dependent efficiencies.
4. It needs to model interactions between any number of assets, and thus be able to be used to build a energy system.
5. It needs to account for the cost of both sizing and operating assets.
6. It needs to be able to account for possible curtailment of energy vectors.
7. It will be used for energy system operation and sizing, it will not be used to develop the asset itself. Thus, the asset model need not be a white-box model, it need only be a black-box model.

To develop the asset model-generator, Section 3.1 first shows how interactions can be modelled using generalized coordinates. Section 3.2 then shows how these interactions can be modelled as discrete flows in a space time energy vector network. Section 3.3 maps flows to the basis functions of an energy system, and uses it to develop the generalized spatio-temporal asset model-generator. The chapter is finally summarised in Section 3.5.

3.1 Modelling Interactions Using Generalized Coordinates

The first step to developing the unified asset model-generator is to model interactions using generalized coordinates. Consider the interaction of an object with its surroundings. Figure 3.1 shows a schematic of how the interaction of an object with its surroundings can be modelled using generalized coordinates.

If the state of an object can be uniquely described by a set of values, or a vector, then these are called generalized coordinates, or the generalized coordinate vector. Generalized coordinates are sometimes referred to as generalized quantities; later parts of the chapter elucidate this connection. Generalized coordinates are conventionally represented by $\vec{q}$; this thesis follows this convention for clarity and consistency. The rate of change of these generalized coordinates with time are called the generalized velocities, $\dot{\vec{q}}$. Generalized coordinates fully describe the state of the object. They are also thermodynamic functions, or variables of the state of the object. I.e. they are path independent, or equivalently, they must not depend on the evolution of the object. For example, a particle's state can be described by its x, y, and z Cartesian coordinates. However, we may also describe the position of the particle in spherical coordinates using its radial distance from an origin point, its polar angle, and its azimuthal angle.

As another example, the state of a cup of water can be described by the volume of water in the cup, or the height of water in the cup. The volume of water in the cup at all previous times, and thus the rate at which the cup was filled does not need to be known to know the volume of water in the cup. This is because the volume of the cup can be measured at the time. Similarly, there are multiple ways in which the

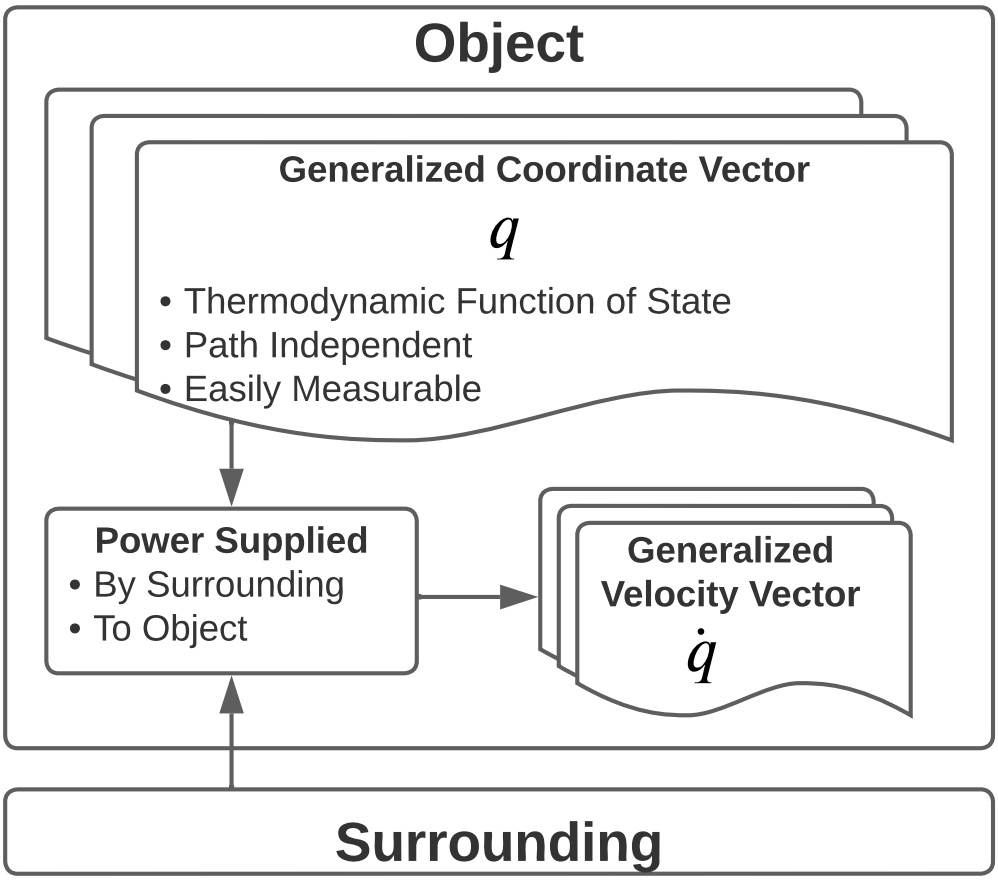

Figure 3.1: The state of an object at a specific time can be represented by a set of generalized coordinates, or equivalently a generalized quantity vector q. q must be a thermodynamic function of the state of the object; i.e. it must be path independent. While there are multiple possible sets of generalized coordinates, coordinates should be chosen that are easily measurable. When the surrounding interacts with the object, it supplies power to the object, P. This leads to a change in q. The rate of change of q is represented as the generalized velocity vector, $\dot{q}$. The $\dot{q}$ at a specific time, in general, depends on both P and q at that time. Examples of generalized coordinates (q) include temperature, pressure, density, internal energy, and entropy.

cup could have been filled which will give the same volume of water in the cup at a certain time. Thus, the volume of water in a cup is "path independent"; i.e. it can be defined independently of other historical values.

As such, there are multiple possible sets of generalized coordinates. However, to model energy assets for energy system sizing and operation, generalized coordinates should be chosen that are easily measurable. For example, it may be tempting to use the internal energy of a battery to describe the state of charge of a battery. However, it is not easy to measure the internal energy of a battery directly. In fact, it is not clear how to define the internal energy of a battery. Instead, consider the chemical composition of a battery. This is proportional to the amount of electrical charge that has flowed in the battery. The amount of electrical charge in a battery (Q) may thus be used as its generalized coordinate. The electrical charge in a battery is simply the integral of the current flowing into the battery (i.e. the charging current, I). The current is consequently the generalized velocity of a battery ($I = \dot{Q}$) . The rest of the chapter uses the example of a battery to illustrate various concepts. Do note however, that $\vec{q}$ refers to the generalized coordinate of any object; it does not specifically refer to the electrical charge in the battery. Q will be used when specifically referring to the electrical charge in the battery, to distinguish it from the symbol for generalized coordinates.

When an object interacts with the surrounding, the surrounding supplies a power, P, to the object. This leads to a rate of change of generalized coordinate, or generalized velocity, $\dot{\vec{q}}$. The generalized velocity at a specific time t, $\dot{\vec{q}}(t)$, also depends on the generalized coordinate at the time, $\vec{q}(t)$.

$$\dot{\vec{q}}(t) = \dot{\vec{q}}(P(t), \vec{q}(t)) \tag{3.1}$$

Where $P(t)$ is the power supplied to the object at time t.

In the example of the battery, P is the electrical power supplied to the battery, $\dot{\vec{q}}$ is the electrical current flowing into the battery (I), and $\vec{q}$ is the electrical charge in the battery (Q). In the example of the battery, the generalized coordinate and velocities are scalars, or vectors with dimension one.

3.1.1 Interaction with Surroundings

When P is negative, power is being supplied from the object to the surrounding. An interaction can thus be split by into two by splitting P into P_{in} and P_{out}. P_{in} is the power entering the object, P_{out} is the power leaving the object; these represent the "charging" and "discharging" interactions of an object, respectively. In the example of a battery, positive and negative P represent charging power (P_c) and discharging power (P_d), respectively. Figure 3.2 illustrates this.

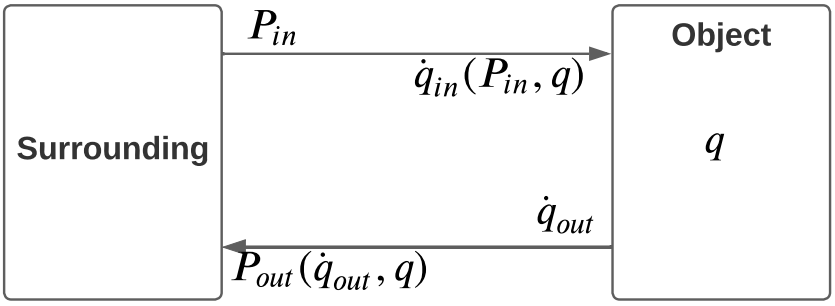

Figure 3.2: The interaction of an object with the surrounding can be split into two parts. When the surrounding does work on the object per unit time, power (P_{in}) flows into the object. P_{in} leads to an increase in the generalized coordinates of the object per unit time, $\dot{q_{in}}$. $\dot{q_{in}}$ is a function of both P_{in} and the generalized coordinate, q. When the object does work on the surrounding per unit time, generalized coordinate flow out the object per unit time, $\dot{q_{out}}$. $\dot{q_{out}}$ leads to power flowing out of the object and into the surrounding, P_{out}. P_{out} depends on both $\dot{q_{out}}$ and q.

$\vec{q}$ can similarly be split into $\vec{q}_{in}$ and $\vec{q}_{out}$, the generalized velocity when P is positive and negative, respectively. In the example of a battery, $\vec{q}_{in}$ and $\vec{q}_{out}$ are the charging current (I_c) and discharging current (I_d), respectively.

Equation 3.1 now transforms to:

$$\dot{\vec{q}}_{in} = \dot{\vec{q}}_{in}(P_{in}, \vec{q}) \tag{3.2}$$

and

$$\dot{\vec{q}}_{out} = \dot{\vec{q}}_{out}(P_{out}, \vec{q}) \tag{3.3}$$

However P_{out} may instead be rewritten as a function of $\vec{q}$ and $\dot{\vec{q}}_{out}$:

$$P_{out} = P_{out}(\dot{\vec{q}}_{out}, \vec{q}) \tag{3.4}$$

When P is positive, the energy flowing out of the surrounding can thus be viewed as being converted to generalized coordinates flowing into the object. Similarly, when P is negative, the generalized coordinates flowing out of the object can be viewed as being converted into energy flowing into the surrounding. The generalized coordinate of an object can thus also be viewed as a "quantity" that flows into and out of the object. When an object interacts with the surrounding, this quantity gets converted to energy, and vice versa.

Consider a simple case of an object that is described by a single generalized coordinate, or equivalently a scalar generalized coordinate, q. A battery is incidentally an example of such an object. Such an object also has a scalar generalized velocity, $\dot{q}$. For such an object, the possible states of the object can be visualized as a surface in P-q-$\dot{q}$ space; Figures 3.3(a) shows this surface. An evolution of the object as it interacts with its surrounding can be visualized as a line or path on the surface. If the object returns to its original state, this line will be a loop on the P-q-$\dot{q}$ surface. For the example of a battery, the loop represents a charge-discharge cycle.

This surface can be easily obtained by treating an object as a black-box, and systematically measuring various points on the surface. In the example of a battery, the method described by Ahsan et al. may be used [108]. The battery is first charged at a constant charging current until the maximum voltage constraints are reached, after which the battery is trickle charged at constant maximum voltage until it is fully charged. The battery is then discharged at constant discharging current until minimum voltage constraints are reached, after which the battery is trickle discharged at constant minimum voltage until it is fully discharged. This process is repeated for multiple charging and discharging currents. The electrical power, and electrical current flowing into or out of the battery is measured at all times during these charge-discharge cycles. The amount of electrical charge is also tracked by integrating the current with time. The electrical charge is set to zero at the end of every discharge to minimize numerical integration errors in the electrical charge. This process allows easy measurement of the P-q-$\dot{q}$ surface of any battery, regardless of its technology by treating it as a black-box.

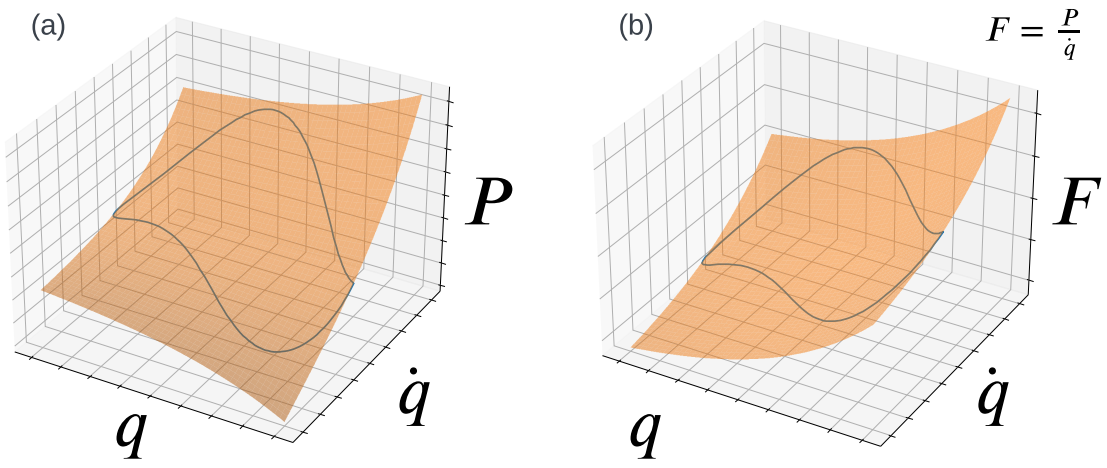

Figure 3.3: Evolution of the sate of an object during a "charge-discharge" cycle.
(a): Evolution of state in q-$\dot{q}$-P space. Consider an object (such as a battery) with a scalar generalized coordinate (q), and scalar generalized velocity ($\dot{q}$). Power supplied by the object to the surrounding is represented as negative values of P. The power supplied to the object by the surrounding, P, is a function of q and $\dot{q}$; this can be visualized as a surface in the P-q-$\dot{q}$ space. This surface represents all the possible states of the object. The evolution of the object can be represented as a path or line on this surface. If an object evolves and returns to its original state, its path on the surface forms a closed loop.
(b): Evolution of state in q-$\dot{q}$-F space. The generalized force (F) on the object is P divided by $\dot{q}$ and is given by Equation 3.5. The corresponding path or line on the surface is again the evolution of the object. For the example of a battery, the generalized force is the voltage across the battery (V), or the electromotive force of the battery (emf).

A similar process can be performed for any object, not just a battery. The electrical charge (Q) is replaced with the object's corresponding generalized coordinate (q). The electrical current (I) is similarly replaced with the object's corresponding generalized velocity ($\dot{q}$).

It is easier to measure the generalized velocity of a battery (the electrical current flowing into the battery, I) than its generalized coordinate (the electrical charge in the battery, Q). This is why it is better to first measure I at each time, and subsequently calculate Q by integrating I. However, this may not be the case for other objects. It may be easier to measure the generalized coordinate of some objects, than their generalized velocities. An example is a pumped hydro storage asset. The state of a pumped hydro storage asset can be defined by the height of water in the top reservoir, h. This can be trivially measured. Its generalized velocity can then be calculated by numerically differentiating h with respect to time.

Thus, to be able to easily model the interaction of an object with its surroundings, a set of generalized coordinates need to be picked such that at least q or $\dot{q}$ can be measured easily and directly. Due to higher numerical errors from integration, it is better to directly measure the generalized coordinate and calculate the generalized velocity, instead of vice versa. The errors will be minimized if both q and $\dot{q}$ can be measured directly; this would be the ideal set of generalized coordinates to use to model an object and its interaction with its surroundings.

3.1.2 Implicit vs Explicit Efficiency

The model in Figure 3.3(a) was first described for a battery by Ahsan et al. in [108]. However, they did not split power and current into charging and discharging powers and currents. They also did not describe how or why this is able to account for state of charge and current (or power) dependent efficiency of a battery. Before the P-q-$\dot{q}$ surface is used for the next step in generating the unified asset model-generator, it needs to be proved why the models in Figures 3.2 and 3.3(a) are implicitly able to account for efficiency of an object. In doing this, it shall be shown how the charging and discharging efficiency, and the internal energy of an object can be explicitly defined.

This will consequently give a consistent definition of the instantaneous charging and discharging efficiency of a battery as well as the internal energy of a battery.

The generalized force on an object by the surrounding, F, shall first be defined. The generalized force is the work done on an object by the surrounding per unit generalized coordinate.

$$F = \frac{dE}{dq} \tag{3.5}$$

Where E is the work done on the object by the surrounding.

The power supplied to the object is the work done on the object per unit time.

$$P = \frac{dE}{dt} \tag{3.6}$$

Combining equations 3.5 and 3.6 gives:

$$F = \frac{dE}{dt}\frac{dt}{dq} = \frac{P}{\dot{q}} \tag{3.7}$$

Thus, the generalized force is the ratio of the power supplied to the object to the generalized velocity.

For the example of the battery, the generalized force is ratio of the electrical power flowing into the battery, and the current flowing into the battery.

$$F = \frac{P}{I} = V \tag{3.8}$$

The generalized force on a battery is thus the voltage across the battery, V. This elucidates the alternate name for voltage: the electromotive force (emf).

P is a function of q and $\dot{q}$, thus we can rewrite F as:

$$F = F(q, \dot{q}) \tag{3.9}$$

This can be visualized as a surface in q-$\dot{q}$-F space, as shown in Figure 3.3(b). This surface again represents all the possible states the object can take. The evolution of the object is again a path on this surface. If the object returns to its original state, this path is a closed loop on the surface.

Projecting this loop onto the force-coordinate (F-q) plane, produces a hysteresis loop. This is shown in Figure 3.4. The area of this loop is the hysteresis energy loss due to inefficiencies. In the case of a battery, this represents the charge-discharge losses.

The area under the top half of the curve is the energy supplied by the surrounding to charge the battery. The area under the bottom half of the curve is the energy supplied to the surrounding while discharging the battery.

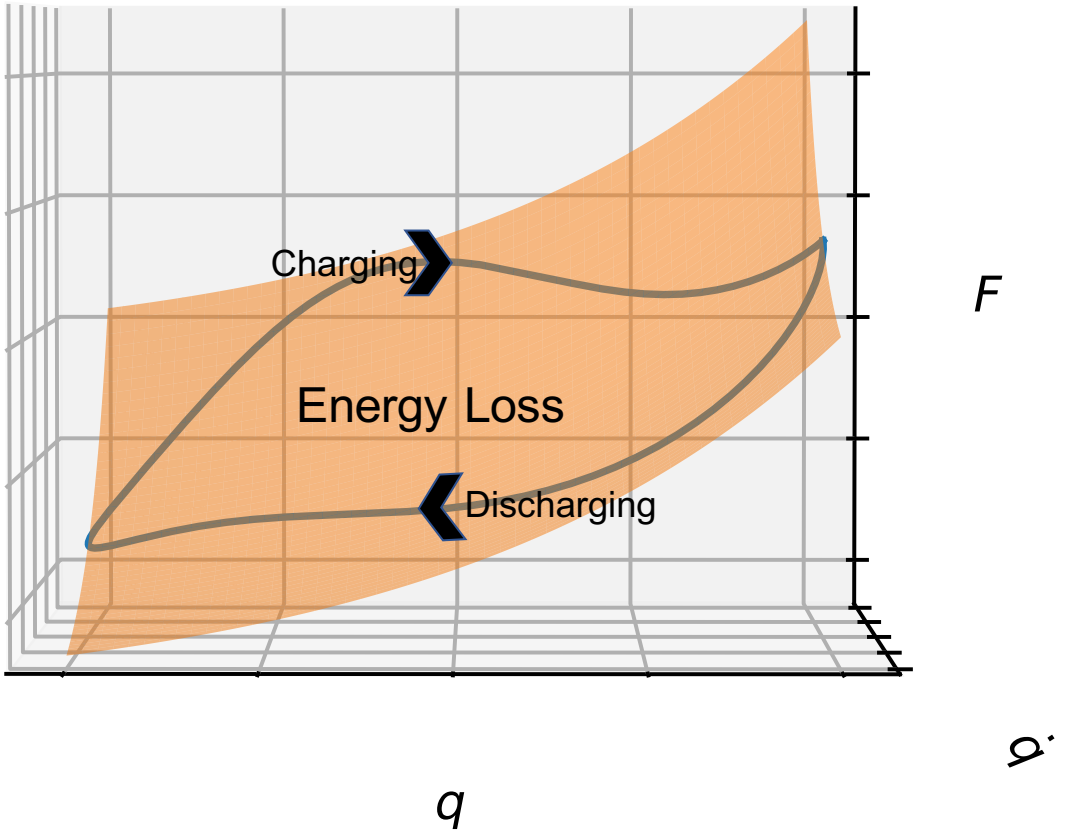

Figure 3.4: Hysteresis loop of the charge-discharge cycle of an object described by a scalar generalized coordinate (such as a battery). If the path of an object in q-$\dot{q}$-F space from Figure 3.3(b) is projected onto the generalized coordinate vs generalized force plane (q-F plane), a hysteresis loop is achieved. The area of this loop is the energy loss during the charge-discharge cycle.

This shows how the q-$\dot{q}$-P curve implicitly accounts for path dependent efficiencies and losses. However, the instantaneous efficiency of the interaction of the object with its surrounding has not been explicitly defined yet. To explicitly define the efficiency, consider the evolution of the object reversibly, i.e. at infinitesimally low speeds. This is equivalent to the path taken by the object at zero velocity, $\dot{q}$. If this path is added to the q-$\dot{q}$-F surface in Figure 3.3(b) and project onto the F-q plane, a line in the middle of the hysteresis loop is produced. Figure 3.5 shows the hysteresis loop with the adiabatic path line.

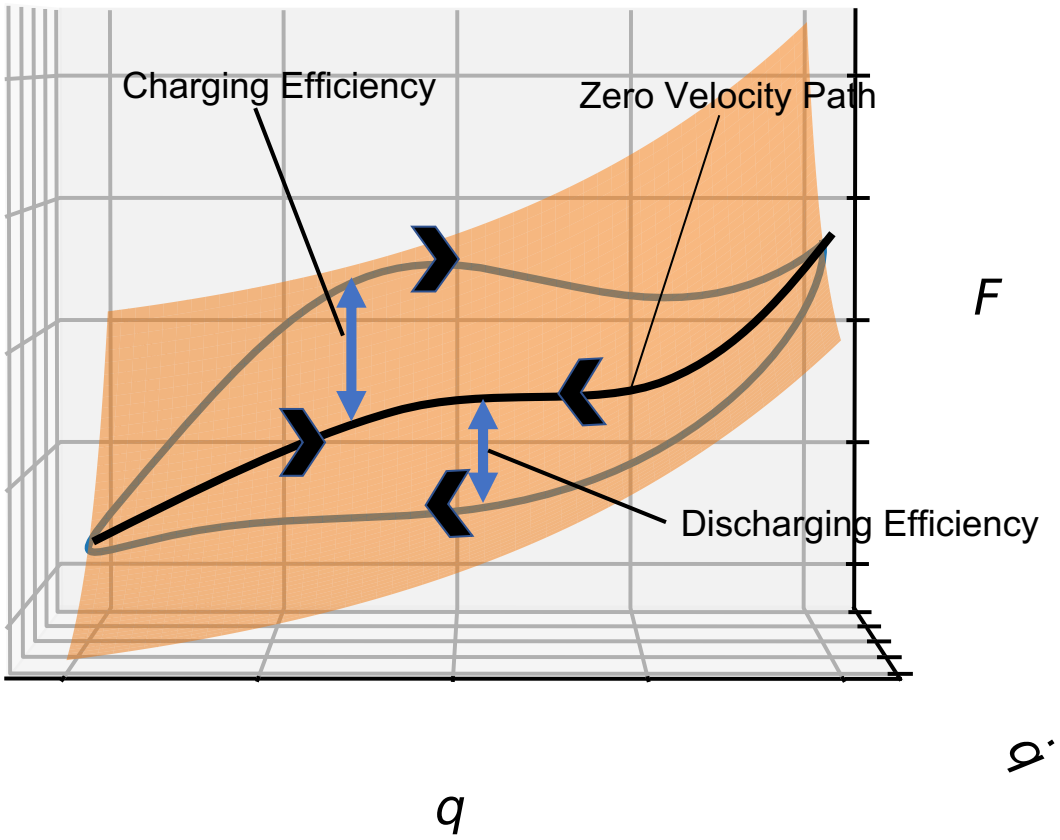

Figure 3.5: Charging and discharging efficiency of an object defined using ratio of generalized forces. The graph shows two charge-discharge cycles. The outer loop represents a charge-discharge cycle with finite charging and discharging currents; this is the same as in Figures 3.4, 3.3(a), and 3.3(b). The line between the loop represents a charge-discharge cycle at zero velocity ($\dot{q} = 0$). This is an adiabatic process and thus represents zero hysteresis energy loss. The instantaneous charging efficiency (η_c) at a specific charging power (P_c) and current ($\dot{q_c}$) is the ratio of the generalized force at zero current ($F(0, q)$) and the generalized force at charging current ($F(\dot{q_c}, q)$). $\eta_c = \frac{F(0,q)}{F(\dot{q_c},q)}$ The instantaneous discharging efficiency (η_d) at a specific discharging power (P_d) and current ($\dot{q_d}$) is the ratio of the generalized force at discharging current ($F(\dot{q_d}, q)$) and the generalized force at zero current ($F(0, q)$). $\eta_d = \frac{F(\dot{q_d},q)}{F(0,q)}$

Consider the "charging" process, when power is supplied from the surrounding to the object. The efficiency is the ratio of the minimum energy supplied per unit coordinate to the object to change its coordinate, to the actual energy supplied per unit coordinate. From equation 3.5, the charging efficiency η_c is:

$$\eta_c = \eta_c(q, \dot{q}) = \frac{F(q, 0)}{F(q, \dot{q}_{in})} \tag{3.10}$$

Similarly consider the "discharging" process, when power is supplied from the object to the surrounding. The efficiency is the ratio of the actual energy supplied per unit coordinate of the object to the maximum energy supplied per unit coordinate of the object to change its coordinate. Again, from equation 3.5, the discharging efficiency η_d is:

$$\eta_d = \eta_d(q, \dot{q}) = \frac{F(q, \dot{q}_{out})}{F(q, 0)} \tag{3.11}$$

Thus, the efficiency of an interaction can be represented as a function of the generalized coordinate and generalized velocity. This is visualized as a surface in Figure 3.6(a).

The internal energy of an object shall now be defined. The internal energy of an object may be defined as the work done on the object adiabatically, i.e. with no heat loss. This is equivalent to the area under the generalized force curve at zero velocity, as in Figure 3.5. The internal energy, E, is thus given by:

$$E(q) = \int_{Q=q_0}^{q} F(Q, 0) dQ \tag{3.12}$$

Where q_0 is the "base" or "default" value of the coordinate of the object. q_0 is arbitrary and can be any value. If the minimum value of q is used as q_0, it will ensure that the value of q will not be negative. Thus, the minimum value of q is a good value to use as q_0. With this definition, the internal energy (E) of an object can be represented as a function of its generalized coordinate (q) as in Figure 3.6(b)

To check if this definition of internal energy is consistent with the definition of efficiency in Equations 3.10 and 3.11, consider the charging and discharging processes. The charging efficiency is the ratio of the change in internal energy of the object to

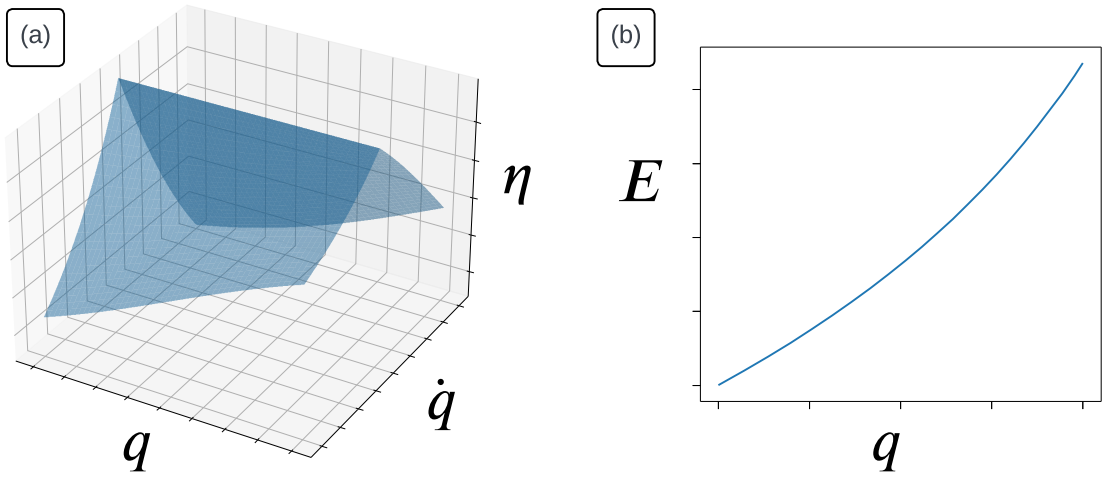

Figure 3.6: (a): Figure of instantaneous charging and discharging efficiency of a battery as a function if q and $\dot{q}$. Using the process described in Figure 3.5 the charging (η_c) and discharging (η_d) efficiency of a battery can be defined as a function of q and $\dot{q}$. The charging and discharging efficiency are used for positive and negative values of $\dot{q}$, respectively. In this example, efficiency is 100% at zero $\dot{q}$. Efficiency goes down as $\dot{q}$ moves away from zero.
(b): Figure of the internal energy of a battery as a function of q and $\dot{q}$. The work done on a battery adiabatically, i.e. zero $\dot{q}$ and no energy loss, can represent the internal energy of a battery E. This is the area under the q-F curve at $\dot{q} = 0$, from $q = 0$ to $q = Q$. I.e. $E(Q) = \int_{q=0}^{Q} F(\dot{q} = 0, q)\, dq$

the energy supplied to the object; this is to change the coordinate of the object from q_1 to q_2.

$$\eta_c = \frac{E(q_2) - E(q_1)}{\int_{q=q_1}^{q_2} F(q, \dot{q}) dq} \tag{3.13}$$

The instantaneous efficiency is the efficiency as the length of the process tends to zero, i.e. $q_2 - q_1 \to 0$. This is equivalent to differentiating the numerator and denominator by q; this gives us the original definition of instantaneous charging efficiency in equation 3.10.

Similarly, the discharging efficiency is the ratio of the energy supplied by the object to the internal energy of the object; this is to change the coordinate of the object from q_2 to q_1.

$$\eta_d = \frac{\int_{q=q_2}^{q_1} F(q, \dot{q}) dq}{E(q_1) - E(q_2)} \tag{3.14}$$

Taking the limits of $q_2 - q_1 \to 0$ again gives the original definition of instantaneous discharging efficiency in equation 3.11.

This shows that the definition of internal energy (in Equation 3.12) and instantaneous efficiencies (in Equations 3.10 and 3.11) are consistent. It also shows that modelling interactions using P as a function of q and $\dot{q}$ as in Figure 3.2 implicitly accounts for q and $\dot{q}$ dependent efficiencies.

The internal energy E as defined by equation 3.12 is a thermodynamic function of the state of the object. Thus, E may be used as the generalized coordinate of an object, including a battery. However, as can be noted, E is not easy to measure for a battery. Thus, it is not always a good choice for use as a generalized coordinate to track the state of a battery. Furthermore, this is only possible for objects with scalar generalized coordinates. If the state of an object needs to be defined by a vector of dimension more than one, its state necessarily cannot be defined just using a scalar internal energy.

The shows that the P-q-$\dot{q}$ curve implicitly contains the q and $\dot{q}$ dependent efficiencies of interactions of an object with its surroundings. Thus the q and $\dot{q}$ dependent efficiencies of an object can be equivalently modelled by simply measuring or modelling the object's P-q-$\dot{q}$ curve. This can be done without explicitly considering the "efficiency" of an interaction.

3.1.3 Interaction with Other Objects

Figure 3.7 shows how the interaction of an object with its surrounding can be modelled as power being converted to generalized velocity, and vice versa. The next step is to model the interaction between two objects defined by their respective generalized coordinates, $\mathbf{q_1}$ and $\mathbf{q_2}$.

To do this, consider the interaction of the two objects with a "virtual surrounding". This is shown in the top diagram in Figure 3.7. Where q, $\dot{q}$ and P have an additional subscript to indicate the object, e.g. q_1 and $\dot{q}_{in_1}$ refer to the generalized coordinate and charging velocity of object 1, respectively.

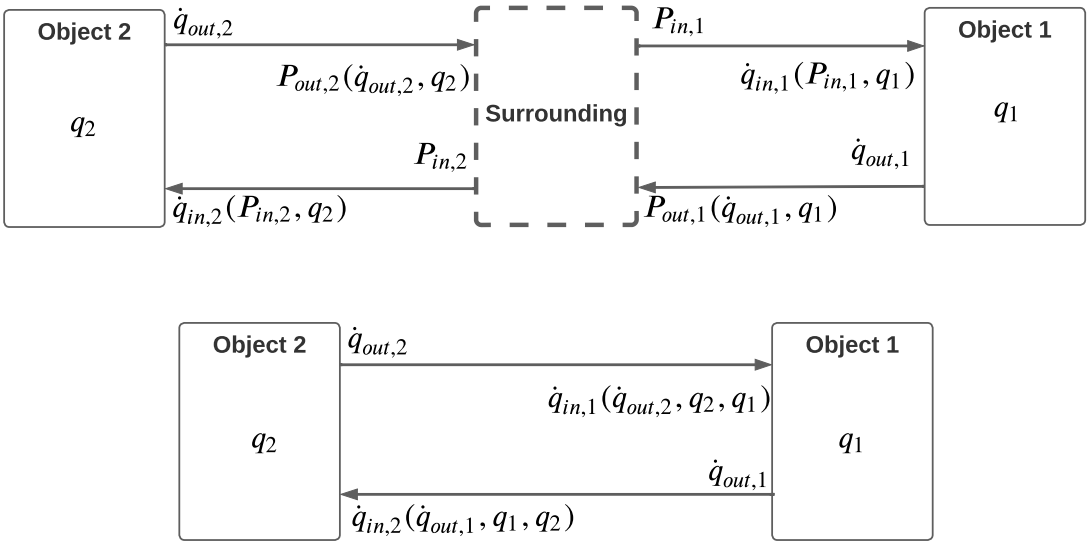

Figure 3.7: Interaction of an object with another object. The interaction of object 1 with object 2 can be split into two interactions (top). The first is the interaction of object 1 with a "virtual" surrounding; the second is the interaction of object 2 with the same virtual surrounding. Combining the two interactions and eliminating the virtual surrounding, we can view object 1 as directly interacting with object 2 (bottom). When generalized coordinates flow out of object 1 ($\dot{q}_{out,1}$), they are converted into generalized coordinates flowing into coordinate 2 ($\dot{q}_{in,2}$). $\dot{q}_{in,2}$ is, in general, a function of the flow out of object 1 ($\dot{q}_{out,1}$) and the coordinates of objects 1 and 2 (q_1 and q_2). Similarly, when coordinates flow out of object 2 and into object 1, $\dot{q}_{in,1} = \dot{q}_{in,1}(\dot{q}_{out,2}, q_2, q_1)$.

Consider the interaction in which object 2 "charges" object 1, i.e. coordinates flow out of object 2 and flow into object 1. This can be viewed as the sum of two interactions: object 2 discharging to the surrounding and object 1 charging from the

surrounding. If the power supplied to the surrounding by object 2 is equal to the power supplied to object 1:

$$P_{out,2}(\dot{q}_{out,2}, q_2) = P_{in,1} \tag{3.15}$$

Combining with the definition of $\dot{q}_{in,1}$ from equation 3.2 gives:

$$\dot{q}_{in,1} = \dot{q}_{in,1}(P_{in,1}, q_1) = \dot{q}_{in,1}(\dot{q}_{out,2}, q_2, q_1) \tag{3.16}$$

These two interactions can be combined to eliminate the "virtual surrounding" to represent the direct charging of object 1 by object 2 as in the bottom diagram in Figure 3.7.

Similarly, consider the charging of object 2 by object 1. From symmetry:

$$\dot{q}_{in,2} = \dot{q}_{in,2}(\dot{q}_{out,1}, q_1, q_2) \tag{3.17}$$

An interaction between two objects can thus be viewed as a combination of three steps. This is the flow of generalized coordinates out of first object, conversion into generalized coordinates of the type of the second object, and flow of generalized coordinates into the second object. Generalized coordinates can thus be viewed as quantities that flow from one object to another object. The next step is to formalize the interaction between objects described using generalized coordinates, as discrete flows in a network.

3.2 Modelling Interactions as Flows

To formally translate interactions from differential equations in generalized coordinates to discrete flows in a space time energy-vector network, three steps are needed. The first step is to convert continuous, differential equations of generalized coordinates into discrete flows of generalized quantities. The second step is to formalize the flow of generalized quantities in time. The final step is to account for conservation and curtailment of quantities in the network as equalities and ineqalities, respectively.

The simplest object of a graph, or network, is a "node". A pair of nodes form an "edge". If the pair of nodes is ordered, the edge is referred to as a "directed edge" or an "arrow". The first node is referred to as the "source node". The arrow points out

of the source node. The second node is referred to as the "target node". The arrow points into the target node. In the rest of the thesis, an "edge" refers to a directed edge or arrow. The rest of the thesis refers to a pair of unordered nodes explicitly as an "undirected edge".

Various information can be encoded in nodes and edges. This is referred to as adding additional structure for nodes and edges. Formalizing interactions as flows involves defining additional structure for these nodes and edges. As later parts of this section show, edges will be associated with the flow of generalized quantities; these will be represented by a vector. Nodes will be associated with the conservation or curtailment of these generalized quantities; these will be represented by an equality or inequality, respectively.

3.2.1 From Continuous to Discrete Flows

The first step to modelling interactions as flows is to convert the continuous model in Figure 3.7 to a discrete model. For simplicity consider the simple case of an evolution of an object from time t, over the timestep δt; this is shown in Figure 3.8.

An object at time t, may be represented as a node. The state of the object at time t, is given by the generalized coordinate of the object at time t, $q(t)$. In the continuous case, $q(t)$ is stored in the node of the object at time t. The second thing stored at the node is an equality that determines how the coordinate at time t depends on the coordinate at the previous time step, $q(t - \delta t)$.

$$q(t) = q(t - \delta t) + \int_{\tau=t-\delta t}^{t} \dot{q} d\tau \tag{3.18}$$

This is because there is a flow of coordinate into the node over that time. This is stored in the edge pointing into the node with the generalized velocity ($\dot{q}(t)$).

To discretize the coordinate at the node, the generalized coordinate as a function of time ($q(t)$) is replaced with the generalized coordinate indexed with the timestep (q_t).

To discretize the coordinate at the edge, the change in coordinate over the timestep due to the velocity, Δq_t, is calculated. Δq_t is again indexed with time and is given

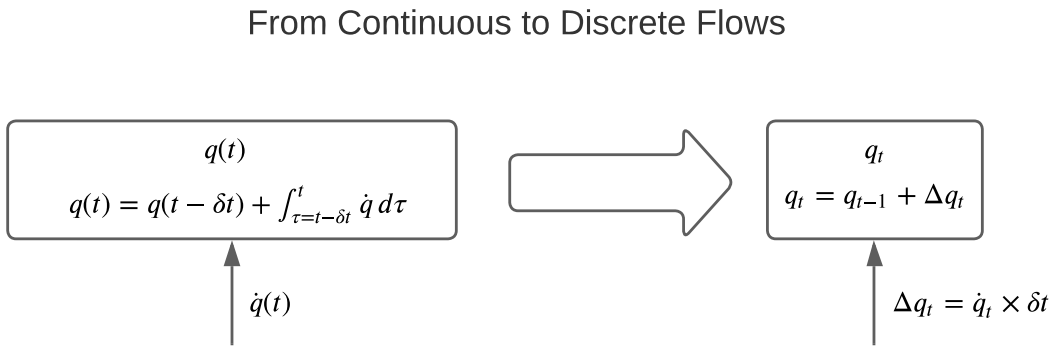

Figure 3.8: Diagram showing the representation of continuous interactions and discrete interactions. The left side shows the representation of the evolution of a generalized coordinate as a function of continuous time ($q(t)$). The rectangle represents the node at time t. The node is associated with two objects: a coordinate $q(t)$; and an equality that describes how $q(t)$ has evolved from the value at the previous timestep ($q(t - \delta t)$). The generalized velocity ($\dot{q}(t)$) can be viewed as a flow into the node, and is associated with the edge. The left side shows the representation of the same evolution of a generalized coordinate as a function of discrete, indexed, time (q_t). The node is again associated with a coordinate q_t, and an equality describes how q_t has evolved from the value at the previous timestep (q_{t-1}). The edge is now associated with the total change in coordinate over the timestep (Δq_t). The coordinate at the node and flowing in from the edge now have the same units and can be simply added.

by:

$$\Delta q_t = \int_{\tau=t-\delta t}^{t} \dot{q} d\tau = \dot{q}_t t \tag{3.19}$$

Where $\dot{q}_t$ is the average generalized velocity over the timestep. To dicretize the equation at the node, equation 3.18 at the node is replaced with:

$$q_t = q_{t-1} + \Delta q_t \tag{3.20}$$

Where q_{t-1} is the generalized coordinate at the previous timestep $(t-1)$, i.e. at the time $t-\delta t$. Note that the units of the flow in the edge (flowing into the node), and the terms in the node are the same. This was not the case for the continuous case as the edge merely represented the differential rate of change of the generalized coordinate, not an actual conserved flow. The rest of the chapter uses the term generalized quantities instead of coordinates as it invokes the intuitive notion of conservation and curtailment.

3.2.2 Formalizing Flow of Energy in Time

The second step to modelling interactions as flows is to formalize the flow of energy in time; this will convert snapshots in time to flows in time. Note that the discretized flow diagram in Figure 3.8 has an asymmetry. Edges have a value, but nodes have both values and equalities. As shall be seen, making this diagram symmetric will in fact formalize the flow of quantities in time.

Consider the simple discretized model from Figure 3.8 for timesteps $t-1$, t, and $t+1$. For simplicity, first consider zero generalized velocity; this is shown in Figure 3.9. The top nodes represent the "snapshots" in time of the nodes at various timesteps. Each node has both a generalized quantity (q) and an equality. Consider moving the generalized quantity from the node at timestep t to an edge flowing out of that node and into the node at the next timestep, $t+1$. This gives the bottom diagram in Figure 3.9

Nodes now only contain equalities, and edges now only contain quantities. The generalized quantity at a specific timestep can thus be viewed as a quantity that is flowing from one timestep to the next timestep.

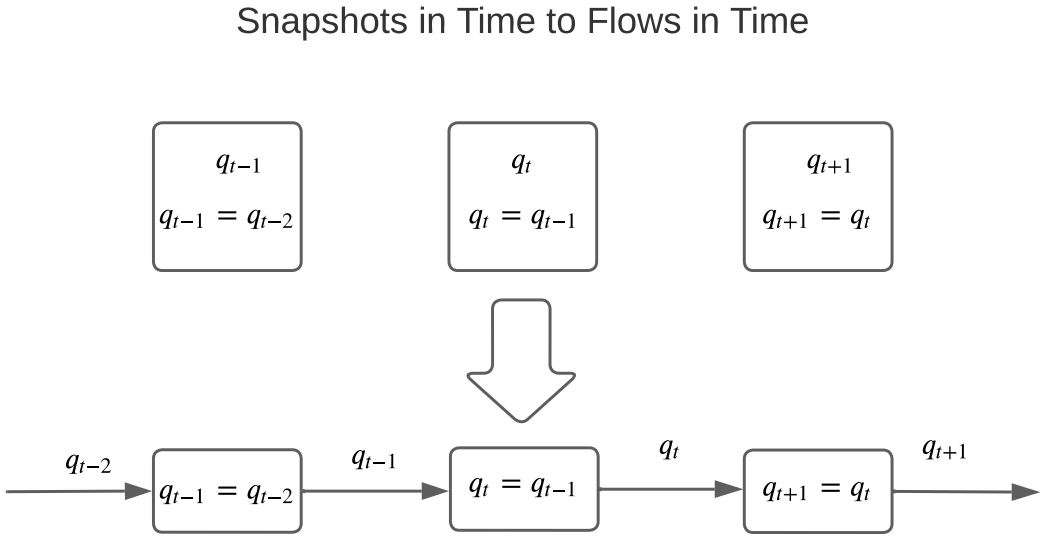

Figure 3.9: Diagram showing the equivalence of snapshots in time and flows of generalized quantities in time. The top shows snapshots in time of an asset that stores a generalized quantity (q). The nodes at each timestep contain the quantity stored at that time (q_t), and an equation relating q_t to the quantity in the asset at the previous time (q_{t-1}). The bottom shows the same asset represented using flows of quantities in time instead of snapshots. The quantity stored in the asset at timestep t is now viewed as the quantity flowing from the node at timestep t to the node at the next timestep $t + 1$. Each edge is now only associated with a coordinate, and each node is now only associated with an equality. Thus, storing a quantity can be viewed as moving that quantity in time. An asset that stores a quantity can equivalently be viewed as an asset that moves that quantity forwards in time.

From Figure 3.9, the equation at each node now represents the conservation of quantities flowing into or out of the node. It says that the sum of quantities going out of the node are equal to the sum of quantities going into the node. To understand this better, consider how to interpret this for a real-life example. In the example of a battery, the node is the state of the battery at time t. The equation thus means that the amount of electrical charges flowing from time t to time t+1 is the same as the amount of electrical charges flowing from time t+1 to time t+2. In terms of the traditional view of snapshots in time, this means that the amount of electrical charges in the battery at time t is equal to the amount of electrical charges in the battery at time t+1. This is expected because no losses are assumed during the charging or discharging of the battery.

To check if this continues to hold true when there are more edges attached to the nodes, consider the same asset in Figure 3.9 but with discrete charging and discharging interactions with the surrounding. This is shown in Figure 3.10. The top diagram models the interactions as snaphots in time. The bottom diagram models these interactions as flows of quantities in time. The top diagram is asymmetric, there are flows in both edges and nodes. However, in the bottom diagram, the symmetry is restored and all flows are in edges, and all equalities are in nodes.

Note that there are now two flows at each edge. The first is the flow out of the source node, which is a variable. The second is the flow into the target node, this is given by a "conversion function" of the flows out of each node as in Figure 3.7. This means that one quantity at the node in the "snapshot" model gets translated to a quantity leaving the node ($q_{t,out}$), and a quantity entering the next node ($q_{t+1,in}$). $q_{t+1,in}$ is given by the conversion function (ψ), where:

$$q_{t+1,in} = \psi(q_{t,out}) \tag{3.21}$$

To understand what this may represent, consider the example of a battery. The conversion function of a battery represents the self discharge of the battery. This is because there may be some storage losses and the quantity stored at the next timestep may not be equal the quantity stored at the previous timestep.

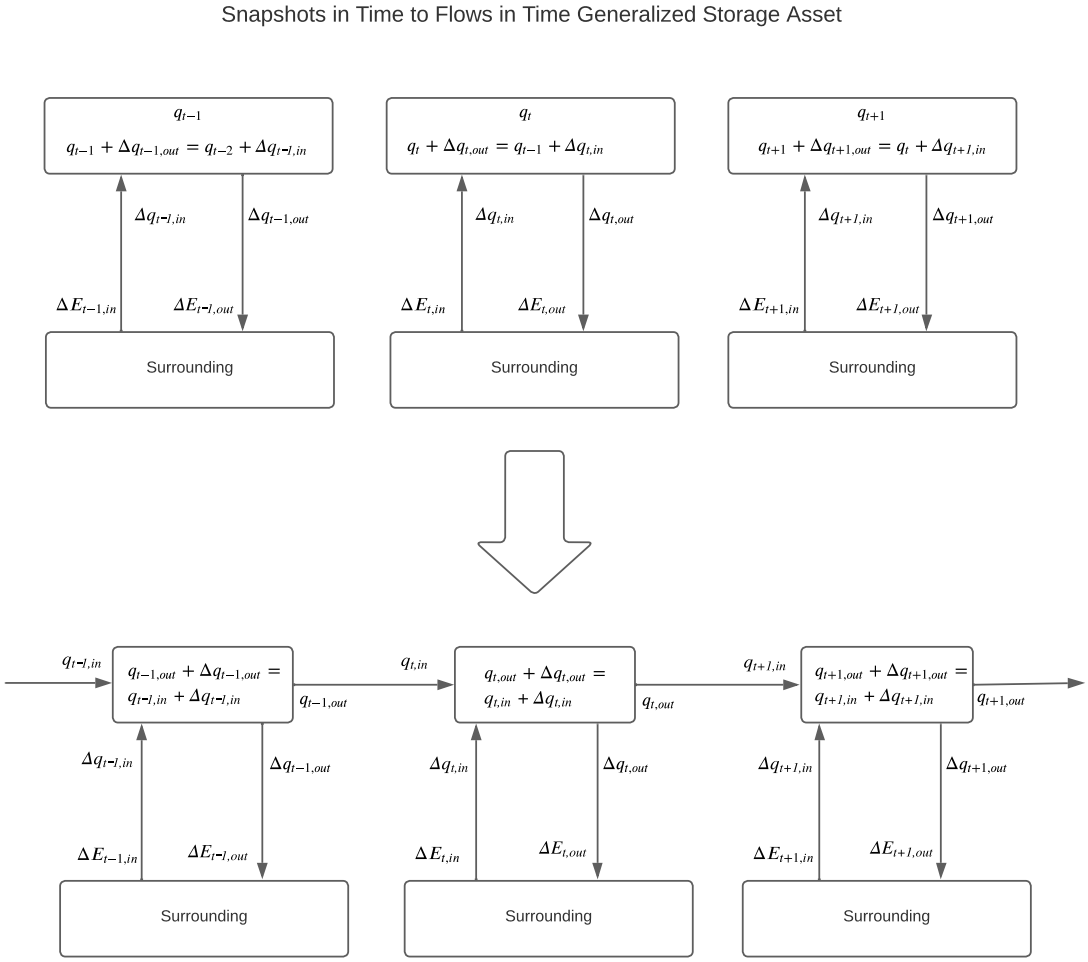

Figure 3.10: Interactions of a generalized storage asset with the surrounding as snapshots in time and as flows in time. Independent variables are represented by non-italic letters; functions are represented by italic letters. The top shows the storage asset in Figure 3.9 as timesteps, but with additional interactions with the surrounding. Flows from the "surrounding" nodes to the storage asset nodes represent "charging" of the storage asset. Flows from the storage asset nodes to the "surrounding" nodes represent "discharging" of the storage asset. Note that each edge contains two quantities: the flow out of the source node (an independent variable), and the converted flow into the target node (given by a "conversion function"). However, nodes have an equality and a quantity (independent variable). The bottom diagram shows the same storage asset but with flows in time instead of snapshots. Here, the symmetry being restored: all flows of generalized quantities, independent values, and conversion functions are associated with edges; all equalities are associated with nodes. Each edge is only associated with a flow out of a node (independent value) and a flow into a node (given by a conversion function). Each node is only associated with an equality constraint.

Finally, the equality at the node at timestep t does indeed represent the sum of flows out of node are equal to the sum of flows into the node:

$$q_{t,out} + \Delta q_{t,out} = q_{t,in} + \Delta q_{t,in} \tag{3.22}$$

This formalizes the concept of "movement of generalized quantities in time".

3.2.3 Conservation and Curtailment

The final step to modelling interactions as flows is to consider the curtailment of flows. The previous sections show how the equalities at each node represent the conservation of generalized quantities leaving the node. To understand how to model curtailment, consider the simple case of just storage without any interactions with the surrounding as in Figure 3.8. Now, consider a possible curtailment flow out of each node at timestep t ($q_{t,curtail}$); this is shown in top diagram of Figure 3.11.

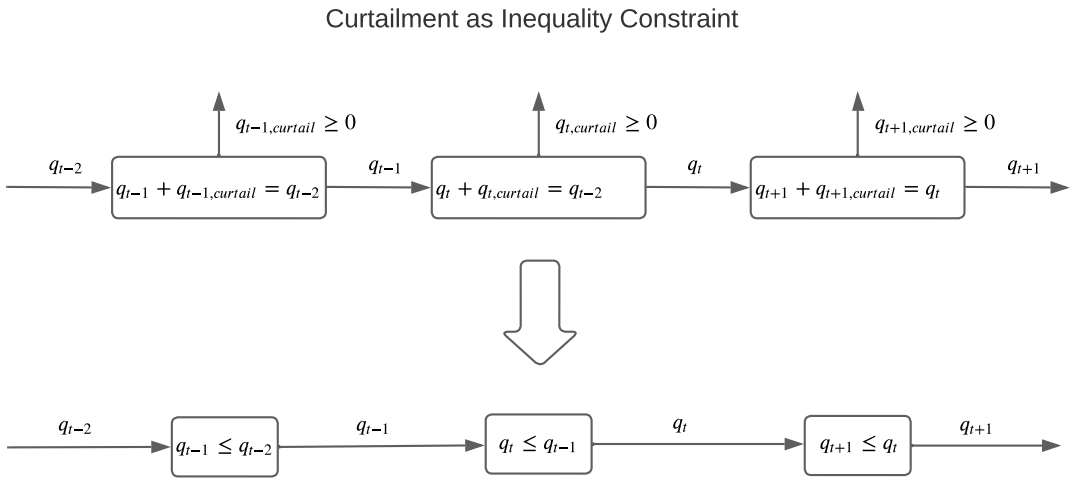

Figure 3.11: Diagram to show how curtailment is represented by an inequality constraint. The top figure shows the simple storage asset from Figure 3.9, but with an additional potential flow out of each node that represents the possible positive curtailment at each time. Combining the equality in the node and the inequality in the curtailment edge gives the bottom diagram. This may be intuitively viewed as the following. As some quantity may be curtailed at each time, the remaining quantity flowing out of a node may be less than the quantity flowing into the node. Note that the symmetry has been recovered again: edges only have flows, and no constraints. However, the equality constraint in Figure 3.9 has been replaced with an inequality constraint. Thus, adding a curtailment of a quantity at a node is equivalent to replacing the equality constraint of that quantity with an inequality constraint.

This curtailment needs to be more than zero. Thus, there is an inequality at each curtailment edge:

$$q_{t,curtail} \geq 0 \tag{3.23}$$

This again breaks the symmetry as there is an inequality at an edge. Instead, consider combining the inequality at the edge with the equality at the node. This eliminates $q_{t,curtail}$, and gives us the inequality:

$$q_t \leq q_{t-1} \tag{3.24}$$

If the curtailment edge is removed and the equality at the node is replaced with Inequality 3.24 the bottom diagram in Figure 3.11 is obtained. This can be interpreted as the sum of flows leaving the node must be less than the sum of flows entering the node. Thus, potential curtailment at a node can be represented by replacing the equality at a node with an inequality. There may be various types of generalized quantities flowing into and out of a node, i.e. $\mathbf{q}$ may be a vector. In such a situation, the equality constraint is replaced with an inequality constraint only for the generalized quantities that can be curtailed.

Finally note that in the bottom figure, the curtailment flow is no longer tracked. This is because curtailment usually does not directly lead to any costs. If this curtailment flow results in costs, then it should enter another node. However, calculating the curtailment flow may be useful for studying the operation of an energy system. The curtailment flow can be easily recovered as the net flow into the node at time t:

$$q_{t,curtail} = q_{t-1} - q_t \tag{3.25}$$

With this, any interaction of objects with other objects may now be represented as flows of generalized quantities in a network. Each node represents either a conservation or a curtailment of generalized quantities as an equality or an inequality, respectively. Each edge represents the flow out of a source node, and a flow into the target node (given by a conversion function). The final step to building the unified asset model-generator is to defined flows as functions of an energy systems and define assets as objects that perform a set of energy system functions.

3.3 From Flows to Assets

The unified asset model-generator models interactions as flows of generalized quantities in a discrete network to unify the six energy system assets: energy generation, consumption, transportation, storage, conversion, and demand response assets. Figure 3.12 shows the structure of the generalized spatio-temporal asset model-generator. In this model-generator, an asset consists of a set of one or more components and a cost function. The basic building block of the asset model-generator is the node. The node contains information about curtailment and conservation of flows as an inequality and equality function, respectively. Two nodes can be linked together using an edge. An edge contains the flow of generalized quantities out of one node (the source node) and into a second node (the target node). A set of edges of the same type over multiple operational times form a component. A component defines one type of interaction over multiple timesteps; an interaction can also be viewed as a function of an energy system. A set of components make up an asset. An asset contains the capital and operational costs of its constituent components.

This structure of the generalized spatio-temporal asset model-generator is designed to take into account the following:

1. It is a hierarchical structure that models all energy systems assets that can perform any combination of energy system functions.

2. It is a highly compressed form of storing and representing the information needed to build an asset. The set of edges and nodes for a component can be systematically reconstructed using just the template edge and the operational times of a component.

3. The information in each part of the structure maps to the most primitive object possible if the asset is implemented in a code using object oriented programming.

4. The use of a template edge insures that all "instructions" are the same for "data" for all operational times. This ensures that the calculations associated with the simulation and optimization steps of a component map to the single

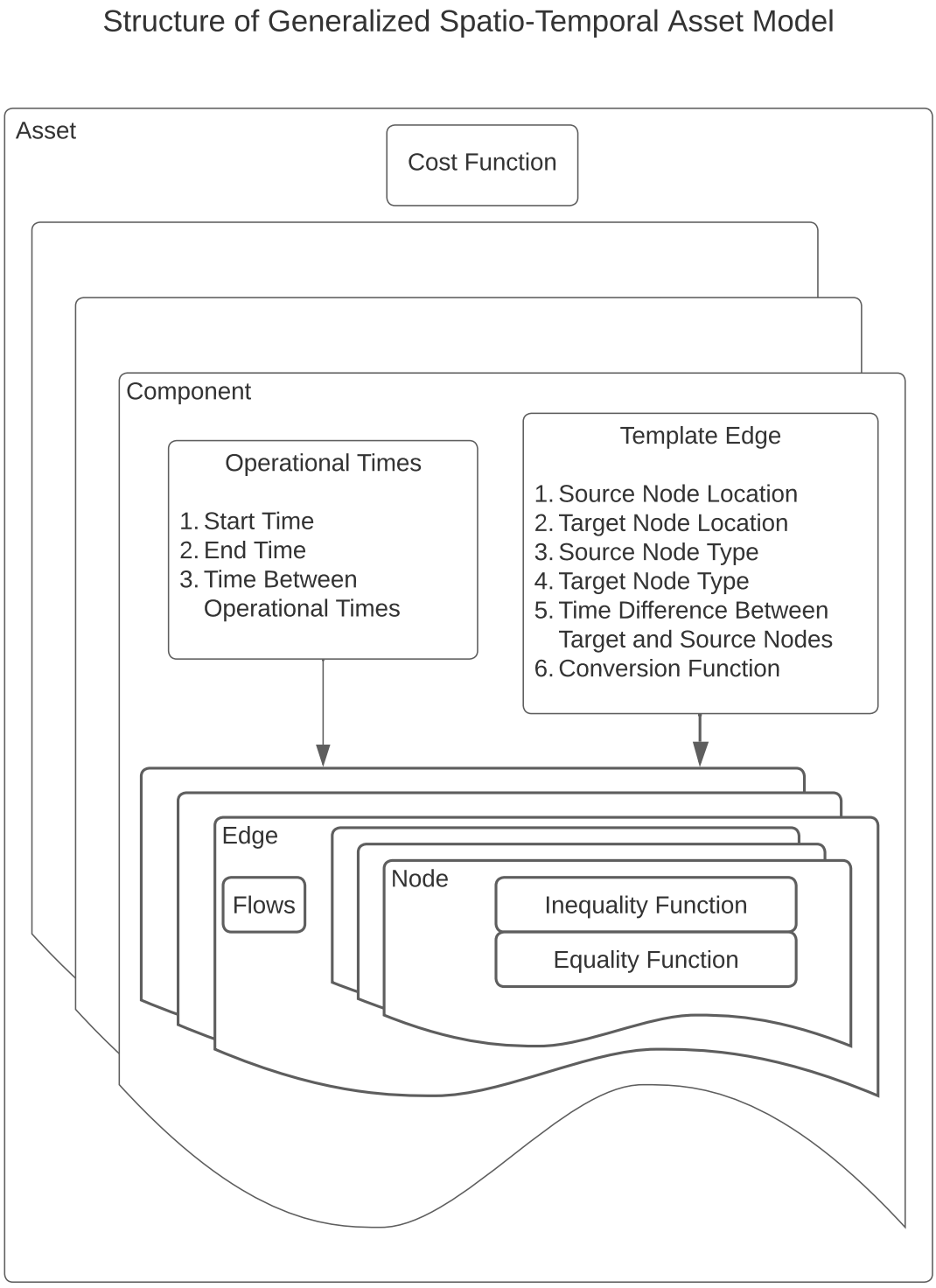
Structure of Generalized Spatio-Temporal Asset Model
Asset
Cost Function
Component
Operational Times
1. Start Time
2. End Time
3. Time Between
Operational Times
Template Edge
1. Source Node Location
2. Target Node Location
3. Source Node Type
4. Target Node Type
5. Time Difference Between
Target and Source Nodes
6. Conversion Function
Edge
Flows
Node
Inequality Function
Equality Function

Figure 3.12:

instruction multiple data (SIMD) architecture of modern graphics processing units (GPUs). This ensures that the problem it represents is highly parallel.

This section details individual parts of the generalized spatio-temporal asset model-generator, starting from the most basic building block, and moving up to the asset.

3.3.1 Nodes

Figure 3.13 shows a schematic of a node in the asset model-generator. The identity of a node is defined by the following three values:

1. Location: this is the physical location of the asset(s) that this node is a part of.
2. Time: this is the temporal location of the node. It is the timestep of objects that this node is a part of.
3. Type: this represents the set of generalized quantities that flow through the node and whether they are conserved or curtailed at the node.

A node contains the following two pieces of information:

1. inequality function ($\vec{g}$): This is the net flow out of generalized quantities that are curtailed at the node. It represents the inequality constraint ($\vec{g} \leq \vec{0}$)
2. equality function ($\vec{h}$): This is the net flow out of generalized quantities that are conserved at the node. It represents the equality constraint ($\vec{h} = \vec{0}$)

Multiple edges may be connected to a node. These represent flows out of the node ($\vec{x}$), and flows into the node ($\vec{y}$). The flow into the node is given by a conversion function ($\vec{\psi}$). These flows are vectors of various generalized coordinates. We may split these generalized quantities into two types. The first type of quantities are curtailed at the node; these are sub-scripted with g. The net flow of these quantities out of the node is curtailed; this is defined using the inequality function g:

$$\vec{g} = \sum_i \vec{x}_{i,g} - \sum_j \vec{y}_{j,g} \leq \vec{0} \tag{3.26}$$

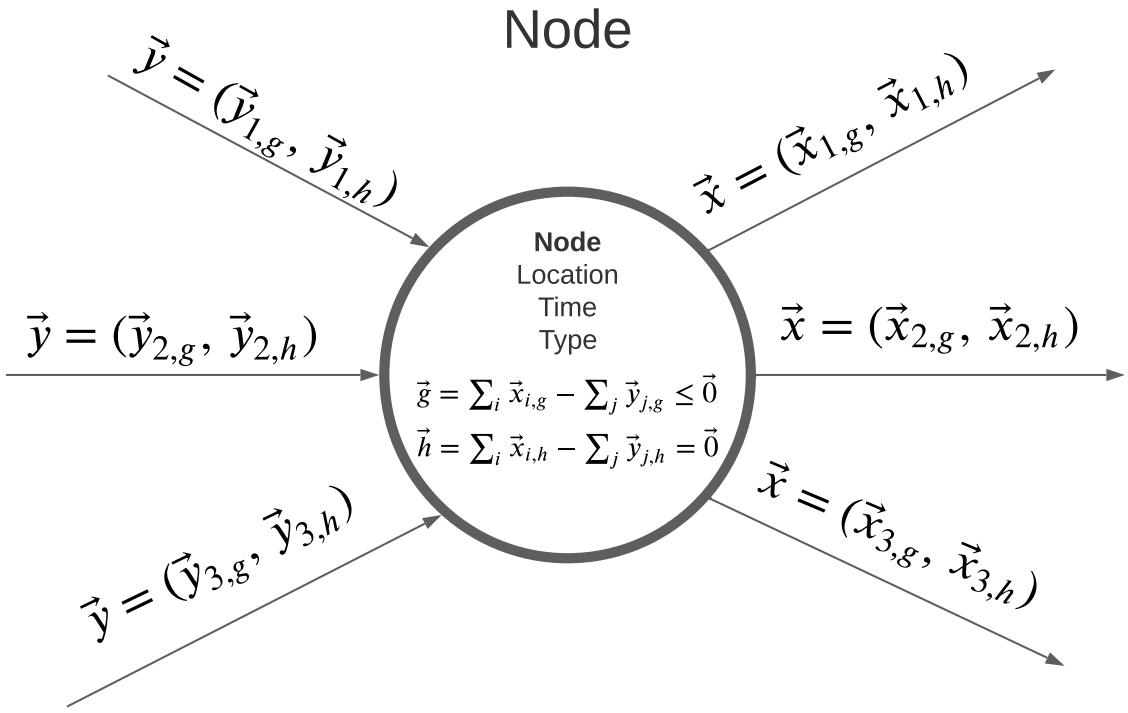

Figure 3.13: Diagram of a node in the asset model-generator. The identity of a node is defined by three values: its location, its time, and its type. A node contains two pieces of information: an inequality constraint function ($\vec{g}$), and an equality constraint function ($\vec{h}$). Multiple edges may be connected to a node. These represent flows out of the node ($\vec{x}$) and flows into the node ($\vec{y}$). These flows are vectors of various quantities. We may split these quantities into two types. The first type of quantities are curtailed at the node; these are sub-scripted with g. $\vec{g}$ is the net flows of curtailed quantities out of the node. This curtailment of quantities is represented in the node as the inequality constraint ($\vec{g} \leq \vec{0}$). The second type are conserved at the node; these are sub-scripted with h. $\vec{h}$ is the net flows of conserved quantities out of the node. This conservation of quantities is represented in the node as an equality constraint ($\vec{h} = \vec{0}$).

Where $\vec{x}_{i,g}$ is the vector of generalized quantities of the i^{th} edge pointing out of the node that are curtailed. $\vec{y}_{j,g}$ is the vector of generalized quantities of the j^{th} edge pointing into the node that are curtailed.

The second type of quantities are conserved at the node; these are sub-scripted with h. The net flow of these quantities out of the node in conserved; this is defined as the equality function h:

$$\vec{h} = \sum_i \vec{x}_{i,h} - \sum_j \vec{y}_{j,h} = \vec{0} \tag{3.27}$$

Where $\vec{x}_{i,g}$ is the vector of generalized quantities of the i^{th} edge pointing out of the node that are conserved. $\vec{y}_{j,g}$ is the vector of generalized quantities of the j^{th} edge pointing into the node that are conserved.

3.3.2 Edges

An edge in the asset model-generator is a directed edge, or an arrow. Figure 3.14 shows a schematic of an edge in the asset model-generator. An edge (i,j) represents the flow of generalized quantities out of its source node (i) and into its target node (j). The identity of an edge is thus defined by its two nodes:

1. Source Node: The node out of which generalized quantities flow via the edge.
2. Target Node: The node into which generalised quantities flow via the edge.

The edge contains two pieces of information:

1. Flow ($\vec{x}$): The generalized quantities flowing out of the source node via the edge.
2. Conversion Function ($\vec{\psi}$): This gives the generalized quantities flowing into the target node via the edge ($\vec{y}$).

The conversion function of an edge (i,j), $\vec{\psi}_{i,j}$, is in general a function of the flows out of its source and target nodes:

$$\vec{y}_{i,j} = \vec{\psi}(\{\vec{x}_{i,k} \forall k\}, \{\vec{x}_{j,l} \forall l\}) \tag{3.28}$$

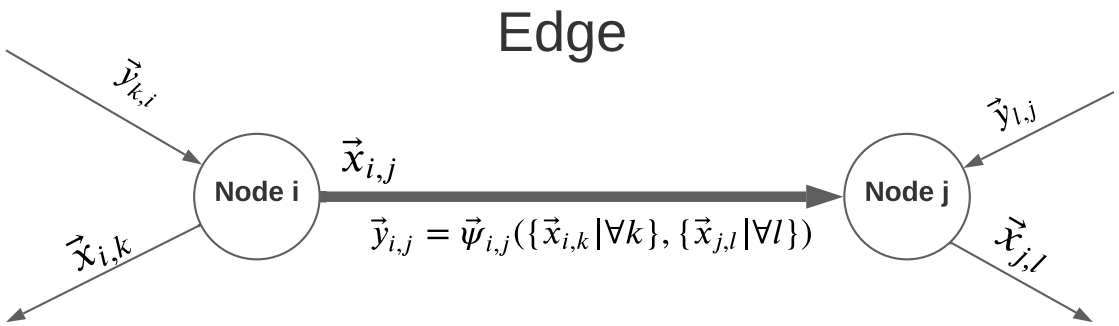

Figure 3.14: Diagram of an edge in the asset model-generator. An edge in the asset model-generator is a directed edge: it is an arrow from its source node i, to its target node j. The identity of an edge is thus defined by its two nodes (i,j). An edge (i,j) contains two pieces of information: a variable called the flow ($\vec{x}_{i,j}$), and a function called the conversion function $\vec{\psi}_{i,j}$. $\vec{x}_{i,j}$ is the flow of the edge; it is the flow of quantities/quantities out of the source node. $\vec{\psi}_{i,j}$ is the conversion function of the edge; it is the flow of quantities/quantities into the target node, $\vec{y}_{i,j}$. The conversion function of an edge, $\vec{\psi}_{i,j}$, in general, depends on all the flows out of its source and target nodes.

Where $\vec{x}_{i,k}$ and $\vec{x}_{j,l}$ are the flows out of the source node (i) and target node (j), respectively. The conversion function can be defined either analytically using white-box models, or black-box models by directly measuring various combinations $\vec{x}$ and $\vec{y}$, as discussed in section 3.1.

3.3.3 Components

A set of edges of the same type over different operational times (timesteps) form a component. A component represents one type of interaction, or energy system function. For example, the charging of a battery, or the transport of hydrogen, or the conversion of electricity to heat. The set of edges in a component can be defined by two things:

1. Template Edge: This represents the generic structure of the edges in the component. This represents a function of an energy system, or a type of interaction.

2. Operational Times: This is a set of timesteps that the interaction occurs over.

One operational time combines with the template edge to define one edge. An edge thus represents an instance of a function of an energy system. Therefore, the set of

operational times and the template edge of a component define the set of edges of the component.

Figure 3.15 shows the schematic of a template edge in the asset model-generator. This schematic is called the "template edge" diagram. The template edge diagram shows examples of three edges of a component. These edges represent the edge of three operational times: t, $t - \delta t$, and $t + \delta t$. The operational times are the times of the source node. δt is the time between operational times.

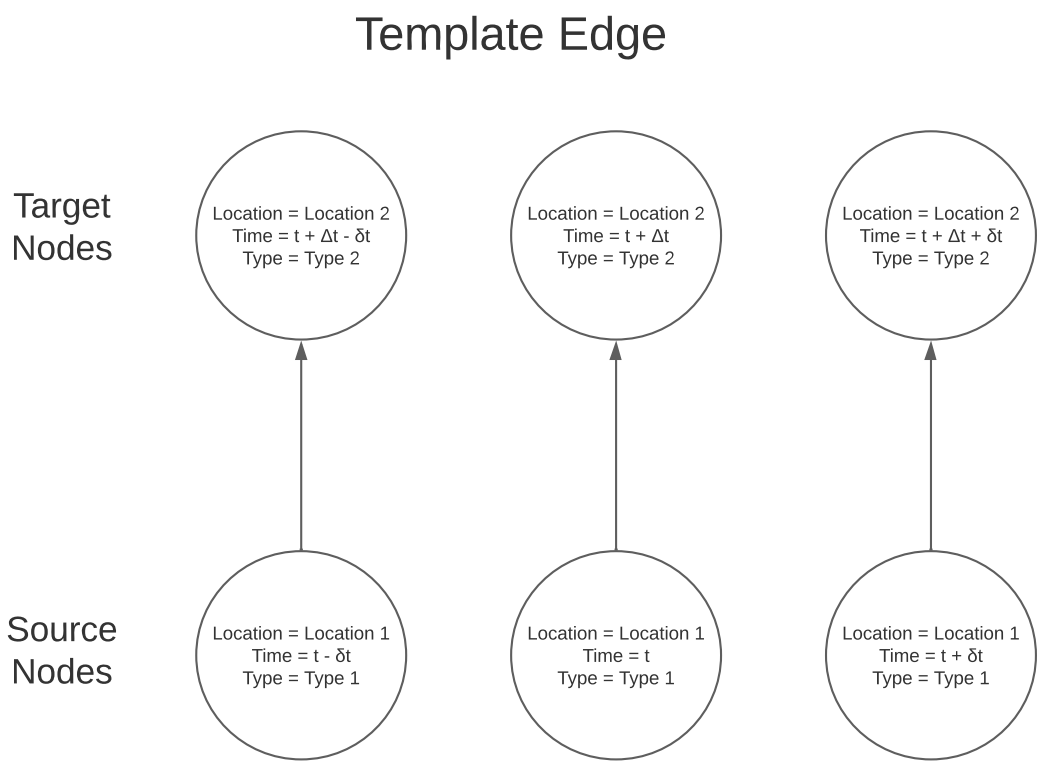

Figure 3.15: Template Edge Diagram for a generic component. A template edge is defined by the its source nodes and target nodes locations and types. There is also a time difference between the target and source nodes, Δt. The template diagram shows three examples of edges. These are for there operational times: t, $t - \delta t$, and $t + \delta t$. The operational times are the times of the source node. δt is the time between operational times. The template edge and the set of operational times define a component.

A template edge is defined by the identity of the source and target nodes, as well as the difference in time between them. A template edge is defined by the following information:

1. Source Node Type: This is the type of the source node of all edges of the component.

2. Target Node Type: This is the type of the target node of all edges of the component.

3. Source Node Location: This is the location of the source node of all edges of the component.

4. Target Node Location: This is the location of the target node of all edges of the component.

5. Time Difference (Δt): This is the difference between the target node and source node times.

6. Conversion Function $\vec{\psi}$: This is the conversion function of the edges of the component.

The operational times of a component are, in general, a set of times $\{t\}$. However, for practical purposes, $\{t\}$ can be represented using three values:

1. Start Time (t_0): This is the time the component is operated from. It is the first operational time.

2. End Time (t_1): This is the time the component is operated until. It is the final operational time.

3. Operational Timestep (δt): The is the time between operational times.

The set of operational times is thus given by:

$$t \in \{t = t_0 + n\delta t | n \text{ is an integer}; t \leq t_1\} \tag{3.29}$$

The operational timestep, δt, is an assumption that the modeller needs to make. This framework can be used to work backwards and adjust the level of detail to determine the level of detail that is useful, i.e. the value of δt that is small enough for the results to be accurate and useful, but not so small that the optimization problem takes too much computational power to solve.

3.3.4 The Five Basis Functions of an Energy System

The asset model-generator unifies the functions of an energy system as flows of generalized quantities in a network; this is shown in Figure 3.16. The asset model-generator represents energy generation and consumption as flows of energy out of a generation node and into a consumption node, respectively. The asset model represents energy transportation, storage, and conversion as flows of energy from nodes of one location to another location, one time to another time, or one type to another type, respectively. As this subsection discusses, demand shifting is a generalization of energy storage; or equivalently, energy storage is a special case of demand shifting. Thus, the six types of energy system assets can be represented by five energy system functions.

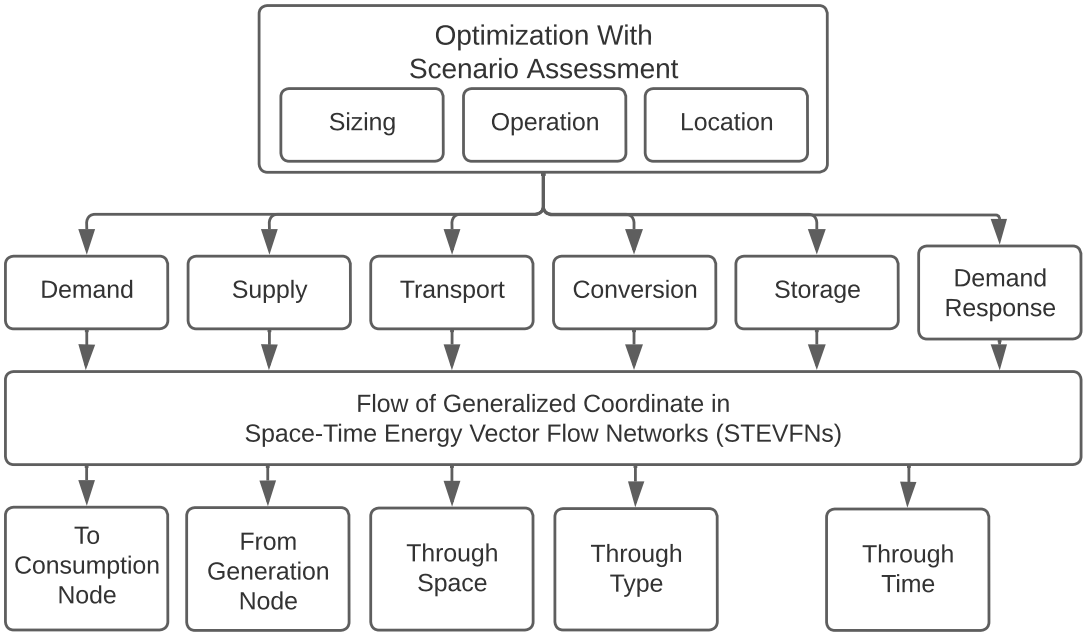

Figure 3.16: Diagram of the unification of energy system functions in the asset model-generator. The asset model-generator is designed for optimal sizing and operation for scenario testing. Asset can perform any combination of the six energy system assets: energy demand, supply, transport, conversion, storage, and demand response assets. Both storage and demand response can be viewed as movement in time. The asset model-generator unifies these different functions as flows in a network. Thus, the six types of energy system assets can be represented by five energy system functions. These represent the flow to a consumption node, from a generation node, through space, through type, or through time, respectively.

If the source and target nodes of the template edge of a component have different locations, the component moves generalized quantities from one location to another location. Such a component can be interpreted as representing the energy system function of energy transportation.

If the template edge of a component has a positive time difference, the component moves generalized quantities from one time to another time in the future. Such a component can be interpreted as representing the energy system function of energy storage.

Note that the time difference of a template edge can be negative. This can be interpreted as moving energy backwards in time. While this may be an alien concept to many, it is found in various fields of theoretical physics. The most famous example of this is found in the interpretation of anti-particles in Feynman diagrams. In Feynman diagrams, an anti-particle flowing in the positive direction along the time axis can be equivalently viewed as its normal particle flowing in the negative direction along the time axis. This is the Feynman–Stueckelberg interpretation of anti-particles [171, 172]. Another example is holes in semiconductor physics. The flow of holes in one direction may be viewed as the flow of electrons in the opposite direction. Similarly, the flow of energy, or energy supply, in one direction may be viewed as the flow of energy demand in the opposite direction.

An example of this is found in demand shifting. If demand is delayed and shifted to the future (e.g. because current electricity prices are higher than future predicted prices), it is equivalent to moving energy supply backwards in time. This would be represented in the asset model as a component with a template edge with negative time difference. For completeness, if energy demand is shifted earlier in time (e.g. because current electricity prices are lower than future projected prices), it is equivalent to moving energy supply forwards in time. This is represented by a template edge with positive time difference. Thus energy storage can be viewed as a special case (or subset) of the more general demand shifting. Or equivalently, demand shifting can be viewed as a generalization of energy storage; demand shifting moves energy both forward and backwards in time. An energy storage only moves energy forwards in time, and is equivalent in function to the shifting of demand earlier in time. If demand

is shifted to the future, it is equivalent to moving energy backwards in time. This formalizes the link between energy storage and demand shifting by unifying them as the same type of function of an energy system.

If the source and target nodes of the template edge of a component have different types, the component moves generalized quantities from one type to another type. Such a component can be interpreted as representing the energy system function of energy conversion.

If a generalized quantity is not constrained at a node, the node is called a "virtual node". If the source node of a template edge is a virtual node, then more generalized quantities may flow out of that node, and that source node is a "generation node" or a "supply node". A component with that template edge may be interpreted to be generating or supplying energy. Such a component can be interpreted as representing the energy system function of energy supply or energy generation. This may be interpreted as generation being unconstrained.

If the target node of a template edge is a virtual node, that target node is a "consumption node" or a "demand node". The component with that template edge may be interpreted to be consuming or demanding energy. Such a component can be interpreted as representing the energy system function of energy demand, or energy consumption.

Any template edge can be split into a sum of the basic five types of edges described above. Thus, any function of an energy system can be represented as a combination of the five basis functions of an energy system:

1. Energy Demand: Flow of quantities into a sink node.

2. Energy Supply: Flow of quantities out of a source node.

3. Energy Transport: Flow of quantities from a node of one spacial location to a node of another spacial location.

4. Energy Storage/Demand Response: Flow of quantities from a node of one time to a node of another time. This also includes demand shifting when as energy can move backwards in time.

5. Energy Conversion: Flow of quantities from a node of one energy vector type to a node of another energy vector type.

3.3.5 Assets

A set of components with interdependent costs combine to form an asset in the asset model. Figure 3.17 shows the representation of an example of an asset with three components. This type of diagram is referred to as the asset-component diagram in the asset model. An asset is identified by its constituent components. Consider the example of a battery. A battery consists of the following three components:

1. Storage Components: This moves electrical charges from one time to the next time.

2. Charging Component: This converts electrical energy in the grid to electrical charges in the battery.

3. Discharging Component: This converts electrical charges in the battery to electrical energy in the grid.

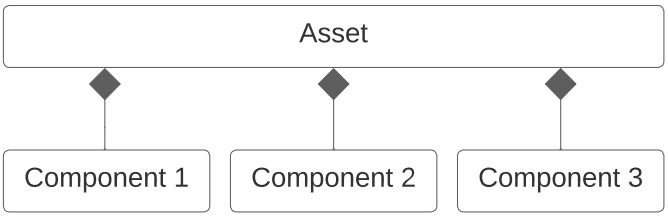

Figure 3.17: Example of an asset-component diagram. This is a generic asset that consists of three components. The asset-component diagram shows the structure of an asset as its constituent components.

An asset contains a cost function, f_{asset}. f_{asset} is, in general, a function of the flows of each edge of each component of the asset.

$$f_{asset} = f_{asset}(\{\{\vec{x}^{\alpha,\beta}|\forall\alpha\}|\forall\beta\}) \tag{3.30}$$

Where $\vec{x}^{\alpha,\beta}$ is the flow of edge α of component β of the asset.

The total cost of an asset includes both the capital, operational, and maintenance costs. It also includes costs and revenues from market participation, regulations,

taxes, etc. There are instances where the size of assets are determined by other factors such as reserves, market power, reliability, etc. In such instances, these other factors either need to be translated to flows, or a new component needs to be build to represent those markets, or other factors and added to the asset as an additional component.

E.g. if the size of a power plant needs to be 20% larger than the maximum demand, then the cost of the power plant can be set to 20% larger than the actual maximum flows in the power plant asset. If the size of the power plant is determined by a day ahead market, then the participation of the power plant in this day ahead market needs to be added as a component of the power plant asset.

An asset can, in theory, contain all components of an energy system. However, this would make it indistinguishable from the energy system, and thus not a useful concept. However, when calculating the cost of a component, its cost may depend on the cost of another component. Thus, to calculate the cost of one component, the cost of the both interdependent components need to be calculated together. If these two components are combined to form an asset, the cost of the asset can be defined and calculated. In general, a set of components may have costs that depend on each other. Assets should be defined by the minimum set of components that have costs that are interdependent. If the cost of a subset of components can be defined independently of the rest of the set, then this subset can be removed from the asset to form another asset.

3.3.6 Energy System

A set of assets combine to form an energy system in the asset model. An energy system is identified by the set of its constituent assets.

The energy system contains the total cost function, F. F is the sum of the cost of the constituent assets of the energy system.

$$F = \sum_{\gamma} f^{\gamma} \tag{3.31}$$

Where f^{γ} is the cost function of asset γ of the energy system.

3.4 Modelling Costs

The costs of an asset are traditionally split into two types: the capital cost, and the operational costs. However, the costs of an asset can also be categorized into two other types: the sizing cost, and the usage cost. These two classifications usually align, but not necessarily. In the unified asset model, costs are categorized based on the latter.

3.4.1 Usage Cost

Define the usage of each flow (i) of an asset as u_i:

$$u_i = u_i(\vec{x}_i) \tag{3.32}$$

Where $\vec{x}_i$ is the i^{th} flow of the asset. The total usage of the asset (U_{asset}) is thus the sum of all usages of the asset:

$$U_{asset} = \sum_i u_i(\vec{x}_i) \tag{3.33}$$

The usage cost of an asset (f_{use}) is a function of the total usage of the asset:

$$f_{use} = f_{use}(U_{asset}) \tag{3.34}$$

Examples of the usage cost include, the total fuel supplied to a generator, or the total amount of electricity consumed by an electric heater. The usage cost thus represents the operation and maintenance cost of an asset.

If all u_i are the same and, and u_i is linear, u_i can be pulled out of the summation in equation 3.33; this gives:

$$U_{asset} = \sum_i u_i(\vec{x}_i) = u\left(\sum_i \vec{x}_i\right) \tag{3.35}$$

Note that in this situation, u_i and u represent the same mapping. U_{asset} from equation 3.35 can then be combined with f_{use} to redefine f_{use} as a function of the sum of flows. In this special case, equation 3.34 then transforms to:

$$f_{use} = f_{use}(\sum_i \vec{x}_i) \tag{3.36}$$

In this special case, the usage cost of an asset is a function of the sum of flows in the asset.

3.4.2 Sizing Cost

Consider the definition of the size. The size of an asset (s_i) required to satisfy the flow (i) of an asset is given by:

$$s_i = s_i(\vec{x}_i) \tag{3.37}$$

Where $\vec{x}_i$ is the i^{th} flow of the asset. The size of the asset (S_{asset}) is the size required to satisfy all flows. The size of the asset is the maximum of the sizes required for individual flows:

$$S_{asset} = \max_i\{s_i\} \tag{3.38}$$

The sizing cost of an asset (f_{size}) is a function of the size of the asset:

$$f_{size} = f_{size}(S_{asset}) \tag{3.39}$$

Examples of sizing cost include the maximum power supplied by a generator, or the maximum power flowing through an electricity line. The sizing cost thus represents the capital cost of an asset.

Similar to the usage cost, if all s_i are the same and linear, then in this special case, equation 3.39 transforms to:

$$f_{size} = f_{size}(\max_i\{\vec{x}_i\}) \tag{3.40}$$

In this special case, the sizing cost is a function of the maximum of the flows. Once again, the size and thus sizing cost, of assets may be determined by different components, or may be a function of the flows due to certain regulations or reserve requirements. A minimum size may also be set if there is existing capacity.

3.4.3 Degradation Costs

Certain energy assets degrade when they are used, and need to be replaced when they are fully degraded. In general their degradation depends on the way they are used. For instance batteries degrade when they are charged or discharged; they degrade at different rates depending on their state of charge and charging/discharging current. These degradation costs can be amortized as an operational cost.

The degradation cost (f_{deg}) represents the cost of purchasing assets and their replacements. Thus, adding the amortized degradation cost and the capital cost will

lead to double counting. If an asset does not fully degrade throughout its lifetime, it only needs to be purchased once, and the cost of purchasing it is the capital cost. However, if an asset is fully degraded during its lifetime, it needs to be replaced and purchased again. The number of assets that need to be purchased is the total amortized cost divided by the cost of purchasing one asset. The actual capital cost ($f_{capital}$) is in fact the maximum of the sizing and degradation costs:

$$f_{capital} = \max\{f_{size}, f_{deg}\} \tag{3.41}$$

In reality this slightly overestimates the levelized cost of an energy system as it assumes that all purchases of future replacements are made at the time of purchase of the first asset. This may be countered by discounting the amortization cost depending on the time the asset is used. This however "splits" the asset into multiple small parts that are purchased at different times. This slightly underestimates the actual cost. In general, trying to account for this cost fully will make the total cost non-convex. This may be dealt with by having multiple types of assets that are purchased at different years. This however, increases the number of assets as there are multiple copies of assets, distinguished by the year they were purchased.

In the asset model, the amortized cost is a type of usage cost. It may initially be unclear how to define these costs, especially when they depend on the way an asset is operated. Consider a process based on the work done by Ahsan et al [108]. Consider the example of a Li-Ion battery to illustrate this process.

The amortized cost of using an asset once is the cost of the asset (C_{CAP}) divided by the number of times the asset can be used (N). A traditional curve found for batteries is the number of lifecyles as a function of depth of discharge (DOD) as shown in Figure 3.18. Where "one use" of a battery is defined as discharging the battery from full to that DOD and then charging it back to full, i.e. a charge-discharge cycle. The degradation cost of one such cycle (f_{cycle}) is thus the cost of the battery divided by the number of lifecycles:

$$f_{cycle} = \frac{C_{CAP}}{N(DOD)} \tag{3.42}$$

Where N is a function of DOD.

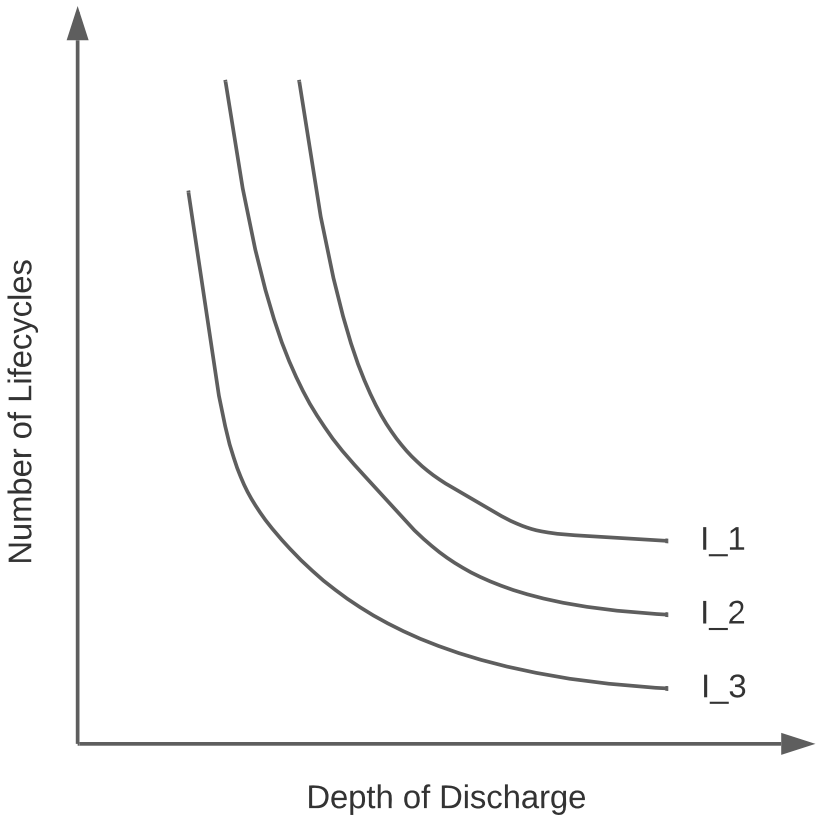

Figure 3.18: Stylized schematic of the Battery Lifecycle vs Depth of Discharge for different currents. The number of lifecycles of a battery depends on the depth of discharge (DOD). At cycles with higher DOD, the battery degrades quicker. The greater the depth of discharge, the lower the number of lifecycles before the battery reaches its end of life. The number of lifecyles also depends on the charge-discharge current. I_1, I_2 and I_3 represent three currents in increasing order. At higher currents, the battery degrades quicker. As the current increases, the number of lifecycles decreases.

C_{cycle} is the cost of a charge-discharge cycle. However, the battery need not fully charge nor fully discharge in a simulation timestep. In fact, the battery does not need to be fully charged before it can begin to be discharged. Consider the definition of the cost of discharging the battery from an initial SOC_i to a future SOC_f. SOC is defined as (1-DOD). This gives:

$$f_{cycle}(SOC) = \frac{C_{CAP}}{N(SOC)} \tag{3.43}$$

The degradation due to the charging and discharging can be split and set as half the cost of a charge-discharge cycle. This is because a battery will have to eventually be charged once it is discharged. This may be split equally or in any other way, but the equal split is considered here for simplicity. When the battery is discharged to SOC_i, it degrades a total of $f_{discharge}(SOC_i)$. When the battery is discharged further to SOC_f, it degrades a total of $f_{discharge}(SOC_i)$. Thus, the additional amount it degrades when it is discharged from SOC_i to SOC_f is the difference of the two:

$$f_{discharge} = f_{cycle}(SOC_f) - f_{cycle}(SOC_i) \tag{3.44}$$

Combining Equations 3.43 and 3.44 gives:

$$f_{discharge}(SOC_i, SOC_f) = \frac{C_{CAP}}{N(SOC_f)} - \frac{C_{CAP}}{N(SOC_i)} \tag{3.45}$$

This is the degradation cost of discharging a battery as a function of SOC_i and SOC_f. However, if a fixed simulation timestep, δt, is assumed:

$$SOC_f = SOC_i - I_d \delta t \tag{3.46}$$

Where I_d is the discharging current. The degradation cost of discharging a battery at timestamp t ($C_{discharge}(t)$) can thus be written as:

$$f_{discharge}(t) = f_{discharge}(SOC(t), I_d(t)) = C_{CAP}\left[\frac{1}{N(SOC(t) - I_d\delta t)} - \frac{1}{N(SOC(t))}\right] \tag{3.47}$$

However, the number of lifecycles of a battery also depends on the current. This is viewed as multiple lines in Figure 3.18. In general, this would give a surface and:

$$N = N(SOC, I) \tag{3.48}$$

The degradation cost of discharging a battery (f_{deg}) is now:

$$f_{deg} = f_{discharge}(SOC(t), I_d(t)) = C_{CAP}\left[\frac{1}{N(SOC(t) - I_d\delta t, I_d)} - \frac{1}{N(SOC(t), I_d)}\right] \tag{3.49}$$

The degradation cost of an asset is thus a type of "capital" cost, as it is the cost of purchasing assets. However, as it depends on the usage of assets, it is a usage cost instead of a sizing cost. If the degradation cost is lower than the sizing cost, an asset is only purchased once. If an asset is only purchased once, the capital cost is just the sizing cost. If the degradation cost is higher than the sizing cost, an asset is replaced, and thus purchased multiple times. If an asset is replaced, the capital cost is the degradation cost. Thus, the overall capital cost is the maximum of the sizing cost and the degradation cost. The switch from sizing cost to degradation cost can also be interpreted as moving from purchasing all consumables at once, to purchasing them bit by bit over a long time.

3.5 Summary

This chapter answers thesis sub-question 1: "what are the minimum and sufficient theoretical basis functions of all assets in an energy system, and can these functions be used to create a unified model of assets?" There are five basis functions of an energy system. Any energy system function can be built from these basis energy functions. Any of the six types of energy system assets can be modelled using the five basis functions of an energy system. This chapter develops a unified generalized spatio-temporal asset model-generator that describe any asset that can perform any combination of energy system functions. The five basis functions of an energy system are:

1. Energy Demand: Flow of quantities into a sink node.
2. Energy Supply: Flow of quantities out of a source node.
3. Energy Transport: Flow of quantities from a node of one location to a node of another location.

4. Energy Storage/Demand Response: Flow of quantities from a node of one time to a node of another time. This also includes demand shifting when as energy can move backwards in time.

5. Energy Conversion: Flow of quantities from a node of one energy vector type to a node of another energy vector type.

In defining the basis functions of an energy system, this chapter is the first to mathematically formalize the link between energy storage and demand shifting. Energy storage only moves energy forwards in time. Energy demand can be considered the anti-particle of energy supply. A flow of demand in one direction, in space-time-type, is the same as the flow of supply in the opposite direction. Demand shifting is a generalization of energy storage as it can move energy both forwards and backwards in time. Equivalently, energy storage is a special case of demand response that only moves energy forward in time.

This chapter utilizes the representation of the basis energy system functions as flows in a space time energy vector network to build a unified model for energy system assets. This is a hierarchical model and is referred to as the asset model. The basic building block is a node. A node is a point in the network defined by its location, time, and type; it models the conservation or curtailment of a set of generalized quantities at that point. A set of ordered nodes define an edge; this contains the flow of generalized quantities out of its source node, and into its target node. The flow into the target node of an edge is in general a function of the output flow of the edge and its neighbouring edges. This models conversions and implicitly models efficiencies. A set of edges of the same type that differ only by operation times form a component. A component represents an energy system function. This function can be described as a combination of the five basis energy system functions. A set of components with interconnected costs form an asset. This asset model is able to account for capital, operational, and degradation costs as sizing and usage costs. A set of assets combine to form an energy system. The cost of an energy system is the sum of the costs of its constituent assets.

The main question of the thesis is to determine if a generalized spatio-temporal model of assets can be developed and utilized to optimize the sizing, operation and location of energy system assets. This chapter develops and presents a spatio-temporal asset model that is able to model any energy system and its costs. The next chapter uses this unified asset model to develop a theoretical framework that can co-optimize the sizing, operation, and location of energy system assets with scenario assessment.

Chapter 4

The Space Time Energy Vector Flow Networks (STEVFNs)

This chapter answers sub-question 2 of the thesis:

"Can a model-generator of energy system design problems be developed, that utilizes the unified model-generator of assets, to co-optimize the sizing, operation, and location of real assets?"

This chapter does this by developing the Space-Time Energy Vector Flow Networks (STEVFNs, pronounced like the name "Steven") model-generator. The STEVFNs model-generator consists of three languages and translations between these languages. The STEVFNs model-generator uses the generalized asset model-generator in chapter 3 as the intermediary language to translate energy system design and operation problems to mathematical optimization problems.

The main question of the thesis is if a generalized spatio-temporal asset model-generator can be utilized to optimally size and operate whole energy systems. Chapter 3 develops and presents a generalized spatio-temporal asset model-generator that is able to model any asset that can perform any combination of the five energy system functions. This chapter uses this unified asset model to develop a framework to translate whole energy system design and operation problems to mathematical optimization problems.

The energy system design problem is to find the optimal size and operation of energy system assets at each location. The set of assets that can be built at each location or between each location pairs is referred to as a "case study". However,

the optimal energy system design for a case study depends on various assumptions. Each set of assumptions is a referred to as a "scenario". Each scenario will have a different optimal energy system design. Studying how scenario assumptions affect the optimal energy system design is referred to as "scenario assessment". The STEVFNs model-generator this chapter develops enables scenario assessment of case studies with optimization.

The STEVFNs model-generator consists of three models, or "languages" and translations between these languages; Figure 4.1 shows a schematic of the structure of STEVFNs. These languages are descriptions of the same energy system design problem, but focus on different aspects of the design problem, and are thus useful for different purposes. The first language is the "system designer language". This describes the structure and scenarios of the energy system design problem in a simple, natural language. This gets translated into the "asset modeller language". The asset modeller language describes the physics of the assets that form the energy system. It is a slight modification of the generalized spatio-temporal asset model presented in chapter 3. This is finally translated into the "optimizer language". The optimizer language describes a mathematical optimization problem. This optimization problem is described using disciplined convex programming (DCP) and disciplined parametrized programming (DPP). Solving this mathematical optimization problem in the optimizer language equivalently solves the original energy system design problem in the system designer language. The STEVFNs model-generator thus uses a generalized spatio-temporal asset model to map, or translate the basic energy system design problem to a mathematical optimization problem.

Finding the ideal energy system design can be understood using the following analogy of writing a beautiful story. To find the ideal story that can be written with some characters, we need to first set the stage by listing the characters in the story. We then define the personalities and motivations of these characters. We then translate this to a language that simulates the actions of these characters. The actions of these characters are then translated into a mathematical optimization problem that intelligently loops through multiple possible stories to find the ideal story given the characters and the personalities of these characters. We then change the personalities

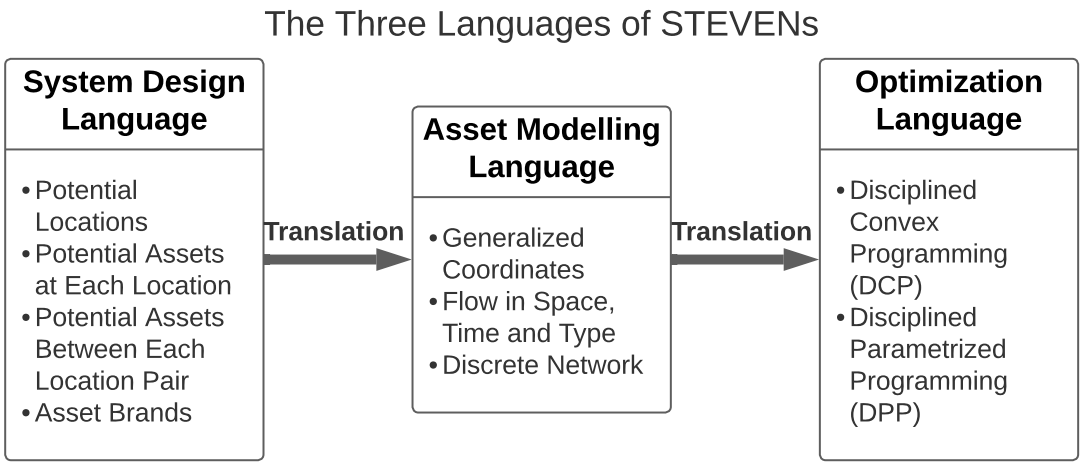

Figure 4.1: Structure of the three languages of the STEVFNs model-generator. The STEVFNs model-generator maps an energy system design and operation problem to a mathematical optimization problem using the generalized spatio-temporal asset model as a bridge. The STEVFNs model-generator consists of three models or "languages", and translations between these languages. The first language is the system design language. The structure of the energy system design and operation problem and the scenario assumptions are described in this simple language. This gets translated to the asset modeller language. The asset modeller language describes the physics of the energy system assets using the generalized spatio-temporal asset model presented in chapter 3. This gets translated into the optimization language. The optimization language describes the mathematical optimization problem that will eventually solve the system design problem. The optimization language uses Disciplined Convex Programming (DCP) and Disciplined Parametrized Programming (DPP).

and motivations of these characters and repeat the process to find the new ideal story given the new scenario. We then study how these scenarios affect the ideal story to find the most beautiful story. The personalities of some seemingly important characters may be inconsequential in the story. Likewise the motivations of some other characters may be pivotal to how the story plays out. The most beautiful story allows the reader to explore the interplay between the personalities of characters and how the story plays out.

In the process of finding the ideal energy system design, the beautiful story is the ideal energy system design and operation. The characters are the assets. The personalities and motivations of the characters are the parameters of the assets, and the latitudes and longitudes (lat-lon) of the locations. The ideal energy system design requires studying which scenario assumptions do not affect the system design. These scenarios become inconsequential in decision making, i.e. a decision may be made without worrying about which of these scenarios actually plays out. The ideal energy system design also requires studying which scenario assumptions critically change the ideal system design. This may dictate what kind of predictions need to improved before a decision can be made. It may, instead, require decisions to be made with these risks in mind.

To develop the STEVFNs model-generator, Section 4.1 first describes the three languages of STEVFNs: the system designer language, the asset modeller language, and the optimizer language. An energy system design problem is first described in the system designer language. This is translated into the asset modeller language that Section 4.2 describes. The asset modeller language describes the physics of the assets that form the energy system. Section 4.3 then presents how the description in the asset modeller language can be translated into a mathematical optimization problem in the optimizer language. The three languages and translations between these languages form the STEVFNs model-generator. Section 4.4 discusses the advantages and disadvantages of the STEVFNs model-generator compared to existing model-generator and tools. Section 4.5 finally summarizes the chapter.

4.1 The Three Languages of STEVFNs

The first part of the STEVFNs model-generator is the three models, or languages of the STEVFNs model-generator. All three languages describe the same energy system design problem; this is the optimal sizing and operation of assets in an energy system. However, they abstract away various aspects of the problem allowing different experts to focus and specialize on their respective roles. These are the design of energy systems, the modelling of the physics of assets, and the solving of mathematical optimization problems.

4.1.1 System Designer Language

The first language of the STEVFNs model-generator is the system designer language. This is the simple language used to describe the structure and scenarios of the energy system design and operation problems described in Figure 4.1. This is the operational or outermost language, and the ultimate purpose of the STEVFNs model-generator. Users of any tool implementation of STEVFNs will interact with and use this language.

Figure 4.2 shows a schematic of the system designer language of STEVFNs. An energy system in the system designer language is defined by a set of assets and locations. These assets and locations have a structure and scenario data. The structure of the assets and locations define the "structure" of the energy system design problem, or the "case study". The scenario data of the assets and locations define the "scenario" of the energy system design problem.

To build the structure of an energy system design problem, potential assets are "added" to either a location or between two locations. This is visualized using the system diagram such as the one Figure 4.2 shows. These assets represent possible assets that can be sized and operated. The optimization can still choose to not use these assets. This will be represented as a zero (or near zero) ideal size of an asset. The structure and scenario data of assets and locations are sufficient to define the energy system problem. However, the energy system diagram is useful for visualizing and systematically building the energy system problem.

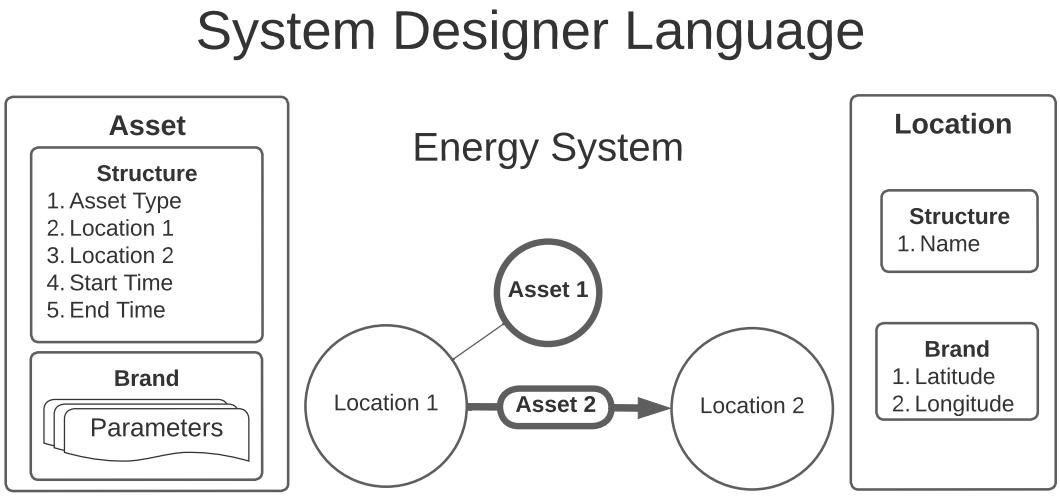

Figure 4.2: Diagram of the system designer language. The system designer language in STEVFNs describes the energy system design and operation problem. It consists of the energy system structure (middle), asset information (left), and location information (right). Middle: Example of a simple energy system diagram. The structure of an energy system is defined by "placing" assets in either one location (Asset 1) or between two locations (Asset 2). Left: An asset is defined by its structure and its scenario information. The information of all assets is sufficient to produce the energy system diagram (middle). Right: A location is defined by its Structure and its scenario information. The asset and location information are sufficient to define the energy system design and operation problem. The energy system diagram (middle) is not necessary to define the energy system problem. However, the energy system diagram is very useful for visualizing the energy system design problem.

In the system designer language, the structure of an asset is described by the following:

1. Asset Type: This is the class of asset.
2. Location 1: This is the name of first location an asset is attached to.
3. Location 2: This is the name of the second location an asset is attached to. If an asset is located at one location, Location 2 is the same as Location 1. If an asset is located between two locations, then Location 2 is different from Location 1.
4. Start Time: This is the first time that the asset is allowed to be used.
5. End Time: This is the last time that the asset is allowed to be used.

The scenario data of an asset is represented by its brand name. The brand name is an alias for the set of parameter data for the asset. This parameter data is either obtained from manufacturer data sheets or via simple black-box experiments (or tests).

The structure of a location is the name of the location. This name is used to identify the location and define the links between assets. The scenario data of a location is the geographical information of the location. One example for the scenario data for locations is the latitude and longitude (lat-lon) of the locations. The geographical information of a location need not be represented by its lat-lon. Other sets of data such as the x-y distance from an origin point may also be used. However, for simplicity, the lat-lon shall be used to represent the scenario data for a location in the rest of the thesis.

4.1.2 Asset Modeller Language

The asset modeller language is used to describe the physics of assets of an energy system. This includes all techno-economic constraints and aspects of assets.

In the STEVFNs model-generator, the asset modeller language is a slight modification of the of generalized spatio-temporal asset model chapter 3 presents. Figure 4.3 shows the structure of assets in the asset modeller language. There are two main

difference between the asset modeller language and the generalized spatio-temporal asset model in chapter 3. The first is that edges contain an additional set of conversion function parameters ($\vec{\mathbf{P}}_\psi$). The second difference is that assets contain an additional set of cost function parameters ($\vec{\mathbf{P}}_f$).

The set of conversion function parameters in each edge ($\vec{\mathbf{P}}_\psi$) affect the conversion function of the edge ($\vec{\psi}$). In STEVFNs asset modeller language, the conversion function is thus a function of the flows out of its source and target nodes, as well as the conversion function parameters. In the asset modeller language, equation 3.28 thus transforms to:

$$\vec{y}_{i,j} = \vec{\psi}(\{\vec{x}_{i,k} \forall k\}, \{\vec{x}_{j,l} \forall l\}, \vec{\mathbf{P}}_{\psi,i,j}) \tag{4.1}$$

Where $\vec{\mathbf{P}}_{\psi,i,j}$ is the conversion function parameters of edge (i,j).

The set of cost function parameters in each asset ($\vec{\mathbf{P}}_f$) affect the cost function of the asset (f). In STEVFNs asset modeller language, the conversion function is thus a function of the flows in each of its edges as well as the cost function parameters. In the asset modeller language, equation 3.30 thus transforms to:

$$f = f\{\{\vec{x}^{\alpha,\beta} | \forall \alpha\} | \forall \beta\}, \vec{\mathbf{P}}_f) \tag{4.2}$$

The rest of the definition of assets in the asset modeller language are the same as that of the generalized spatio-temporal asset model chapter 3 presents.

4.1.3 Optimizer Language

The optimizer language in the STEVFNs model-generator describes a mathematical optimization problem. This mathematical optimization problem represents the optimal sizing and operation of assets in the energy system. Thus, solving this mathematical optimization problem is equivalent to finding the optimal design of the energy system.

The optimizer language in the STEVFNs model-generator uses the syntax used for disciplined convex programming (DCP) with disciplined parametrized programming (DPP) [25, 26, 24]. Figure 4.4 shows the parts of an optimization problem in the optimizer language. The optimization problem is to find the values for all components of the vector of control variables ($\vec{x}$) that minimize the value of the scalar cost function

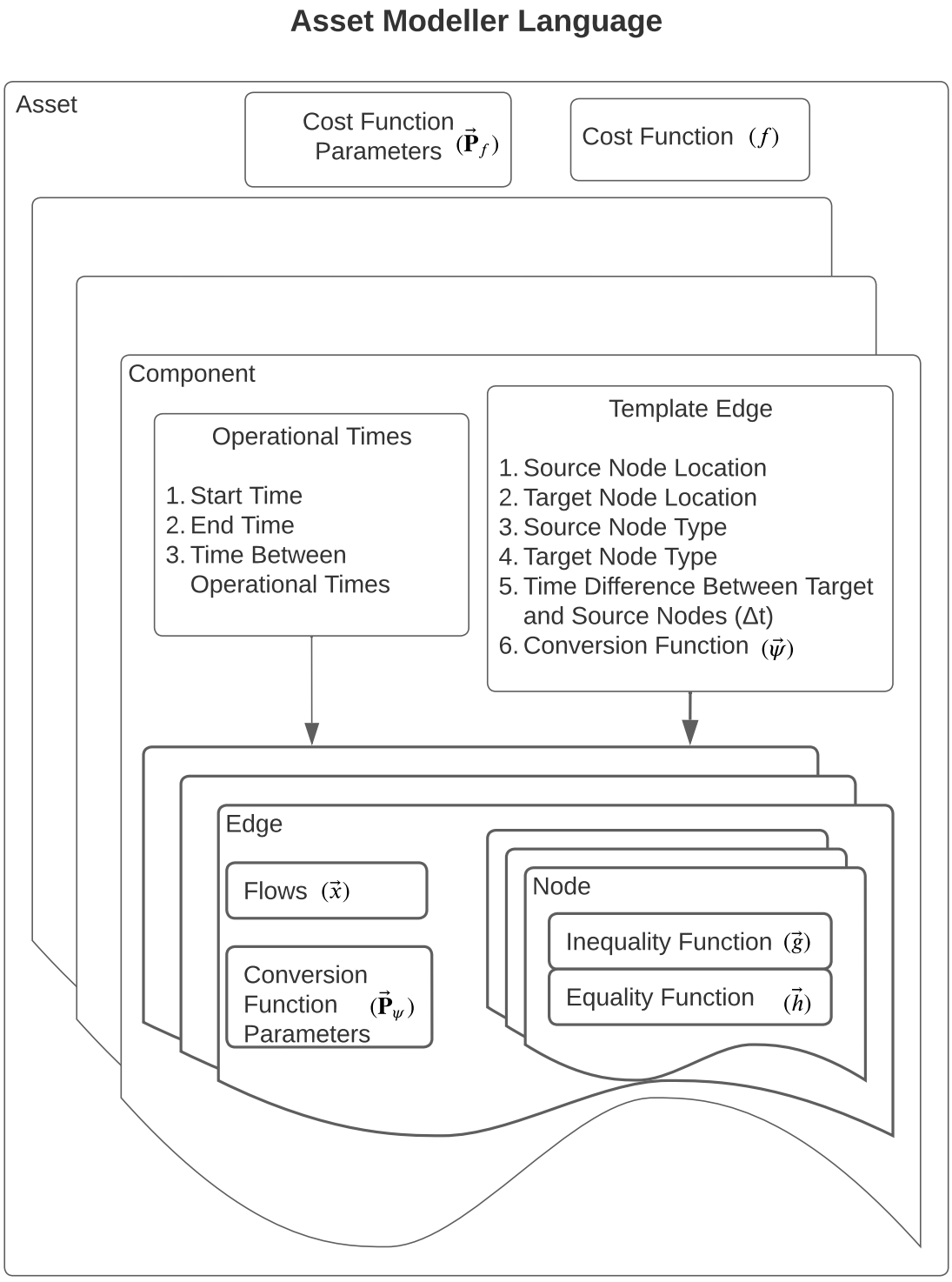

Figure 4.3: Structure of the asset modeller language. The asset modeller language in STEVFNs is a slight modification to the generalized spatio-temporal asset model presented in chapter 3. There are two main differences. Firstly, the edge contain conversion function parameters ($\vec{\mathbf{P}}_\psi$). Secondly, the asset contains cost function parameters ($\vec{\mathbf{P}}_f$).

f. This is subject to the value of all components of the vector inequality constraint function ($\vec{g}$) being less than zero. This is also subject to the value of all components of the vector equality constraint function ($\vec{h}$) being equal to zero. f, $\vec{g}$, and $\vec{h}$ are also functions of the vector of parameters ($\vec{\mathbf{P}}$).

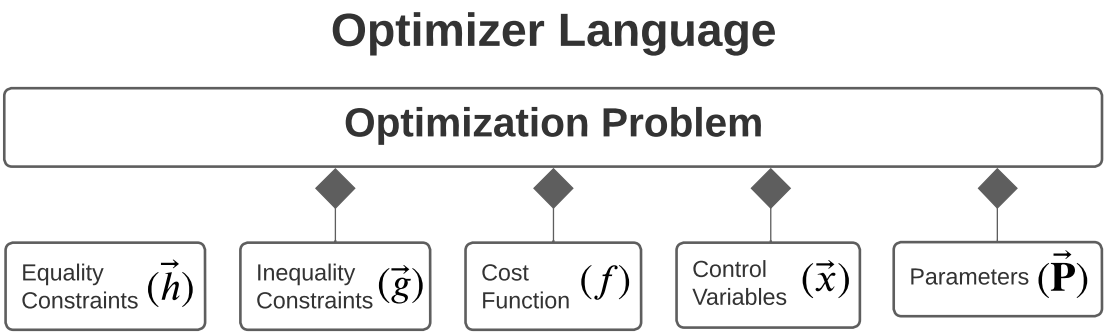

Figure 4.4: Diagram of the optimizer language. The optimizer language defines an optimization language using DCP and DPP. In this, an optimization problem consists of minimizing a cost function (f). This is subject to inequality constraints functions ($\vec{g}$), and equality constraints functions ($\vec{h}$). These functions are convex functions of the control variables ($\vec{x}$), and follow DCP rules. The functions are also parametrized by the parameters ($\vec{P}$), and follow DPP rules.

We can write the mathematical optimization problem of the optimizer language in the standard form as:

$$\begin{aligned} \text{minimize} \quad & f = f(\vec{x}, \vec{\mathbf{P}}) \\ \text{with respect to} \quad & \vec{x} \\ \text{subject to} \quad & \vec{g}(\vec{x}, \vec{\mathbf{P}}) \leq \vec{0} \\ & \vec{h}(\vec{x}, \vec{\mathbf{P}}) = \vec{0} \end{aligned} \tag{4.3}$$

As the optimizer language of STEVFNs uses the syntax of DCP and DPP, it also imposes DCP and DPP rules. Functions f and $\vec{g}$ must be convex with respect to $\vec{x}$. $\vec{g}$ is the net flows of generalized coordinates that are curtailed. Thus, for $\vec{g}$ to be convex, the conversion functions ($\vec{\psi}_g$) of curtailed coordinates of all edges connected to a node must be concave and positive, or convex and negative.

Function $\vec{h}$ must be affine with respect to $\vec{x}$. $\vec{h}$ is the net flows of generalized coordinates that are conserved. Thus, for $\vec{h}$ to be affine, the conversion functions ($\vec{\psi}_h$) of curtailed coordinates of all edges connected to a node must be affine.

f, $\vec{g}$, and $\vec{h}$ must also be parameter affine with respect to the parameters $\vec{\mathbf{P}}$. The full set of rules that define whether a function is convex, affine, or parameter affine is described in the literature [25, 26, 24]. A tutorial for DCP and DPP is presented in the CVXPY user guide [173].

The relevant parts of the DCP and DPP rules are reproduced for convenience [173]. DCP analysis of an expression consists of analyzing the expression as atomic functions of its sub-expressions. This process is continued until the final sub-expressions are atomic functions. Atomic functions are functions that have known convexity.

$f(expr_1, expr_2, ..., expr_n)$ is convex if f is a convex function and for each $expr_i$, one of the following conditions hold:

- f is increasing in argument i (i.e. f increases as i increases) and $expr_i$ is convex.
- f is decreasing in argument i and $expr_i$ is concave.
- $expr_i$ is affine or constant.

Similarly, $f(expr_1, expr_2, ..., expr_n)$ is concave if f is a concave function and for each $expr_i$, one of the following conditions hold:

- f is increasing in argument i and $expr_i$ is concave.
- f is decreasing in argument i and $expr_i$ is convex.
- $expr_i$ is affine or constant.

An expression is affine if it is both convex and concave. The list of atomic, or basic functions are provided in CVXPY user guide [173].

For DCP expression to be DPP with respect to parameters, the expression must be affine with respect to its parameters. Under DPP, the following two rules apply:

1. Parameters are parameter affine.
2. The product of two expressions is affine if at least one of the expressions is constant, or when one of the expressions is parameter-affine and the other is parameter-free.

Note that while ensuring the problem is DCP and DPP compliant allows us to ensure the problem is convex and use DPP to rerun problems quickly, it is not required to model a system. Relaxing the DCP or DPP compliance loses some associated benefits, but the optimization problem can still be formulated. In such situations, the solvers used simply need to be changed.

If any f, $\vec{g}$, and $\vec{h}$ are not DPP compliant, alternate formulations or approximations could be made to make them DPP compliant; examples of this are given in CVXPY examples []. If a component cannot be made DPP compliant, the component can still be modelled and the optimization can still be solved; only the ability to resolve problems quickly via DPP is lost.

Similarly, if any f, $\vec{g}$, and $\vec{h}$ are not DCP compliant, approximations could be systematically made to make them DPP compliant; Chapter 5 describes this in further detail with examples. If a component cannot be made DCP compliant via reasonable approximations, then the resulting optimization problem can still be solved. However, the solution cannot be guaranteed, and an approximate solution may not be able to be found in reasonable time. Furthermore, in such cases heuristic solvers need to be used like machine learning, swarm optimization, etc.

4.2 Translation from System Designer to Asset Modeller Language

The previous section introduces the three languages of the STEVFNs model-generator. With the three languages defined, the next step is to define the translations between the three languages. The energy system design and operation problem is first described by the system designer in the system designer language. This first needs to be translated to the asset modeller language. This section describes the translations from the system designer language to the asset modeller language. Figure 4.5 shows a schematic of the translations from the system designer language to the asset modeller language.

Defining the asset type name in the system designer language defines the type of asset; cost function; list of components; and the conversion function of the components. The start time and end time are defined in the system designer language;

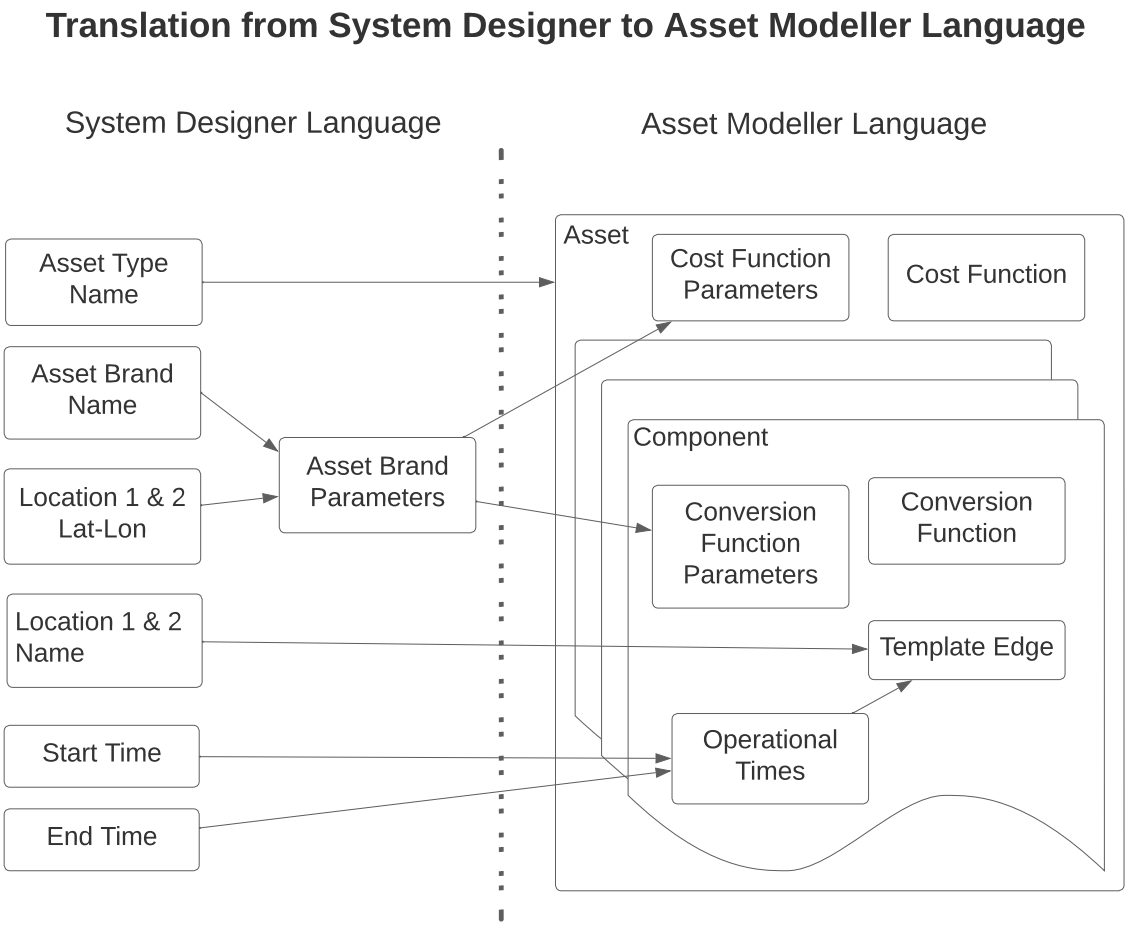

Figure 4.5: Diagram of the translation from the system designer to asset modeller language. An asset is described in the system designer language, these are then translated to descriptions in the asset modeller language. Defining the asset type name in the system designer language defines the type of asset; cost function; list of components; and the conversion function of the components. The start time and end time are defined in the system designer language; these gets translated to the operational times of components in the asset modeller language. Locations 1 and 2 in the system designer language combine with the operational times in the asset modeller language to define the template edge of various components in the modeller language. These define the structure of the asset, and are sufficient to build the asset. To update the asset, the system designer needs to define the asset brand name, and location 1 and 2 lat-lon. These link to predefined asset brand parameters in the system designer language. These asset brand parameters get translated to cost function parameters of the asset, and conversion function parameters of the asset's components in the asset modeller language. These define the parameters of the asset, and are sufficient to update the asset.

these gets translated to the operational times of components in the asset modeller language. Locations 1 and 2 in the system designer language combine with the operational times in the asset modeller language to define the template edge of various components in the modeller language. These are the source and target node locations of template edges. These define the structure of the asset, and are sufficient to build the asset.

To update the asset for a new scenario, the system designer needs to define the asset brand name, and location 1 and 2 lat-lon. These link to predefined asset parameters in the system designer language. These asset parameters get translated to cost function parameters of the asset, and conversion function parameters of the asset's components in the asset modeller language. These define the parameters of the asset, and are sufficient to update the asset.

With this, system designers will be able to define an energy system design problem in the system designer language and have it translated to the asset modeller language.

4.3 Translation from Asset Modeller to Optimizer Language

The previous section describes how energy system design and operation problems can be translated from the system designer language to the asset modeller language. This section describes how the description of the same problem can be translated from the asset modeller language to the optimizer language.

Figure 4.6 shows a schematic of the translations from the asset modeller language to the optimizer language. An energy system in the asset modeller language maps to an optimization problem in the optimizer language. Each asset has a cost in the asset modeller language; these add up to form the objective cost function of the optimization problem. Each asset is also associated with optimization parameters. Each edge is associated with a set of optimization control variables. Each node is associated with a set of optimization constraints.

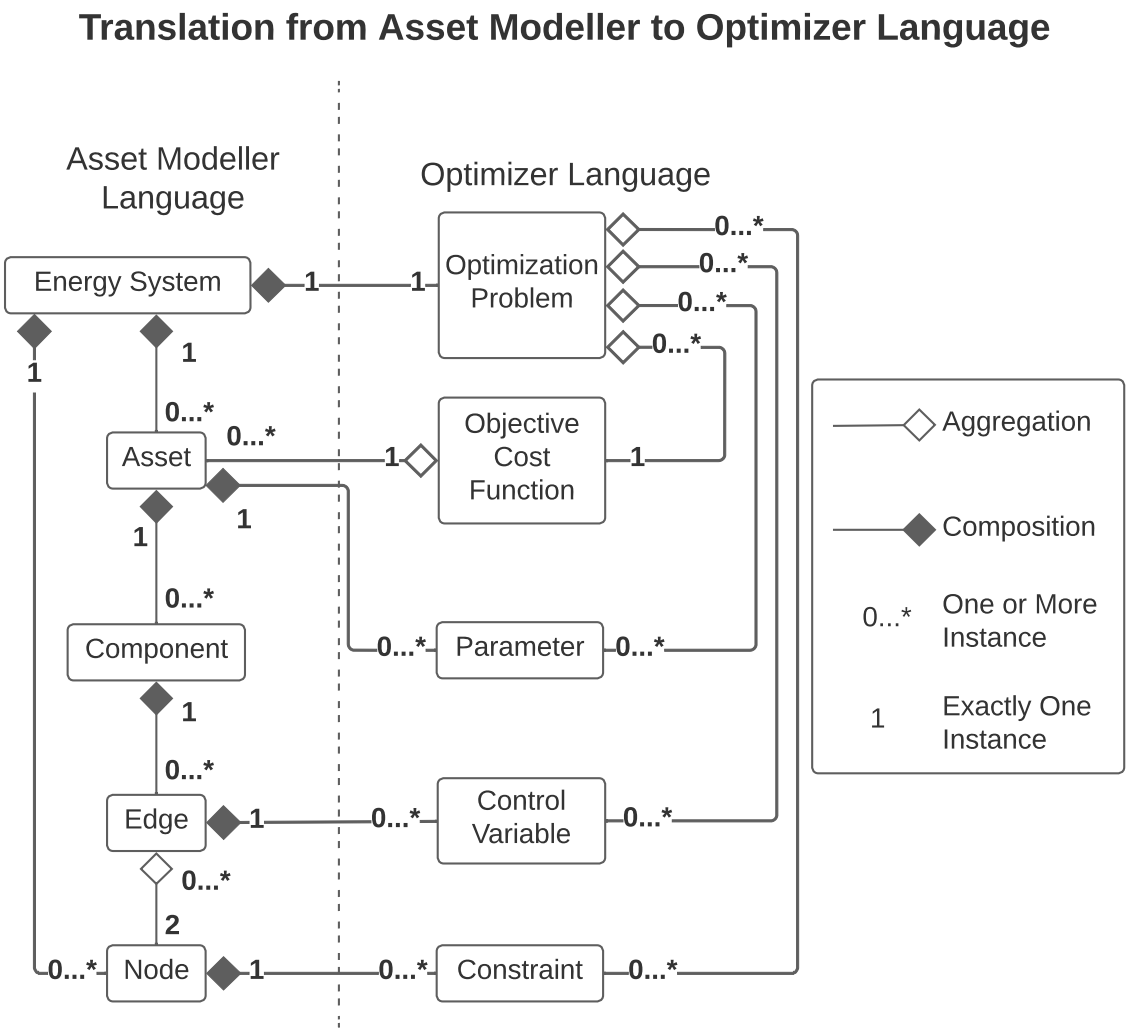

Figure 4.6: Diagram of translations from the asset modeller language to the optimizer language. An energy system in the asset modeller language maps to an optimization language in the optimizer language. Each asset has a cost in the asset modeller language that add up to form the objective cost function of the optimization problem. Each asset is also associated with optimization parameters. Each edge is associated with a set of optimization control variables. Each node is associated with a set of optimization constraints.

Each asset (α) has a cost (f_α) in the asset modeller language; these add up to form the objective cost function of the optimization problem f.

$$f = \sum_{\alpha} f_\alpha \tag{4.4}$$

Each asset (α) has parameters ($\vec{\mathbf{P}}_\alpha$). The set of parameters of all assets form the parameters of the optimization problem in the optimization language ($\mathbf{P}$).

$$\vec{\mathbf{P}} = \{\vec{\mathbf{P}}_\alpha | \forall \alpha\} \tag{4.5}$$

$\vec{P}$ can also be written as a vector of the parameters of the n assets in the energy system:

$$\vec{\mathbf{P}} = (\vec{\mathbf{P}}_1, \vec{\mathbf{P}}_2, ..., \vec{\mathbf{P}}_n) \tag{4.6}$$

The flow ($\vec{x}_\beta$) of each edge (β) in the asset modeller language is a control variable in the optimizer language. Thus, the control variable in the optimization language ($\vec{x}$) is the set of flows of all assets in the asset modeller language.

$$\vec{x} = \{\vec{x}_\beta | \forall \beta\} \tag{4.7}$$

$\vec{x}$ can also be written as a vector of the flows of the n assets in the energy system:

$$\vec{x} = (\vec{x}_1, \vec{x}_2, ..., \vec{x}_n) \tag{4.8}$$

Each node (i) in the asset modeller language has an inequality function ($\vec{g}_i$) and an equality function ($\vec{h}_i$). The inequality and equality constraints of the optimization problem in the optimizer language are the union of these constraints. The inequality constraint function ($\vec{g}$) in the optimizer language can be written as a vector of inequality functions of the n assets in the energy system:

$$\vec{g} = (\vec{g}_1, \vec{g}_2, ..., \vec{g}_n) \tag{4.9}$$

Similarly, the equality constraint function ($\vec{h}$) in the optimizer language can be written as a vector of inequality functions of the n assets in the energy system:

$$\vec{h} = (\vec{h}_1, \vec{h}_2, ..., \vec{h}_n) \tag{4.10}$$

This fully describes the translations from the asset modeller language to the optimizer language, and thus the STEVFNs model-generator. With this, a system designer can now describe an energy system design problem in the simple system designer language and have it systematically translated into a mathematical optimization problem in the optimizer language. This is possible because the asset modeller language and the two translations act as a bridge between the two languages.

4.4 Advantages and Limitations of STEVFNs

This section discusses the advantages and disadvantages of the STEVFNs model-generator compared to existing model-generators or tools in the literature.

4.4.1 Unified Energy Model

Model-generators in the literature have different models for different assets e.g. batteries, hydrogen, electricity lines, EVs, heating demand, solar panels, fossil fuel generators, etc. Model-generators such as OSeMOSYS, TIMES, and MESSAGE use "generalized technologies" and define them using input output matrices. However, they still fundamentally treat models for transport, conversion, storage and demand response energy services differently. E.g. storage is usually treated using snapshots in time, and the state of charge is a function not a decision variable: it is the cum-sum of all charging and discharging power in the past timesteps. This makes it difficult to model and study various assets and services together, especially when building optimization problems. STEVFNs provides a unified model-generator to model different energy assets, and different services using a common framework. This makes it very easy to model or study any generic energy systems asset. Insights from one type of asset or energy system function can then be easily translated to another asset or function. It also makes it easy to implicitly and systematically model the optimization problem. This is demonstrated in the implementation of STEVFNs as a tool in Chapter 7.

However, even though STEVFNs is able to model a lot of different energy assets, it will usually run slower than models that only simulate one type of energy asset or energy system function. More specialized models in the literature take advantage of

the specific structures of the assets or energy system functions that they are simulating. Thus, in these specific instances, they will run quicker than STEVFNs as they are specialized and optimized for their bespoke use case.

Existing models in the literature may be able to model individual assets more accurately than STEVFNs because they are not restricted to convex functions. The STEVFNs model-generator tries to guarantee convexity. This creates constraints on the type of functions that can be used to model assets. Some other models in the literature do not have such constraints, e.g. ACOPF. Thus, other models can be more accurate in simulating individual assets. However, we may relax the condition of convexity in STEVFNs. This just means that we cannot guarantee global optimality. This would mean we would need to use heuristic algorithms such as Machine Learning to solve the problem. However, we still have the rest of the benefits of STEVFNs and may be able to use it as a better simulation framework rather than an optimization framework. E.g. it could be used during training during reinforcement learning. The only change we would need to make in the model-generator is the optimization method adopted in the optimizer language.

4.4.2 Combined Sizing and Operation

Most energy systems optimization model-generators either do optimal sizing or optimal operation. Some models that try to do both do so by assuming a very simple operational strategy. However, different sized systems have different optimal operational strategies, and vice versa. Some research in the literature try to do bi-level optimization to solve this. They have an optimization problem for sizing an energy system, and have an optimal operation/control problem at each iteration of the sizing problem. This is very confusing to model and study, and the computational complexity of the problem grows quickly as the number of assets grows. In particular because they do not use the formalized notion of movement in time, they cannot harness parallel processing and the time complexity of problems increases. STEVFNs implements sizing costs as a function of the maximum of flows, rather than as constraints on flows at each time. This allows both sizing and operation at the same

time without the need for bi-level or multi-level optimization. This allows the harnessing of parallel architectures and reduces the time complexity of such problems. Some model-generators such as EFOM[174] and PREP-SHOT[175] are attempting to use the multi-level optimization or and other ways of splitting to apply parallel algorithms such as benders decomposition. However, the parallizability of these problems are limited because they treat time as snapshots.

Although STEVFNs is able to do both optimal sizing and operation concurrently, it may be slower than existing model-generators that only do either of these. Some model-generators in the literature may even be able to optimize for some operation alongside sizing. However, these models make very simple assumptions about the assets, such as linearity and number of timesteps, and take approximately the same time to rerun when parameters are updated. Examples of such tools include MARKAL/TIMES [9] or OSeMOSYS [8]. There are extensions to these models that try to relax these approximations, but these become limited due to computational run times.

Model-generators in the literature that only do optimal control/operation may be able to work faster than STEVFNs. This is obviously true if STEVFNs is optimizing for both sizing and operation. However, this may also be true for just operation. This is because these specialized model-generators are able to take advantage of special structures of the optimization problem. E.g. they may use the fact that the size of assets is constant. They may also take advantage of usage patterns, i.e. data, and apply heuristic algorithms for quick yet relatively accurate results. These include model predictive control and machine learning. However, researchers are working on machine learning algorithms, to train on ACOPF, and generate accurate inference functions that are convex [176]. STEVFNs will be able to use such machine learning algorithms to generate approximate convex functions. Machine learning algorithms can also be used to solve the optimization problem in STEVFNs when allowing the assets and thus problems to be non-convex.

4.4.3 Computable General Equilibrium Models

Most energy system optimization models or model-generators usually assume a fixed demand, such as OSeMOSYS. However, the quantity of energy service demanded could depend on the cost of the service. STEVFNs represents utility of quantity demanded as a negative cost. This thus allows STEVFNs to model market equilibrium similar to tools such as MARKAL/TIMES. However, MARKAL/TIMES explicitly models these costs and thus needs to distinguish different markets. It thus is only a partial equilibrium model: the equilibrium at each market is calculated separately, and we cannot see how one market affects another. This is because MARKAL/TIMES is restricted to a linear model. Some, such as Lavigne [157], attempt to introduce price elasticity, but need to use step functions that can cause numerical stability issues during optimization. Some also try to link macroeconomic models together such as with TIMES-MACRO [56] and TIMES MACRO Plus[177]. However, as both TIMES and MACRO linked models perform optimization, this leads to inefficiencies in optimization as well as obfuscation of how to simply models. STEVFNs allows for convex costs, not just linear costs. STEVFNs calculates the total cost of a system, and thus the total welfare of a system, i.e. all markets. It is thus able to maximize the total welfare of all markets and is able to account for the effect of one market equilibrium on another. STEVFNs is thus, a computable general equilibrium model, rather than a partial equilibrium model.

In the current formulation and implementation, the STEVFNs model-generator is only able to account for a traditional market equilibrium. However, there are various methods in the literature that model novel energy markets such as by using agent based decision making, stochastic decision making, least regret decision making, and hierarchical prioritization of demands. The current formulation and implementation of STEVFNs is currently unable to model these special markets. However, individual players in these markets may be modelled as assets. Their actions, or choices would then be modelled using flows along edges. This would thus allow STEVFNs to model a wide class of novel energy markets, not just traditional ones.

4.4.4 Rerunning Problems Quickly Using CVXPY

There are three main types of tools available in the literature: accounting tools such as MAED; scenario simulation tools such as MUSE; and optimization tools such as OSeMOSYS, MARKAL/TIMES, MESSAGE, PyPSA and Calliope. Accounting or simulation tools can run different scenarios very quickly (within seconds or minutes), and allow policymakers to quickly test the effect of different energy systems. However, while these tools allow users to predict the impact of different assumptions and system sizes, they require users to manually find the ideal size and operation for each set of scenario assumptions. This is where optimization tools come in; these are able to optimize the ideal system size (and sometimes some of the operation) for given scenario assumptions. However, these optimization tools take very long, hours or even days, to run one scenario. Modules such as OSeMOSYS-PuLP are able to do batch processing of scenarios, potentially in parallel. However, they require the list of scenarios to be tested to be know in advance. This limits the functionality of such tools as scenarios cannot be tested "on the fly". Because STEVFNs is able to take advantage of similar problem structures, solving optimization problems for different scenarios can be done orders of magnitude quicker. If a STEVFNs problem takes a few hours to run once, it can be rerun for another scenario, i.e. with updated parameters, in a matter of seconds. This is because STEVFNs is able to utilize disciplined convex programming and disciplined parametrized programming using CVXPY [173].

4.4.5 Convex Analysis

STEVFNs was built ground up with convexity in mind. It is thus very easy to guarantee that the optimization problem of an energy system design problem is convex using STEVFNs. As long as the conversion function of each component is concave, the component is convex. As long as each component of an asset is convex, and the conversion function of an asset is convex, the asset is convex. As long as each asset of an energy system is convex, the energy system (and its design problem) is convex. STEVFNs is implemented as a tool in Chapter 7 using CVXPY. This allows the convexity of each conversion function or cost function to be tested automatically

using CVXPY. CVXPY also automatically flags if any of these functions are non-convex.

Even when a problem is non-convex, STEVFNs allows quick and easy visualization of the non-convexity. It can then easily visualize approximations for those surfaces or functions that can make the problem convex. This is demonstrated further in modelling batteries in Chapter 5. Thus, STEVFNs also allows easy identification of assumptions that make a problem non-convex, and find good approximations to make the problem convex. This visualization can also show if no "good" convex approximation exists and quantify how "non-convex" a problem is. If no good approximations exist, heuristic algorithms should be used to solve the problem.

4.4.6 Parallel Computing

Most of the recent increases in computational speed have been achieved by parallelization. The increase in serial computational speed is now minimal, dwarfed by the increase in the number of cores of modern computers with massively parallel architectures such as multicore CPUs, GPUs and FPGAs. And STEVFNs uses the formalized notion of movement in time, the constraint at each time only depends on the neighbouring flows. This means that the problem can be naturally, and systematically split into various subproblems that can be solved independently. This allows the harnessing of the power of massively parallel architectures of modern computers. While the number of assets may only be of the order of tens, or hundreds; the number of processors in modern GPUs for example is of the order of thousand or tens of thousands. The number of timesteps of a simulation is of the order of tens or hundreds of thousands, thus allowing the harnessing of the power of increasingly parallel computers. This thesis only uses serial optimization algorithms. This is because SCS indirect GPU parallel solvers are still experimental and the author was unable to implement them on their machine. This is an easy extension for future research. The author of the thesis has tried using CUDA and GPU programming to build their own solver for a very small test case. This was able to run a few thousand times quicker than the equivalent sequential algorithm for that test case. Future research could build custom parallel convex solvers for CVXPY that can harness the structure of STEVFNs to

run quickly on parallel architectures, specifically Nvidia or AMD GPUs using CUDA or ROCm, respectively. Enzyme AD is a new tool that provided automatic differentiation for arbitrary kernels on the GPU [178, 179]. This is an excellent starting point for implementing custom parallel optimization implementation of STEVFNs on the GPU.

The full details of how STEVFNs can be parallelized by utilizing locality is beyond the scope of this thesis and will be developed in subsequent work. However, the following is an outline for how this parallelization can be done. This is to provide an intuitive understanding of locality and how the parallelization can be achieved without needing to understand the deep intricacies of GPU architecture.

In STEVFNs the constraints at a node can be added to the optimization cost using either a barrier or penalty function. The constraints at a node depend only on the input and output edges connected to the node. The flow into a node via an edge is a function of the flow of the edge. Thus, the constraint at a node depends only on the flow in the edges connected to the node. Thus, the constraint functions, and thus the associated barrier or penalty functions at each node can be calculated independently.

Figures 4.7(a) and 4.7(b) show schematics of computational dependencies for simulating a BESS using snapshots in time and flows in time, respectively. When snapshots in time are used, the constraint at a node depends on the values of all the edges at all previous times. The number of edges represent both computation and communications. However, when flows in time are used, the number of edges are reduced. More importantly, the average number of edges connected to each node is also reduced. This reduces the computation and communication times. Furthermore, this allows the parallelization of the problem as each node only depends on the flows at the immediately previous and next time.

When snapshots in time are used as in Figure 4.7(a), the SOC at a specific time is a function of the P at all previous times. Thus, the total number of edges, and thus the computational complexity, grows as $O(T^2)$, i.e. quadratic with time. Where T is the total number of timesteps. Because each subsequent SOC requires more

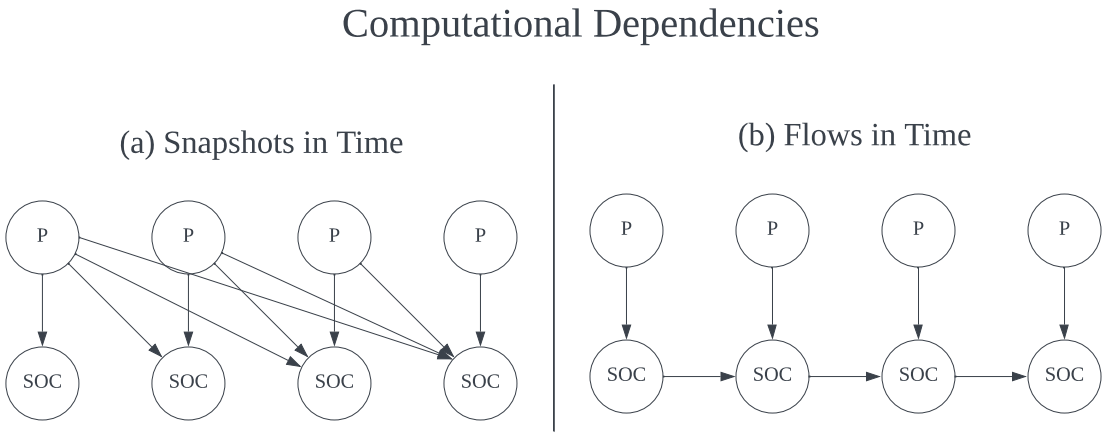

Figure 4.7: Computational Dependencies with Snapshots and Flows in Time. This is an example of calculations needed to simulate a BESS. P refers to the charging/discharging power at different times. SOC refers to the state of charge at different times. (a) When the BESS is simulated using snapshots in time, the SOC at a specific time is a function of the P at all previous times. Thus, the number of connections, and thus computations, grow as $O(T^2)$, i.e. quadratic with time. Where T is the number of timesteps. As the calculation of subsequent SOC requires more and more computations, the total computation cannot be split evenly to multiple processors. (b) When the BESS is simulated using snapshots in time, the SOC constraint at a specific time is only a function of the current SOC, previous SOC, and the current P. Thus, the total number of connections, and thus computations, grow as O(T), i.e. linearly with time. Furthermore, computational burden can be split evenly to different processors as the total number of timesteps grows.

computation than the previous, the total computation cannot be split equally to different processors.

When flows in time are used as in Figure 4.7(b), the SOC constraint at a specific time is only a function of the current SOC, previous SOC, and the current P. Thus, the total number of connections, and thus computations, only grow as O(T), i.e. linearly with time. Furthermore, each SOC constraint calculation requires the same amount of computation and the total computation can be equally split to different processors.

Figure 4.8 shows a schematic of the computation and communication in a parallel architecture using STEVFNs. The flows in the edges represent optimization control variables. The nodes contain optimization constraints. The information that needs to be stored is only the actual flows in the network, i.e. connections between nodes that are not connected, do not need to be stored. This eliminates the problem of "sparse matrices".

However, note that modern highly parallel GPU architecture consists of single instruction multiple data (SIMD) architecture. Thus, to take advantage of this, the same function needs to be performed on different values. The definition of "components" follows this structure. All edges of a component have the same conversion function, as they perform the same operation between different different times. Thus, GPUs can be used to perform these parallel operations, especially when timesteps of optimization increases dramatically. This allows the increase in optimization time resolution and time horizon by splitting the task to different GPUs. By not needing to calculate the constraints at different times sequentially, the overall time to calculate each timestep can be kept near constant. In practice, this time will slightly increase due to overheads in communications between GPU cores.

Even though less information needs to be stored, each edge is connected to two nodes, thus this information needs to be stored in both nodes, or in a shared location. During each optimization step, the change in the variable at each node is determined by the differential of the constraint function at both nodes, and the final value then needs to be communicated back to the two nodes. Thus, the communication between nodes is given by the edges surrounding a node. Nodes can also be considered as

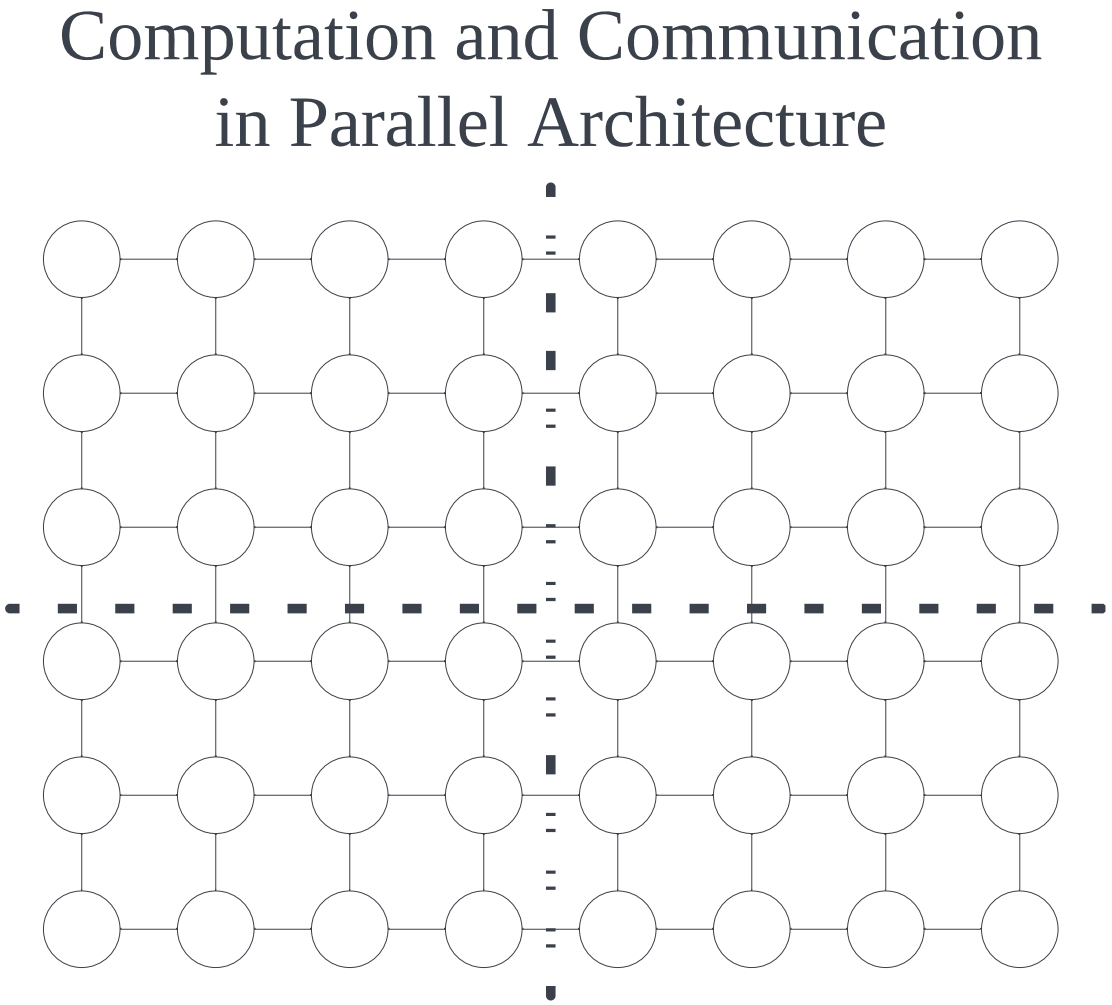

Figure 4.8: Computation and Communication in Parallel Architectures. Each node represents a computation. The number of edges connected to a node is the total calculations required at each node. Each edge represents the communication required between two computations. The dotted lines represent splittings of the total computation into different regions. Each region represents the total computation that will be completed by a processor. The only communication require between processors is the edges between processors. This is represented by the number of edges cut by the dotted line.

representing the "calculations" that need to be performed. Thus, multiple nodes can be mapped to one processor, this can be represented by the dotted lines creating regions in Figure 4.8. Thus, the total computation that needs to be completed by each processor is represented by the "area" of these regions, split by the dotted lines. The communication between processors is represented by the number of edges cut by the dotted surface splitting these regions. As communication costs are very high in parallel architectures, the splitting of processing needs to be done in such a way as to minimize the surface area to volume ratio. This is similar to packing problems, and intuitive solutions could be hexagons or spheres. However, GPUs have further sub-structures that make it more efficient if the number of computations are multiples of 32 or 64 depending on the specific architecture. This would mean that the ideal "shape" of the computation regions may be slightly ellipsoidal.

These highlight some intuitions of how locality is achieve in STEVFNs and how it can be harnessed to parallelize not just simulations, but optimization problems. These also give a general roadmap of how GPU architecture can be naturally mapped with the STEVFNs hierarchical framework of components and assets to harness the power of massively parallel SIMD architecture of modern and upcoming GPUs.

4.4.7 Sensitivity Analysis

The STEVFNs model-generator uses DPP from CVXPY. Recent developments allow for the differentiation of solutions (costs and control variables) with respect to the optimization parameters [24]. Even if optimization problems are rerun with DPP, it allows the measurement of how the optimal design of a system is affected by changes in parameters. This can be done much quicker than traditional methods as it employs DPP. This allows for incredibly quick and efficient sensitivity analysis of optimal energy system design that is currently not possible in the literature.

4.5 Summary

This chapter answers the thesis sub-question 2: "Can a model-generator of energy system design problems be developed, that utilizes the unified model-generator of assets, to co-optimize the sizing, operation, and location of real assets?" This chapter

develops the Space Time Energy Vector Flow Networks (STEVFN; pronounced like the name "Steven") model-generator to co-optimize the sizing, operation, and location of energy system assets with scenario assessment.

The STEVFNs model-generator translates energy system design problems into mathematical optimization problems. The STEVFNs model-generator consists of three languages and translations between these languages. A system designer describes the energy system problem in a simple, natural language. This gets translated into the asset modeller language; this is a slight modification of the generalized spatio-temporal asset model in chapter 3. Descriptions in the asset modeller language then get translated into a mathematical optimization problem described in the optimizer language. The optimizer language uses the syntax of disciplined convex programming (DCP) and disciplined parametrized programming (DPP).

The main question of the thesis is to determine if a generalized spatio-temporal model-generator of assets can be utilized to optimize the sizing, operation, and location of energy system assets. This chapter utilizes the generalized spatio-temporal model-generator of assets from chapter 3 to build the STEVFNs model-generator to optimize the sizing, operation, and location of any energy system assets. This chapter theoretically shows that this can be done for any energy system built of any energy system asset that can perform any combination of five energy system functions. While this chapter shows that solutions exist for building models for any energy system asset using the STEVFNs system design and unified asset model-generators, it does not show how assets can be built using the model-generators. It is still non-trivial to model concrete, real-world assets in STEVFNs using manufacturer data or simple black-box experimental measurements. Concrete, real-world examples of energy assets need to be modelled in STEVFNs before the STEVFNs model-generators may be used for a real case study. The next chapter models eleven classes of energy system assets using the STEVFNs model-generators.

Chapter 5

Modelling Real Assets Using STEVFNs

This chapter answers sub-question 3 of the thesis:

"How are models for real-world assets generated from traditional data using the model-generators?"

This chapter models eleven classes of simple and complex energy system assets using STEVFNs asset modeller language and manufacturer data-sheets, or simple black-box measurements.

The main question of the thesis is if a generalized spatio-temporal asset model-generator can be developed and used for the optimal sizing, operation and location of energy system assets. Chapter 3 develops and presents a generalized spatio-temporal asset model-generator that can model any energy asset that can perform any combination of the five basis functions of an energy system. Chapter 4 uses this asset model-generator as an intermediary "asset modeller" language to build a system design model-generator to map whole energy system design and operation problems to mathematical optimization problems. This model-generator is called STEVFNs. While chapters 3 and 4 theoretically answer the thesis question, it is non-trivial to model concrete, real-life energy assets in STEVFNs. This consists of both describing an asset in the asset modeler language using the generalized spatio-temporal asset model-generator, and defining the translations to the system designer language. This needs to be done before STEVFNs can be used to solve real case studies.

This chapter models various concrete, real-world assets in STEVFNs. The real-world data required is easily obtainable. I.e. it is either present in asset datasheets, or

can be easily measured by treating the asset as a black-box. This chapter models assets that consist of only one component and that can perform any one of the five basis functions of an energy systems, individually; these are referred to as simple assets. As there are only five types of simple assets, this chapter models all five of these simple assets. This chapter also models six assets that consist of multiple components and/or can perform multiple energy system functions; these are are referred to as complex assets. As there are potentially infinite number of complex assets, this chapter only models a few common complex assets. This set of assets includes assets with multiple components and/or that perform multiple basis functions of an energy system. This demonstrates how any complex asset may be modelled. In modelling these assets in the asset modeller language and translating them to the system designer language, this chapter demonstrates how to easily identify what might make the optimization problem non-convex. And if so, it demonstrates how STEVFNs makes apparent the class of approximations that can be made to make the problem convex.

Section 5.1 first models the five types of simple energy assets. With this, the reader should become accustomed to the process of modelling assets in STEVFNs. Section 5.2 then models six complex energy assets. Modelling these complex energy assets also demonstrates how STEVFNs can help make clear what asset assumptions make an energy system design problem non-convex. And in those situations, it demonstrates how to find approximations to make the asset, and thus the energy system optimization problem, convex. Section 5.3 finally concludes the chapter by summarizing the limitations of the models presented in the chapter as well as future assets that need to be modelled in STEVFNs.

5.1 Simple Energy Assets

To get accustomed to modelling assets in STEVFNs, this chapter first models the five simple energy assets. These are one asset for each of the five basis functions of an energy system: energy demand, energy supply, energy transportation, energy storage and energy conversion. This will allow the reader to understand the basics of the languages in STEVFNs and the process of building translations between them. It

Table 5.1: Template Edge of Electricity Transport Component

Source Node Type	Electricity Grid (EL)
Target Node Type	Electricity Grid (EL)
Source Node Location	Location 1
Target Node Location	Location 2
Operational Time Difference (δt)	1 hour
Time Difference Between Target and Source Node (Δt)	0 hour

will also help the reader get accustomed to thinking in the languages of STEVFNs when describing assets.

5.1.1 Electricity Line

Consider a simple asset that only performs the energy system function of energy transportation, i.e. it only transports a flow from one location to another location without any change in time or type. An example of this is an electricity line, such as a HVDC or AC transmission line. For simplicity, consider one electricity line that can be operated independently, i.e. the power going through the line can be controlled independently of other electricity lines. Also assume that electricity can only flow in one direction along this line.

In the asset modeller language, we can model such an electricity line as an asset with one component: the electricity line component. The electricity line component represents the flow of electricity along the electricity line in one direction.

The electricity line component moves electricity from the electricity grid node at a specific location and time, to the electricity grid at a different location but same time. An illustration of the template edge of the electricity transport component is shown in Figure 5.1. This diagram is referred to as the "Template Edge Diagram". The template edge of the electricity transport component is defined by the following:

Consider the conversion function (ψ) of the electricity line component. The flow leaving the source node and the flow entering the target node are both of type "electricity". Thus, the conversion function of the edges of the forward component can be viewed as containing the transport efficiency. The power flowing out of the electricity grid and into the electricity line at location 1 at time t is $P_{in}(t)$. The power flowing into the electricity grid and out of the electricity line at location 2 is P_{out}. Assume

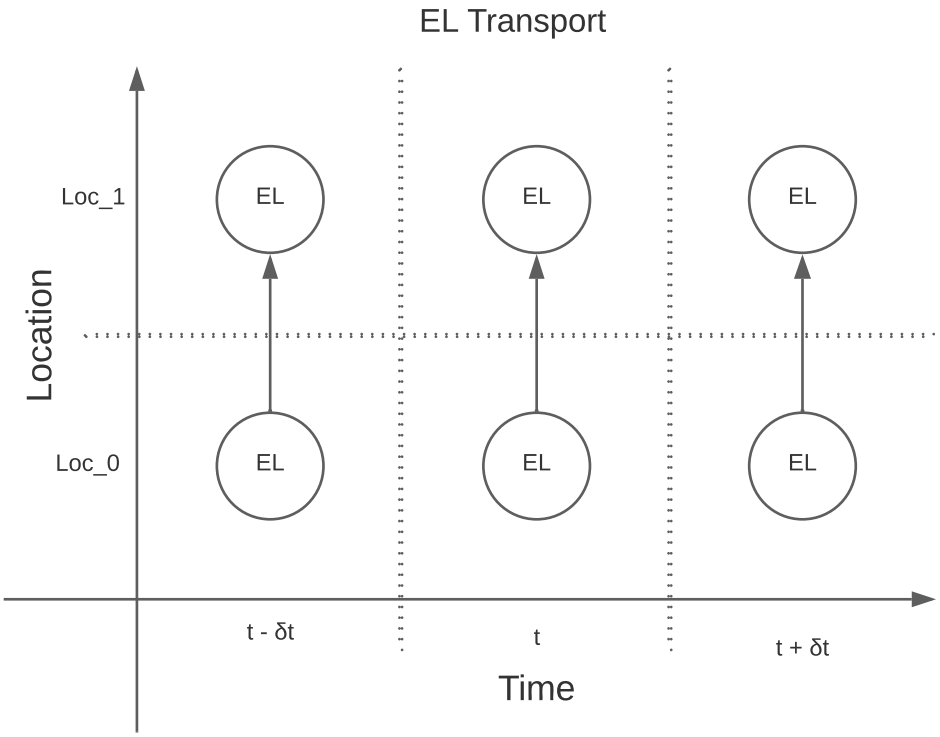

Figure 5.1: Template Edge Electricity Line. The single directional electricity line asset only has one component. The template edge of this component moves electricity from the "Electricity Grid" node (EL) at a specific location and time to the Electricity Grid node (EL) at a different location but same time.

that the electricity line has resistance R, and the voltage at the source node and target nodes are V_0 and V_1, respectively. Let I_t be the current along the line at time t, thus:

$$V_1 = V_0 - I_t R \tag{5.1}$$

P_{in} is given by:

$$P_{in} = V_0 I_t \tag{5.2}$$

P_{out} is similarly given by:

$$P_{out} = V_1 I_t \tag{5.3}$$

Combining Equations 5.1, 5.2, and 5.3 gives:

$$P_{out} = P_{in} - (I_t)^2 R = P_{in} - \frac{R}{V_0^2}(P_{in})^2 \tag{5.4}$$

This is a concave function in P_{in}, and will keep the optimization problem convex. Thus, the quadratic losses in an electricity line can be simulated to optimize the operation of an electricity line.

Consider the sizing cost of this electricity line. The capital cost of the electricity line (f_{cap}) is proportional to the length (L) of the line and the cross-sectional area (A) of the line.

$$f_{cap} = C_{cap} L A \tag{5.5}$$

C_{cap} is the capital cost of the electricity line per unit length, per unit area. Where C_{cap} and L are parameters and can be combined into one parameter. A is a decision variable. This gives us a linear sizing cost for the asset.

However, the resistance of the line also depends on the length and cross-sectional area:

$$R = \frac{\rho L}{A} \tag{5.6}$$

Where ρ is the resistivity of the electricity line.

Equation 5.4 now transforms to:

$$P_{out} = P_{in} - \frac{\rho L}{V_0^2} \frac{(P_{in})^2}{A} \tag{5.7}$$

This is shown in Figure 5.2.

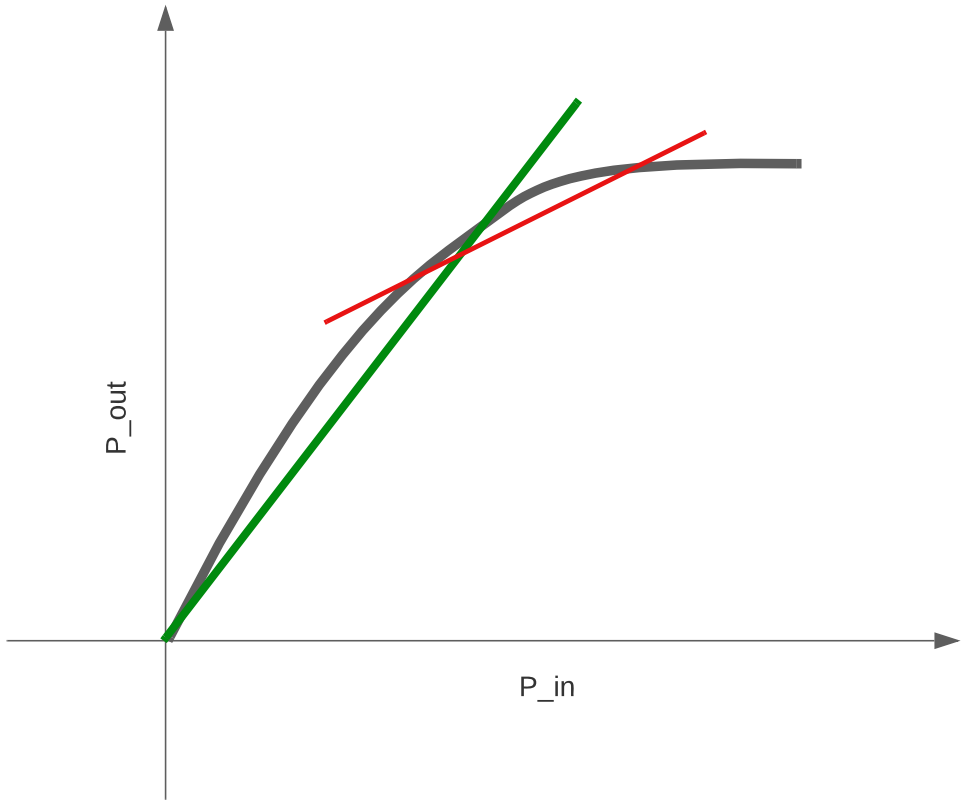

Figure 5.2: I^2R Losses. An electricity line may be represented as a resistor. The output power (P_{out}) is a function of the input power (P_{in}). If we assume a constant voltage at the start of the line and constant resistance, this will be a quadratic curve. This curve may be approximated by assuming P_{out} is proportional to P_{in}; this is shown using the green line. This is equivalent to saying that the electricity line has fractional losses, or constant efficiency. If we know that we will only be operating the electricity line at higher powers, we may instead use a linear approximation closer to the region of operation; this is shown as the red line.

Even if the various parameters are combined into one parameter, the P_{out} is now no longer concave with the decision variables P_{in} and A. Thus, the combined optimal operation and sizing of a single electricity line will be a non-convex problem.

A similar situation occurs when trying to optimize the sizing and operation of a line with DCOPF in PyPSA. Even though optimizing the operation with DCOPF is a convex (linear) problem, the co-optimization of sizing and operation in DCOPF is non-convex as the admittance matrix values become variables. This is why PyPSA uses domain specific heuristic algorithms and bi-level optimization when performing sizing and operation of power grids [11]. Similar techniques can be applied to other model-generators such as MARKAL and OSeMOSYS using NLP techniques with similar associated computational time penalties.

Consider an approximation for the conversion function to make the problem convex. In the literature, the losses of a HVDC line are assumed to be proportional to the length of the line [180, 181, 182]. This is equivalent to a straight line as shown in Figure 5.2. The straight line is a reasonable approximation if the line operates over a certain power region. If it is known that the electricity line will be operated in a much smaller region away from zero power, the second line may be used to better approximate that region of the curve. For simplicity, assume that losses are a fixed fraction of the energy transported, i.e. the line that goes through the origin.

The flow along the edges of the electricity line component at operational time t (x_t) is the amount of electrical energy that moves out of the electricity grid node at location 1 from time t to time $t + \delta t$. y_t is the flow of electrical energy into the electricity grid node at location 2 at time t, and is given by the conversion function, ψ. The conversion function of the electricity line component (ψ) is given by:

$$y_t = \psi(x_t) = (1 - L\mu)x_t \tag{5.8}$$

Where μ is the fractional loss per unit distance, and is an asset brand parameter in the system designer language. μ has units m^{-1} L is the length of the electricity line, and is defined by the lat-lon of locations 1 and 2 in the system designer language. L has units m.

For simplicity, the electricity line can be assumed to go along the shortest path, or "as the bird flies", and L can be approximated as:

$$L(\phi_1, \lambda_1, \phi_2, \lambda_2) = R \cos^{-1}\left(\sin\phi_1 \sin\phi_2 + \cos\phi_1 \cos\phi_2 \cos\left(\lambda_2 - \lambda_1\right)\right) \tag{5.9}$$

Where R is the radius of the earth and is a constant, ϕ_1 and λ_1 are the latitudes and longitudes of location 1 in the system designer language, and ϕ_2 and λ_2 are the latitudes and longitudes of location 2 in the system designer language.

Equation 5.8 is not DPP with respect to μ and the lat-lon of locations 1 and 2. However, the expression with μ and L can be combined to define a new parameter η:

$$\eta = 1 - L\mu \tag{5.10}$$

Where η is unitless and can be interpreted as the efficiency of the electricity line. The conversion function of the electricity line from Equation 5.8 now transforms to:

$$y_t = \psi(x_t) = \eta x_t \tag{5.11}$$

And this conversion function is now DPP.

The conversion function parameters ($\vec{\mathbf{P}}_\psi$) of the electricity line component is just η:

$$\vec{\mathbf{P}}_\psi = (\eta) \tag{5.12}$$

The cost of the electricity line component (and thus asset) can be separated into the sizing and operational costs. The sizing cost for the electricity line is the capital cost of the line. In the literature, the capital cost of an electricity line can be assumed to be proportional to the length of the line and the maximum power rating of the line. The maximum power rating of the line can be defined as the maximum power going through the line. The cost of sizing the electricity line ($f_{size,t}$) to meet the flow at time t is given by:

$$f_{size,t}(x_t) = \frac{C_{size} L}{\delta t} x_t \tag{5.13}$$

Where C_{size} is an asset brand parameter in the system designer language; this is the capital cost per peak power capacity of the line, per unit distance. C_{size} has units $[\$\,\mathrm{kW_p^{-1}\,km^{-1}}]$. C_{size}, L and δt can be combined into one parameter ($\mathbf{P}_{f_{size}}$):

$$\mathbf{P}_{f_{size}} = \frac{C_{size} L}{\delta t} \tag{5.14}$$

The cost of sizing the electricity line (f_{size}) to meet the flow at all times is the maximum of $f_{size,t}$ across all times:

$$f_{size} = \max_t\{f_{size,t}\} = \mathbf{P}_{f_{size}} \max_t\{x_t\} \tag{5.15}$$

The operation of the electricity line causes some degradation and thus requires maintenance. Assume that the maintenance cost is proportional to the total energy that flows through the line. The usage cost of the electricity line ($f_{use,t}$) at operational time t is given by:

$$f_{use,t} = C_{use} L x_t \tag{5.16}$$

Where C_{use} is an asset brand parameter in the system designer language; this is the operation and management cost per energy shifted, per unit distance. C_{use} has the units [\$ $\mathrm{kWh}^{-1}\,\mathrm{km}^{-1}$]. C_{use} and L can be combined to form the parameter ($\mathbf{P}_{f_{use}}$)

$$\mathbf{P}_{f_{use}} = C_{use} L \tag{5.17}$$

The usage cost of operating the electricity line over all times (f_{use}) is the sum of $f_{use,t}$ over all operational times, t:

$$f_{use} = \sum_t f_{use,t} = \mathbf{P}_{f_{use}} \sum_t x_t \tag{5.18}$$

The total cost of the electricity line asset (f_{asset}) is the sum of the sizing and usage costs and is given by:

$$f_{asset} = f_{size} + f_{use} = \mathbf{P}_{f_{size}} \max_t x_t + \mathbf{P}_{f_{use}} \sum_t x_t \tag{5.19}$$

The cost function parameters of the electricity line asset ($\vec{\mathbf{P}_f}$) is given by:

$$\vec{\mathbf{P}_f} = (\mathbf{P}_{f_{size}}, \mathbf{P}_{f_{use}}) \tag{5.20}$$

Where $\mathbf{P}_{f_{size}}$ and $\mathbf{P}_{f_{use}}$ are defined by the asset brand parameters using Equations 5.14 and 5.17, respectively.

The flows, asset brand parameters, conversion function parameters, cost function parameters of the electricity line, and their units, are compiled in Table 5.2.

Table 5.2: Flows and Parameters of Electricity Line Asset

Symbol	Meaning	Units	Language
ϕ_i	Latitude of location i	rad	System Designer
λ_i	Longitude of location i	rad	System Designer
μ	losses per distance	m^{-1}	System Designer
C_{size}	Capital cost per peak power capacity	$\$\,\mathrm{W_p^{-1}\,m^{-1}}$	System Designer
C_{use}	Operational cost per distance per energy shifted	$\$\,\mathrm{Wh^{-1}\,m^{-1}}$	System Designer
η	Transport Efficiency	unitless	Asset Modeller
$\mathbf{P}_{f_{use}}$	Cost per energy moved	$\$\,\mathrm{Wh^{-1}}$	Asset Modeller
$\mathbf{P}_{f_{size}}$	Cost per peak energy moved	$\$\,\mathrm{Wh_p^{-1}}$	Asset Modeller
x	Electrical energy leaving source node	Wh	Asset Modeller
y	Electrical energy entering target node	Wh	Asset Modeller

5.1.2 Fossil Fuel Power Generator

Consider a simple energy asset that only performs the basis function of energy generation. A conceptually simple energy generation asset is a fossil fuel electricity power generator. This is referred to as the "fossil fuel power generator asset". This power generator can be for example a natural gas power plant, a coal power plant, or a diesel generator. Ramp rate constraints may be added, but they will make the asset more complex (i.e. require multiple components). For simplicity, assume that there are no ramp rate constraints. The sizing cost is the cost of purchasing the power plant. The usage cost is the fuel cost, which the power plant consumes and converts to electricity.

To model a power plant, the conversions, or flows of energy in a power plant need to be considered. A fossil fuel power plant takes fuel (chemical potential energy) as an input, and outputs electrical energy. This would make a fossil fuel power plant perform the energy conversion function and will be useful for building circular economy models. However, for simplicity, assume that the power plant generates electrical power and moves it to the electricity grid, and has a cost associated with it. The cost associated with using the power plant is the fuel consumed by the power plant. Thus, a fossil fuel power plant asset can be described in the asset modeller language as an asset with one component: the "electricity generator" component.

The electricity generator component moves electricity out of the power plant node at a specific time and location, and moves it into the electricity grid node at the same

Table 5.3: Template Edge of Electricity Transport Component

Source Node Type	Power Plant (PP)
Target Node Type	Electricity Grid (EL)
Source Node Location	Location 1
Target Node Location	Location 1
Operational Time Difference (δt)	1 hour
Time Difference Between Target and Source Node (Δt)	0 hour

time and location. The template edge diagram of the electricity generator component is shown in Figure 5.3. The template edge of the electricity generator component is defined in Table 5.3.

As this is a generation component, the conversion function at the source node does not get added as a constraint to the optimization problem. Such a node is referred to as a "virtual node". It represents the fact that the amount of energy flowing out of the node is unconstrained.

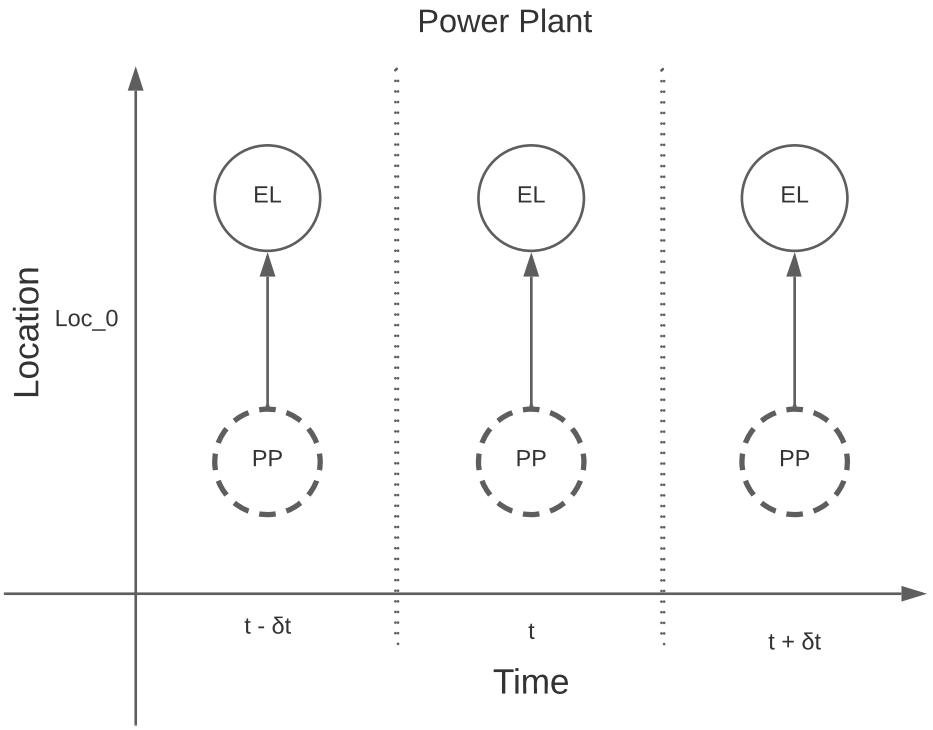

Figure 5.3: Template Edge of the electricity generator component. The power plant asset only has one component. The template edge of this component moves electricity from the "Power Plant" node at a specific location and time to the "Electricity Grid" node at a same location and time.

Consider the conversion function of the electricity generator component. Consider the edge at operational time t. The flow out of the power plant is of type "electrical energy". This is the electrical energy produced by the power plant during that timestep. The flow going into the electricity grid node is also of type "electrical energy". This is energy entering the grid from the power plant. In this simple case, these two values are equivalent, thus the conversion function of the edge of the electricity generation component at operational time t is:

$$y_t = \psi_t(x_t) = x_t \tag{5.21}$$

Where x_t is the flow of the edge, i.e. the flow out of the power plant node. y_t is the flow into the electricity grid node, and is defined by the conversion function (ψ). x_t is an optimization decision variable with a dimension of one. This conversion function has no parameters as it is simply the unity function.

The total cost of the fossil fuel power plant asset is the sum of the sizing cost (f_{size}) and the usage cost(f_{use}) of the electricity generation component. The total cost of the fossil fuel power plant can also be split into the capital cost and fuel cost. The capital and O&M costs may not coincide with the sizing and usage costs. The sizing cost only depends on the size of the power generation component. The sizing cost can be split into two parts: the capital cost of the power plant, and the cost of the fixed fuel consumption. The usage cost is the variable fuel consumption cost at each operational time.

The size of a power plant can be determined by various factors such as reserve constraints, and market requirements. For this example, consider a power plant that is sized to provide peak power demand. The stylized capital cost of a power plant as a function of the maximum power generated by the power plant is shown in Figure 5.4(a). For simplicity, the capital cost can be assumed to be proportional to the peak power supplied. The capital cost of sizing the electricity generator component ($f_{cap,t}$) to satisfy the operation of the component at time t is thus given by:

$$f_{cap,t} = \frac{C_{cap}}{\delta t} x_t \tag{5.22}$$

Where C_{cap} is a parameter in the system designer language. C_{cap} is the capital cost of the fossil fuel power plant per unit peak power and has the units $\$\,\mathrm{kWp}^{-1}$.

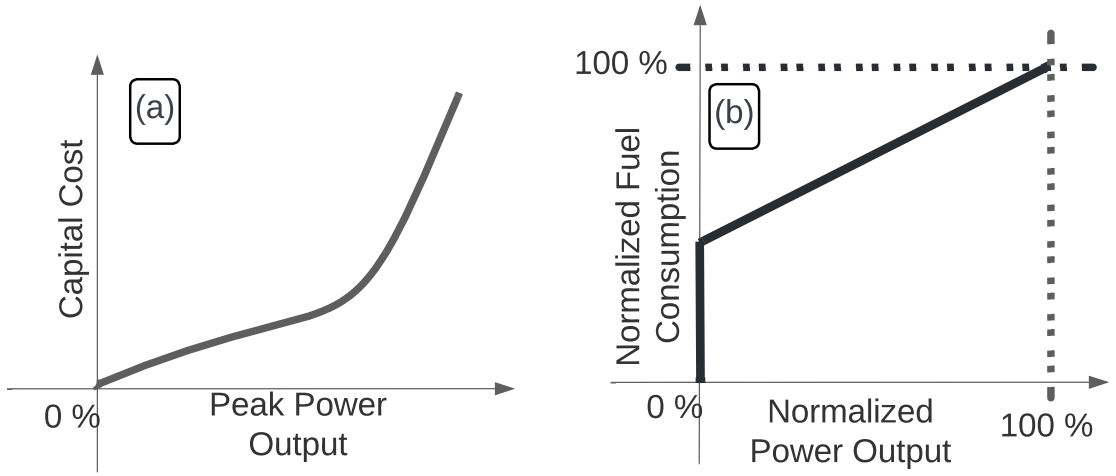

Figure 5.4: (a): Stylized Capital Cost Power Plant The capital cost of a power plant depends on the peak power output or capacity of the power plant.
(b): Stylized Fuel Consumption Power Plant. The fuel consumption of a power plant depends on its peak power and the power produced. We may normalize this by looking at the fraction of maximum fuel consumed as a function of fraction of maximum power produced. We note that a power plant has some "standing" losses. I.e. some fuel is still consumed even if no power is being produced. These go down to zero if we wish to simulate switching the power plant on or off. This would make the cost concave, and thus the problem non-convex. We may instead assume the power plant is always being operated. The standing costs may then be considered as sizing costs as they depend on the maximum power of the power plant and not their operation.

The stylized fuel consumption as a function of normalized power is given in Figure 5.4(b). For simplicity this can be fit to a linear function:

$$\alpha = \alpha_0 + (1 - \alpha_0)\frac{P}{P_{max}} \tag{5.23}$$

Where α is the normalized fixed fuel consumption. When $P = P_{max}$, $\alpha = 1$. I.e. when the power is equal to the maximum power, the fuel consumption is equal to the maximum fuel consumption. α_0 is an asset brand parameter and is unitless. The hourly fuel consumed (β) at time t is the product of the normalized fuel consumption and the peak capacity of the power plant:

$$\beta = A_{max}P_{max}\alpha = A_{max}\alpha_0 P_{max} + A_{max}(1 - \alpha_0)P \tag{5.24}$$

Where A_{max} is the maximum hourly fuel consumption of a power plant per peak power of the power plant and has the units [$\mathrm{kg\,h^{-}1\,kW_p^{-1}}$]. α_0 and A_{max} are brand parameters for the power plant. The first term can be seen as the fixed fuel consumption, the fuel consumption even when the plant is not producing any power. It is thus the minimum amount of fuel that the plant consumes. This fixed fuel consumption may be taken as part of the sizing cost as it depends only on the sizing of the plant, and not its operation. The fixed fuel consumption cost ($f_{fixed,t}$) of sizing the electricity generator component to operate time t is:

$$f_{fixed,t} = C_{fuel}A_{max}\alpha_0 T_{lifetime}x_t \tag{5.25}$$

Where C_{fuel} is the price of fuel and has the units [$\mathrm{\$\,kg^{-1}}$]. $T_{lifetime}$ is the lifetime that the asset will be run for, and has the units [h]

The total sizing cost (f_{size}) of the asset is the maximum of the total sizing cost required at each time t, and is given by:

$$f_{size} = \max_t\{f_{cap,t} + f_{fixed,t}\} = (\frac{C_{cap}}{\delta t} + C_{fuel}A_{max}\alpha_0 T_{lifetime})\max_t\{x_t\} \tag{5.26}$$

All the asset brand parameters can be combined into one parameter ($\mathbf{P}_{f_{size}}$):

$$\mathbf{P}_{f_{size}} = \frac{C_{cap}}{\delta t} + C_{fuel}A_{max}\alpha_0 T_{lifetime} \tag{5.27}$$

Where C_{cap} is the capital cost per unit peak power in [$\mathrm{\$\,kWp^{-1}}$]. A_{max} is the peak hourly fuel consumption per peak power of a power plant in [$\mathrm{kg\,h^{-}1\,kW_p^{-1}}$]. α_0 is the

fraction of fuel that is fixed fuel consumption of a power plant and is unitless. C_{fuel} is the cost per unit fuel, i.e. fuel price in [$\$\,\mathrm{kg}^{-1}$]. $t_{lifetime}$ is the total lifespan of the power plant asset in [h].

Equation 5.26 thus transforms to:

$$f_{size} = \mathbf{P}_{f_{size}} \max_t\{x_t\} \tag{5.28}$$

The second part of the fuel cost is the usage cost of the asset. The cost of using the asset at time t is $f_{use,t}$, and is given by:

$$f_{use,t}(x_t) = C_{fuel} A_{max}(1 - \alpha_0)x_t \tag{5.29}$$

The various asset brand parameters can be combined to one cost function parameter ($\mathbf{P}_{f_{use}}$):

$$\mathbf{P}_{f_{use}} = C_{fuel} A_{max}(1 - \alpha_0) \tag{5.30}$$

The total usage cost over all times (f_{use}) is the sum of the usage costs:

$$f_{use} = \sum_t f_{use,t} = \mathbf{P}_{f_{use}} \sum_t x_t \tag{5.31}$$

The total cost of the asset (f_{asset}) can thus be written as:

$$f_{asset} = f_{size} + f_{use} = \mathbf{P}_{f_{size}} \max_t\{x_t\} + \mathbf{P}_{f_{use}} \sum_t\{x_t\} \tag{5.32}$$

The conversion function parameter (P_f) in the asset modeller language is thus:

$$\vec{\mathbf{P}_f} = (\mathbf{P}_{f_{size}}, \mathbf{P}_{f_{use}}) \tag{5.33}$$

The flows, asset brand parameters, conversion function parameters, cost function parameters of the fossil fuel power generator, and their units, are compiled in Table 5.4.

5.1.3 Elastic Temporal Demand

Consider an asset that only performs the energy system function of energy demand, i.e. it moves quantities into a virtual sink node. An example of this is the elastic demand for electricity at each hour.

Table 5.4: Flows and Parameters of Fossil Fuel Power Generator Asset

Symbol	Meaning	Units	Language
$T_{lifetime}$	Operational Lifetime	h	System Designer
C_{cap}	Capital cost per peak power capacity	$\$\,\mathrm{W_p^{-1}}$	System Designer
C_{fuel}	Fuel Price	$\$\,\mathrm{kg^{-1}}$	System Designer
A_{max}	Maximum fuel consumption rate per peak power	$\mathrm{kg\,h^{-1}\,W_p^{-1}}$	System Designer
α_0	Minimum fractional fuel consumption	unitless	System Designer
$\mathbf{P}_{f_{use}}$	Cost per electricity generated	$\$\,\mathrm{Wh^{-1}}$	Asset Modeller
$\mathbf{P}_{f_{size}}$	Cost per peak electricity generated	$\$\,\mathrm{Wh_p^{-1}}$	Asset Modeller
x	Electrical energy leaving source node	Wh	Asset Modeller
y	Electrical energy entering target node	Wh	Asset Modeller

Table 5.5: Template Edge of Elastic Electricity Demand Component

Source Node Type	Electricity Grid (EL)
Target Node Type	Electricity Demand ($\mathrm{EL_D}$)
Source Node Location	Location 1
Target Node Location	Location 1
Operational Time Difference (δt)	1 hour
Time Difference Between Target and Source Node (Δt)	0 hour

In the asset modeller language, the elastic electricity demand asset can be modelled as an asset with one component: the elastic electricity demand component. The elastic electricity demand component represents the amount of electricity consumed at a specific location at each hour.

The elastic electricity demand component moves electrical energy out of the electricity grid node at a specific location and time, and into the electricity demand node at the same location and time. The template edge diagram of the electricity transport component is shown in Figure 5.5. The template edge for the elastic electricity demand component is defined by Table 5.5:

The electrical energy flowing into the electricity demand node is equal to the electrical energy flowing out of the electricity grid node. Thus, the conversion function (ψ) of the elastic electricity demand component is given by:

$$y_t = \psi(x_t) = x_t \tag{5.34}$$

Where y_t is the flow of electricity into the electricity demand node at time t. Where x_t is the electrical energy flowing out of the electricity grid node at time t.

As the flow of energy into the electricity demand node is not constrained, the electricity demand node is a virtual node. And, the elastic electricity demand component

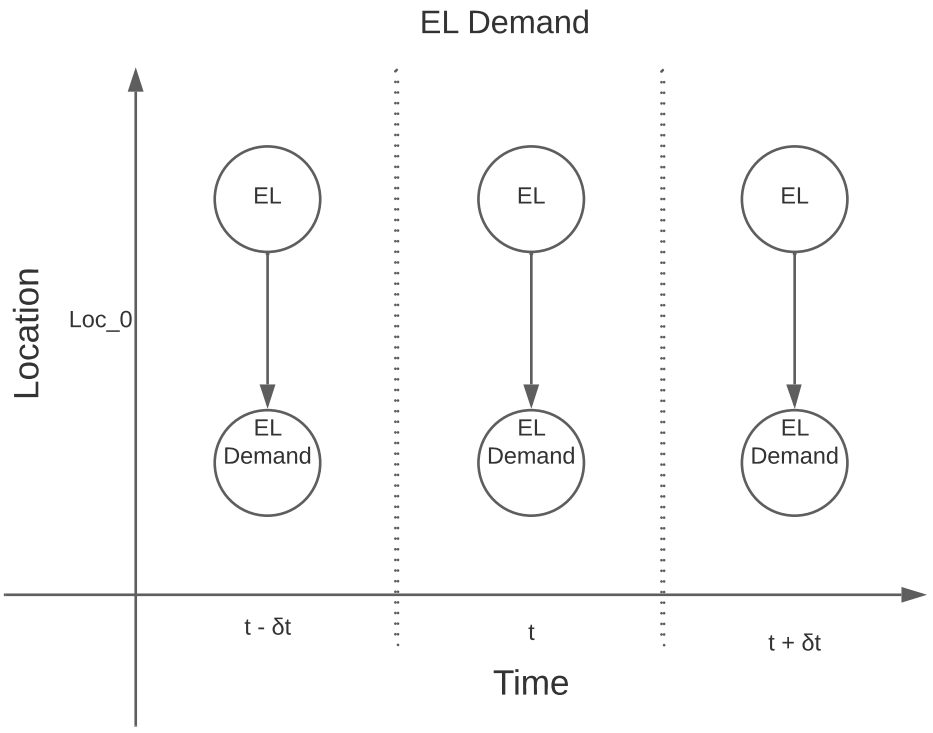

Figure 5.5: Template Edge Elastic Electricity Demand Asset. The elastic electricity demand asset only has one component. The template edge of this component moves electricity out of the "Electricity Grid" node (EL) at a specific location and time, and into the "Electricity Demand" node (D_{EL}).

fulfils the energy system function of energy demand, or consumption.

The elastic electricity demand component has no conversion function parameter, i.e.:

$$\mathbf{P}_{\psi} = \emptyset \tag{5.35}$$

The cost function of the elastic electricity demand at each timestep can be viewed as the negative of the utility of consuming that amount of electricity demand. The utility of consumption is the integral for the demand curve in economics. The price of electricity demanded at each time (C_t) is a linear function of quantity of electricity demanded at that time (x_t), and is given by:

$$C_t(x_t) = A_t - B_t x_t \tag{5.36}$$

Where A_t and B_t are asset parameters in the system designer language. A_t is the price of electricity demanded, at time t, when the quantity demanded is zero. B_t is the reduction in price of electricity demanded per increase in quantity of electricity demanded at time t.

The total utility at a specific time is the integral of Equation 5.36. The total cost at a specific time (f_t) is the negative of that integral and is given by:

$$f_t = -\int_{x=0}^{x_t} C_t dx = -A_t x_t + \frac{B_t}{2}(x_t)^2 \tag{5.37}$$

The cost function of the elastic electricity demand asset (f_{asset}) is the sum of f_t over all times:

$$f_{asset} = \sum_t f_t = \sum_t \left[-A_t x_t + \frac{B_t}{2}(x_t)^2 \right] \tag{5.38}$$

The cost function parameters for the elastic electricity demand asset ($\vec{\mathbf{P}}_f$) are:

$$\vec{\mathbf{P}}_f = (\vec{A}, \vec{B}) \tag{5.39}$$

Where $\vec{A}$ and $\vec{B}$ are the set of values of A_t and B_t at each time. All A_t and B_t are asset brand parameters in the system designer language.

In general, the demand curve represents the negative differential of the cost function. For the cost function of a demand asset to be convex, the demand curve needs to be not increasing. Thus, if an asset has a demand curve that is upwards sloping

Table 5.6: Flows and Parameters of Elastic Temporal Demand Asset

Symbol	Meaning	Units	Language
A	Vertical intersection of demand curve	$\$\,\mathrm{Wh}^{-1}$	System Designer Asset Modeller
B	Downwards slope of demand curve	$\$\,\mathrm{Wh}^{-2}$	System Designer Asset Modeller
x	Electrical demand leaving source node	Wh	Asset Modeller
y	Electrical energy entering target node	Wh	Asset Modeller

at any point, it will be concave. Assets with upwards sloping demand curves are referred to as "luxury goods". Thus, optimizing an energy system with demand assets that are luxury goods is non-convex, and thus, in general, a computationally hard problem. Energy systems with markets with luxury goods must thus be optimally designed using heuristic algorithms such as machine learning. Lavigne attempts to introduce elasticity in OSeMOSYS [157], but is only able to approximate it using step functions. By allowing the cost function to be convex, all downward sloping demand curves can be fully modelled, i.e. even ones with changing elasticity.

The flows, asset brand parameters, conversion function parameters, cost function parameters of the Elastic Temporal Demand asset, and their units, are compiled in Table 5.6.

5.1.4 Hydrogen Storage Tanks

Consider the modelling of a simple asset that only fulfils the energy system function of energy storage, or flow in time. As an example, consider a hydrogen storage tank. Assume that there are some losses or "self discharge" of hydrogen that depends on the hydrogen stored in the tank. The hydrogen in the tank is a function of the state of the storage tank. Thus to model this asset, consider the flow of hydrogen from one time to the next time.

In the asset modeller language, a hydrogen storage tank can be described as an asset with one component: the hydrogen storage component. The hydrogen storage component moves hydrogen from the hydrogen node at a specific location and time to the hydrogen node at the same location but a future time. The template edge of the hydrogen storage component is shown in Figure 5.6. The template edge of the hydrogen storage component is defined in Table 5.7.

Table 5.7: Template Edge of Hydrogen Storage Component

Source Node Type	Hydrogen (H_2)
Target Node Type	Hydrogen (H_2)
Source Node Location	Location 1
Target Node Location	Location 1
Operational Time Difference (δt)	1 hour
Time Difference Between Target and Source Node (Δt)	1 hour

To account for boundary condition, i.e. the start and end of the simulation time period, assume that the edge at operational time t_1 moves energy to the start time t_0. This is the same as saying that the amount of hydrogen at the end of the simulation is the same as the amount of hydrogen at the start of the simulation. These define the structure of the hydrogen storage asset and its components.

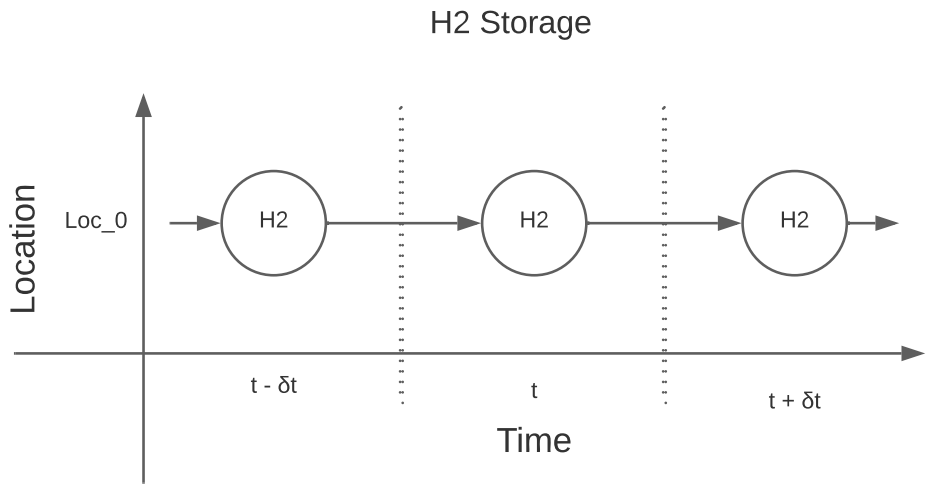

Figure 5.6: Template Edge Hydrogen Storage. The Hydrogen Storage asset only has one component. Storage of hydrogen can be interpreted as movement of hydrogen in time. Keeping everything else equal, the amount of hydrogen at a specific time, will be the amount of hydrogen at the next time. Thus, the amount of hydrogen at a specific time can be viewed as the amount of hydrogen moving from one time to the next time. The template edge of this component moves hydrogen from the "Hydrogen Storage" node at a specific location and time, to the "Hydrogen Storage" node at a same location but a time δt later. The component has edges every δt, the time between operation. Unlike other components, the template edges of a component that only moves energy in time creates a "chain" of edges.

Consider the conversion function of the storage component. This is the amount of hydrogen that moves from one operational time to the next. As the type of flow

out of the source node and into the target node are the same, this can be viewed as the storage efficiency of the hydrogen storage device. In the literature, the standing losses or self discharge of hydrogen is a fraction of the current amount of hydrogen [73]. E.g. if μ fraction of the hydrogen is lost when hydrogen is stored each month, then:

$$E_{out} = E_{in}(1 - \mu) \tag{5.40}$$

Where E_{in} is the amount of hydrogen at the start of the month. E_{out} is the amount of hydrogen at the end of the month. However, the storage losses of hydrogen may be given at much longer timescales than the operational period of hydrogen. Thus, if the time used to define the storage losses is $t_{storage}$, then the amount of hydrogen in the storage at the end of an operational time period is given by:

$$y_t = \psi(x_t) = (1 - \mu)^{\frac{t_{storage}}{\Delta t}} x_t \tag{5.41}$$

Where x_t is the amount of hydrogen flowing out of the hydrogen node at time t, and represents the amount of hydrogen stored at time t. y_t is the amount of hydrogen flowing into the hydrogen node at time $t + \Delta t$, and is defined by the conversion function ψ.

μ and $t_{storage}$ are asset brand parameters in the system designer language. μ is unitless, and $t_{storage}$ has units [h]. The asset brand parameters can be combined into a conversion function parameter, η, given by:

$$\eta = (1 - \mu)^{\frac{t_{storage}}{\Delta t}} \tag{5.42}$$

The conversion function of the hydrogen storage component is now given by:

$$y_t = \psi(x_t) = \eta x_t \tag{5.43}$$

The conversion function parameter of the asset ($\vec{\mathbf{P}}_{\psi}$) only consists of one parameter:

$$\vec{\mathbf{P}}_{\psi} = (\eta) \tag{5.44}$$

Assume that the cost of the asset does not depend on the operation of the asset and only the sizing of the asset. Assume that the sizing cost of the asset is proportional to the size of the asset. The cost of the asset ($f_{size,t}$) to satisfy the flows at time t is:

$$f_{size,t} = C_{size} x_t \tag{5.45}$$

Table 5.8: Flows and Parameters of Hydrogen Storage Asset

Symbol	Meaning	Units	Language
μ	Loss per typical storage time	unitless	System Designer
$t_{storage}$	Typical storage time	h	System Designer
C_{size}	Capital cost per peak storage capacity	$\$\,\mathrm{kg_p^{-1}}$	System Designer Asset Modeller
η	Efficiency	unitless	Asset Modeller
x	Hydrogen leaving source node	kg	Asset Modeller
y	Hydrogen entering target node	kg	Asset Modeller

Where C_{size} is an asset brand parameter in the system designer language. It is the cost of sizing the hydrogen storage asset per amount of maximum hydrogen stored, and has the units $[\$\,\mathrm{kg}^{-1}]$.

The cost of sizing the asset to satisfy all times (f_{size}) is the maximum of $f_{size,t}$ over all times:

$$f_{asset} = f_{size} = \max_t\{f_{size}\} = C_{size} \max_t\{x_t\} \tag{5.46}$$

As there is no other cost of the asset, this is also equal to the cost of the asset, f_{asset}.

The cost function parameter of the asset ($\vec{\mathbf{P}}_f$) only consists of one parameter:

$$\vec{\mathbf{P}}_f = (C_{size}) \tag{5.47}$$

The flows, asset brand parameters, conversion function parameters, cost function parameters of the Hydrogen Storage asset, and their units, are compiled in Table 5.8.

5.1.5 Hydrogen Water Heater

Consider the modelling of assets that perform the energy system basis function of energy conversion function, i.e. it moves energy from one type to another. These are assets such as hydrogen heating, water electrolysis, and electric heat pump. As an example, consider the hydrogen water heater.

The hydrogen water heater asset can be described using the asset modeller language as an asset with one component: the hydrogen water heater component. The hydrogen water heater component moves hydrogen out of the hydrogen node at a location and time, and moves hot water into the hot water node at the same location and time. Figure 5.7 shows the template edge of the hydrogen water heater component. The template edge of the hydrogen water heater component is defined in Table 5.9.

Table 5.9: Template Edge of Electricity Transport Component

Source Node Type	Hydrogen (H_2)
Target Node Type	Hot Water
Source Node Location	Location 1
Target Node Location	Location 1
Operational Time Difference (δt)	1 hour
Time Difference Between Target and Source Node (Δt)	0 hour

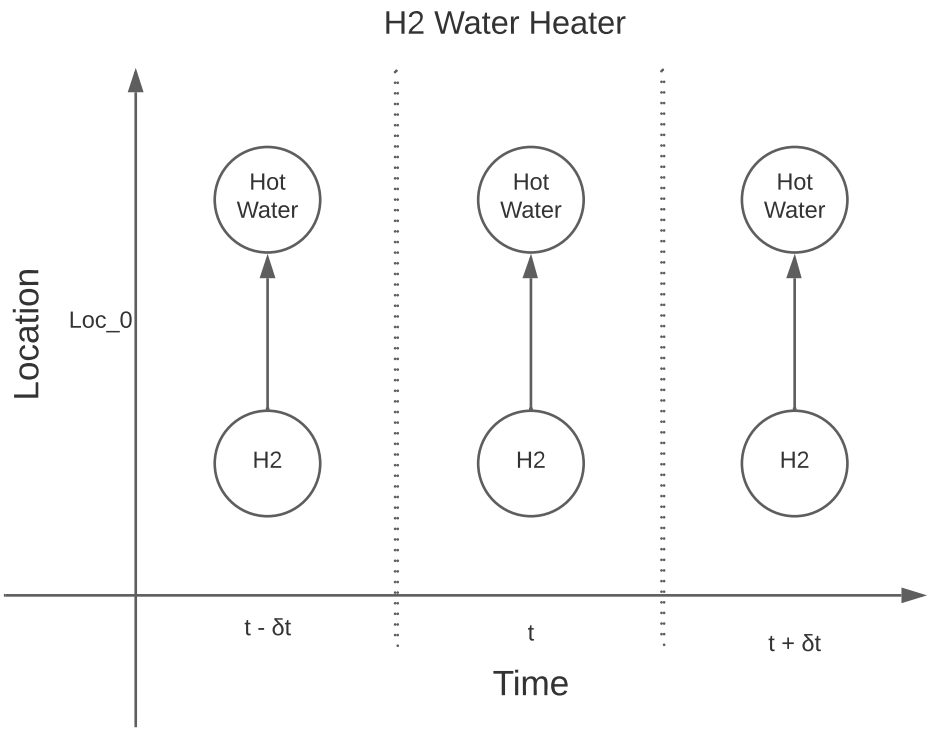

Figure 5.7: Template Edge Hydrogen Water Heater. The hydrogen water heater asset only has one component. The template edge of this component converts hydrogen from the "Hydrogen" node at a specific location and time, to hot water in the "Hot Water" node at a same location and time. The component has edges every δt, the time between operation.

The hydrogen water heater component converts hydrogen to hot water. The flow from the source node to the edge is of type "hydrogen". The flow from the edge to the target node is type "hot water". Thus the conversion function of the edges of the heater component depends on the hourly hot water production per hourly hydrogen consumption. This hot water production per unit hydrogen consumption can be obtained from heater data. This is in general a function of the initial and final temperatures of the water. To model this completely, the generalized coordinates of the system are amount of water and temperature. The equation for amount of water and temperature would be similar to the equation for mass and velocity in a rocket. For simplicity, consider fixed initial and final temperatures of water that is being heated. The amount of hot water produced is now assumed to be proportional to the hydrogen consumed. The amount of hot water produced (y_t) and thus the conversion function of the hydrogen water heater component at operational time t (ψ) is given by:

$$y_t = \psi(x_t) = \eta x_t \tag{5.48}$$

Where η is an asset brand parameter in the system designer language. It represents the amount of hot water produced per unit hydrogen and has the unit [$\mathrm{L\,kg^{-1}}$]. The conversion function parameter of the asset ($\vec{\mathbf{P}}_\psi$) thus only has one parameter, and is given by:

$$\vec{\mathbf{P}}_\psi = (\eta) \tag{5.49}$$

The cost of the hydrogen water heater asset can be split into the sizing (f_{size}) and usage costs (f_{use}).

The usage cost of the heater component depends only on the operation of the assets, and not the size of the asset. It may be intuitive to consider the cost of hydrogen as a usage cost of the hydrogen water heater. However, that is an implicit cost and will be accounted for by the asset that produces the hydrogen. Thus, adding the cost of hydrogen here will lead to double counting. In fact, the cost of hydrogen here is not well defined as it may be produced by various other assets. In STEVFNs, the cost of assets is the explicit cost of assets. For the hydrogen water heeater, these are the maintenance costs for repairing the heater. In datasheets, these could be labeled as the hot water produced before maintenance need to be performed, A_0. A_0

has the units [L]. The cost per maintenance is $C_{maintenance}$, and has the units [$]. This assumes that the maintenance cost depends on the production of hot water, not the size of the heater. A bigger heater should in theory need to be maintained less often, but the cost for each maintenance is higher. If the maintenance cost is proportional to the size of the heater, the maintenance cost per amount of hot water produced is the same. The maintenance cost can be amortized as a degradation cost similar to a battery as described in Section 3.4.3. The usage cost ($f_{use,t}$) of operating the hydrogen water heater at time t is:

$$f_{use,t} = \frac{C_{maintenance}}{A_0} x_t \tag{5.50}$$

Where the two asset brand parameters can be combined to form a cost function parameter (C_{use}):

$$C_{use} = \frac{C_{maintenance}}{A_0} \tag{5.51}$$

The total usage cost of the asset (f_{use}) is the sum of all usage costs over all times:

$$f_{use} = \sum_t f_{use} = C_{use} \sum_t x_t \tag{5.52}$$

The cost of sizing the heater ($f_{size,t}$) to meet the operation at time t is given by:

$$f_{size,t} = \frac{C_{cap}}{\delta t} y_t = \frac{C_{cap}\eta}{\delta t} x_t \tag{5.53}$$

Where C_{cap} is an asset brand parameter. It is the capital cost of the hydrogen heater per peak amount of hot water produced per hour and has the units [$\$\,\mathrm{L_p^{-1}\,h^{-1}}$]. The asset brand parameters can be combined to form a cost function parameter (C_{size}):

$$C_{size} = \frac{C_{cap}\eta}{\delta t} \tag{5.54}$$

The total sizing cost of the asset (f_{size}) is the maximum of the sizing cost requried for all times:

$$f_{size} = \max_t\{f_{size,t}\} = C_{size} \max_t\{x_t\} \tag{5.55}$$

The total cost of the asset (f_{asset}) is the sum of the sizing and usage costs:

$$f_{asset} = f_{size} + f_{use} = C_{size} \max_t\{x_t\} + C_{use} \sum_t x_t \tag{5.56}$$

Table 5.10: Flows and Parameters of Hydrogen Water Heater Asset

Symbol	Meaning	Units	Language
C_{cap}	Capital cost per peak hot water output rate	$\$\,\mathrm{L_p^{-1}\,h^{-1}}$	System Designer
$C_{maintenance}$	Cost per maintenance	\$	System Designer
A_0	Hot water produced per maintenance	L	System Designer
η	Water heated per hydrogen	$\mathrm{L\,kg^{-1}}$	System Designer Asset Modeller
C_{size}	Sizing cost per peak hydrogen input	$\$\,\mathrm{kg_p^{-1}}$	Asset Modeller
C_{use}	Usage cost per hydrogen input	$\$\,\mathrm{kg^{-1}}$	Asset Modeller
x	Hydrogen leaving source node	kg	Asset Modeller
y	Hot Water entering target node	L	Asset Modeller

The cost function parameters ($\vec{\mathbf{P}}_f$) are given by:

$$\vec{\mathbf{P}}_f = (C_{use}, C_{size}) \tag{5.57}$$

The flows, asset brand parameters, conversion function parameters, cost function parameters of the Hydrogen Storage asset, and their units, are compiled in Table 5.10.

5.2 Complex Energy Assets

The previous section models five simple assets that perform the five energy system functions. This helps the reader become comfortable with describing assets in the various languages of STEVFNs and defining their translations. This section models complex assets; these are assets that perform more than one basis function of an energy system, consist of more than one component, and/or are conceptually difficult to understand. As these assets are more complex, they are used to demonstrate how the impact of modelling assumptions on the convexity of the eventual optimization problem can be studied. Furthermore, when an asset does make the optimization problem non-convex, this section demonstrates how to find good approximations for the asset model to make the asset model, and thus the optimization problem, convex.

5.2.1 Bi-Directional Electricity Line

Revisit the electricity line asset presented in Section 5.1.1. That electricity line only moved electricity in one direction. Consider modelling an asset that moves electricity in both directions; this referred to as the "bi-directional electricity line" asset.

It is initially tempting to simply use the electricity line asset and allow for negative flow of electricity. However, the magnitude of the electricity at locations 1 and 2 depend on the direction of the flow. If the electricity is flowing from location 1 to 2, i.e. positive flow, the electrical energy flowing out of location 1 is larger than the electrical energy flowing into location 2. However, if the electricity is flowing from location 2 to 1, i.e. negative flow, the electrical energy flowing into location 1 is smaller than the electrical energy flowing out of location 2. Thus, the conversion function will now become:

$$\psi(x_t) = \begin{cases} \eta x_t, & x_t \geq 0 \\ \frac{x_t}{\eta}, & x_t \leq 0 \end{cases} \tag{5.58}$$

This is a concave function and thus the problem is still convex.

Since the flow can now take a negative value, the sizing and operational costs functions also need to be updated. They now depend on the magnitude of the flows rather than the flows. The total cost now becomes:

$$f_{asset} = \mathbf{P}_{f_{size}} \max_t |x_t| + \mathbf{P}_{f_{use}} \sum_t |x_t| \tag{5.59}$$

Where $|x_t|$ is the absolute value of the flow along the edge of operational time t. As f_{asset} is convex and increasing in $|x_t|$, and $|x_t|$ is convex with x_t, f_{asset} is convex with x_t. Thus, this bi-directional asset will be convex. The rest of the descriptions in both the asset modeller and system designer languages, as well as the translations between them, will be the same as for the single directional electricity line asset in Section 5.1.1.

However, this introduces negative variables as the energy flowing along the edges can be negative. Some algorithms may benefit from ensuring that all variables are positive. Furthermore, the piece-wise nature of the conversion function may not be desirable by some algorithms too. Lastly, some piece-wise functions may not be concave. For example, if we considered full I^2R losses, the conversion function will no longer be convex. In fact, it will have two potential values when the flow is negative.

In such a situation, the asset can still be modelled by splitting the flows into positive and negative flows; these will be represented as flows in the forward and reverse directions, respectively. The bi-directional electricity line can thus be described using only positive flows instead. To do this, the bi-directional electricity line asset

can be described in the asset modeller language as an asset with two components. Figure 5.8 shows the UML diagram of the bi-directional electricity line asset. The first component is the "forward component"; the second component is the "reverse component".

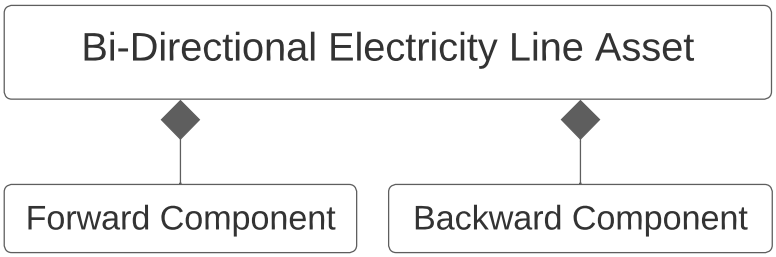

Figure 5.8: UML Bi-Directional Electricity Line A Bi-Directional Electricity Line asset consists of two components: the forward and backwards components.

The template edges of components of the bi-directional electricity line are given in Figure 5.9. The forward component has the same template edge and conversion function as the component of the electricity line asset. The conversion function is given by equation 5.11. The reverse component also has the same template edge and conversion function as the component of the electricity line asset, the source and target nodes of the reverse component are reversed.

Both the forward and backward components of the bi-directional electricity line also have the same sizing and operational cost functions as the component of the electricity line asset. The sizing cost of the components is given by equation 5.15. The operational cost of the components is given by equation 5.18. However, as the bi-directional electricity line asset has two components, its total cost is different from the total cost of the electricity line asset. The size of the bi-directional electricity line asset is determined by the maximum requirement of both the forward and backwards flow of electricity. Thus, the sizing cost of the bi-directional electricity line asset is given by:

$$f_{size} = \max\{f_{size}^{forward}, f_{size}^{reverse}\} \tag{5.60}$$

Where $f_{size}^{forward}$ and $f_{size}^{reverse}$ are the sizing costs of the forward and reverse components, respectively.

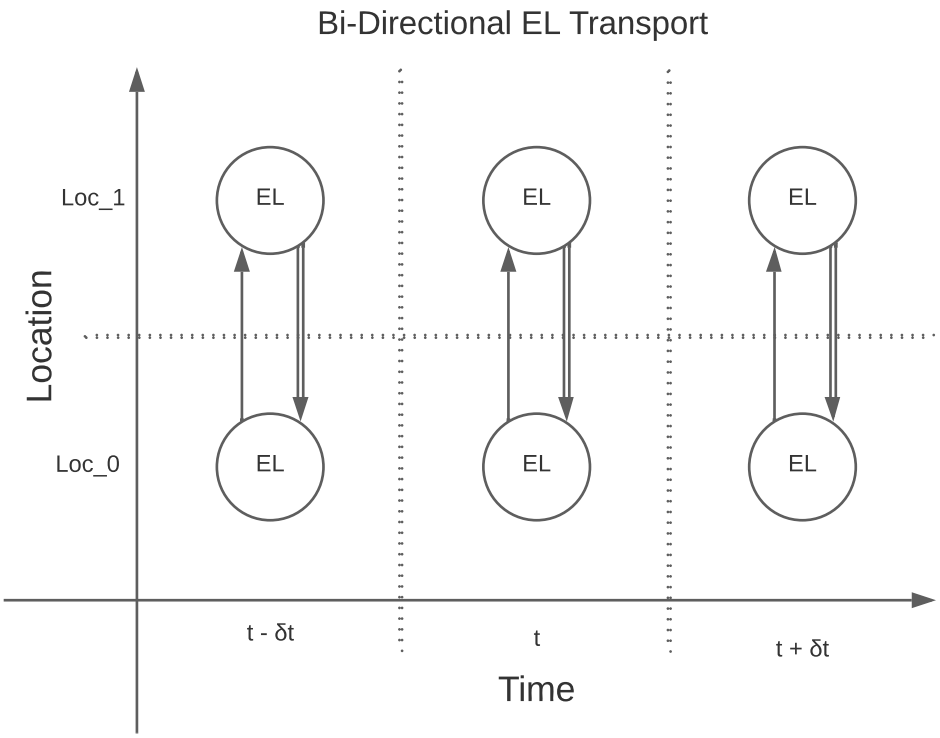

Figure 5.9: Template Edge Bi-Directional Electricity Line. The Bi-Directional Electricity Line asset only has two components: the forward component, and the backward component. The single lined arrows represent the template edges of the forward component. The double lined arrows represent the template edges of the backward component. The template edge of the forward component moves electricity from the "Electricity Grid" node at a specific location and time, to the "Electricity Grid" node at a different location but same time. The component has edges every δt, the time between operation. The template edge of the backward component moves electricity in the opposite direction as the template edge of the forward component.

The total degradation of the bi-directional electricity line is the sum of the degradation of the forward and reverse usages of the line. The total operational cost of the asset (f_{use}) is thus the sum of the operational cost of the forward ($f_{use}^{forward}$) and reverse ($f_{use}^{reverse}$) components:

$$f_{use} = f_{use}^{forward} + f_{use}^{reverse} \tag{5.61}$$

The total cost of the asset (f_{asset}) is thus given by:

$$f_{asset} = f_{size} + f_{use} = \max\{f_{size}^{forward}, f_{size}^{reverse}\} + f_{use}^{forward} + f_{use}^{reverse} \tag{5.62}$$

The conversion functions of all components of the bi-directional electricity line asset are concave, thus they will keep the optimization problem convex. The total cost of the asset is convex. Thus, the optimal operation and sizing of the bi-directional electricity line asset is convex.

It might initially seem strange that we have allowed electricity to flow in both directions at the same time. However, note that if the flow in the edges of the forward and reverse components of a specific operational time are both non-zero, the operational cost of the asset can always be reduced by reducing both the flows until one of the flows is zero. Thus, in the optimal solution, at least one of the flows will be zero. Therefore, splitting the flow of electricity into the forward and reverse flows is a convex relaxation of the problem and will lead to the same solution as the original problem. This assumption needs to be revisited if the "price" of electricity generation is negative or if there is multi-node wheeling. In such situations, the inequality constraints may need to be converted to an equality constraint or the bi-directional flow may need to be combined to a single flow that can be negative.

5.2.2 Perfectly Inelastic Temporal Demands

Consider the modelling of a perfectly inelastic temporal demand. This is a fixed demand of a certain type of end-use energy or service that needs to be met at regular intervals of time. The demand at each operational time can be different but is fixed, and is usually treated as a constraint for an energy system design problem. Examples of fixed temporal demands include average hourly electricity demand at a certain

Table 5.11: Template Edge of Fixed Electricity Demand Component

Source Node Type	Electricity Demand
Target Node Type	Electricity Grid (EL)
Source Node Location	Location 1
Target Node Location	Location 1
Operational Time Difference (δt)	1 hour
Time Difference Between Target and Source Node (Δt)	0 hour

location, hourly hot water demand, daily demand for coffee at a cafe, etc. Consider the example of hourly electricity demand. This is a special case of the elastic electricity demand where the elasticity is set to infinity.

The perfectly inelastic temporal demand can be described in the asset modeller language as an asset with one component, the fixed electricity demand component. As this is a special case of the elastic electricity demand, it is tempting to use the same template node definition as the elastic electricity demand component in Section 5.1.3. The template edge diagram for the fixed electricity demand component is thus also given by Figure 5.5. The template edge is also defined by Table 5.5.

Consider the conversion function of the demand component. Equation 5.34 now transforms to:

$$y_t = \psi(P_{D,t}) = P_{D,t}\delta t \tag{5.63}$$

Where $P_{D,t}$ is the flow along the edge and is a conversion function parameter. $P_{D,t}$ is the power demanded at time t, and is an asset brand parameter in the system designer language. Note that for the case of fixed electrical demand, $P_{D,t}$ is a parameter, not a decision variable. Thus, the edges of this component only contain optimization parameters, and no optimization decision variables. However, for consistency, flows along edges should be optimization variables. All optimization parameters should be in the conversion function. To do this, consider the flow of demand instead of the flow of energy to model fixed electrical demand.

This new demand component moves electricity demand out of the demand node at a specific location and time, converts it to electricity, and moves electricity into the electricity grid node at the same location and time. The template edge of the demand component is shown in Figure 5.10. The template edge for the fixed electricity demand component is defined by Table 5.11.

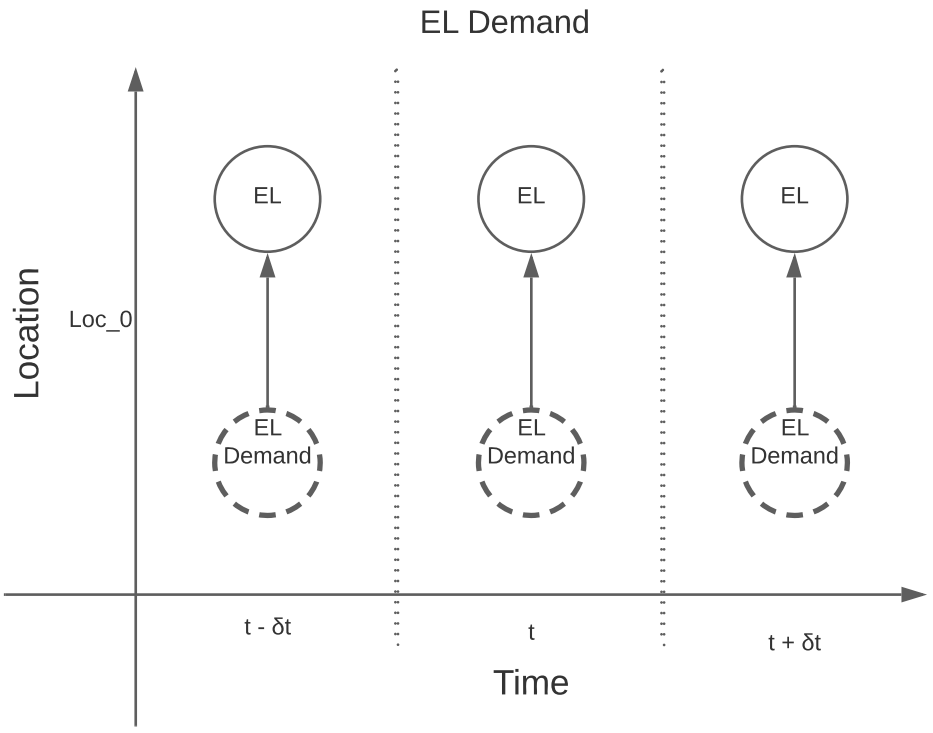

Figure 5.10: Template Edge Fixed Demand. The Fixed Demand asset only has one component. In this formulation, we are tracking the movement of demand instead of energy. The flow of demand is in the opposite direction as it would be for energy. This is because demand can be viewed as negative energy. The template edge of this component moves demand from the "Electricity Demand" node at a specific location and time, to electricity in the "Electricity Grid" node at a same location and time. The component has edges every δt, the time between operation. The dotted line represents a "virtual node" that does not have any optimization constraints.

Consider the conversion function of the new demand component. Unlike the previous case, the flow out of the electrical demand node is of type "electrical demand". The flow into the electrical grid node is of type "electrical energy". Thus, the flow into and out of the node are of different types. Consider the impact of the demand on the electricity grid node. When there is a positive demand of electricity, there is less electricity available at the electricity grid node. The reduction in available electricity at the grid node is equal to the quantity demanded. Thus, the electricity into the electrical grid node is equal in magnitude but of the opposite sign as the electrical demand flowing in the edge. The conversion function is thus given by:

$$y_t = \psi_t(x_t) = -P_{D,t}\delta t \tag{5.64}$$

Where y_t represents electricity moved out of the electricity grid between times t and $t + \delta t$. Where, x_t is now a zero dimensional control variable. $P_{D,t}$ is the electrical power demanded at time t, and is an asset brand parameter. $P_{D,t}$ and δt can be combined to form a conversion function parameter, D_t, the total energy demand in timestep t:

$$D_t = P_{D,t}\delta t \tag{5.65}$$

The conversion function is now given by:

$$y_t = \psi(x_t) = -D_t \tag{5.66}$$

The flow in each edge is now a control variable (x_t), and has no parameters; even if the variables has zero dimensions and is thus a null variable. As the dimension of the flow out of the electrical demand node is zero, the dimension of the conversion function at that node is zero and it is a null constraint. The electrical demand nodes are "virtual nodes" because they do not contain any optimization constraints. Similarly the edges are referred to as "virtual edges" because they do not contain any optimization variables.

The conversion function parameters ($\vec{\mathbf{P}}_\psi$) for the asset are:

$$\vec{\mathbf{P}}_\psi = \{D_t\,, \forall t\} \tag{5.67}$$

Table 5.12: Flows and Parameters of Perfectly Inelastic Temporal Demand Asset

Symbol	Meaning	Units	Language
$P_{D,t}$	Power demanded at time t	W	System Designer
D_t	Electrical energy demand at timestep t	Wh	Asset Modeller
y	Electrical energy entering target node	Wh	Asset Modeller

As there are no operational or sizing decisions to be made, the fixed temporal electricity demand asset does not have any cost, or has a cost of zero. Thus the cost of the asset, f_{asset}, is given by:

$$f_{asset} = 0 \tag{5.68}$$

The flows, asset brand parameters, conversion function parameters, cost function parameters of the Perfectly Inelastic Temporal Demand asset, and their units, are compiled in Table 5.12.

5.2.3 Solar PV Farm

Consider the modelling of a more complex energy asset that performs the energy generation function, a DER farm. A DER farm is a mathematically simpler but conceptually more complicated energy generation asset to model than a fossil fuel power generator. A DER farm extracts energy from its surroundings to generate electricity. However, "we cannot control when the wind blows or the sun shines". Thus, the output of a RE farm is intermittent. Examples of RE farms include wind, solar PV, hydro, and wave power. By modelling a DER farm in STEVFNs, all types of DER farms are modelled as different brands of the same asset. The important thing is that this DER asset moves DER equipment requirement from the "DER farm" node at a specific time and location moves electricity to the "electricity grid" node at the same time and location.

Consider a DER farm as a black box that encapsulates all parts of the farm such as PV panels, inverters, etc. A DER farm can be described in the asset modeller language as an asset with one component. The only component in the DER farm asset is the extractor component. The extractor component moves "DER farm size requirement" out of the DER node at a specific time and location, and moves electrical energy into the electricity grid node at the same time and location. Figure 5.11 shows

Table 5.13: Template Edge of Backward Demand Shifting Component

Source Node Type	DER Farm (DER)
Target Node Type	Electricity Grid (EL)
Source Node Location	Location 1
Target Node Location	Location 1
Operational Time Difference (δt)	1 hour
Time Difference Between Target and Source Node (Δt)	0 hour

the template edge diagram of the extractor component. The template edge of the extractor component is defined by Table 5.13:

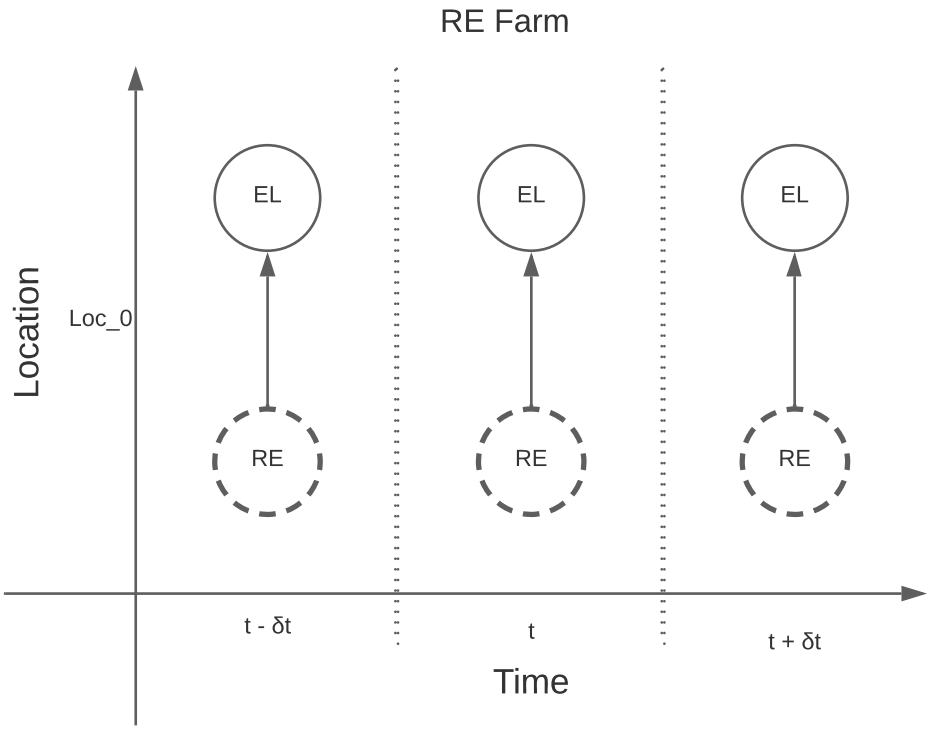

Figure 5.11: Template Edge DER Farm. The DER Farm asset only has one component. The template edge of this component converts DER requirement from the "DER Farm" node at a specific location and time, to electricity in the "Electricity Grid" node at a same location and time.

The extractor component can be viewed as converting DER farm size requirement (DER peak) to electricity. The flow from the source node to the edge is of type "DER size requirement". The flow from the edge to the target node is type "electricity". Thus the conversion function at the edge at an operational time depends on the amount of natural resource available at that time ($DEROUT_t$), and the rated power

of the DER farm (i.e. the size of the DER farm). $DEROUT$ can be obtained for specific locations around the world at different times. They can also be estimated by using historical data, as in the literature. Consider the historical global solar and wind outputs at hourly resolution calculated by Renewables.ninja. This uses historical irradiance, temperature and wind speed data from NASA's MERA 2 satellite to calculate the average hourly $DEROUT$ for 30 years at each point on the globe at 0.5 and 0.625 degrees latitude and longitude resolution, respectively. Example of the spatial and temporal distribution of PV around the world is shown in Figure 5.12. If the flow out of the RE farm node is the size of the RE farm, the electricity flowing into the electricity grid node (y_t) of operational time t (ϕ_t) is given by the conversion function of the edge (ψ_t) at that time:

$$y_t = \psi_t(x_t) = DEROUT_t \, \delta t \, x_t \tag{5.69}$$

Where x_t is the size of the DER farm required to produce electricity y_t at time t. $DEROUT_t$ is an asset brand parameter in the system designer language. $DEROUT_t$ is the power produced at time t per peak power rating of the DER asset, and has the units $[\mathrm{kW\,kW_p^{-1}}]$.

$DEROUT_t$ and δt can be combined to form the conversion function parameter, E_t:

$$E_t = DEROUT_t \, \delta t \tag{5.70}$$

The conversion function parameter ($\vec{\mathbf{P}}_\psi$) of the asset has all E_t over all times:

$$\vec{\mathbf{P}}_\psi = \vec{E} = \{DEROUT_t \, \delta t \, , \forall t\} \tag{5.71}$$

Where $\vec{E}$ is the vector of E_t over all operational times of the component t.

The operation of a DER asset does not significantly affect the cost of an RE farm. Thus, an RE farm may be assumed to only have a sizing cost and no usage cost. The cost of sizing a DER farm ($f_{size,t}$) to satisfy the flows at time t is given by:

$$f_{size,t} = \frac{C_{cap}}{\delta t} x_t \tag{5.72}$$

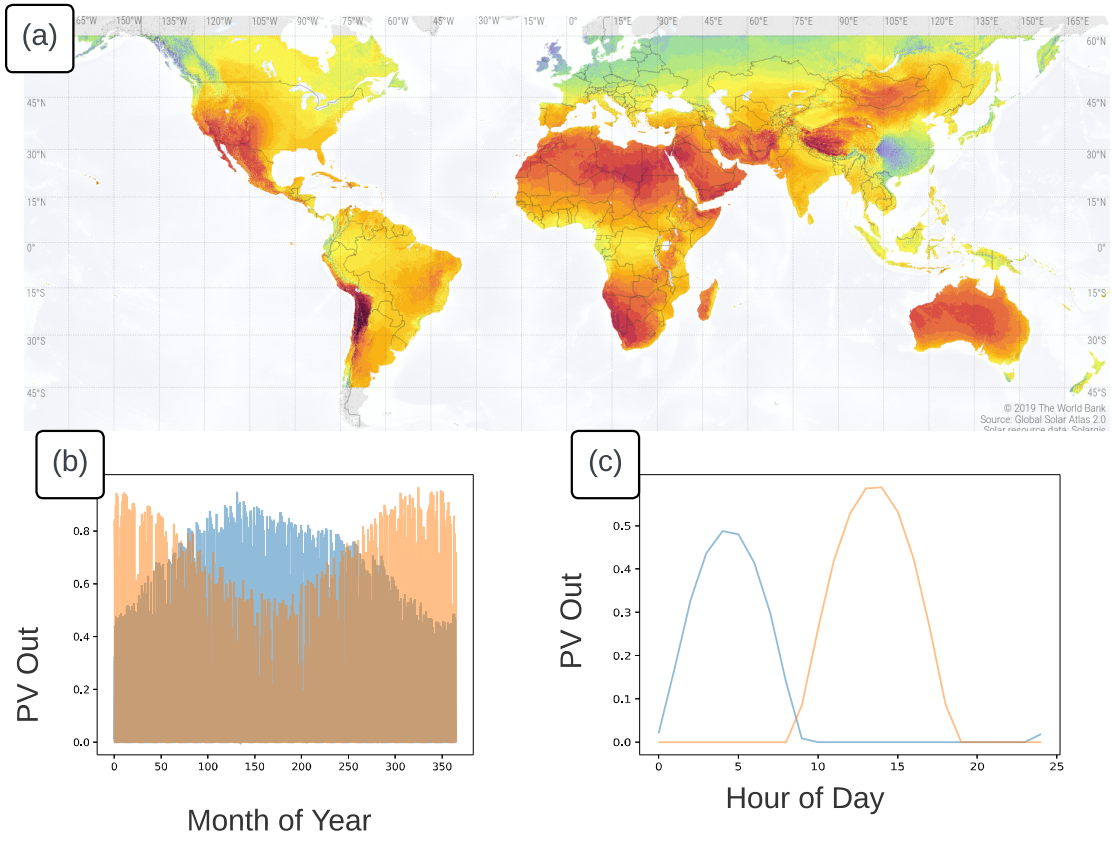

Figure 5.12: Spatiotemporal Distribution of PV [5] Renewable electricity output per unit rated power can be obtained for all parts of the world at hourly time intervals. We may use historical or simulated data.
a. Shows the annual PV output at each point in the world.
b. Shows the temporal PVOUT for one year of two points with different latitudes. This illustrates the north-south seasonal variation of PV.
c. Shows the temporal PVOUT for one day of two points with different longitudes. This illustrates the east-west daily variation of PV.

Table 5.14: Flows and Parameters of PV Farm Asset

Symbol	Meaning	Units	Language
$DEROUT_t$	Power generated at time t per rated power	$\mathrm{W\,W_p^{-1}}$	System Designer
C_{cap}	Capital cost per rated power t	$\mathrm{\$\,W_p^{-1}}$	System Designer
C_{size}	Sizing cost per peak electrical energy	$\mathrm{\$\,Wh^{-1}}$	Asset Modeller
x	PV farm size requirement leaving source node	$\mathrm{Wh_p}$	Asset Modeller
y	Electrical energy entering target node	Wh	Asset Modeller

Where C_{cap} is an asset brand parameter in the system designer language. It is the capital cost of the DER farm, per peak power capacity, and has the units $[\mathrm{\$\,W_p^{-1}}]$. C_{cap} can be combined with δt to get the parameter (C_{size}):

$$C_{size} = \frac{C_{cap}}{\delta t} \tag{5.73}$$

Where C_{size} is an cost function parameter in the asset modeller language. C_{size} has the units $[\mathrm{\$\,Wh_p^{-1}}]$.

The size of the extractor component may be interpreted as the highest DER farm size required over all times. The total sizing cost of the DER asset (f_{size}) is thus the maximum of the cost required to meet the requirements at all times. This is also the total cost of the DER asset (f_{asset}) and is given by:

$$f_{asset} = f_{size} = \max_t\{f_{size,t}\} = C_{size} \max_t\{x_t\} \tag{5.74}$$

The cost function parameter of the asset ($\vec{\mathbf{P}}_f$) only consists of one value:

$$\vec{\mathbf{P}}_f = (C_{size}) \tag{5.75}$$

The flows, asset brand parameters, conversion function parameters, cost function parameters of the PV farm asset, and their units, are compiled in Table 5.14.

5.2.4 Demand Shifting

Consider the modelling of demand shifting. An example of this is the shifting of electricity demand. Electricity demand shifting can be modelled in the asset modeller language as the Electricity Demand Shifting Asset. This is an asset with two components: the forward demand shifting component, and the backward demand shifting component. The UML diagram for the electricity demand shifting asset is shown in Figure 5.13. The forward demand shifting component shifts demand forwards in

time. This may be done because there is an anticipated greater supply in the future. The backward shifting component shifts demand backwards in time. This may be done because there is an anticipated greater supply at an earlier time.

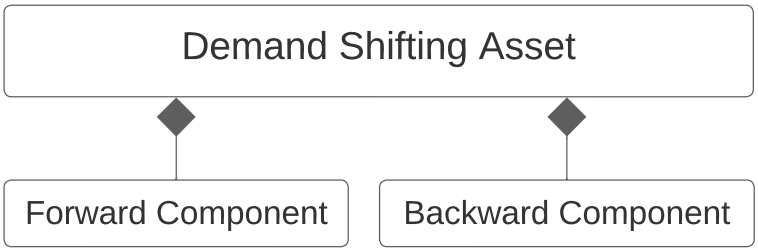

Figure 5.13: UML Demand Shifting Asset. The demand shifting asset consists of two components: the forward and backwards components.

The backward demand shifting component shifts electricity demand from the electricity grid node at a specific location and time, to the electricity grid node at the same location but a past time. However, the electricity grid node tracks the flow of electrical energy, not demand. Electricity demand can be viewed as negative electricity supply. The flow of demand out of a node is the flow of negative energy out of the node, and thus the flow of positive supply into the node. Similarly, the flow of demand into a node is flow of negative energy into the node, and thus the flow of positive energy out of the node. Therefore, the flow of electrical demand in one direction is equivalent to the flow of electrical energy in the opposite direction. As Section 3.3.4 discusses, demand can thus be viewed as the anti-particle of energy supply.

The backward demand shifting component can thus be modelled as moving electrical energy out of the electrical grid node at a specific location and time, and into the electrical grid node at the same location but at a future time. In this interpretation, the template edge diagram of the backward demand shifting component is shown in Figure 5.14. The template edge for the backward demand shifting component is defined by Table 5.15:

Note that this is the same as the hydrogen storage component in Figure 5.6, with hydrogen replaced with electricity. Thus, storage can be viewed as having the equivalent energy system function of shifting demand backwards in time, and vice

Table 5.15: Template Edge of Backward Demand Shifting Component

Source Node Type	Electricity Grid (EL)
Target Node Type	Electricity Grid (EL)
Source Node Location	Location 1
Target Node Location	Location 1
Operational Time Difference (δt)	1 hour
Time Difference Between Target and Source Node (Δt)	1 hour

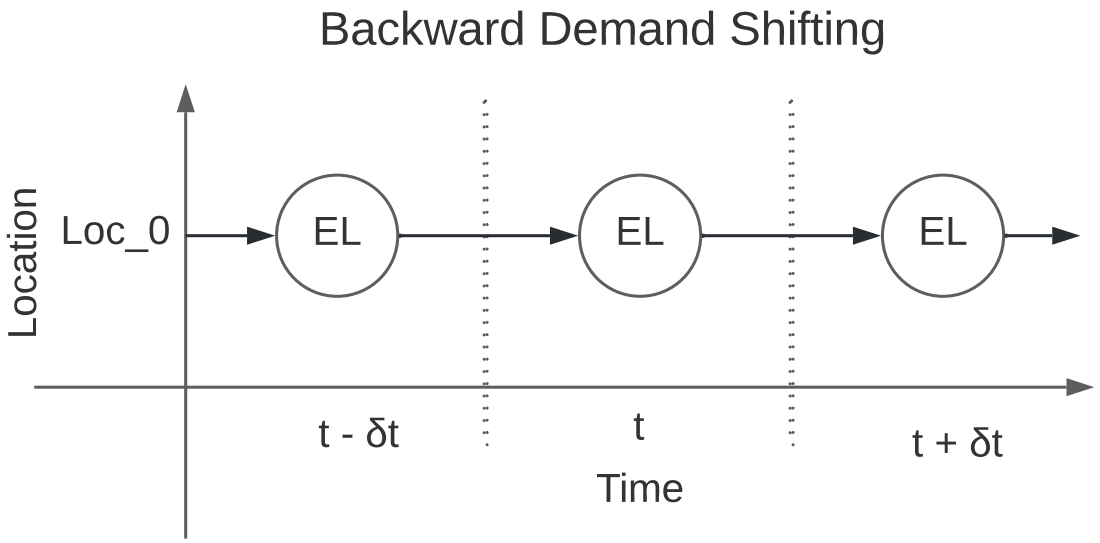

Figure 5.14: Template Edge Backward Demand Shifting Component. The backward demand shifting component moves electricity demand to the past. Demand can be viewed as negative supply, and thus the anti-particle of supply. Thus, the flow of electricity demand into the past is equivalent to the flow of electricity supply into the future. The template edge of the backward demand shifting component thus moves electricity out of the "Electricity Grid" node (EL) at a specific location and time, and into the "Electricity Grid" node (EL) at at same location but a future time. Note that this is the same as the hydrogen storage component in Figure 5.6, with hydrogen replaced with electricity. Thus, storage can be viewed as having the equivalent function of shifting demand backwards in time.

Table 5.16: Template Edge of Forward Demand Shifting Component

Source Node Type	Electricity Grid (EL)
Target Node Type	Electricity Grid (EL)
Source Node Location	Location 1
Target Node Location	Location 1
Operational Time Difference (δt)	1 hour
Time Difference Between Target and Source Node (Δt)	-1 hour

versa. This is because they both decrease the amount of a generalized quantity available now, and increase the amount of generalized quantity available in the future.

The forward demand shifting component can be defined similar to the backward shifting component, with the direction of flow reversed. the template edge diagram of the backward demand shifting component is shown in Figure 5.14. The template edge for the forward demand shifting component is defined by Table 5.16:

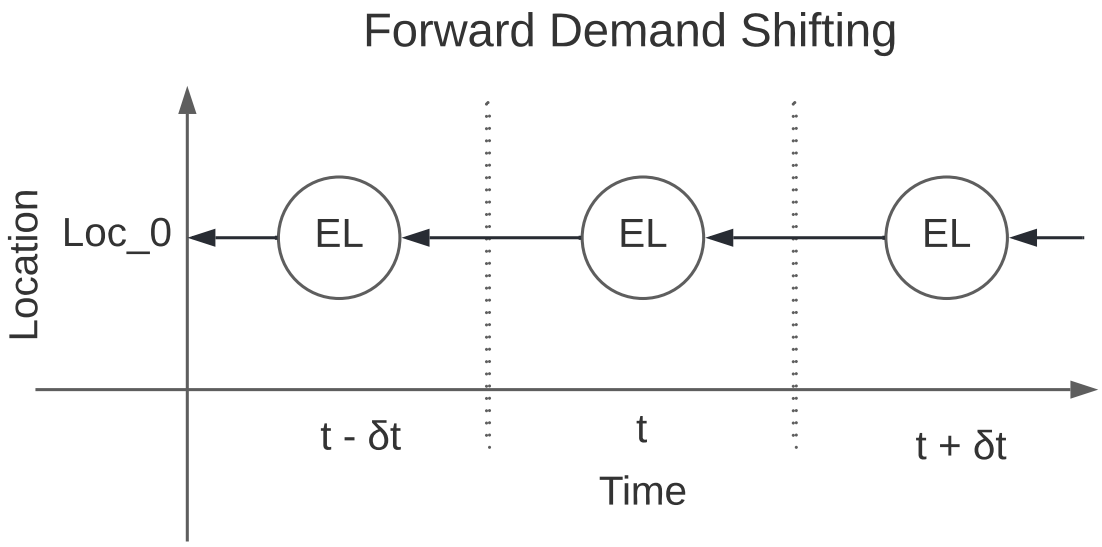

Figure 5.15: Template Edge Forward Demand Shifting Component. The forward demand shifting component moves electricity demand to the future. Demand can be viewed as negative supply, and thus the anti-particle of supply. Thus, the flow of electricity demand into the past is equivalent to the flow of electricity supply into the future. The template edge of the forward demand shifting component thus moves electricity out of the "Electricity Grid" node (EL) at a specific location and time, and into the "Electricity Grid" node (EL) at at same location but a past time. Note that this is similar to the hydrogen storage component in Figure 5.6, with hydrogen replaced with electricity, and the flow direction reversed.

Note that the time difference between the target and source node is a negative value. This indicates that forward demand shifting component moves electrical energy

backwards in time. Thus, demand response can also be viewed as a generalization of energy storage. While storage only moves energy forwards in time, demand response can also move energy backwards in time. The forward and backward demand shifting components thus formalize the link between demand response and energy storage, by unifying them.

As the amount of electricity demanded does not change when demand is moved forwards or backwards in time, the amount of energy flowing into and out of nodes in both components are the same. The conversion function for both the forward and backward demand shifting components ($\psi_{forward}$, and $\psi_{backward}$, respectively) is thus given by:

$$y_{forward} = y_{backward} = \psi_{forward}(x) = \psi_{backward}(x) = x \tag{5.76}$$

Where $y_{forward}$ and $y_{backward}$ are the flows of electrical energy into the electricity grid nodes via the forward and backward shifting components, respectively. This is equivalent to a generalized storage with no storage losses.

The forward and backward demand shifting components have no conversion functions parameters, ie.:

$$\mathbf{P}_{\psi_{forward}} = \mathbf{P}_{\psi_{backward}} = \emptyset \tag{5.77}$$

Where $\mathbf{P}_{\psi_{forward}}$ and $\mathbf{P}_{\psi_{backward}}$ are the conversion function parameters of the forward and backward demand shifting components, respectively.

The cost function of the forward and backward demand shifting components can be viewed as the inconvenience cost of needing to shift demand forwards or backwards in time, respectively. Consider the backward demand shifting component. Consider the inconvenience of shifting demand for one timestep ($f_{backward,use,t}$), i.e. during the operational time t. This is a usage cost of the component, as it depends on the way the component is used. The larger the amount of demand shifted, the larger the inconvenience cost. Furthermore, every additional demand shifted is more expensive. Thus, can be modelled with a convex function. For simplicity, consider the quadratic inconvenience cost:

$$f_{backward,use,t}(x_t) = A_{backward,use,t}x_t + B_{backward,use,t}(x_t)^2 \tag{5.78}$$

Where $A_{backward,use,t}$ and $B_{backward,use,t}$ are parameters. The total inconvenience cost of all energy shifting is thus the sum of the costs over all operational times.

$$f_{backward,use} = \sum_t f_{backward,use,t} = \sum_t \left[A_{backward,use,t} x_t + B_{backward,use,t}(x_t)^2\right] \quad (5.79)$$

There may be an additional inconvenience cost that depends on the maximum amount of shifting that a consumer needs to prepare for. These could represent additional precautions that a consumer needs to put in place. E.g. there is an additional fixed cost of being prepared to shift the usage of one computer vs two. The inconvenience cost of preparing for shifting demand backward at time t ($f_{backward,size,t}$) can again be modelled as a convex function. For simplicity consider the quadratic cost:

$$f_{backward,size,t}(x_t) = A_{backward,size,t} x_t + B_{backward,size,t}(x_t)^2 \quad (5.80)$$

Where $A_{backward,size,t}$ and $B_{backward,size,t}$ are parameters.

The overall inconvenience of preparing for all times ($f_{backward,size}$), is the maximum of the preparation cost over all times:

$$f_{backward,size} = \max_t\{f_{backward,size,t}\} = \max_t\{C_{backward,size,t} x_t + D_{backward,size,t}(x_t)^2\} \quad (5.81)$$

The total cost of the forward demand shifting component is the sum of the usage and sizing costs, $f_{backward,use}$ and $f_{backward,size}$, respectively.

The costs for the forward demand shifting component can be defined in the same way as the backward demand shifting component:

$$f_{forward,use,t}(x_t) = A_{forward,use,t} x_t + B_{forward,use,t}(x_t)^2 \quad (5.82)$$

$$f_{forward,use} = \sum_t f_{forward,use,t} = \sum_t \left[A_{forward,use,t} x_t + B_{forward,use,t}(x_t)^2\right] \quad (5.83)$$

$$f_{forward,size,t}(x_t) = A_{forward,size,t} x_t + B_{forward,size,t}(x_t)^2 \quad (5.84)$$

$$f_{forward,size} = \max_t\{f_{forward,size,t}\} = \max_t\{A_{forward,size,t} x_t + B_{forward,size,t}(x_t)^2\} \quad (5.85)$$

The cost of the forward demand shifting component is similar: the sum of its usage and sizing costs, $f_{forward,use}$ and $f_{forward,size}$, respectively.

The total cost of the demand shifting asset (f_{asset}) is thus the sum of the costs of its constituent components:

$$f_{asset} = f_{forward,size} + f_{forward,use} + f_{backward,size} + f_{backward,use} \tag{5.86}$$

In this situation, the costs of the forward and backward demand shifting components are decoupled and the two components should be viewed as separate assets. If however, the sizing cost of the two components are linked, then it will be beneficial to view them as one asset. E.g. if the inconvenience of preparing to shift the demand of a computer use does not depend on the direction in time in which it is shifted. The sizing cost ($f_{asset,size}$) of the demand shifting asset is the maximum of the sizing costs of the forward and backward components:

$$f_{asset,size} = \max\{f_{forward,size}, f_{backward,size}\} \tag{5.87}$$

The total cost of the demand shifting asset is now given by:

$$f_{asset} = f_{forward,size} + f_{backward,size} + \max\{f_{forward,size}, f_{backward,size}\} \tag{5.88}$$

The costs of the forward and backward shifting components are now coupled and it is beneficial to combine them into one asset.

The cost function parameter of the asset ($\vec{P_f}$) is thus given by:

$$\vec{\mathbf{P}_f} = \{X_{i,j,t} | \forall X, i, j, t\} \tag{5.89}$$

Where $X \in \{A, B\}$; $i \in \{forward, backward\}$; $j \in \{use, size\}$;and t for all operational times defined by Equation 3.29. All $X_{i,j,t}$ are asset brand parameters in the system designer language.

The flows, asset brand parameters, conversion function parameters, cost function parameters of the Demand Shifting asset, and their units, are compiled in Table 5.17.

5.2.5 Hydrogen/Ammonia Transport

Consider the modelling of the transport of an object that takes time. This could be for example the transport of fuels via pipeline, via land vehicles, or via sea freight. Transport via pipeline van be considered to be a continuous process and can be

Table 5.17: Flows and Parameters of Demand Shifting Asset

Symbol	Meaning	Units	Language
$A_{i,j,t}$	Linear inconvenience cost at time t $\forall i \in \{forward, backward\}$ $\forall j \in \{size, use\}$	$\$\,\mathrm{Wh}^{-1}$	System Designer Asset Modeller
$B_{i,j,t}$	Quadratic inconvenience cost at time t $\forall i \in \{forward, backward\}$ $\forall j \in \{size, use\}$	$\$\,\mathrm{Wh}^{-2}$	System Designer Asset Modeller
x	Electrical energy leaving source node	Wh	Asset Modeller
y	Electrical energy entering target node	Wh	Asset Modeller

modelled similar to an electricity line in Section 5.1.1. Consider a discrete process of transporting fuels such as via land vehicles or sea freight. Hydrogen and Ammonia are being widely studied as potential chemical energy vectors that can be used for both transport and storage [110]. These are referred to as chemical energy vectors that can be used to move energy in space, time, and type. As an example, consider an asset that transports hydrogen via a discrete process. This asset is referred to this as the "chemical transport asset". This asset moves hydrogen from one location to another. However, unlike electricity transport, it takes time for it to transport hydrogen.

The hydrogen transport asset can be described in the asset modeller language as an asset with one component: the "hydrogen transport" component. The hydrogen transport component moves hydrogen out of the hydrogen storage node at a specific location and time, and moves hydrogen into the hydrogen storage node at a different location and future time. The hydrogen transport component represents the flow of chemicals along in one direction, just like the simple electricity line in Section 5.1.1. This can be easily extended to the bi-directional case just like for the bi-directional electricity line using the method in Section 5.2.1.

Consider the case of one-directional flow. Figure 5.16 shows the template edge diagram of the hydrogen transport component. The template edge of the hydrogen transport component is defined by Table 5.18.

Unlike the transport of electricity, the transport of hydrogen may only occur at lower time intervals, e.g. 24 hours. An operational time (δt) of 24 hours could for example represent shipments of hydrogen leaving every one day.

Table 5.18: Template Edge of Hydrogen Transport Component

Source Node Type	Hydrogen Storage (H_2)
Target Node Type	Hydrogen Storage (H_2)
Source Node Location	Location 1
Target Node Location	Location 2
Operational Time Difference (δt)	24 hour
Time Difference Between Target and Source Node (Δt)	48 hour

A time difference between the target and source nodes (Δt) of 48 hours for hydrogen transport component could represent it taking two days to transport each hydrogen shipment.

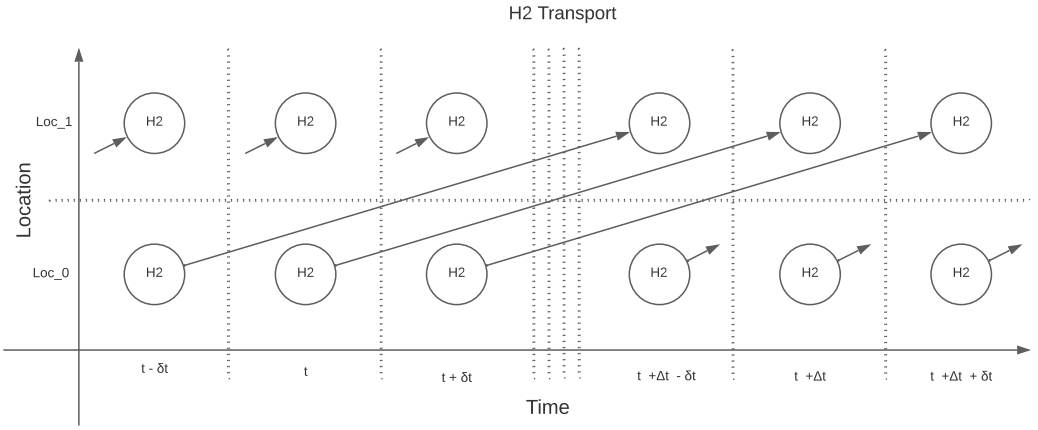

Figure 5.16: Template Edge Hydrogen Transport. The hydrogen Transport asset only has one component. The template edge of this component moves hydrogen from the "Hydrogen Storage" node at a specific location and time, to the "Hydrogen" node at a different location and a time Δt in the future. The component has edges every δt, the time between operation. Hydrogen is transported every δt interval of time. Each time hydrogen is transported, it takes Δt amount of time.

Consider the conversion function of the hydrogen transport component. Energy is used to transport the hydrogen such as the energy used to pump the hydrogen along a pipeline, or power the vehicles used to transport the hydrogen. The transport could use any forms of energy, such as electricity, heat, or hydrogen; this can be modelled by using a flow of two types of quantities. However, for simplicity, assume that a constant fraction of the chemical energy vector is consumed to transport it per unit distance. This is similar to the fractional loss per unit distance of the electricity lines. Assuming linear losses, the conversion function of the hydrogen transport component

(ψ) is given by:

$$y_t = \psi(x_t) = (1 - L\mu)x_t \tag{5.90}$$

Where x_t and y_t are the amount of hydrogen moving out of the source location and into the target location, respectively. μ is an asset brand parameter in the system designer language; it is the fractional loss of energy per unit distance, and has the units [km^{-1}]. L is the distance between the source and target node locations.

For simplicity, L can be assumed to be the great circle distance, similar to the electricity line asset, and is given by Equation 5.9. In general, a different distance metric that takes into account different routes may be used. As this is only used to set the value of the conversion function parameter, a more complex path generation algorithm may be used to define L.

Similar to the electricity line asset, the conversion function parameters asset brand parameters can be combined to form the conversion function parameter η.

$$\eta = (1 - L\mu) \tag{5.91}$$

The conversion function parameter can thus be written as:

$$y_t = \psi(x_t) = \eta x_t \tag{5.92}$$

The conversion function parameters ($\vec{\mathbf{P}_\psi}$) of the hydrogen asset only consist of one parameter:

$$\mathbf{P}_\psi = (\eta) \tag{5.93}$$

The cost of chemical transport can be split into its sizing (f_{size}) and usage costs (f_{use}). The sizing cost could be the capital cost of building pipelines, or securing trading route rights, or the cost of ships. The usage cost is the cost of renting or repairing ships.

The usage cost of the hydrogen transport asset could be assumed to be proportional to the amount of hydrogen energy vector transported and the distance it is transported for. The cost of using the hydrogen transport asset ($f_{use,t}$) at time t is thus:

$$f_{size,t} = C_{use} L x_t \tag{5.94}$$

Where C_{use} is an asset brand parameter in the system designer language; it is the O&M cost of transporting the hydrogen per amount of hydrogen per distance, and has the units [$\$\,\mathrm{kg}^{-1}\,\mathrm{km}^{-1}$].

C_{use} and L can be combined to form the cost function parameter $\mathbf{P}_{f_{use}}$:

$$\mathbf{P}_{f_{use}} = C_{use} L \tag{5.95}$$

The total usage cost of the asset (f_{use}) is the sum of usage costs over all times:

$$f_{use} = \sum_t f_{use,t} = \mathbf{P}_{f_{use}} \sum_t x_t \tag{5.96}$$

The cost of sizing the hydrogen transport asset ($f_{size,t}$) to meet the requirements at time t is given by:

$$f_{size,t} = C_{cap} x_t \tag{5.97}$$

Where C_{cap} is an asset brand parameter in the system designer language; it is the capital cost per unit peak hydrogen transported, and has the units [$\$\,\mathrm{kg}^{-1}$].

The total sizing cost of the asset (f_{size}) is the maximum of the sizing costs over all times:

$$f_{size} = \max_t\{f_{size,t}\} = C_{cap} \max_t\{x_t\} \tag{5.98}$$

The total cost function of the hydrogen transport asset (f_{asset}) is thus:

$$f_{asset} = f_{size} + f_{use} = C_{cap} \max_t\{x_t\} + \mathbf{P}_{f_{use}} \sum_t x_t \tag{5.99}$$

The cost function parameters ($\vec{\mathbf{P}_f}$) of the hydrogen transport asset consist of two parameters:

$$\vec{\mathbf{P}_f} = (C_{cap}, \mathbf{P}_{f_{use}}) \tag{5.100}$$

The flows, asset brand parameters, conversion function parameters, cost function parameters of the Hydrogen Transport asset, and their units, are compiled in Table 5.19.

Table 5.19: Flows and Parameters of Hydrogen Transport Asset

Symbol	Meaning	Units	Language
ϕ_i	Latitude of location i	rad	System Designer
λ_i	Longitude of location i	rad	System Designer
μ	losses per distance	m^{-1}	System Designer
C_{use}	Capital cost per hydrogen moved per distance	$\$\,\mathrm{kg}^{-1}\,\mathrm{m}^{-1}$	System Designer Asset Modeller
C_{cap}	Cost per peak hydrogen moved	$\$\,\mathrm{kg}_{\mathrm{p}}^{-1}$	Asset Modeller Asset Modeller
η	Transport Efficiency	unitless	Asset Modeller
$\mathbf{P}_{f_{use}}$	Cost per hydrogen moved	$\$\,\mathrm{kg}^{-1}$	Asset Modeller
x	Hydrogen leaving source node	kg	Asset Modeller
y	Hydrogen entering target node	kg	Asset Modeller

5.2.6 Battery Energy Storage System

Section 5.1.4 models a hydrogen storage tank as a simple example of an asset that performs the function of energy storage, i.e. movement of energy in time. However, "energy storage system" is traditionally viewed as an asset that is also able to be "charged" and "discharged". Thus, an energy storage system is a complex asset in STEVFNs. Examples of energy storage systems include batteries, pumped hydro storage, compressed-air energy storage (CAES), hydrogen energy storage (hydrogen storage tank, electrolyzer, and fuel cell), flow batteries, flywheel, capacitor, and inductor. These may seem like very different assets and are usually modelled very differently. However, all types of ESS can be modelled using the same model by replacing the generalized coordinates of the ESS with their respective ones. Table 5.20 shows the generalized coordinates and velocities for a variety of ESS.

Consider the modelling of the ESS asset in STEVFNs. An ESS essentially performs three functions, it "charges", "discharges" and "stores"; these are interpreted as moving energy in type, in type, and in time, respectively. An ESS can thus be described in the asset modeller language as an asset with three components: the "charging" component, "discharging" component, and the "storage" component. Figure 5.17 shows the UML diagram of the ESS asset.

The charging, discharging and storage components of some ESS can be sized and operated independently. Examples of such ESS include flow batteries and hydrogen electrical energy storage systems. The costs of such ESS can thus be separated into

Table 5.20: Generalized Coordinates of ESS

ESS Technology	Generalized Coordinate	Generalized Velocity
Chemical Battery	Electrical Charge ($Q = \int I\,dt$)	Electrical Current (I)
Flow Battery	Electrical Charge ($Q = \int I\,dt$)	Electrical Current (I)
Capacitor	Electrical Charge ($Q = \int I\,dt$)	Electrical Current (I)
Pumped Hydro	Volume of Water (V)	Flow of Water ($\frac{dV}{dt}$)
Pumped Hydro	Reservoir Water Level Height (h)	Rate of Change of Reservoir Height ($\frac{dh}{dt}$)
Hydrogen Energy Storage	Mass of Hydrogen (m)	Flow of Hydrogen ($\frac{dm}{dt}$)
Inductor	Electrical Current (I)	Rate of Change of Electrical Current ($\frac{dI}{dt}$)
Flywheel	Angular Velocity (ω)	Angular Acceleration($\frac{d\omega}{dt}$)
Isothermal CAES	Volume of Air Flowed ($\int J\,dt$)	Flow Rate of Air from Surrounding (J)
Thermal Energy Storage	Temperature (T)	Rate of Change of Temperature ($\frac{dT}{dt}$)
Phase Change Energy Storage	Mass of Material in New Phase (m)	Mass Rate of Material Changing to New Phase ($\frac{dm}{dt}$)
Gravitational Energy Storage	Height of Payload (h)	Velocity of Payload ($\frac{dh}{dt}$)

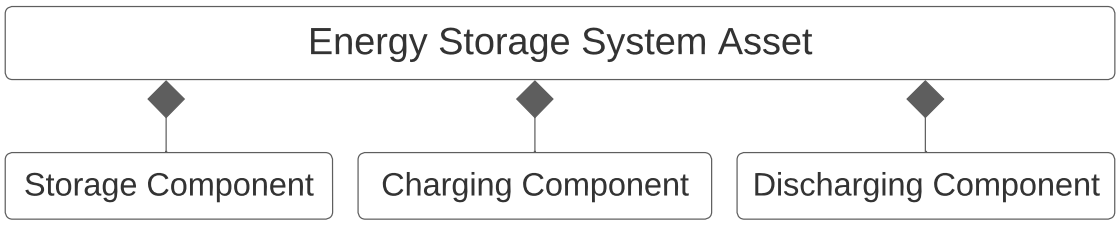

Figure 5.17: UML ESS. An energy storage system asset consists of three components: storage, charging, and discharging components.

Table 5.21: Template Edge of Storage Component

Source Node Type	Energy Storage System (ESS)
Target Node Type	Energy Storage System (ESS)
Source Node Location	Location 1
Target Node Location	Location 1
Operational Time Difference (δt)	1 hour
Time Difference Between Target and Source Node (Δt)	1 hour

the sum of the costs of the individual components. The sizing, operation and cost of these components are decoupled, and thus the components are decoupled. When the components of an ESS are decoupled, they can be modelled separately as three simple assets instead of a complex asset with three components. The charging asset and discharging asset are simple conversion assets like the hydrogen water heater in Section 5.1.5; they convert electricity to the respective generalized coordinates that describe the asset. The storage asset is a simple storage asset such as the hydrogen storage tank in Section 5.1.4; these move the respective generalized coordinates in time. Thus, these ESS can be modelled without any additional information.

Consider now ESS whose components cannot be decoupled and need to be modelled as complex assets. Examples of such assets include Li-ion batteries and lead-acid batteries. The charging, discharging, and storage components of these assets are modelled similar to their simple asset counterparts. Figure 5.18 presents the template edges of the charging, discharging and storage components of an ESS asset.

Consider the storage component of the ESS asset. The storage component moves generalized coordinates out of the ESS node at a specific location and time, and moves generalized coordinates into the ESS node at the same location but a future time. The template edge of the storage component is defined by Table 5.21.

In general, the conversion function of the storage component (ψ_s) is given by:

$$y_{s,t} = \psi_s(x_{s,t}) \tag{5.101}$$

Where x_t is the amount of generalized quantities flowing out of the ESS node at time t; this can also be interpreted as the state of charge of the ESS at time t ($Q_t = x_t$). y_t is the amount of generalized quantities flowing into the ESS node at time t. ψ_s can be interpreted as representing the self-discharge losses of an ESS.

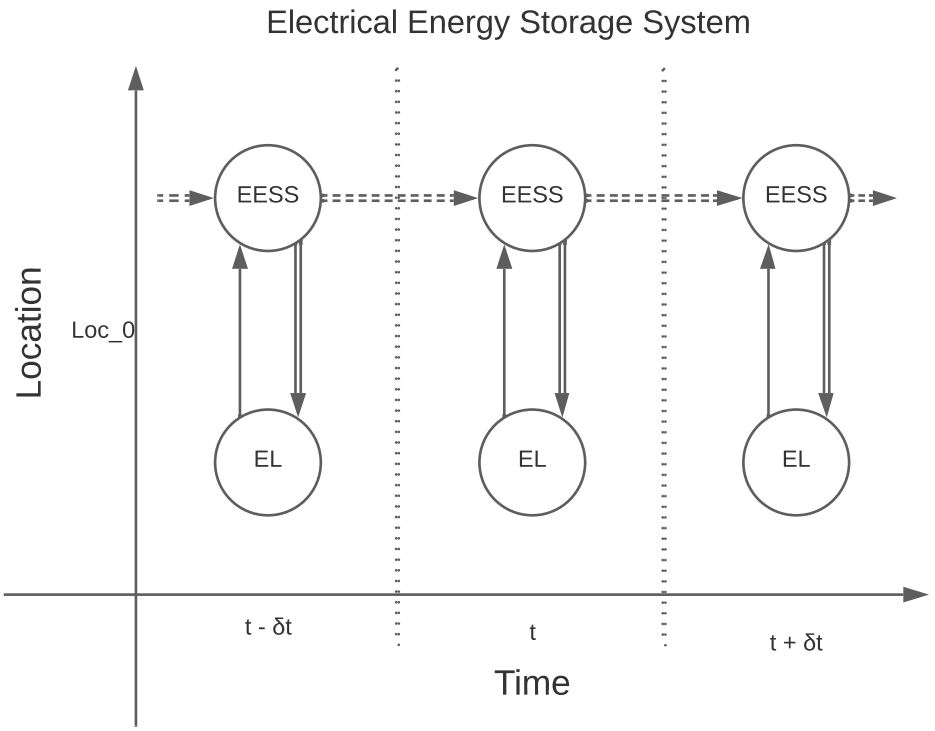

Figure 5.18: Template Edge EESS. The electrical energy storage system asset (EESS) has three components: storage, charging, and discharging components. The template edge of the storage component is represented by the double dotted-lined arrow. The storage component moves the generalized coordinate from the "EESS" node at a specific location and time, to the "EESS" node at a same location and at a time δt in the future. The template edge of the charging component is represented by the single solid-lined arrow. The charging component converts the electricity from the "Electricity Grid" node at a specific location and time, to generalized coordinate in the "EESS" node at a same location and time. The template edge of the discharging component is represented by the double solid-lined arrow. The discharging component's template edge has the opposite direction as the charging component's template edge. The discharging component converts the generalized coordinate from the "EESS" node at a specific location and time, to electricity in the "Electricity Grid" node at a same location and time. All three components have edges every δt, the time between operation.

Table 5.22: Template Edge of Charging Component

Source Node Type	Electricity Grid (EL)
Target Node Type	Energy Storage System (ESS)
Source Node Location	Location 1
Target Node Location	Location 1
Operational Time Difference (δt)	1 hour
Time Difference Between Target and Source Node (Δt)	0 hour

Table 5.23: Template Edge of Discharging Component

Source Node Type	Energy Storage System (ESS)
Target Node Type	Electricity Grid (EL)
Source Node Location	Location 1
Target Node Location	Location 1
Operational Time Difference (δt)	1 hour
Time Difference Between Target and Source Node (Δt)	0 hour

Consider the charging component. The charging component moves electrical energy out of the electricity grid node (EL) at a specific location and time, converts it to the generalized coordinate of the ESS, and moves it into the ESS node at the same location and time. The template edge of the charging component is defined by Table 5.22.

In general, the conversion function of the charging component (ψ_c) is given by:

$$y_{c,t} = \psi_c(x_{s,t}, x_{c,t}) \tag{5.102}$$

$x_{c,t}$ is the amount of generalized quantities flowing out of the electricity grid node at time t; this is also the product of the charging power and operational time $P_{c,t}\delta t = x_{c,t}$. $y_{c,t}$ is the amount of generalized coordinate that flows into the ESS node at time t; this is also the product of the charging current and operational time $I_{c,t}\delta t = y_{c,t}$.

The discharging component has the opposite function of the charging component. It moves generalized quantities out of the energy storage system (ESS) node at a specific location and time, converts it into electrical energy, and moves electrical energy into the electricity grid (EL) node. The template edge of the Discharging component is defined by Table 5.23.

In general the conversion function of the discharging component (ψ_d) is similarly defined by:

$$y_{d,t} = \psi_d(x_{s,t}, x_{d,t}) \tag{5.103}$$

$x_{d,t}$ is the amount of generalized coordinates flowing out of the ESS node at time t; this is also the product of the discharging current and operational time $I_{d,t}\delta t = x_{d,t}$. $y_{c,t}$ is the amount of electrical energy that flows into the electricity grid node at time t; this is also the product of the discharging power and operational time $P_{d,t}\delta t = y_{d,t}$.

Note that splitting the conversion between electricity and generalized quantities into two directions is similar to the splitting of electricity flow to two directions space in the bi-directional electricity line. In the bi-directional electricity line, the movement was from one location to another. In the case of an EESS, the movement is from one type to another.

To demonstrate the process of analyzing the convexity of modelling and EESS, consider a Li-ion battery, such as the one used by Ahsan et. al [108]. A Li-ion battery can be implemented in STEVFNs using a white-box or a black-box model. A white-box model is a bottom-up model that starts with internal physics of the asset to derive the conversion functions of the components of the asset. A black-box model is top-down model that directly builds the conversion functions of components by fitting measurements of the asset to concave functions.

Set the generalized coordinate of a Li-ion battery as the amount of electrical charge (Q) that has moved through the battery. The generalized velocity is thus the DC current (I) in the battery.

First consider finding a good approximation for the conversion functions by modelling it bottom-up, as a white box. The generalized force of a battery is the voltage across the battery (V). Consider the discharging power of a battery. The discharging power (P_d) of a battery is given by:

$$P_d = I_d V \tag{5.104}$$

Where I_d is the discharging current. However, the voltage is a function of I_d and Q. The higher the charge of a battery, the higher the voltage. The higher the discharging current, the lower the voltage. A linear approximation for the voltage may be tried as an example:

$$V(Q, I_d) = a_0 + a_1 I_d - a_2 Q \tag{5.105}$$

Where a_0, a_1 and a_2 are parameters. The discharging power now becomes:

$$P_d = a_0 I_d + a_1 (I_d)^2 - a_2 I_d Q \tag{5.106}$$

Using Disciplined Convex Programming (DCP), $I_d Q$ is a product of two variables, thus its curvature cannot be determined automatically using CVXPY. Instead test if P_d is a concave function by testing if the Hessian matrix of P_d is negative semi-definite. The determinant of the Hessian matrix of P_d is $-(a_2)^2$. As a_2 is a positive and real, the determinant of the Hessian matrix is always less than zero. Because the Hessian matrix is two dimensional, this means that its eigenvalues have opposite signs, and P_d is not convex. Explicitly finding the eigenvalues of the Hessian matrix confirms this as the eigenvalues $\lambda_\pm$ are:

$$\lambda_\pm = a_1 \pm \sqrt{a_1^2 + \frac{a_2^2}{4}} \tag{5.107}$$

Guessing could be continued manually to find an appropriate function for V that will result in a good approximation for the conversion function. Instead, consider instead finding a good approximation for the conversion function using empirical methods, by modelling the battery top-down as a black-box.

The DC current in a battery can be easily measured. As the current is easier to measure then the total charge that has moved through the battery, the charge is calculated as the integral of the current over time. This allows the measurement of the active charging and discharging power of the battery as a function of its charge and charging or discharging current. The power-charge-current surface for a Li-ion battery reproduced from Ahsan el. al [108] is shown in Figure 5.19. As discussed by Ahsan et. al [108], this is a non-concave surface, and will make the optimization problem non-convex. Ahsan et. al did not try to find a convex approximation for the battery model. They let the battery model make the optimization problem become non-convex and tried to solve it using heuristic methods.

Consider instead convex approximations for the battery model. Attempts can be made to find a concave function for P as a function of Q and I that is able to approximate this surface. This general concave function can be defined by a vector

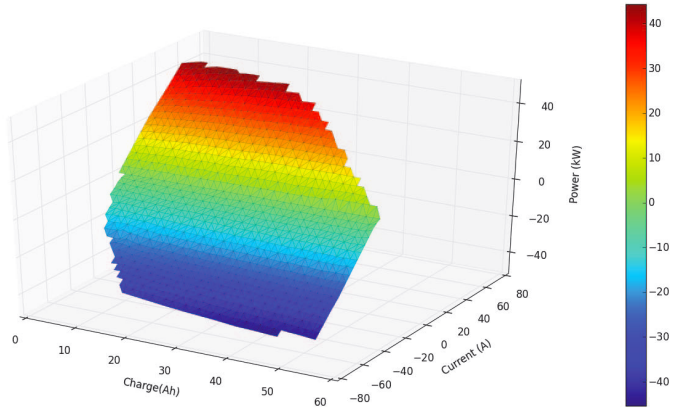

Figure 5.19: Li-Ion P-Q-I surface reproduced from Ahsan el. al [108]. The charging or discharging power of a Li-ion battery depends in the charging or discharging current, and the electrical charge in the battery. The electrical charge in the battery is the integral of the current and is a function of its state. We may use that as the generalized coordinate to describe a battery. Charging and discharging are represented by positive and negative powers and currents, respectively. The surface represents all possible states that the battery can be in. A charge discharge cycle is represented by a loop on the surface.

of parameters $\vec{A}$. These parameters can be fit by using a fitting method such as least square errors.

This is just an example of finding a good function to fit this surface. Any curve fitting methods may be adopted, including machine learning algorithms using only convex functions as basis functions. The system designer can measure the $P-Q-I$ surface as in Figure 5.19, and perform "model learning" offline to find the asset brand parameters $\vec{A}$ that fit the surface. These parameters A are also conversion function parameters in the asset modeller language. The conversion function is thus the convex function that was learnt, and the quicker "model inference" is performed during the overall optimization of the energy system design.

Further convexity analysis to find better implementation of Li-ion batteries in STEVFNs is beyond the scope of this thesis, and is left for future research. For the purposes of this chapter, consider an example of fractional losses in a Li-ion battery. Section 3.1 provided a definition for the instantaneous efficiencies and how they relate to the generalized force (Voltage for a Li-ion battery). A constant charging and discharging efficiency is equivalent to assuming that the battery has constant open circuit voltage (V_0), charging voltage (V_c) and discharging voltage(V_d). V_0, V_c and V_d are asset brand parameters of the battery in the system designer language. In this case, η_c is given by:

$$\eta_c = \frac{V_0}{V_c} \tag{5.108}$$

η_d is similarly given by:

$$\eta_d = \frac{V_d}{V_0} \tag{5.109}$$

The conversion function of the discharging component is thus given by:

$$y_{d,t} = \psi_d(x_{d,t}) = I_{d,t} V_d \delta t = V_0 \eta_d x_{d,t} \tag{5.110}$$

The conversion function of the charging component is similarly given by:

$$y_{c,t} = \psi_c(x_{c,t}) = \frac{P_{c,t}\,\delta t}{V_c} = \frac{\eta_c}{V_0} x_{c,t} \tag{5.111}$$

Note that if the only edges attached to the ESS node are the flows from the charging, discharging, and storage components, then V_0 can be freely chosen in this simple case of constant charging and discharging voltages. V_0 can be interpreted as

the "nominal conversion rate" between electrical energy and generalized quantities of the ESS. If V_0 is set normalized one, the corresponding normalized generalized quantity of the ESS is the internal energy of the ESS as described by Equation 3.12. Thus, the third asset brand parameter V_0 is not necessary to model the ESS.

In general the charging ratio ($\mathbf{P}_{\psi_c}$) can be defined as a conversion function parameter in the asset modeller language:

$$\mathbf{P}_{\psi_c} = V_0 \eta_c \tag{5.112}$$

Similarly, the discharging ratio ($\mathbf{P}_{\psi_d}$) can be defined as a conversion function parameter in the asset modeller language:

$$\mathbf{P}_{\psi_d} = V_0 \eta_d \tag{5.113}$$

If V_0 is set to one, the conversion function of the charging component in Equation 5.111 transforms to:

$$y_{c,t} = \psi_c(x_{c,t}) = \eta_c \, x_{c,t} \tag{5.114}$$

Where η_c is a conversion function parameter in the asset modeller language.

Similarly, the conversion function of the discharging component in Equation 5.110 transforms to:

$$y_{d,t} = \psi_d(x_{d,t}) = \eta_d \, x_{d,t} \tag{5.115}$$

Where η_d is a conversion function parameter in the asset modeller language.

The battery operational voltage curves are not always easily available from manufacturers. Manufacturers sometimes provide the "roundtrip" efficiency ($\eta_{roundtrip}$) of batteries. If $\eta_{roundtrip}$ is the asset brand parameter in the system designer language, η_c and η_d may be derived in a different way. The charge-discharge cycle losses may be assumed to be equally divided into the charging and discharging processes. η_c and η_d are thus given by:

$$\eta_c = \eta_d = \sqrt{\eta_{roundtrip}} \tag{5.116}$$

The conversion function of the storage component of the EESS asset is the same as the storage component of the hydrogen storage tank asset in Section 5.1.4. The

conversion function and conversion function parameters for the storage asset are thus given by Equations 5.43 and 5.44, respectively. The conversion function is given by:

$$y_{s,t} = \psi_s(x_{s,t}) = (1-\mu)^{\frac{t_{storage}}{\Delta t}} x_{s,t} \tag{5.117}$$

Where $x_{s,t}$ is the amount of generalized quantities flowing out of the ESS node at time t, and represents the state of charge at time t. $y_{s,t}$ is the amount of generalized quantities flowing into the ESS node at time $t + \Delta t$, and is defined by the conversion function ψ_s. μ is the fractional storage or self-discharge loss of the ESS per storage time $t_{storage}$. μ is unitless, and $t_{storage}$ has units [h].

μ and $t_{storage}$ are asset brand parameters in the system designer language and can be combined to form a conversion function parameter of the storage component ($\mathbf{P}_{\psi_s}$):

$$\mathbf{P}_{\psi_s} = (1-\mu)^{\frac{t_{storage}}{\delta t}} \tag{5.118}$$

The conversion function parameters of the full ESS asset ($\vec{\mathbf{P}}_{\psi_{asset}}$) are thus given by:

$$\vec{\mathbf{P}}_{\psi_{asset}} = (\mathbf{P}_{\psi_c}, \mathbf{P}_{\psi_d}, \mathbf{P}_{\psi_s}) \tag{5.119}$$

The sizing cost of the storage component ($f_{size,s}$) is similarly given by Equations 5.45 and 5.46.

$$f_{size,s} = C_{size,s} \max_t\{x_{s,t}\} \tag{5.120}$$

Where $C_{size,s}$ is an asset brand parameter and a cost function parameter. $C_{size,s}$ is the capital cost of the ESS per storage capacity. If the generalized quantity of a battery is modelled as the electrical charge in the battery, $C_{size,s}$ has units [$\$\,\mathrm{Ah_p^{-1}}$]. If the generalized quantity is modelled as energy (by assuming $V_0 = 1$), $C_{size,s}$ has units [$\$\,\mathrm{kWh_p^{-1}}$].

The sizing cost of the charging ($f_{size,c}$) components can be modelled as:

$$f_{size,c} = \frac{C_{size,c}}{\delta t} \max_t\{x_{c,t}\} \tag{5.121}$$

Where the asset brand parameters $C_{size,c}$ is the capital cost of the ESS per peak charging power. $C_{size,c}$ has the units [$\$\,\mathrm{kW_p^{-1}}$].

The asset brand parameters can be combined to form the cost function parameter for the charging component ($\mathbf{P}_{f_{size,c}}$):

$$\mathbf{P}_{f_{size,c}} = \frac{C_{size,c}}{\delta t} \tag{5.122}$$

The sizing cost of the discharging ($f_{size,c}$) components can be similarly modelled as:

$$f_{size,d} = \frac{C_{size,d} V_0}{\delta t} \max_t \{x_{d,t}\} \tag{5.123}$$

Where the asset brand parameters $C_{size,d}$ is the capital cost of the ESS per peak discharging power. $C_{size,d}$ has the units [$\$\,\mathrm{kW_p^{-1}}$].

The asset brand parameters can be combined to form the cost function parameter for the charging component ($\mathbf{P}_{f_{size,c}}$):

$$\mathbf{P}_{f_{size,d}} = \frac{C_{size,c} V_0}{\delta t} \tag{5.124}$$

The ESS asset meets to be sized to meet all sizing requirements. Thus, the sizing cost of the ESS asset ($f_{size,asset}$) is the maximum of the sizing costs of its three components:

$$f_{size,asset} = \max\{f_{size,s}, f_{size,c}, f_{size,d}\} \tag{5.125}$$

Section 3.4.3 discusses the degradation costs of discharging a battery ($f_{use,d}$). Equation 3.49 can be rewritten using the notation of this section as:

$$f_{use,d,t} = C_{size,s} \left[\frac{1}{N(x_{s,t} - x_{d,t}, x_{d,t})} - \frac{1}{N(x_{s,t}, x_{d,t})} \right] \tag{5.126}$$

Where $f_{use,d,t}$ is the degradation cost of discharging the ESS at time t. Where N is the number of lifecycles of a ESS, and is in general a function of the state of charge of the ESS and discharging current of the ESS. An appropriate convex function can be found using various white-box or black-box models just like the conversion function for charging and discharging components as is discussed in earlier parts of this section. Figure 5.20 shows a plot of the number of times a Li-ion battery can be used depending on the depth of discharge of its cycle, reproduced from the literature [108].

As an example consider a fixed degradation proportional to the total throughput of the ESS. A lot of the literature assumes a fixed ESS throughput [183]. This is equivalent to fixed degradation cost per unit energy or charge moved and a typical

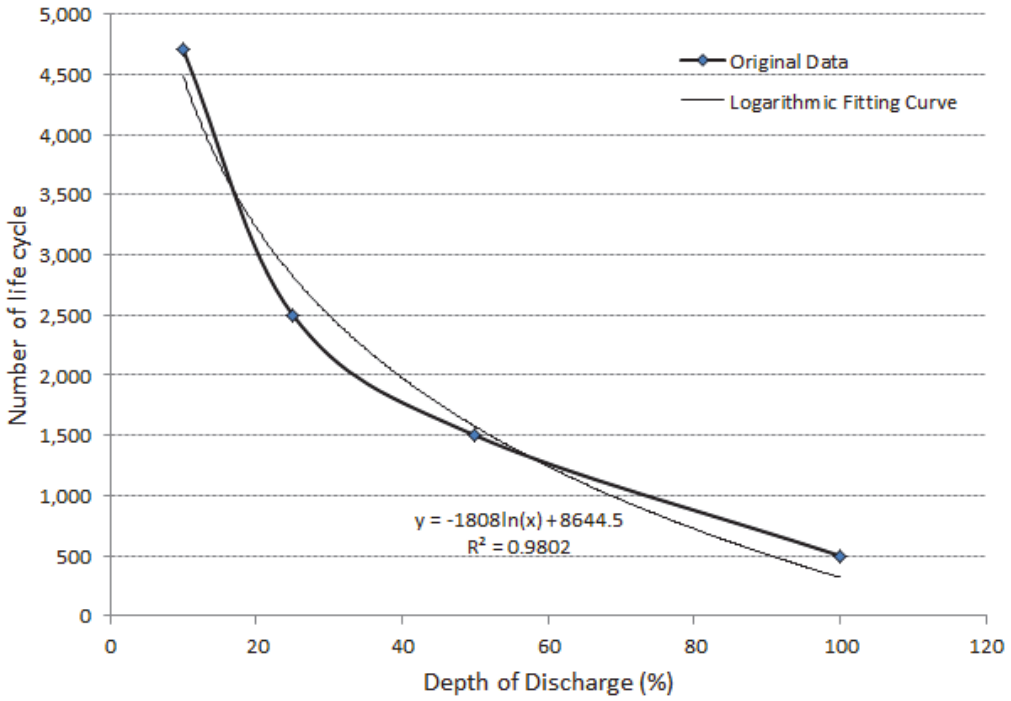

Figure 5.20: Li-Ion N Lifecycle vs DOD reproduced from the literature [108]. The number of times a Li-ion battery can be used depends on the depth of discharge of its cycle. A charge-discharge cycle in this case assumes charging a battery to maximum state of charge and discharging it to a specific value. The number of lifecycles also depends on the charging and discharging current. These will be represented by similar curves for different charging or discharging currents. They can be represented as a surface if we take the continuous limit.

method used is called "rainfall counting" [184, 108]. If the degradation costs of the charge-discharge cycle is equally distributed between the two processes, the total degradation cost of discharging ($f_{use,d}$) is thus given by:

$$f_{use,d} = \frac{C_{size,s}}{2N} \sum_t x_{d,t} \tag{5.127}$$

Where N is a unitless asset brand parameter and is the number of lifecycles an ESS can be operated at full depth of discharge before it needs to be replaced. The asset brand parameters can be combined to form the cost function parameter ($\mathbf{P}_{f_{use,d}}$):

$$\mathbf{P}_{f_{use,d}} = \frac{C_{size,s}}{2N} \tag{5.128}$$

The degradation cost for the charging component ($f_{use,c}$) can be similarly defined as:

$$f_{use,c} = \frac{C_{size,s} V_0}{2N} \sum_t x_{c,t} \tag{5.129}$$

The asset brand parameters can be combined to form the cost function parameter ($\mathbf{P}_{f_{use,c}}$):

$$\mathbf{P}_{f_{use,c}} = \frac{C_{size,s} V_0}{2N} \tag{5.130}$$

The degradation of the storage component is the degradation of having the ESS too full or empty, this is an issue for batteries such as Li-ion batteries. A quadratic cost may be assumed based on the fractional state of charge of the ESS:

$$f_{use,s,t} = \mathbf{P}_{f_{use,s}} \left[\frac{x_{s,t}}{\max_t\{x_{s,t}\}} \right] \tag{5.131}$$

While this captures the degradation costs of a Li-ion storage, it is not a convex function due to the $\max_t\{x_{s,t}\}$ term at the denominator. This represents the size of the ESS. If the size of the ESS is fixed and the ESS is only operated, then these storage degradation costs can be modelled. This is similar to including I^2R losses for electricity lines in Section 5.1.1.

As the degradation costs increase if the ESS is too much or too little charged, taking an average degradation cost will simply result in the lifetime or shelf-life of the ESS. Thus the degradation costs of the storage component can be ignored for an ESS, in particular Li-ion batteries, to first order approximation.

Table 5.24: Flows and Parameters of BESS Asset

Symbol	Meaning	Units	Language
V_0	Nominal Voltage	V	System Designer
η	Roundtrip efficiency	unitless	System Designer
μ	Self-discharge loss per typical storage time	unitless	System Designer
$t_{storage}$	Typical storage time	h	System Designer
N	Number of lifecycles	unitless	System Designer
$C_{size,s}$	Capital cost per electrical charge capacity	$\$\,\mathrm{Ah_p^{-1}}$	System Designer
$C_{size,c}$	Capital cost per peak charging power	$\$\,\mathrm{W_p^{-1}}$	System Designer
$C_{size,d}$	Capital cost per peak discharging power	$\$\,\mathrm{W_p^{-1}}$	System Designer
$\mathbf{P}_{\psi_s}$	Storage Efficiency	unitless	Asset Modeller
$\mathbf{P}_{\psi_c}$	Charging Ratio	$\mathrm{V^{-1}}$	Asset Modeller
$\mathbf{P}_{\psi_d}$	Discharging Ratio	V	Asset Modeller
$\mathbf{P}_{f_{use,c}}$	Degradation cost per charging electrical energy	$\$\,\mathrm{Wh^{-1}}$	Asset Modeller
$\mathbf{P}_{f_{use,d}}$	Degradation cost per discharging electrical charge	$\$\,\mathrm{Ah^{-1}}$	Asset Modeller
$\mathbf{P}_{f_{size,s}}$	Cost per peak electrical charge stored	$\$\,\mathrm{Ah^{-1}}$	Asset Modeller
$\mathbf{P}_{f_{size,c}}$	Cost per peak electrical energy charged	$\$\,\mathrm{Wh^{-1}}$	Asset Modeller
$\mathbf{P}_{f_{size,d}}$	Cost per peak electrical charge discharged	$\$\,\mathrm{Ah^{-1}}$	Asset Modeller
x	Electrical energy leaving source node	Wh	Asset Modeller
y	Electrical energy entering target node	Wh	Asset Modeller

The degradation, and thus usage cost of the ESS asset ($f_{use,asset}$) is the sum of the degradation costs of the charging and discharging components:

$$f_{use,asset} = f_{use,c} + f_{use,d} \tag{5.132}$$

The total cost of the ESS asset (f_{asset}) is the maximum of the sizing and degradation costs:

$$f_{asset} = \max\{f_{size,asset}, f_{use,asset}\} \tag{5.133}$$

The cost function parameters ($\vec{\mathbf{P}_f}$) of the asset are:

$$\vec{\mathbf{P}_f} = (\mathbf{P}_{size,s}, \mathbf{P}_{size,c}, \mathbf{P}_{size,d}, \mathbf{P}_{use,c}, \mathbf{P}_{use,d}) \tag{5.134}$$

The flows, asset brand parameters, conversion function parameters, cost function parameters of the BESS asset, and their units, are compiled in Table 5.17.

5.3 Summary

This chapter answers thesis sub-question 3:"How are models for real-world assets generated from traditional data using the model-generators?" This chapter solves the problem and implements five simple and six complex real-world assets in the

STEVFNs system design and unified model-generators using manufacturer data or simple black-box measurements.

A simple asset is an asset that consists of only one component that performs only one basis function of an energy system. This chapter models the following five simple energy system assets in STEVFNs:

1. Electricity Line
2. Fossil Fuel Power Generator
3. Elastic Temporal Demands
4. Hydrogen Storage Tanks
5. Hydrogen Water Heater

A complex asset is an asset that consists of two or more components or performs more than one basis function of an energy system. This chapter models the following six complex energy system assets in STEVFNs:

1. Bi-Directional Electricity Line
2. Perfectly Inelastic Temporal Demand
3. Solar PV Farm
4. Demand Shifting
5. Hydrogen/Ammonia Transport
6. Battery Energy Storage System

This chapter demonstrates the process of describing an energy system in STEVFNs asset modeller and system designer language, and defining the translations between the two. Describing an asset in the asset modeller language automatically translates it to optimizer language if we use DCP and DPP to define the various functions in the asset modeller language.

This chapter demonstrates with these eleven examples, how modelling these assets in STEVFNs makes it easy to see if an asset is non-convex, and thus the energy system

design problem non-convex, and hard to solve. When these assets are non-convex, it becomes apparent what assumptions make the assets non-convex. Finally, this chapter demonstrates how good approximations can be found to make these assets convex. Modelling assets in STEVFNs also makes it easy to show if certain assets are strongly non-convex and thus no good approximations exist. Thus, energy system design problems with those assets should be solved using heuristic algorithms such as machine learning. Examples of these assets include batteries, and the electricy grid.

Future research can develop more accurate implementations of these assets in STEVFNs: for example, the implementation of the fossil fuel power generator in this chapter does not take into account ramp rate constraints. Furthermore, it assumes a "generation" of electricity with an explicit cost instead of converting fossil fuels to electricity and the storage of the fossil fuels to consider the implicit costs. Future research can use the method of using machine learning to find good convex approximations for assets, in particular batteries. Future work also needs to be done to implement other energy systems asset in STEVFNs such as buildings with space heating or cooling.

Finally, modelling assets in STEVFNs has revealed the lack of some data needed to model assets. These can be easily obtained by simply treating energy assets as black-boxes and measuring the required data. Future researchers can obtain the data highlighted in this chapter to model these assets more accurately in optimization systems while keeping the problems convex and easy to solve. The same will also happen when we try to model other complex assets not modelled in this chapter. This will help us inform asset manufacturers the kind of data required to properly assess their value in a whole energy system.

The main question of the thesis is to determine if a generalized spatio-temporal model of assets can be utilized to optimize the sizing, operation and location of energy system assets. This chapter applies the unified asset model-generator from Chapter 3, and the STEVFNs system design model-generator from chapter 4 to model eleven real-world assets. This enables the building of energy systems design problems with these assets in STEVFNs. However, the STEVFNs system design and unified asset

model-generators are only described mathematically. To be of practical use, the next chapter implements the STEVFNs model-generators as an open source tool.

Chapter 6

The Open-Source STEVFNs Tool

This chapter answers sub-question 4 of the thesis:

"Can the model-generators be implemented as an easily accessible tool?"

This chapter implements the theoretical STEVFNs model-generators as an open source tool in Python.

The main question of the thesis is if a generalized spatio-temporal asset model can be developed and used for the optimal sizing, operation and location of energy system assets. Chapter 5 models eleven classes of energy system assets using the unified asset model-generator in Chapter 3 and the STEVFNs system design model-generator from Chapter 4. While the STEVFNs model-generators have been developed, and models for real-world assets have been generated using STEVFNs, the STEVFNs system design and unified asset model-generators need to be implemented as a tool before they can be used to conduct case studies and get insights into energy system design. This chapter implements the STEVFNs model-generators as an open-source tool.

Section 6.1 gives an overview of the inputs needed by the three types of end-users to use the STEVFNs tool. The three end-users are the system designers, asset modellers, and optimizers. Section 6.2 gives an overview of the modular structure of the code and how it increases accessibility for all three types of end-users. Section 6.3 describes the work being done to increase the accessibility of the code to the three types of end-users. Section 6.4 summarizes the chapter and discusses the future improvements that need to be made to the STEVFNs tool.

6.1 The Three End-Users

The STEVFNs tool has three main types of users, system designers, asset modellers, and optimizers. There are other more "fundamental" types of users of STEVFNs such as those trying to improve the STEVFNs model-generators (e.g.relationships between nodes and edges), those trying to implement STEVFNs into a different language (e.g. Julia, C, C++, or CUDA), or those trying to improve the UI/UX. These other types of users will be discussed in further communications. Figure 6.1 displays the inputs that the three main end-users need to provide to use the STEVFNs tool.

The system designer defines the case study using a single file with the structure of all assets in the system designer language. The system designer defines each scenario using two files: a file with the brand of each asset in the energy system, and a file with the latitude and longitude of each location in the energy system. The system designer also defines the brand parameters for each brand of each asset. This is stored in a database and is stored as part of the definition of the asset. With just these inputs, the system designer is able to define a case study, its scenarios, and assumptions for scenarios and use the STEVFNs tool. In its current form, all of these files are simple CSV files that can be edited in Excel.

The asset modeller is a developer that defines new types of assets in the STEVFNs tool. The asset modeller does this by providing a single .py file with the code for the asset model implemented in STEVFNs. This code defines the components of the asset, the template edge of each component, and the translation between the brand parameters in the system designer language and the cost and conversion function parameters in the asset modeller language.

The optimizer is also a developer that defines how the optimization problem is solved. The STEVFNs tool currently uses CVXPY to define the optimization problem. The optimizer only handles the "CVXPY Problem" object; they do not deal with case study, scenarios, or assets. Thus, the optimizer deals with the CVXPY Problem in exactly the same way as they would normally deal with CVXPY problems. This means that the optimizer needs minimal expertise in energy system design or the physics of asset modelling.

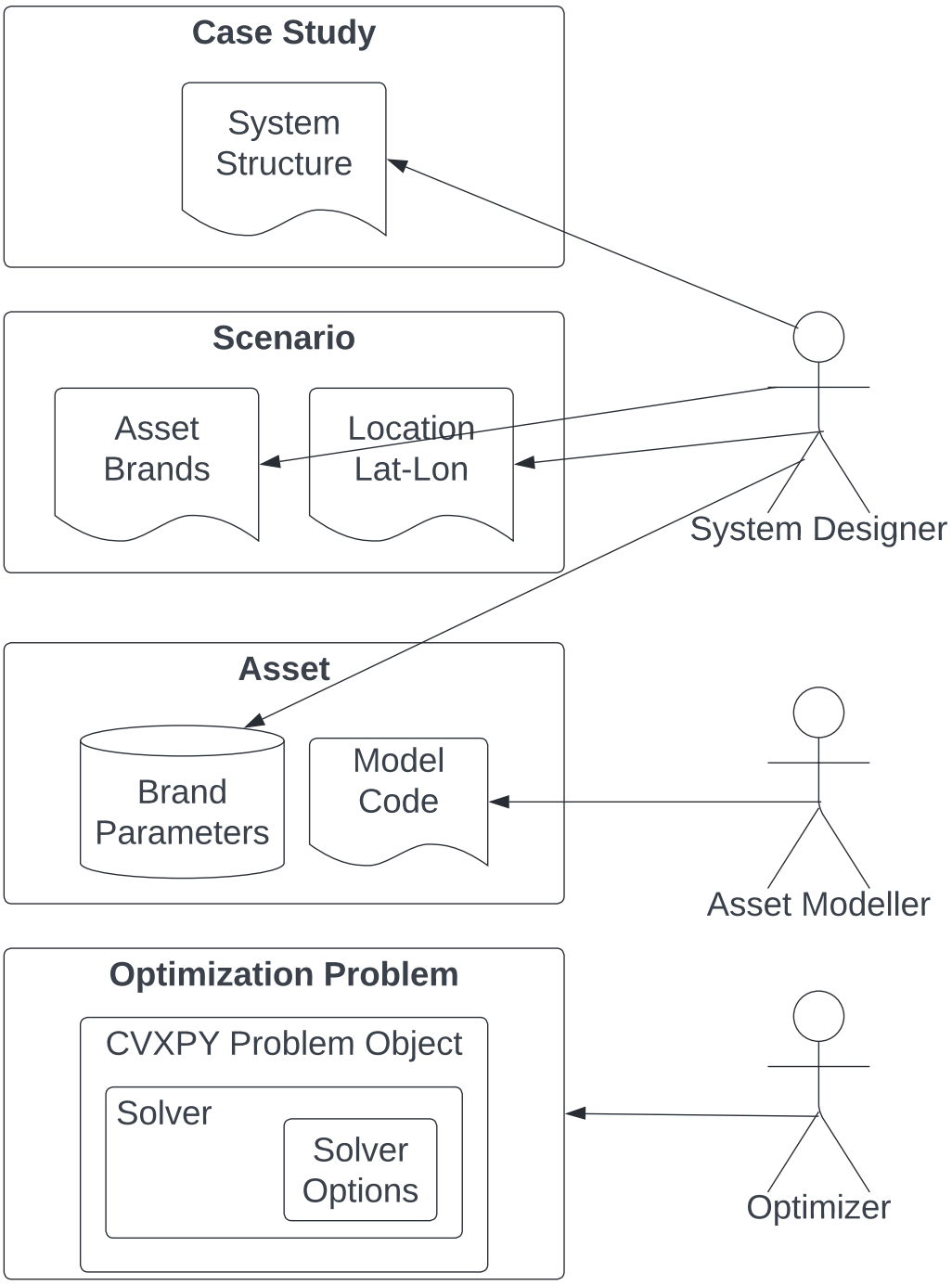

Figure 6.1: User inputs for STEVFNs tool. The system designer defines the case study using a system structure file. The system designer defines each scenario using an asset brands file, and a location lat-lon file. The system designer defines the asset brand parameters for each brands of each assets. The asset modeller defines an asset using a file with the model code. The optimizer manages the optimization problem by defining the CVXPY Problem object, solver, and solver options.

6.2 Modular Approach

The STEVFNs model-generators and tool are designed with modularity in mind. This makes it easy for three types of end-users to use the STEVFNs tool in parallel. The code, and data used by all three types of end-users are kept separate. Improvements and additions can thus be made without any conflicts.

The case study and scenario definitions are kept separate from the asset data, data pre-processing, and the rest of the code. This makes it easy to handle as users do not need to open very large Excel files which process data such as the starter data kits provided for OSeMOSYS [7].

System designers only need to add one csv file to define a case study; this is the list of assets and their locations. They only need to add two csv files per scenario; these are the asset brands, and the lat-long of the locations. They can also add new brand information by adding an additional line in a csv file that stores the brand data for the particular asset.

Asset definitions are kept separate from the rest of the code. The main code defines template base asset classes. Asset modellers can implement new assets by defining them as child classes of the template base asset classes. This dramatically reduces the effort needed to defined a new asset class.

Asset modellers can easily add a new asset by defining the template edges, conversion functions, and cost functions of assets. They define the brands by adding translations between brand data and their implementations.

The following assets have been implemented in the STEVFNs tool:

1. Battery Energy Storage System
2. RE Farm (Wind and Solar)
3. Hourly Electricity Demand
4. Hourly High Temperature Heating Demand (HTH)
5. Electric Heater (EL_to_HTH)
6. Ammonia Heater (NH_3_to_HTH)

7. EL_to_NH_3(produces ammonia from electricity)
8. NH_3_to_EL (produces electricity from ammonia)
9. Ammonia Storage Tanks
10. HVDC Inter-connector
11. Ammonia Transport

The STEVFNs tool uses CVXPY as the optimization language. Optimizers can change the solvers by changing the solver used in the CVXPY solve method; this is just one line of code. They can similarly add their own optimizer as they would normally do in CVXPY and all other benefits of CVXPY.

The STEVFNs tool currently forces the use of the ECOS solver that comes pre-packaged with CVXPY. This is because CVXPY sometimes uses an inappropriate solver and gives an error. This bug has been reported and is being dealt with by the managers of CVXPY. Future optimizers can import other existing solver and use them with their respective solver options. They can also define custom solvers for CVXPY and import them. An important future extension is the use of reverse mode automatic differentiation methods implemented on the GPU. These can be combined with parallel versions of penalty or barrier methods on the GPU.

Even with these limitations, as the tool uses DCP and DPP using CVXPY, the tool is able to rerun optimizations for scenarios in fractions of the original solving time. The tool was able to run the first scenario in about 16 hours and subsequent scenarios in about 15 seconds, for about a 4000 times speedup.

6.3 Accessibility

The STEVFNs model-generators were implemented into an open-source tool referred to as the STEVFNs tool. The STEVFNs tool was written in Python and is available freely on GitHub under the MIT licence [1]. The documentation for the tool is available on the GitHub repository. The STEVFNs tool is also being validated against similar existing tools such as OSeMOSYS [8], and TIMES/MARKAL [10, 9]. Organizations that require it are encouraged to validate the STEVFNs tool in-house.

Third-parties are also being approached to certify and validate the STEVFNs tool independently. This increases the transparency, trustworthiness, and credibility of the tool, compared to closed-source tools.

A video tutorial for the tool is also available on YouTube [185]. The theoretical STEVFNs system design model-generators have been disseminated via two seminars in the Energy and Power Group in Oxford [185, 186], and a seminar at the Delta E-plus group at Simon Fraser University [187]. The use of the STEVFNs tool has been taught to PhD students, masters students, research assistants, and energy consultants via multiple seminars. Other academics and industry members have requested seminars for STEVFNs model-generators and tool. These future seminars are being organized. The outputs of the seminars and tutorials will be compiled as a course on the Open University, and there are plans to make more detailed training courses available for policy makers, industry, and academics in energy modelling summer schools such as the ICTP CCG joint summer school on modelling tools for sustainable development [188].

6.4 Summary

This chapter answers thesis sub-question 5: "Can the model-generators be implemented as an easily accessible tool?" This chapter implements the STEVFNs model-generators as an open-source tool for the co-optimization of sizing, operation, and location of energy system assets with scenario assessment. This tool is called the STEVFNs tool and is available on GitHub [1].

The STEVFNs tool is designed ground up to be modular, and easy to use. This makes it possible for three types to end-users to concurrently work on the tool. These end-users are the system designers, asset modellers, and optimizers.

An online tutorial for the tool has be made available on YouTube. Multiple workshops, and seminars have been conducted to train users to use the tool, and are made available online. The tool is currently being used for two international academic collaborations and to guide policy makers in Singapore. More seminars are planned, these will be converted into an Open University course. Additional deep training for the STEVFNs tool will be made available in joint summers schools.

This chapter implements the STEVFNs model-generators in an open-source tool. To demonstrate the power of the STEVFNs tool, the next chapter uses the STEVFNs tool to perform a case study of Singapore.

Chapter 7

Optimal Design and Operation of Whole Energy Systems Using STEVFNs

This chapter answers sub-question 5 of the thesis:

"How do these model-generators and tool yield insights into real world energy system problems?"

This chapter demonstrates how the open-source STEVFNs tool can be used to study the effect of scenario assumptions on optimal system design, and provides a stress test to validate the dynamics of the STEVFNs tool using a hypothetical case study of Singapore.

The main question of the thesis is if a generalized spatio-temporal asset model-generator can be developed and utilized to optimally size, operate and locate energy system assets. Chapter 4 uses the unified asset model-generator developed in Chapter 3 to develop the STEVFNs system design model-generator. The STEVFNs system design model-generator enables the optimal design of an energy system. Chapter 5 develops models for eleven classes of real assets using STEVFNs. Chapter 6 implements the STEVFNs model-generators as an open-source tool. This chapter demonstrates the power of the STEVFNs tool by using it to perform a hypothetical case study of Singapore. The case study and scenarios are not chosen to be directly utilized by policymakers. The main purpose of this chapter and its case study is to demonstrate how the tool can be used, and provide a stress test to validate the dynamics of the STEVFNs tool.

Section 7.1 describes the case study, the scenarios tested, and the brand parameters of the assets used in the scenarios. The results of the case study are presented and discussed in Section 7.2. Section 7.3 concludes the chapter with examples insights and policy recommendations from the hypothetical case study, compares it to existing insights in the literature, and recommends future improvements to the hypothetical case study that can make the results more directly usable by policymakers.

7.1 Case Study: Singapore

Singapore is a severely resource constrained region (SRCR): the amount of energy it consumes is more than it can produce, locally, using RE sources [189]. Singapore is a city-state with an area of 725 km^2 and a population of 5.7 million [190, 20]. Singapore annually consumes 182 PJ of electricity, 92 PJ of oil for transportation, and 320 PJ of various fossil fuels for low and high temperature heating applications [191, 192]. Currently, 95% of Singapore's electricity is generated using natural gas, 1% using coal, 1% using other petroleum products and the remaining 3% is generated using other sources (mainly waste incineration). Local PV accounts for less than 1% of Singapore's total electricity generation [191]. Thus, if Singapore wishes to produce all its energy from renewables, it will have to import RE from other countries.

Figure 7.1 shows the energy system diagram for the case study in the system designer language of STEVFNs. This shows the list of possible assets at each location and between each location pairs. Figures 7.2 and 7.3 show the template edge diagrams in STEVFNs asset modeller language for Singapore and the three RE-locations, respectively.

For the case study in this chapter, the STEVFNs tool was run on an AMD Ryzen 7 5800H. The case study, scenario, and asset brand files used for the case study are available in the "Aniq_DPhil" branch in the GitHub repository.

The case study consists of satisfying hourly electricity (EL) and high temperature heating (HTH) demand at Singapore (SG); these are referred to as EL_Demand and HTH_Demand assets, respectively. HTH refers to heating demand at temperatures so high (more than 200° C) that the COP of heat pumps is close to one, thus these are satisfied by direct heating. These demands can be supplied from DER farms

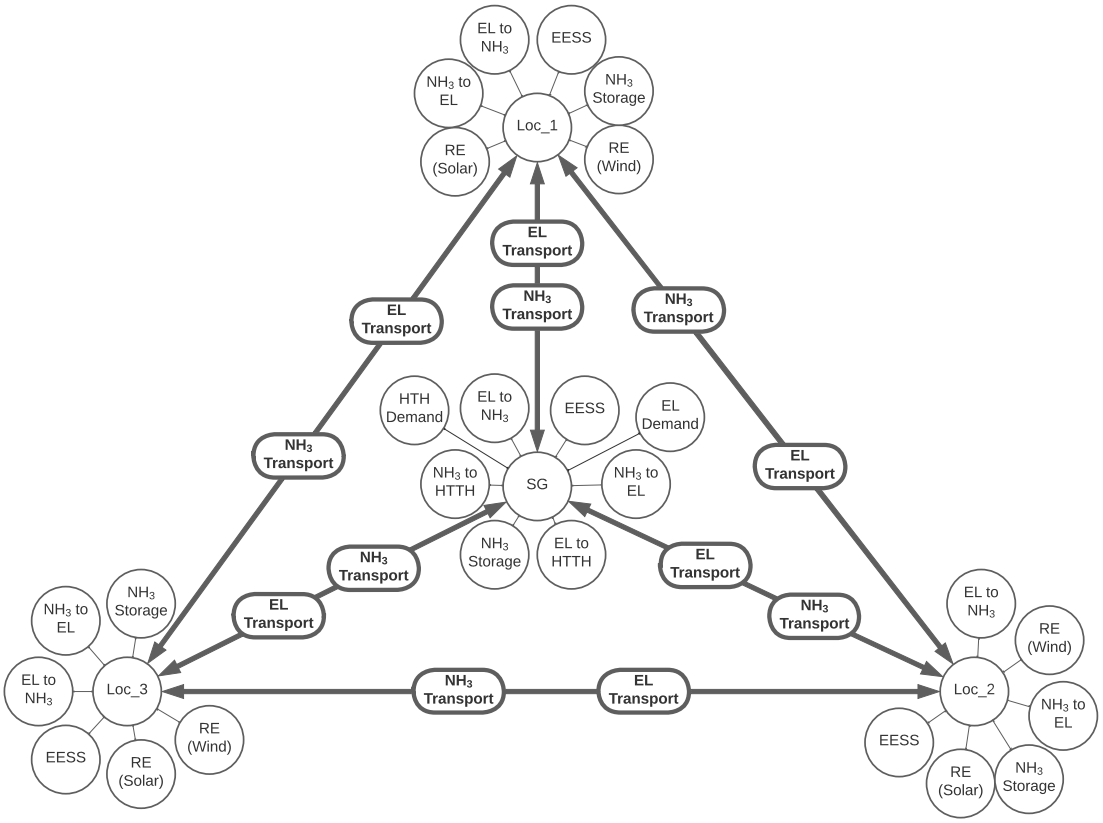

Figure 7.1: Energy System Diagram for the Singapore Case Study. This is the energy system diagram in the system designer language. This simple diagram only defines the possible assets at each location, or between each location pair. There are four locations: one demand location at Singapore (SG), and supply locations (Loc_1, Loc_2 and Loc_3). Demand assets are only present at SG. Supply assets are only present at the RE-farm locations. Various assets that move energy in time and type are present at all locations. There are bi-directional hydrogen and electricity transport assets that move energy in space between each location pair. In theory, the latitude and longitude of each location can be changed between scenarios. However, all scenarios tested will assume the demand location (SG) is fixed at Singapore.

at three potential locations (Loc_1, Loc_2 and Loc_3) around the world. Each DER location can contain solar PV farms and/or Wind farms, referred to as RE(PV) and RE(Wind) assets, respectively.

Energy can be moved in space (transported) via potential bi-directional HVDC lines and NH_3 transport between each of the four locations, i.e. there are six potential links. These are referred to as EL_Transport and NH_3_Transport assets, respectively. Ammonia transport refers to sea and land freight, but is modelled as sea freight for simplicity. Energy can be moved in time (stored) via battery energy storage systems (BESS), or via NH_3 storage assets at all four locations; these are referred to as BESS and NH_3_Storage assets, respectively.

NH_3 is conventionally viewed as better for seasonal storage, and BESS are usually considered less ideal for seasonal storage. However, in this case study, both BESS and NH_3 are allowed to provide seasonal storage; this allows the optimization to determine which storage is utilized to meet seasonal or daily demand shifting requirements.

Electricity can be converted to NH_3 via a combination of N_2-air separators, water electrolyzers and Haber-Bosch plants, with H_2 storage tanks and BESS in ratios described by Salmon et al. [73]. The additional H_2 storage tanks and BESS are required to allow for flexible operation of the Haber-Bosch process. In general these assets should be separated and optimized. However, for simplicity, these are combined as a black-box and treated as a simple asset that converts electricity to NH_3. This asset is referred to as the EL_to_NH_3 asset. There are potential EL_to_NH_3 assets at all four locations.

NH_3 can be converted back to electricity via NH_3 combined cycle gas turbines (CCGT) as described by Cesaro et al. [193]. Some of these are NH_3 CCGTs that crack all or some of the NH_3 to H_2 before feeding them to the CCGTs. However, these crackers can be combined with the CCGT plants as a black-box and treated as a simple asset. This asset is referred to as the NH_3_to_EL asset. There are potential NH_3_to_EL assets at all four locations.

Finally, electricity or NH_3 can be converted to HTH via electric heaters and NH_3 burners, respectively. These are referred to as EL_to_HTH and NH_3_to_HTH assets, respectively. There are potential EL_to_HTH and NH_3_to_HTH assets at Singapore.

These are not at RE-farm locations as the there are no electricity or HTH demands at the RE-farm locations in this case study.

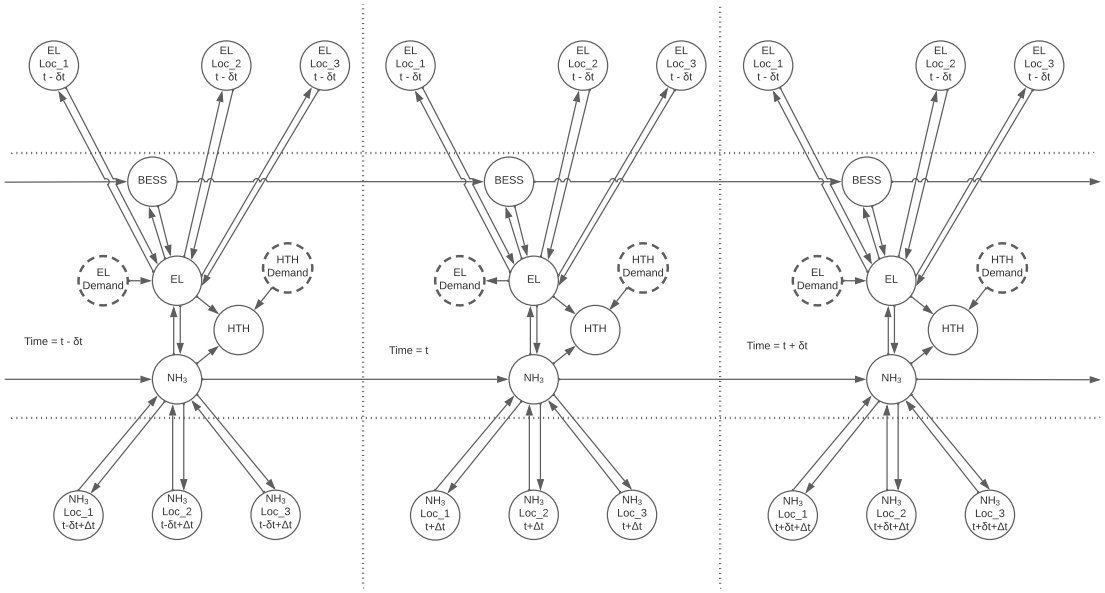

Figure 7.2: Template Edge Diagram SG Location. This is the template edge diagram for the demand location (Singapore) in the asset modeller language of STEVFNs. For simplicity, only the assets at Singapore or between Singapore and other locations are shown.

7.1.1 Asset Brand Parameters

With the case study defined, the set of brand parameters of the assets at each location can be defined. The asset brand parameter for the electricity demand is the electricity demanded for each hour. This was obtained from Singapore's historical wholesale electricity demand for 2019, obtained from the energy market company [194].

The asset brand parameter for the high temperature heating demand is the amount of heating required at each hour. As most policy studies only require annual consumption of fuels, hourly high temperature or industrial heating demand profile is not readily available, or even measured. As the purpose of this hypothetical case study is to perform as stress test, the HTH demand profile was assumed to follow the electricity demand profile of random days throughout the year. This ensures that there is variation between the EL and HTH demand profiles at each time, thus creating more interesting system dynamics and requiring the optimization to find more sophisticated operational strategies. The Ministry of Trade and Industry of Singapore

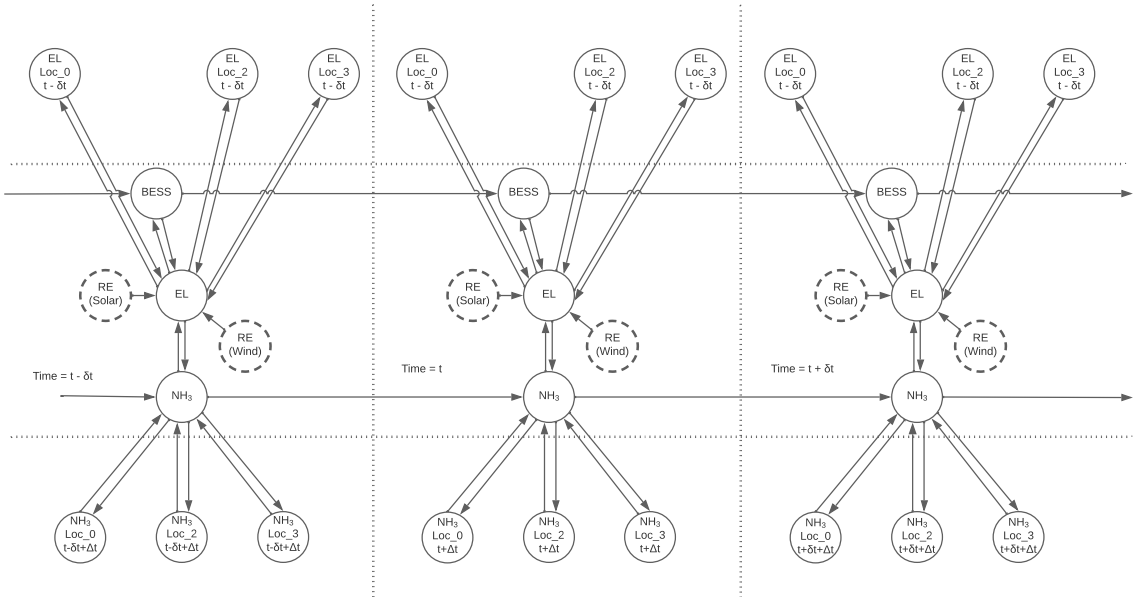

Figure 7.3: Template Edge Diagram RE Location. This is the template edge diagram for the first RE-farm location (Loc_1) in the asset modeller language of STEVFNs. For simplicity, only the assets at Loc_1 or between Loc_1 and other locations are shown. The template edge diagram for Loc_2 and Loc_3 are symmetric, with their locations replaced with Loc_1.

(MTI), and the Economic Development Board of Singapore (EDB) were consulted for estimates on the profile of industrial heating if electrified. Based on their current estimates and future plans, the majority of industrial HTH that has not been electrified in Singapore is used for oil refining. This process requires near constant demand of power with a few shorts periods of downtime throughout the year. To model this, HTH demand would need to assume to follow a flat profile. Future research may obtain and use more accurate profiles. Profiles for other industries or countries could be estimated using typical industrial load patterns. This is also provides a reason future researchers can use to request for such data to be gathered. The profile was linearly scaled to HTH demand by using the 2019 annual industrial fuel consumption from Singapore's energy balance table, and the fuel consumed for process heating from Singapore's industrial roadmap [192].

The asset brand parameter required for the RE supply asset is the hourly normalized power output per peak power (REOUT). REOUT was obtained for PV by using hourly global solar iradiance and temperature data from NASA's MERA-2 Satellite [195, 196]. These were obtained for the whole world at 0.5 and 0.625 degree latitude

Table 7.1: Table of RE Brands

Brand	Resource Type	Capital Cost ($\$\,W_p^{-1}$)
PV_BAU [193]	Solar PV	0.6
WIND_BAU [201]	Wind	0.858
WIND_Cheaper [1]	Wind	0.429

and longitude resolutions, respectively. This was then processed to obtain REOUT for PV using the method used by Renewables Ninja [197, 198, 199], implemented into an open source code in python by Ahsan and Walker. [200]. The exact location of the PV farms for different locations is given in Table 7.11.

REOUT was obtained for Wind "brand" of the RE asset by using hourly global 50m northward and eastward wind data from NASA's MERA-2 Satellite [195, 196]. These were obtained for the whole world at 0.5 and 0.625 degree latitude and longitude resolutions, respectively. This was then processed to obtain REOUT for Wind using the method used by Renewables Ninja [197, 198, 199], implemented into an open source code in python by Ahsan et al. [200]. The exact location of the wind farms for different locations is given in Table 7.11.

The costs per peak power capacity of BAU PV farms were obtained from the analysis of ammonia to power by Cesaro et al. [193]. The costs per peak power capacity of BAU wind farms were obtained from the techno-economic study of green ammonia costs in Australia by Salmon et al. [201]. Detailed future costs of PV and Wind farms can be projected via learning curves or by considering material and processing costs [202]. However, the purpose of this case study is to perform a stress test of the model-generator and tool to observe system dynamics. For these purposes, the cost of "cheaper" brand of wind farms was assumed to be half of the BAU costs. This models a hypothetical future scenario where wind farm costs are lower or fall lower than the costs of other technologies. Again, this is not meant to be a realistic scenario, this value is chosen to show the kinds of dynamics that can be simulated, and the type of insights that can be generated. The cost parameters of various brands of the RE asset are given in Table 7.1.

[1] 50% of BAU value

Table 7.2: Table of BESS Brands

Brand	Storage		Charging	Discharging	Number	Roundtrip
	Capital Cost ($\$/\mathbf{Wh}_p$)	Self Discharge ($\%/\mathbf{yr}$)	Capital Cost ($\$/\mathbf{W}_p$)	Capital Cost ($\$/\mathbf{W}_p$)	of Lifecycles	Efficiency ($\%$)
BAU [193]	0.271	10	0.542	0.271	5000	95
Cheaper [2]	0.136	10	0.271	0.136	5000	95

Table 7.3: Table of Electricity Transport Asset Brands

Brand	Transmission Line			Converter Pair		
	Capital Cost ($\$\,\mathrm{W_p^{-1}\,m^{-1}}$)	O & M Cost ($\$\,\mathrm{Wh^{-1}\,m^{-1}}$)	Losses ($\%\,\mathrm{m^{-1}}$)	Capital Cost ($\$\,\mathrm{W_p^{-1}}$)	O & M Cost ($\$\,\mathrm{Wh^{-1}}$)	Losses ($\%$)
BAU [180, 181, 182]	8.75×10^{-7}	1.0×10^{-12}	1.6×10^{-6}	2.28×10^{-1}	1.8×10^{-6}	1.4

The brand parameters for BESS are the roundtrip efficiency, self discharge rate per month, the cost per peak charging power, cost per peak discharging power and the cost per peak energy. The BAU BESS brand parameters were obtained from the works of Cesaro et al. [193]. The cheaper BESS brand was assumed to cost 50% of the price of the BAU BESS brand. Again, the values for cheaper BESS brand was chosen to study the effects of BESS cost on optimal system design. Realistic future cost projections can be obtained from detailed technology cost projections [203]. The BESS brand parameters are listed in table 7.2.

The brand parameters for the electricity transport asset are the loss per unit distance, the capital cost per unit peak power per unit distance, and the maintenance cost per unit energy per unit distance. The converter losses are fixed fractional losses that do not depend on distance. Converter costs are costs per peak power capacity. These were obtained from the literature [180, 181, 182]. The brands of electricity transport used in this chapter are given in table 7.3.

The brand parameters of the ammonia storage asset are the fractional losses per month and the cost per peak mass of ammonia stored; these were obtained from the works of Salmon et al. [110]. This is using ammonia storage technologies that have lower capital costs, but need frequent re-condensation. This assumes re-condensing is done via electricity produced from the ammonia. Future research could model this

[2] 50% of BAU value

Table 7.4: Table of Ammonia Storage Asset Brands

Brand	Capital Cost ($\$/\mathbf{kg}_p$)	Self Discharge (%/day)
BAU [204]	0.5	0.0308
Cheaper	0.25	0.0308

Table 7.5: Table of Ammonia Transport Asset Brands

Brand	Losses ($\% \, \mathrm{m}^{-1}$)	Berthing Cost ($\$ \, \mathrm{kg}^{-1}$)	Charter Cost ($\$ \, \mathrm{kg}^{-1} \, \mathrm{m}^{-1}$)
BAU [110]	1.21×10^{-7}	1.93×10^{-3}	1.56×10^{-9}

as a component with vector inputs, where the electricity could come from the grid and does not need to come from the ammonia. However, for this case study, this is modelled as a scalar flow for simplicity. Modelling re-condensing this way leads to an effective "self-discharge" loss. Other ammonia storage technologies can store ammonia at higher pressures but lower temperatures leading to lower re-condensation costs, and thus lower effective self-discharge losses. However, these technologies have higher capital costs [110]. Various ammonia storage technologies can be studied, but to study the impact of reducing storage costs, similar to that of other assets, a hypothetical "cheaper" brand of ammonia storage were assumed to cost 50% of the BAU brand. The brands of ammonia storage considered in this chapter are given in table 7.4.

The brand parameters of the ammonia transport asset are the fractional losses per month and the cost per peak mass of ammonia stored; these were obtained from the works of Salmon et al. [110]. The fractional loss per distance was calculated by assuming that the ammonia being transported is used to run the ships. The berthing costs were calculated assuming an average 24 hour berthing time. The brands of ammonia transport considered in this chapter are given in table 7.5.

The brand parameters of the ammonia to electricity asset are the conversion factors, the capital cost per peak ammonia consumption rate, and the maintenance cost per ammonia consumed. These were obtained by Phase 3 NH_3 CCGT plants from the works of Cesaro et al. [193]. To study the impact of cheaper NH_3 to electricity assets, for example retrofitting existing CCGT plants, a hypothetical cheaper brand

Table 7.6: Table of Ammonia to Electricity Asset Brands

Brand	Capital Cost ($\$\,kg_p^{-1}\,h$)	Conversion Factor ($kWh\,kg^{-1}$)
BAU [193]	2385	3.11
Cheaper	1193	3.11
Efficient	2385	4.152

Table 7.7: Table of Electricity to Ammonia Asset Brands

Brand	Capital Cost ($\mathbf{\$/kW}_p$)	Conversion Factor (**kg/kWh**)
BAU [73]	1718	0.101
Cheaper	589	0.101
Efficient	1718	0.135

was assumed to cost 50% of the BAU brand. To study the impact of increased NH_3 to electricity conversion efficiency on optimal system design, a hypothetical "more efficient" brand was assumed to produce 34% more electricity for the same amount of ammonia for an effective increase in efficiency from 60% to 80%, with respect to a lower heating value of $5.19 kWh\,kg^{-1}$. I.e. the more efficient asset is assumed to have a conversion factor closer to the theoretical value. The brands of ammonia to electricity asset considered in this chapter are given in table 7.6.

The brand parameters of the electricity to ammonia asset are the conversion factors, the capital cost per peak electricity power consumption, the maintenance cost per electricity consumed. These were obtained from the works of Salmon et al. [73]. To test the impact of a potentially cheaper electricity to ammonia asset, a hypothetical "cheaper" brand was assumed to cost 50% of the BAU brand. To test the impact of a potentially more efficient electricity to ammoina asset, a hypothetical "more efficient" brand was assumed to produce 34% more ammonia for the same amount of electricity for an effective increase in efficiency from 52.4% to 70%, with respect to a lower heating value of $5.19 kWh\,kg^{-1}$. I.e. the more efficient asset is assumed to have a conversion factor closer to the theoretical value. The brands of electricity to ammonia asset considered in this chapter are given in table 7.7.

The brand parameters of the electricity to high temperature heating asset are the conversion factors, the capital cost per peak electricity power consumption, the main-

Table 7.8: Table of Electricity to High Temperature Heating Asset Brands

Brand	Capital Cost ($\$/\mathbf{kW}_p$)	O & M Cost ($\$/\mathbf{kWh}$)	Conversion Factor
BAU [205]	50	1.0×10^{-3}	1

Table 7.9: Table of Ammonia to High Temperature Heating Asset Brands

Brand	Capital Cost ($\$/(\mathbf{kg/h})_p$)	O & M Cost ($\$/\mathbf{kg}$)	Conversion Factor ($\mathbf{kWh/kg}$)
BAU [205]	260	5.19×10^{-3}	5.19

tenance cost per electricity consumed. These were obtained directly as quotes from wholesale sellers of steel furnaces [205]. The brands of electricity to high temperature heating asset considered in this chapter are given in table 7.8.

The brand parameters of the ammonia to high temperature heating asset are the conversion factors, the capital cost per peak ammonia consumption rate, the maintenance cost per ammonia consumed. The conversion factors was assumed to be the lower heating value of ammonia. As these values are difficult to find in the literature, the capital costs were assumed to be the same capital cost per peak power output as commercial gas to HTH heaters [206]. The brands of ammonia to high temperature heating asset considered in this chapter are given in table 7.9.

7.1.2 List of Scenarios

With the brand parameters for each brand defined, scenarios can be defined by referring to the brands of the asset used in each scenario. The list of scenarios and their respective asset brands are given in Table 7.10. Some assets only have one brand (BAU), and are thus removed from the list for clarity. The locations considered in this case study and their details are given in Table 7.11. The first scenario is the business as usual (BAU) scenario; it considers RE farms at Tibet, India and North-West Australia. The second scenario is the "Cheaper Batteries" scenario; it assumes that batteries will become cheaper. The third scenario is the "Cheaper Wind" scenario; it assumes that wind farms will become much cheaper. The fourth scenario is the "Cheaper Ammonia" scenario; it assumes that ammonia conversion and storage

Table 7.10: Table of Brands and Locations for Scenarios

	Business as Usual	Cheaper Batteries	Cheaper Wind	Cheaper Ammonia	Efficient Ammonia	Different Locations
BESS	BAU	Cheaper	BAU	BAU	BAU	BAU
RE(WIND)	BAU	Wind_{BAU}	$\text{Wind}_{Cheaper}$	Wind_{BAU}	Wind_{BAU}	BAU
NH_3 Storage	BAU	BAU	BAU	Cheaper	Efficient	BAU
EL to NH_3	BAU	BAU	BAU	Cheaper	Efficient	BAU
NH_3 to EL	BAU	BAU	BAU	Cheaper	Efficient	BAU
Location 1	Tibet	Tibet	Tibet	Tibet	Tibet	Somalia
Location 2	India	India	India	India	India	Sudan
Location 3	Australia	Australia	Australia	Australia	Australia	Mongolia

Table 7.11: Table of Details of Locations

Location Name	Location Code	Latitude [°]	Longitude [°]
Australia	AU	-20	123.125
India	IN	10	77.5
Mongolia	MN	43.5	106.25
Singapore	SG	1.4	103.75
Somalia	SO	10	50
Sudan	SU	19	28.75
Tibet	TB	30.5	84.375

technologies will become cheaper. The fifth scenario is the "Efficient Ammonia" scenario; it assumes that the efficiency of ammonia conversion assets will become more efficient. The sixth (and last) scenario is the "Different Locations" scenario; in this scenario, the location of the RE farms are changed to Somalia, Sudan and Mongolia. All locations were chosen because they have good PV and/or wind potential. The set of locations for all scenarios were chosen to cover a variety of latitudes and longitudes. This is to allow the combined RE output to be able to better match Singapore's demand pattern. The locations in the sixth scenario "different loctions" were chosen to demonstrate the impact of increasing the distance between the demand location and RE farms. The distances between the various RE locations and Singapore varied between 3000km and 8400km.

7.2 Results and Discussion

7.2.1 Optimization Time

To test the time taken to build and run the optimizations, each scenario was run fresh, as if it was the first scenario. The time taken to run the optimization for the whole year was too long as the number of optimization parameters grow very quickly because each of the demand, solar, and wind profiles had a parameter for every timestep. Thus, the number of parameters grow almost linearly with T, and the time taken to solve the problem the first time grew as approximately T^3. The optimization was thus first run for eight, one-week chunks of time, equally spaced throughout the year. Changing the starting week only changed the results by less than 5%. Inter-annual variation was not studied in this stress test as only 2019 data was used. However, inter-annual variation can be easily studied using the same methods. The time taken to build the energy system structure and run the optimization the first time was $59000s \pm 1000s$. The optimization had hundreds of thousands of variables, constraints, and parameters.

To test the time taken to run subsequent scenarios, the simulation was run once with the DPP tag set to True when using the CVXPY solver. The optimization was then run again 100 times using randomly selected scenarios. The time taken to rerun each scenario was $15s \pm 3s$. This is an almost 4000 times speedup compared to the first run. This quick testing allowed the testing of various different scenarios in near real time.

A total of more than 50 different scenarios were tested. The six most interesting scenarios were selected and are presented in this chapter to demonstrate the STEVFNs tool and insights gained from it. With the number of scenarios narrowed down, the optimization was repeated for the whole year but without using DPP. This was done by setting DPP value to False when solving the CVXPY problem. By ignoring the parameters, the optimization was able to be run for the whole year at hourly timesteps. The optimization for each scenario took $3200s \pm 500s$.

The optimal system sizes and costs were for the eight one-week, and whole year optimizations were within 5% of each other. Thus, using a lower number of timesteps

is useful when narrowing down scenarios. The rest of the results are for optimizations run for the whole year.

The summary of the size of assets in the optimal system design for all six scenarios is shown in Figure 7.4. The summary of the cost of assets in the optimal system design for all six scenarios is shown in Figure 7.5. The cost of an assets includes both the explicit sizing and usage costs.

7.2.2 Business as Usual

The first scenario tested is the business as usual scenario. Figures 7.6 and 7.7 show the size and cost of assets in the optimal system design for the BAU scenario, respectively.

Solar farms were built at all three RE farm locations: Tibet, India, and Australia. This allowed for a better temporal match between demand and total RE supply. Solar was much cheaper than wind, thus wind was not expected to be built at all. However, a small amount of wind was still built in Tibet and Australia. This is because it helped to balance periods of poor solar irradiance and reduce the size of storage required throughout the system.

HVDC lines were built between Singapore and all three RE-locations: Tibet, India, and Australia. There were no HVDC lines built between pairs of RE-farm locations.

Batteries were built at all three RE-farm locations, but not at Singapore. This is because placing the batteries directly at the RE locations meant that electricity was moved in time before it was moved in space. This means that the electricity moved in space was lower, as some of the energy was lost while being moved in time. This reduced the size and usage cost of the HVDC lines. This is because the total cost of moving electricity in space (via HVDC lines) is similar to the total cost of moving electricity in time (via batteries), as can be seen in Figure 7.7. The flow of electricity into and out of the four locations are shown in Figures 7.9, 7.10, 7.11, 7.12, 7.13, 7.14, 7.15 and 7.16.

Ammonia storage was built at Singapore and Australia. There was ammonia transport between Australia and Singapore.

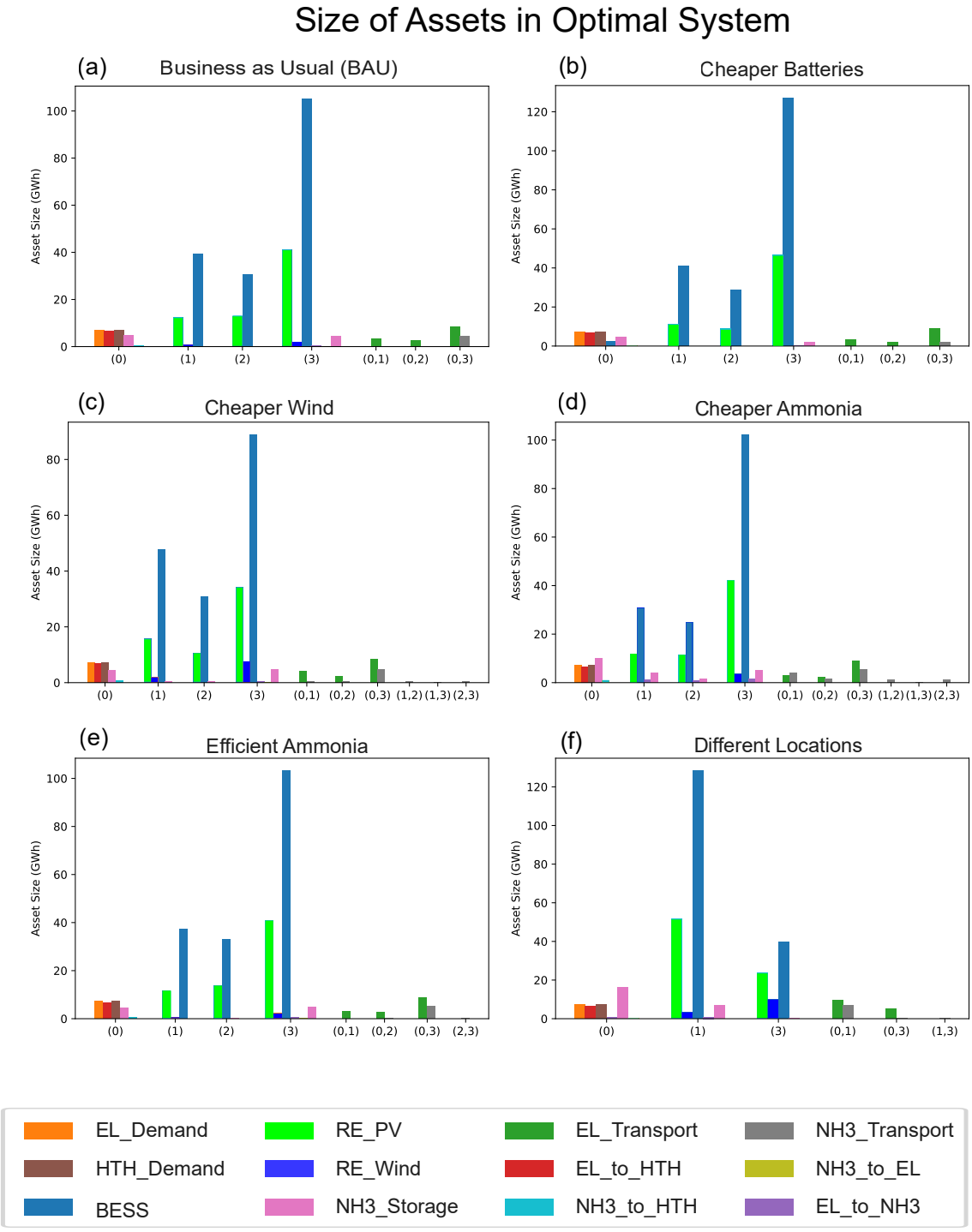

Figure 7.4: Size of Assets in Optimal System. This is the optimal size of assets at locations or between two locations. These are for all six scenarios tested. The brands of these scenarios are given in Table 7.10. Location (0) refers to Singapore for all scenarios. Location (1) is Tibet for scenarios (a)-(e). Location (2) is India for scenarios (a)-(e). Location (3) is Australia for scenarios (a)-(e). Location (1) is Somalia for scenario (f). Location (2) is Sudan for scenario (f). Location (3) is Mongolia for scenario (f). Columns with a pair of locations refer to assets that are place from the first to second location. E.g. (0,1) EL_Transport refers to an electricity line from Location (0) to Location (1).

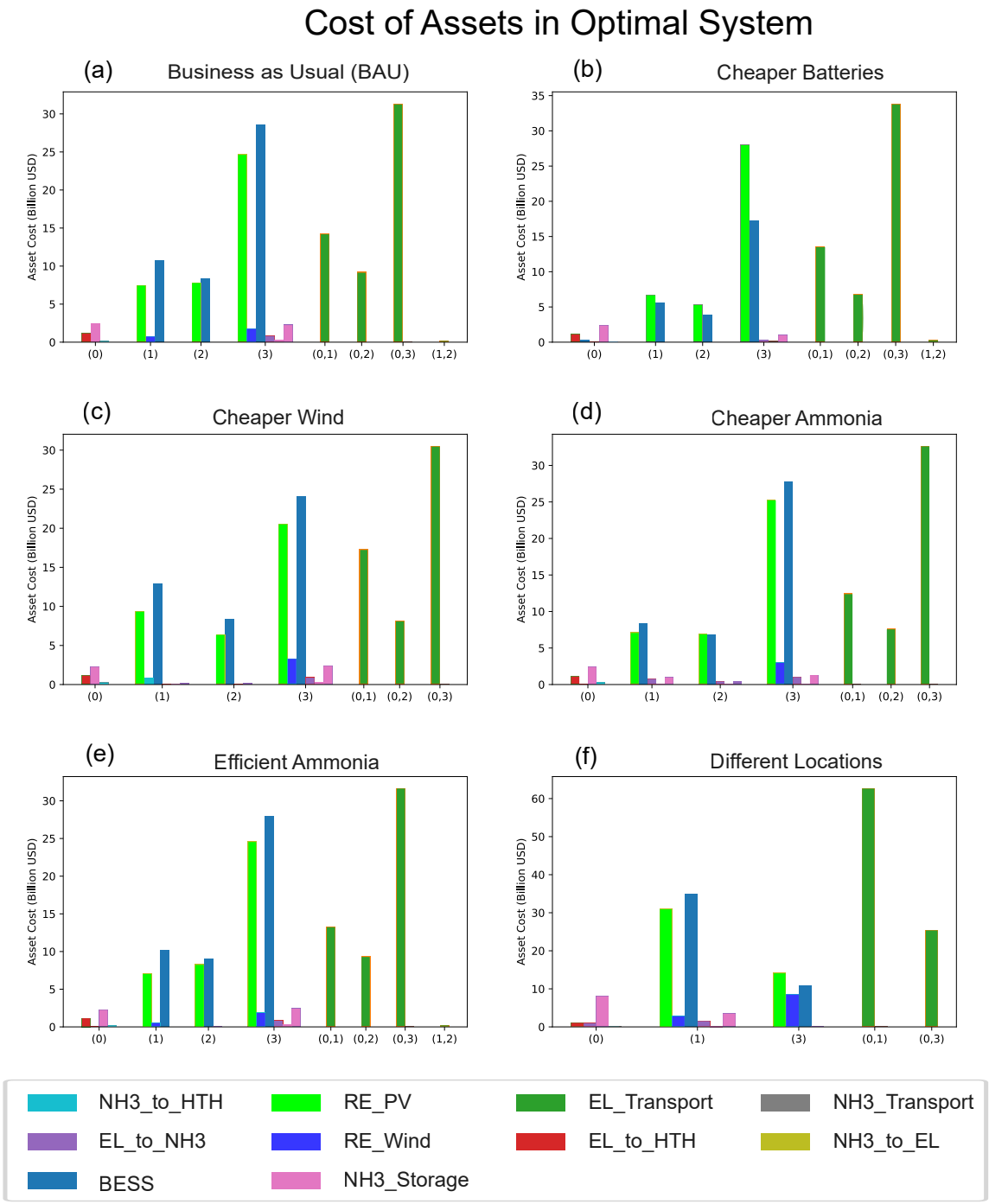

Figure 7.5: Cost of Assets in Optimal System. This is the cost of assets in optimal systems at locations or between two locations. These are for all six scenarios tested. The brands of these scenarios are given in Table 7.10. Location (0) refers to Singapore for all scenarios. Location (1) is Tibet for scenarios (a)-(e). Location (2) is India for scenarios (a)-(e). Location (3) is Australia for scenarios (a)-(e). Location (1) is Somalia for scenario (f). Location (2) is Sudan for scenario (f). Location (3) is Mongolia for scenario (f).

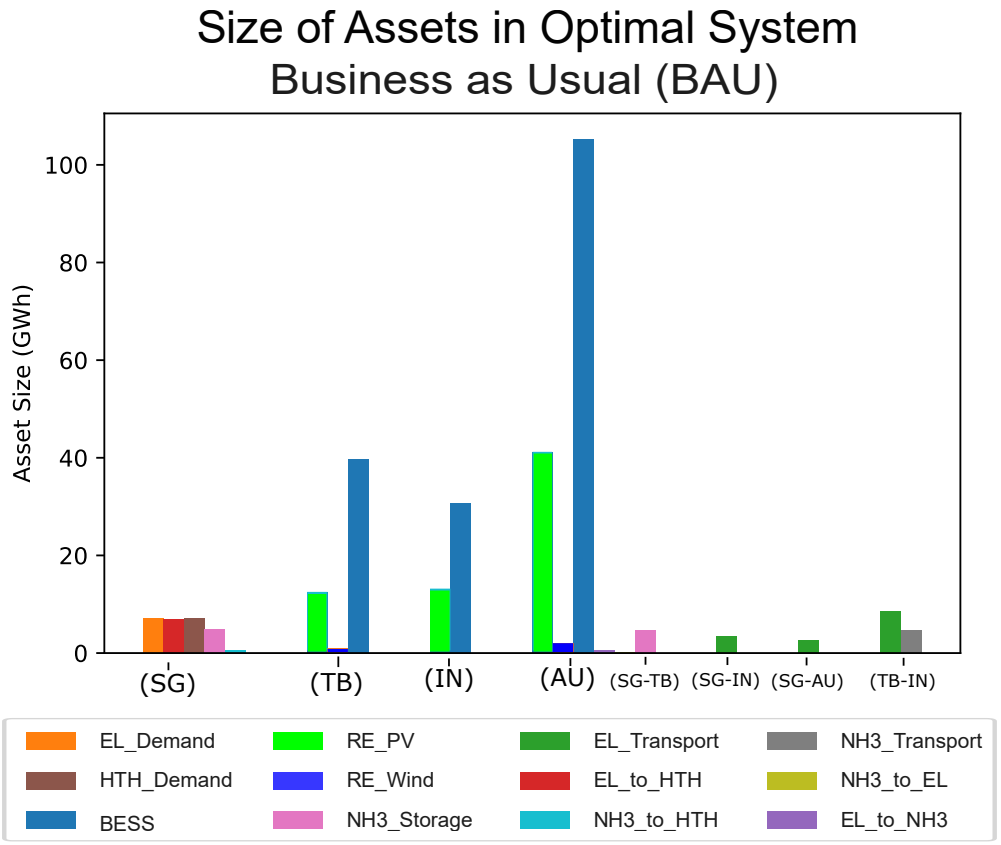

Figure 7.6: Size of Assets in Optimal System for Business as Usual Scenario (BAU). Columns with a pair of locations refer to assets that are place from the first to second location. E.g. (SG,TB) EL_Transport refers to an electricity line from Location SG (Singapore) to Location TB (Tibet). The brands of these scenarios are given in Table 7.10.

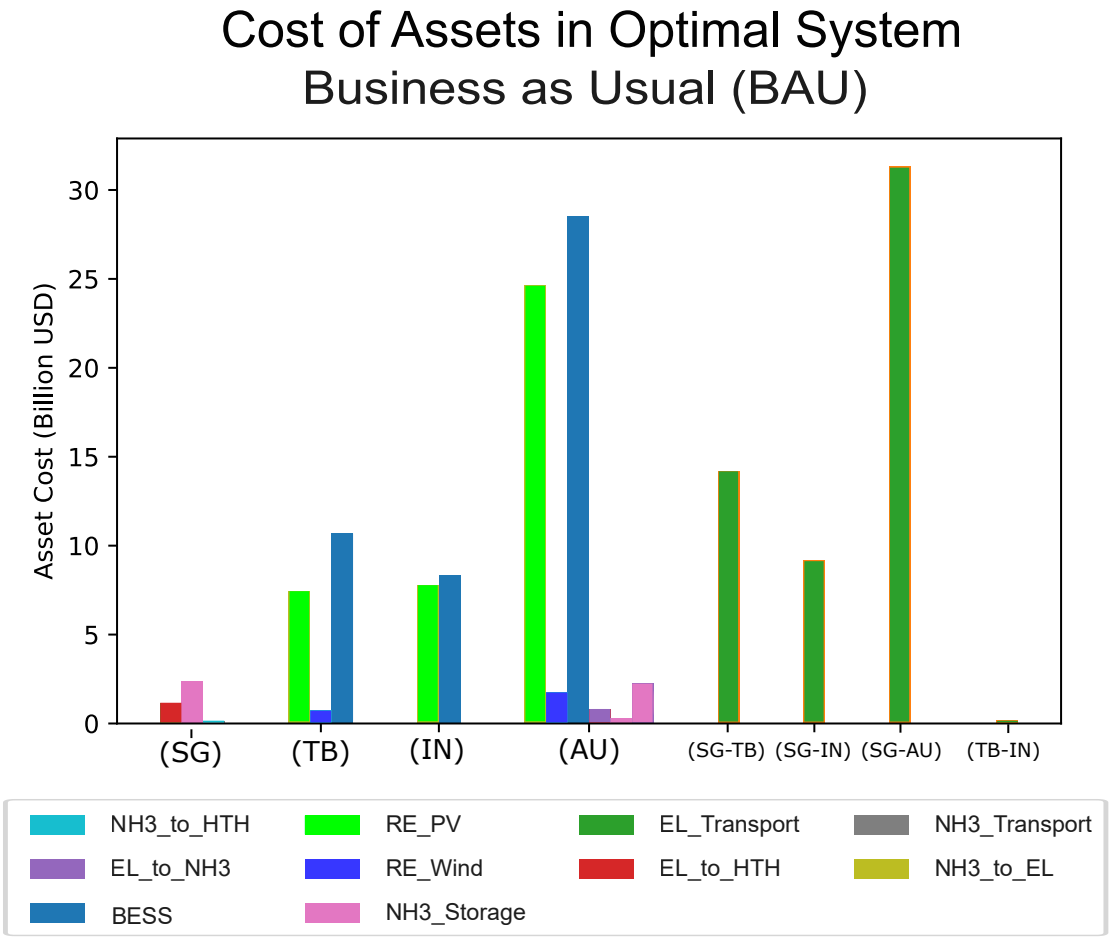

Figure 7.7: Cost of Assets in Optimal System for Business as Usual Scenario (BAU). This is the cost of assets in optimal systems at locations or between two locations. The brands of these scenarios are given in Table 7.10.

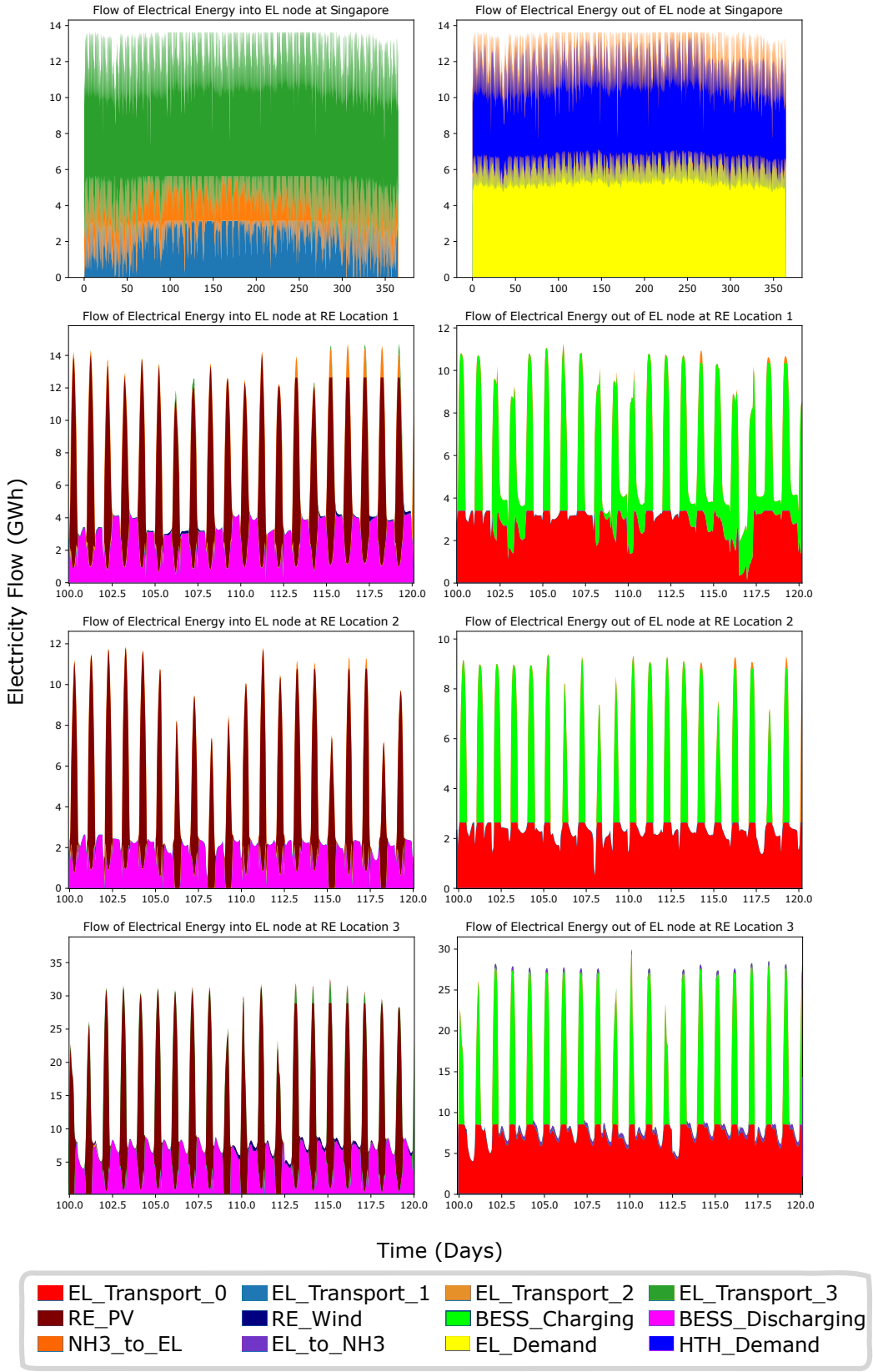

Figure 7.8: Flow of Electricity in BAU Scenario at selected times.

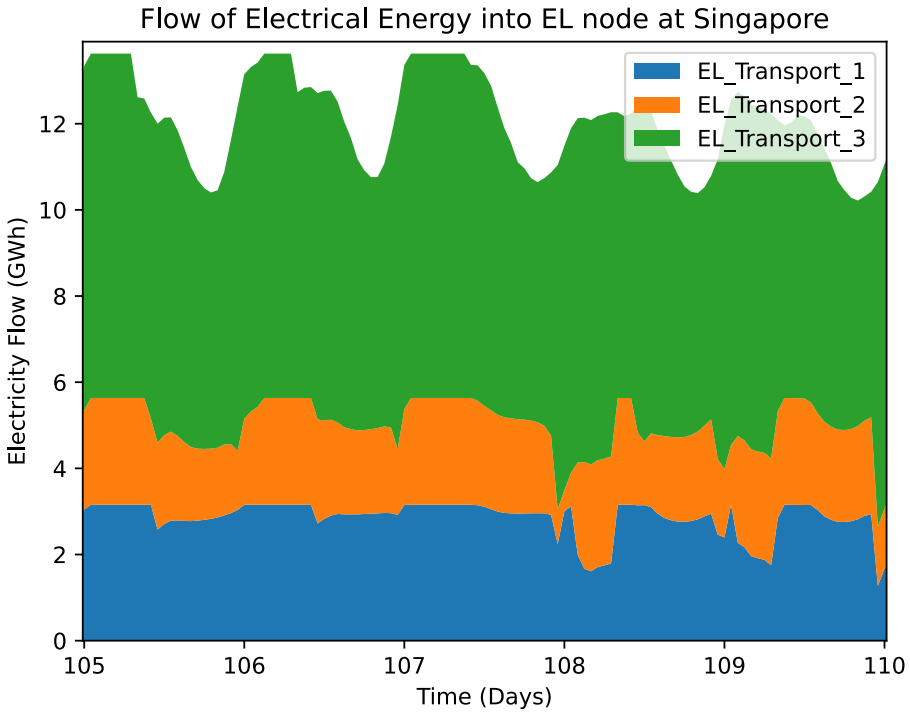

Figure 7.9: Flow of Electricity into Singapore in BAU Scenario at selected times.

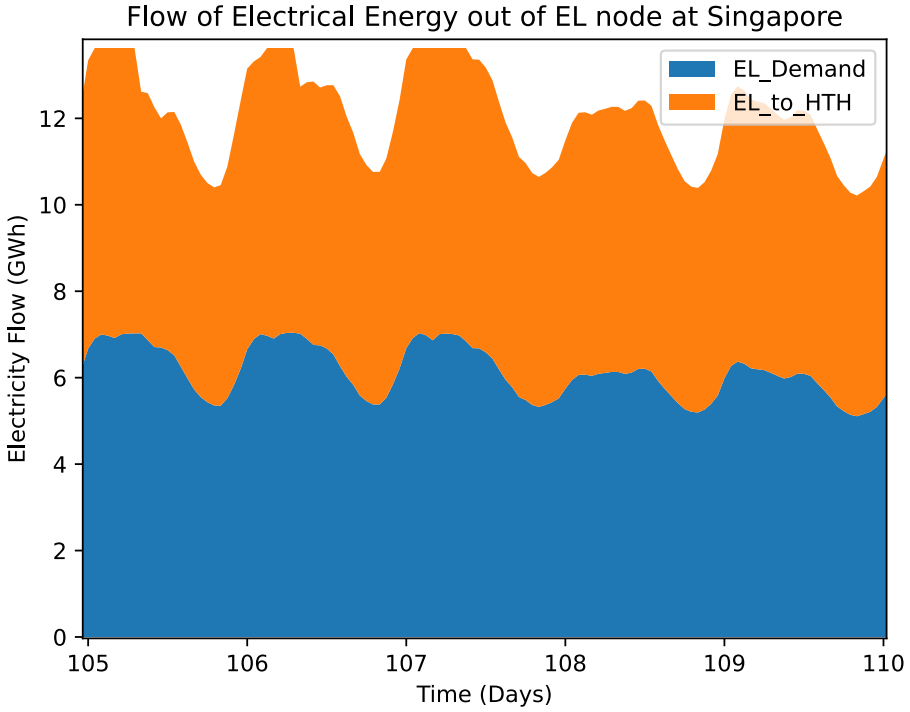

Figure 7.10: Flow of Electricity out of Singapore in BAU Scenario at selected times.

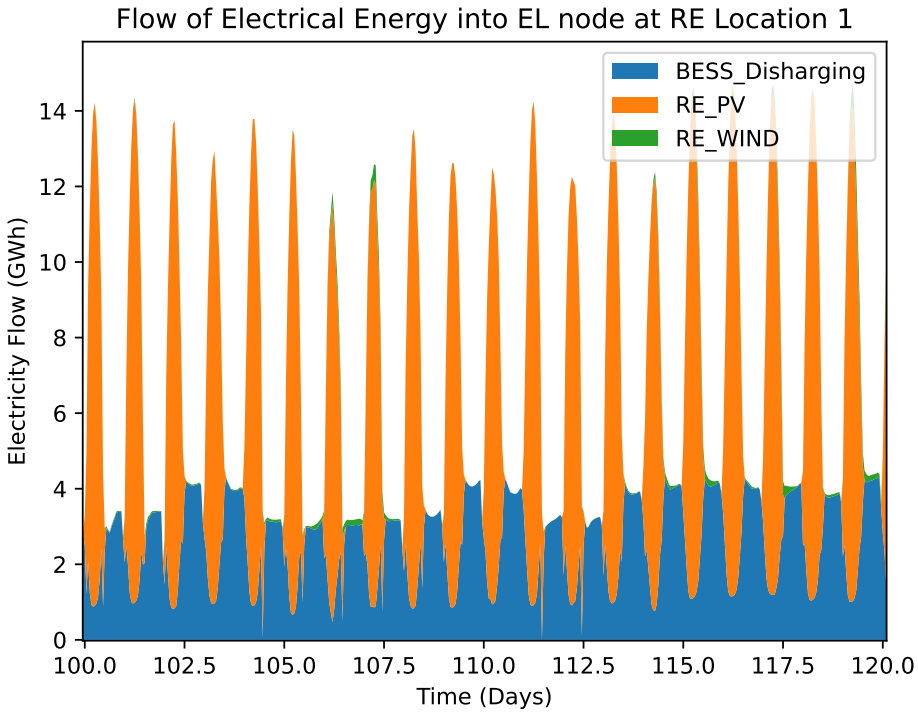

Figure 7.11: Flow of Electricity into Tibet in BAU Scenario at selected times.

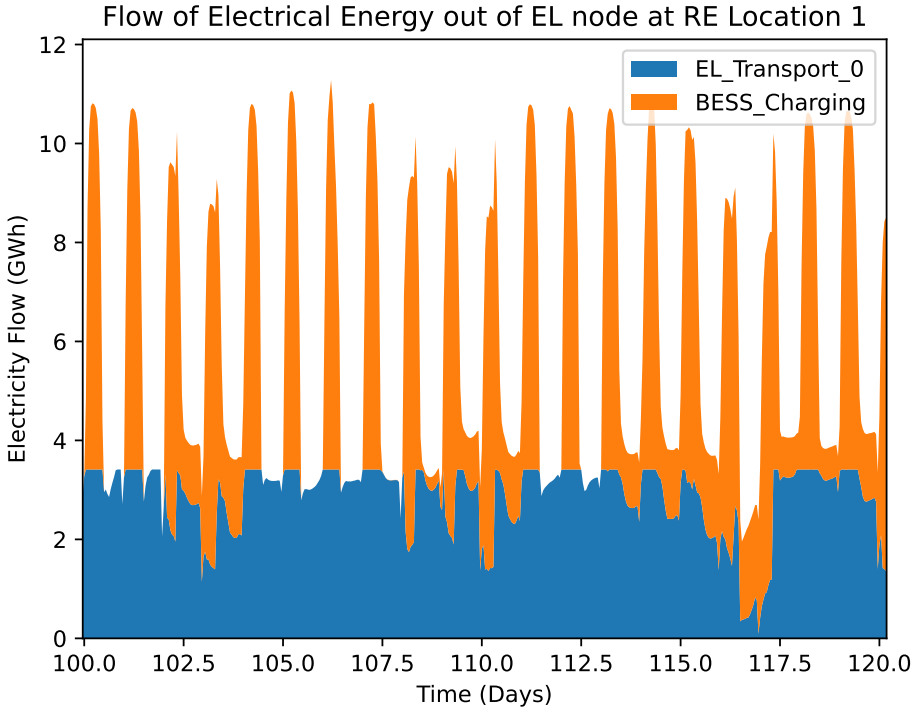

Figure 7.12: Flow of Electricity out of Tibet in BAU Scenario at selected times.

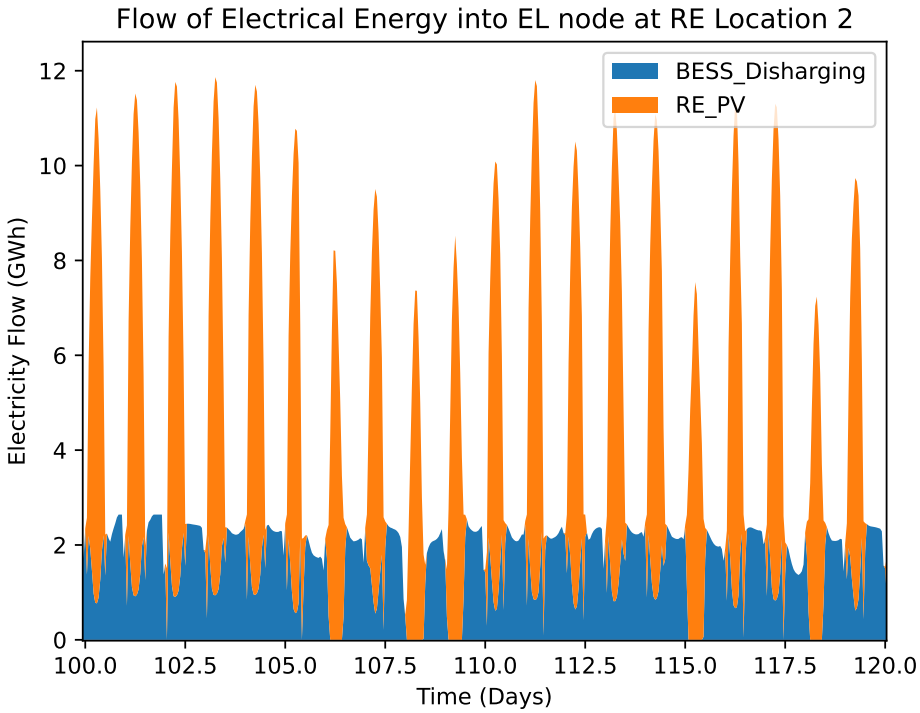

Figure 7.13: Flow of Electricity into India in BAU Scenario at selected times.

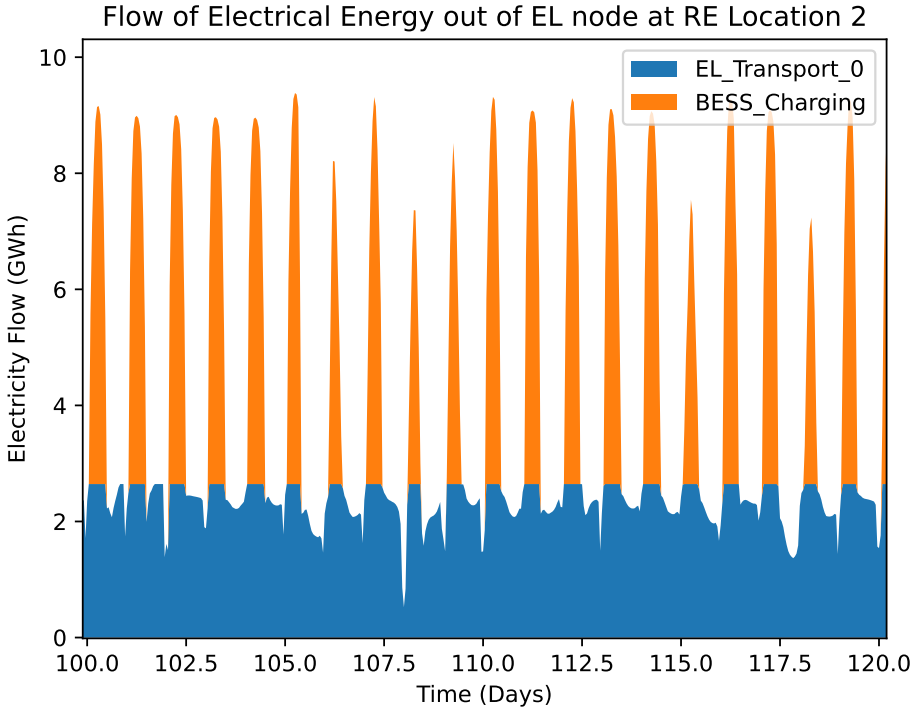

Figure 7.14: Flow of Electricity out of India in BAU Scenario at selected times.

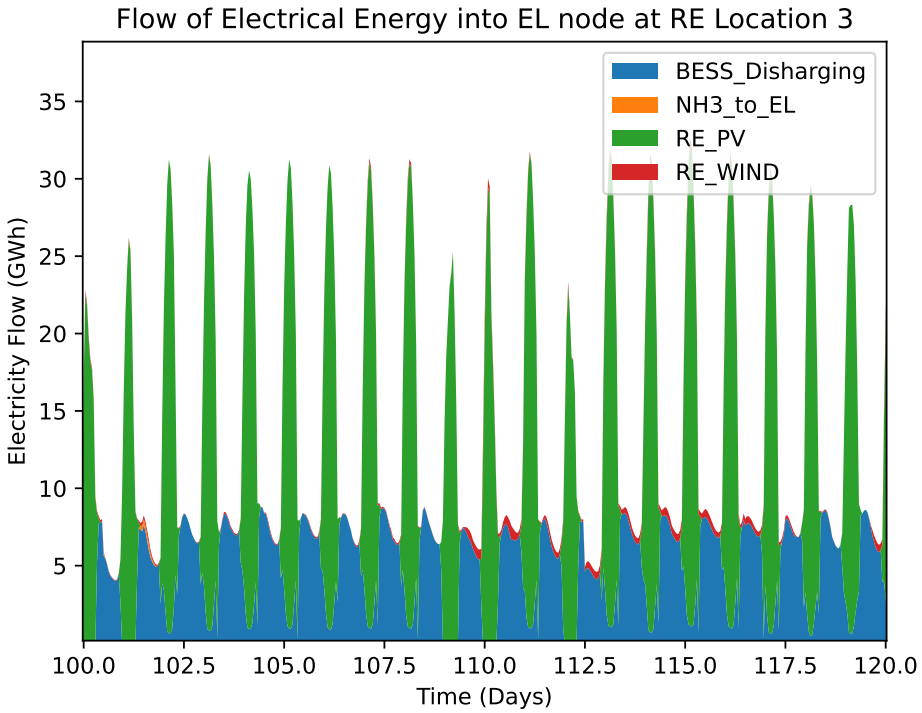

Figure 7.15: Flow of Electricity into Australia in BAU Scenario at selected times.

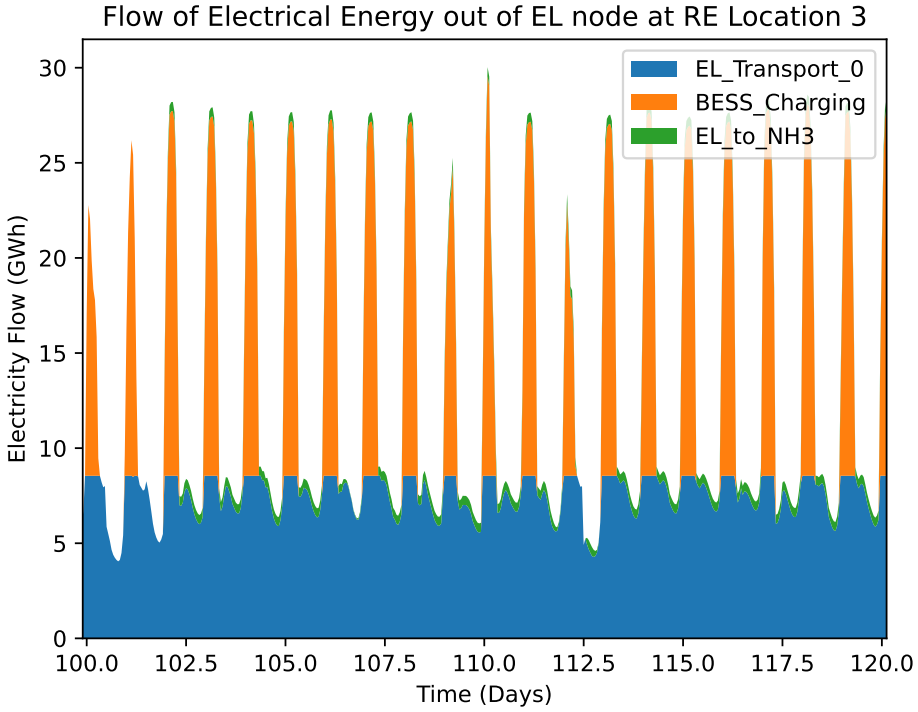

Figure 7.16: Flow of Electricity out of Australia in BAU Scenario at selected times.

There were almost no NH_3_to_EL assets in the system. This indicates that ammonia was only used to satisfy HTH demand, but not electricity demand. This is because converting ammonia to electricity is very inefficient and expensive. To get an insight into this, consider a simple back-of-the-envelope calculation of the difference in efficiency of using electricity vs ammonia to move energy in space and time to satisfy electricity and HTH demands.

To satisfy electricity demand via electricity, electricity is moved in space via HVDC lines, moved in type to charge batteries, moved in time in batteries, and moved back in type to electricity by discharging. Moving energy in space via AC lines leads to about 10% losses per 1000km. Moving energy in space via HVDC lines leads to about 1% losses per 1000km. Moving energy in space via ammonia leads to about 0.1% losses per 1000km. Thus, it may seem like ammonia is an efficiency energy vector. However, charging or discharging a battery leads to about 4% losses each way. Charging or discharging ammonia storage leads to about 40-50% losses each way.

Thus, using HVDC lines and batteries to satisfy electricity demand leads to an overall efficiency of about 90% (97.5% $\times$ 97.5% $\times$ 95%, assuming 5000km distance). Using ammonia transport and storage to satisfy electricity demand leads to an overall efficiency of about 31% (60% $\times$ 52% $\times$ 99.5%). This leads to an implicit over-sizing cost of 111% (1/90%) vs 322% (1/31%), or almost 3 times the cost of the rest of the system to generate the energy.

However, the overall efficiency to satisfy HTH are 90% vs 60%, using electricity and ammonia, respectively. This is because ammonia does not have to be converted back to electricity and is burnt directly. Thus the using ammonia for HTH only costs 1.5 times the costs of the rest of the system compared to using electricity. Thus, ammonia is used to satisfy HTH, but is rarely used to satisfy electricity.

One initially paradoxical behaviour observed was the transport of ammonia from Singapore (the demand location) to Australia (the supply location). An example of this is shown in Figure 7.17. Ammonia was transported from Singapore to Australia from days 136 to 144. However, a closer examination explains that this was a use of distributed storage of ammonia.

On day 136, the ammonia storage tanks in Singapore were very full, thus they would not have been able to accept the next shipment of Ammonia. Instead of increasing the size of ammonia storage at Singapore, the optimizer transported ammonia to Australia as the ammonia storage tanks in Australia were under-utilized. This is because there was a period of low ammonia production in Australia at the same time, between days 145 and 155.

However, note that ammonia was being shipped both to and from Singapore for a week between days 136 and 144. This is because the optimization was also using the ammonia in transit on ships, as temporary storage. This allowed the optimization to reduce the size of ammonia storage required in Singapore and Australia. This is counter intuitive as the ideal action would be to just dock the ships at Singapore during that time. This is a limitation of the case study as the NH_3_Transport asset can only ship ammonia from one location to another. It is not modelled to be able to just store ammonia and be docked.

Future case studies can rectify this by modelling an additional asset that just docks ammonia. Another way to fix this would be to model the ammonia transport asset with two components, one to "load the ammonia on storage tanks on the ship", and another to transport the ammonia to a different location. This would lead to lower losses (from transport) and costs (from chartering).

However, in the current case study, the costs of using ships as temporary storage is overestimated. More accurate modelling of this transport will lead to lower ammonia consumption to transport ammonia. Furthermore, the chartering costs will be replaced with berthing costs. The fuel costs of ammonia transport are very low (about 0.1% losses per 1000km). The difference between berthing and chartering costs is also low. And these scenarios only occur a few times. Thus this has a negligible impact on the overall sizing and costs of the system and thus the results of the optimization.

7.2.3 Cheaper Batteries

The second scenario considered in the case study is the cheaper batteries scenario. In this scenario, batteries are assumed to cost 50% of the BAU cost. Figures 7.18 and

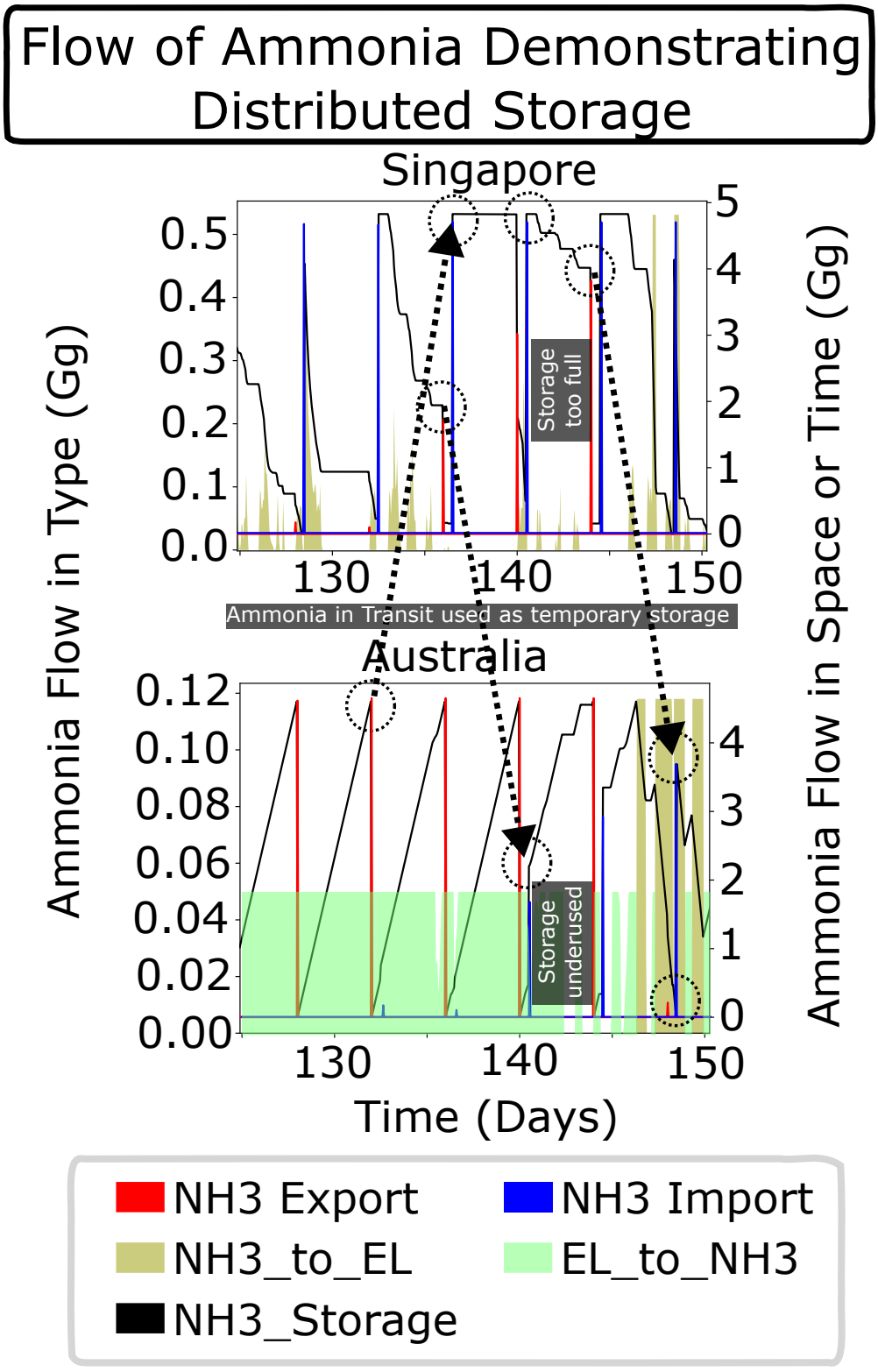

Figure 7.17: Flow of Ammonia in BAU Scenario showing the operation of distributed ammonia storage. When ammonia storage tanks in Singapore were full, ammonia is transported back from Singapore to Australia. This allows the system to use the empty ammonia storage tanks in Australia instead of increasing the size of storage tanks in Singapore. During a short period, ammonia is transported both to and from Singapore, at the same time. This indicates that the system is using ammonia in transit as temporary storage, instead of increasing the size of storage tanks in Singapore or Australia.

7.19 show the size and cost of assets in the optimal system design for the cheaper batteries scenario, respectively.

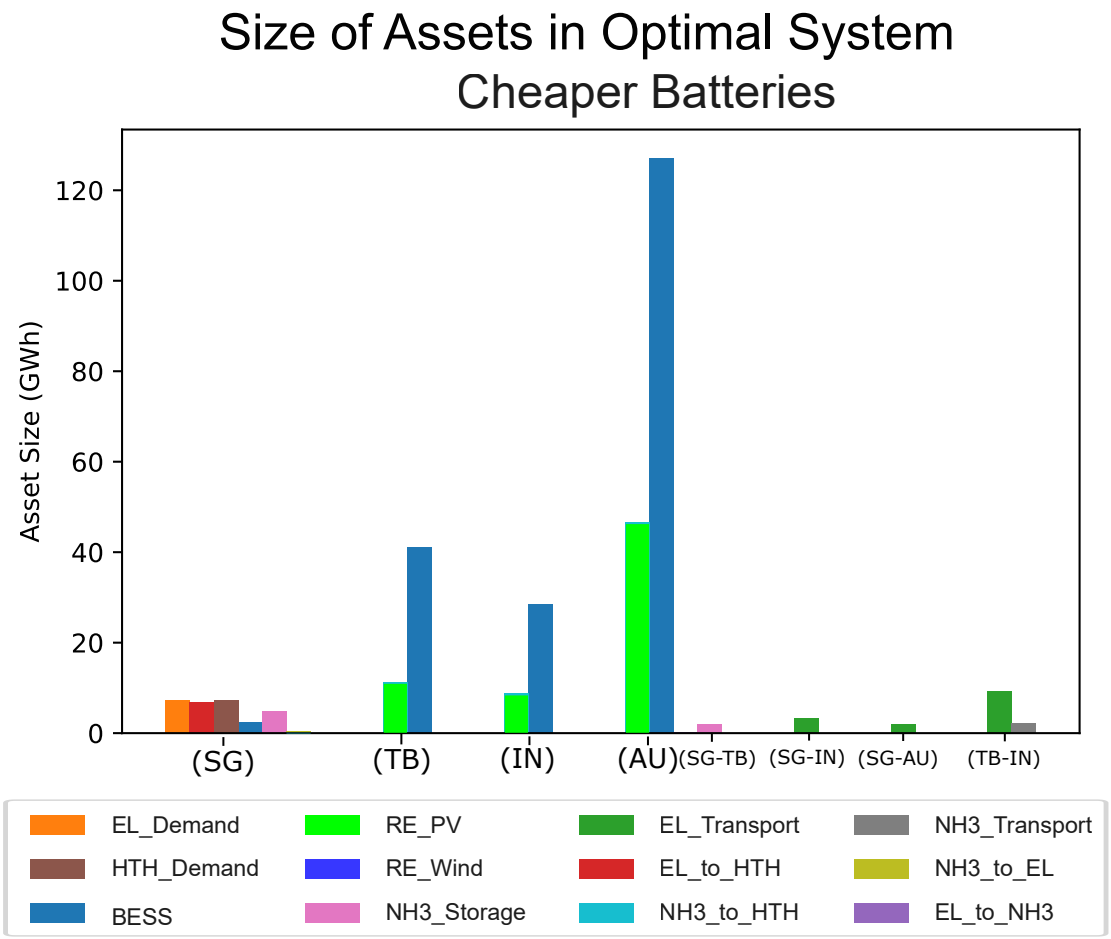

Figure 7.18: Size of Assets in Optimal System for Cheaper Batteries Scenario. Columns with a pair of locations refer to assets that are place from the first to second location. E.g. (SG,TB) EL_Transport refers to an electricity line from Location SG (Singapore) to Location TB (Tibet). The brands of these scenarios are given in Table 7.10.

Unlike to the BAU scenario, no more wind farms are built when batteries are cheaper. Furthermore, the solar farms in Tibet and India are smaller, while the solar farms in Australia are bigger. This indicates that there is less benefit of spreading out the generation of electricity. This is because the cost of moving energy in time is cheaper, thus there is less need to more closely match total RE supply profile with the demand profile in Singapore. Thus, the system builds more of the cheapest RE: solar farms in Australia.

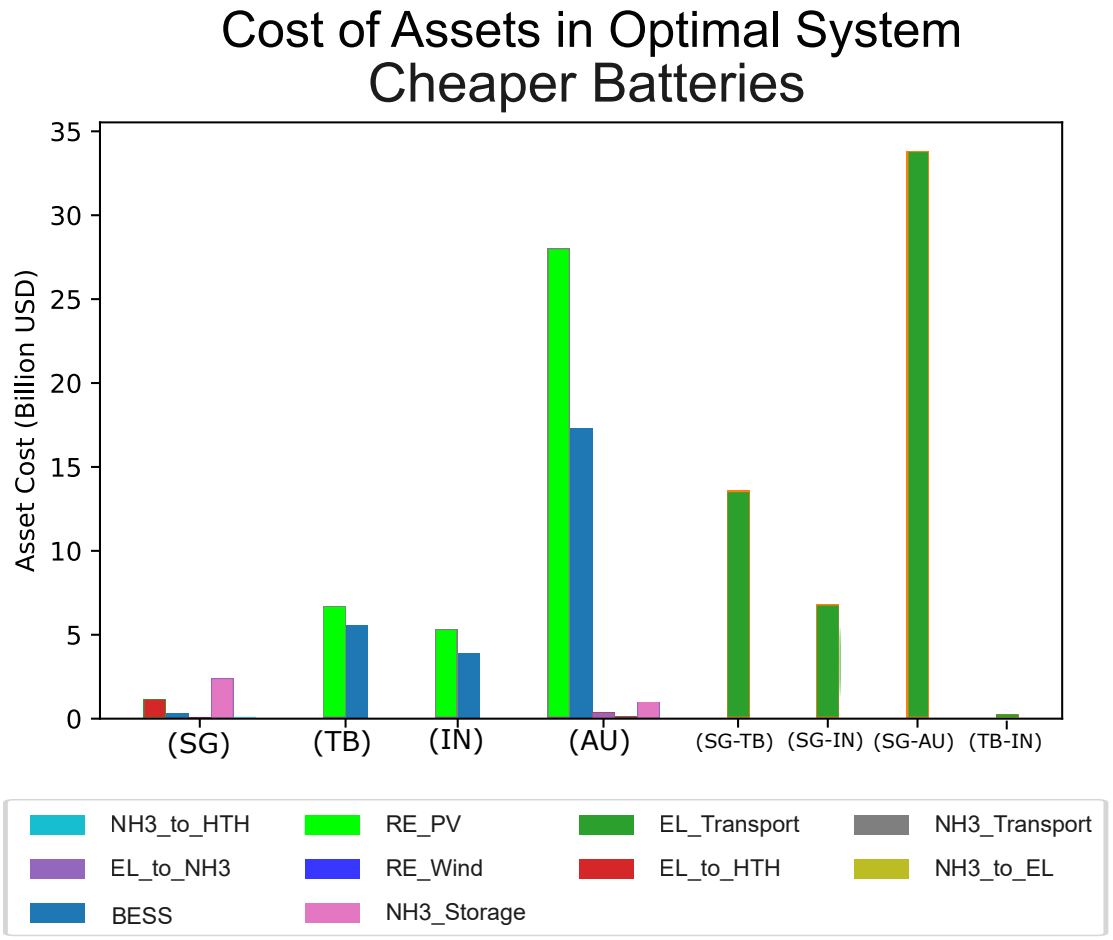

Figure 7.19: Cost of Assets in Optimal System for Cheaper Batteries Scenario. This is the cost of assets in optimal systems at locations or between two locations. The brands of these scenarios are given in Table 7.10.

When batteries are cheaper, ammonia storage and transport is also reduced. This is because batteries become an even cheaper way of moving energy in time compared to ammonia. Note that even when battery prices are halved, the system still uses some ammonia storage and transport. Thus, there is a small value of ammonia even when battery prices drop dramatically. This is because the ammonia production and ammonia storage assets can be sized independently to produce an overall storage system that is ideal for long term storage of energy.

Also note that the reduction in ammonia usage is correlated with the reduction in wind usage. This will be discussed again in the cheaper wind scenario.

7.2.4 Cheaper Wind

The third scenario considered in the case study is the cheaper wind scenario. In this scenario, wind farms are assumed to cost 50% of the BAU cost. Figures 7.4 and 7.21 show the size and cost of assets in the optimal system design for the cheaper wind scenario, respectively.

As expected, when the cost of wind is assumed to be lower, the ideal system has more wind and less solar PV at all RE locations. Note that even when wind costs are assumed to be 50% of BAU values, the optimal system predominantly consists of solar farms. This is probably because wind has very high seasonal variability that requires higher amounts of long term storage. This long term storage is most effectively satisfied with ammonia storage.

This leads to the next big difference compared to BAU scenario: when wind power is cheaper, and the system contains more wind, the ideal system also has more ammonia storage and transport. This is again because wind requires longer term storage solar. This is why wind and ammonia storage are observed to be complementary in optimal energy systems. Similarly, solar and shorter term battery storage are observed to be complementary.

These "pairs" of generation and storage technologies are also seen in the cheaper batteries scenario. When battery prices were cheaper, the optimal system consisted of more batteries and less ammonia storage. It thus contained more solar and less wind power.

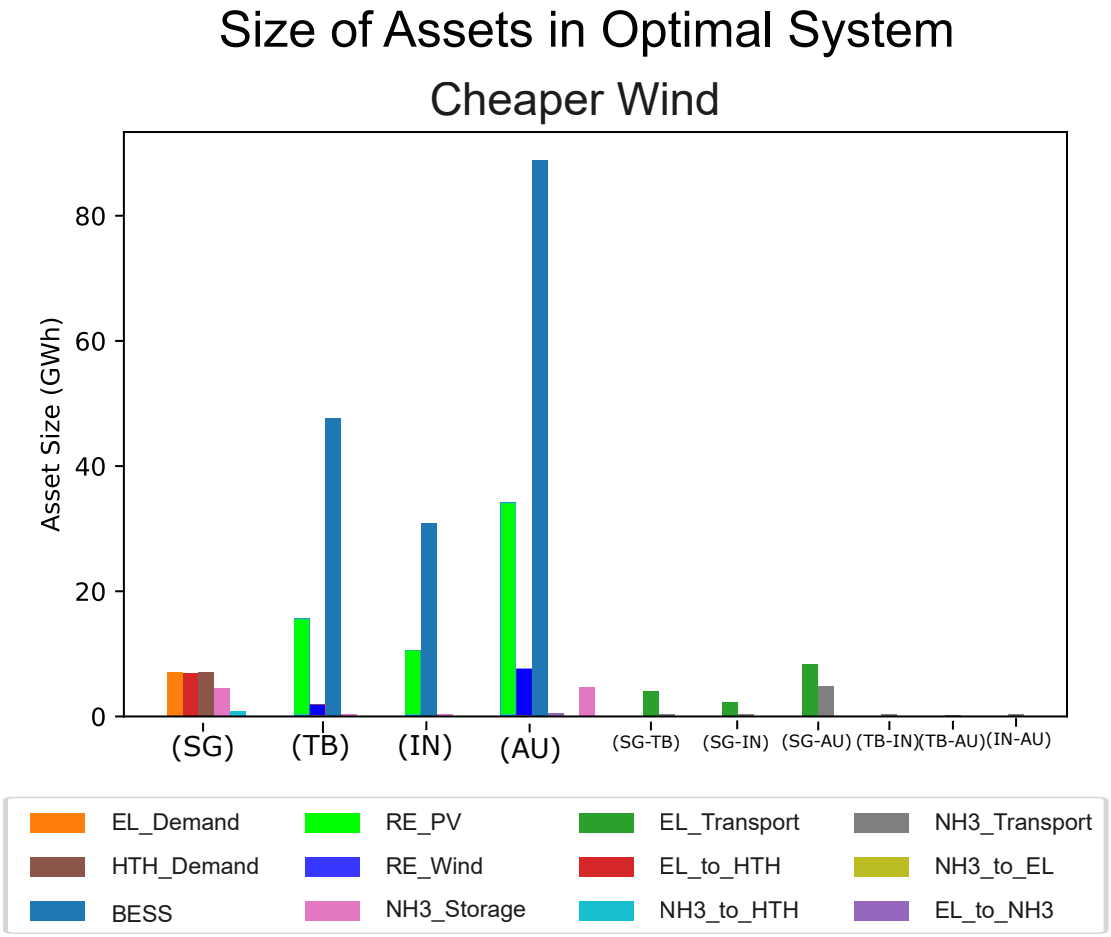

Figure 7.20: Size of Assets in Optimal System for Cheaper Wind Scenario. Columns with a pair of locations refer to assets that are place from the first to second location. E.g. (SG,TB) EL_Transport refers to an electricity line from Location SG (Singapore) to Location TB (Tibet). The brands of these scenarios are given in Table 7.10.

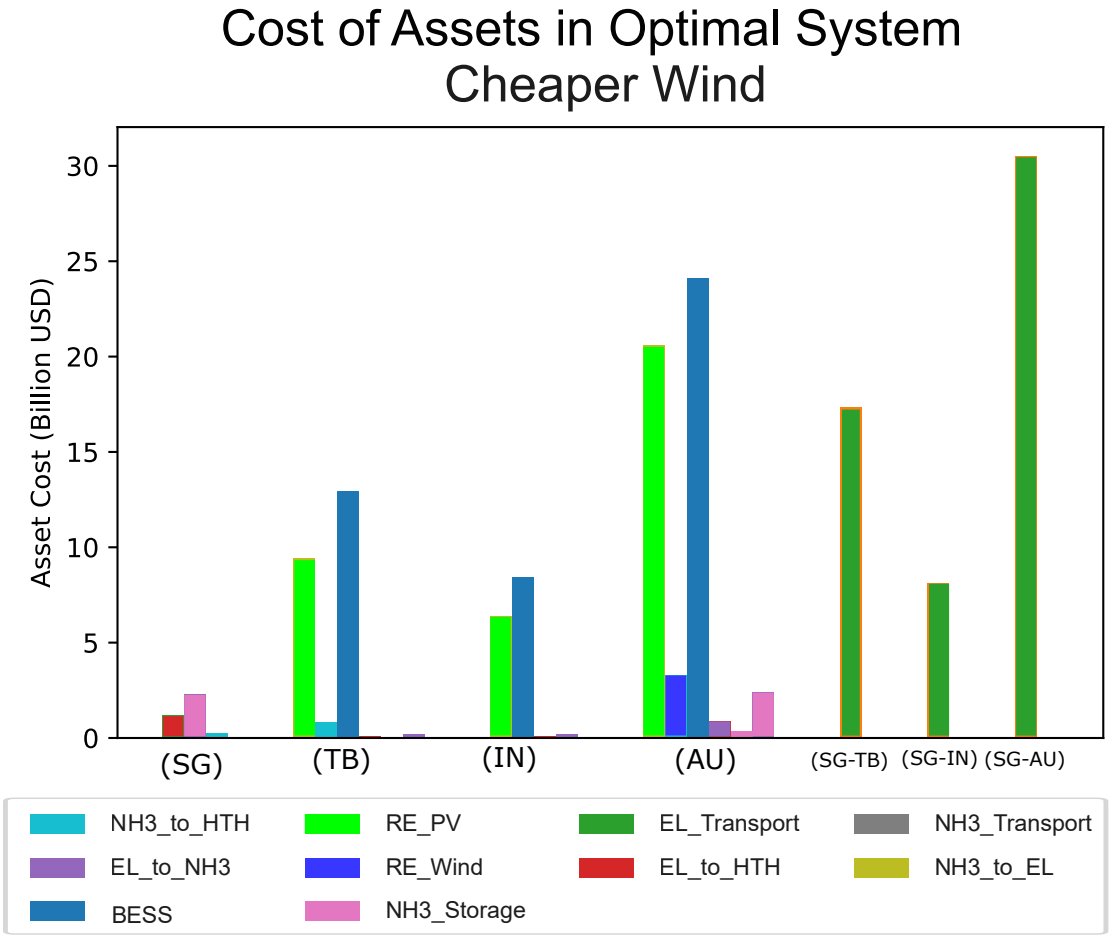

Figure 7.21: Cost of Assets in Optimal System for Cheaper Wind Scenario. This is the cost of assets in optimal systems at locations or between two locations. The brands of these scenarios are given in Table 7.10.

7.2.5 Cheaper Ammonia Storage

The fourth scenario considered in the case study is the cheaper ammonia storage scenario. In this scenario, ammonia storage tanks, NH_3_to_EL and EL_to_NH_3 technologies are assumed to cost 50% of their respective BAU costs. Figures 7.22 and 7.23 show the size and cost of assets in the optimal system design for the cheaper ammonia storage scenario, respectively.

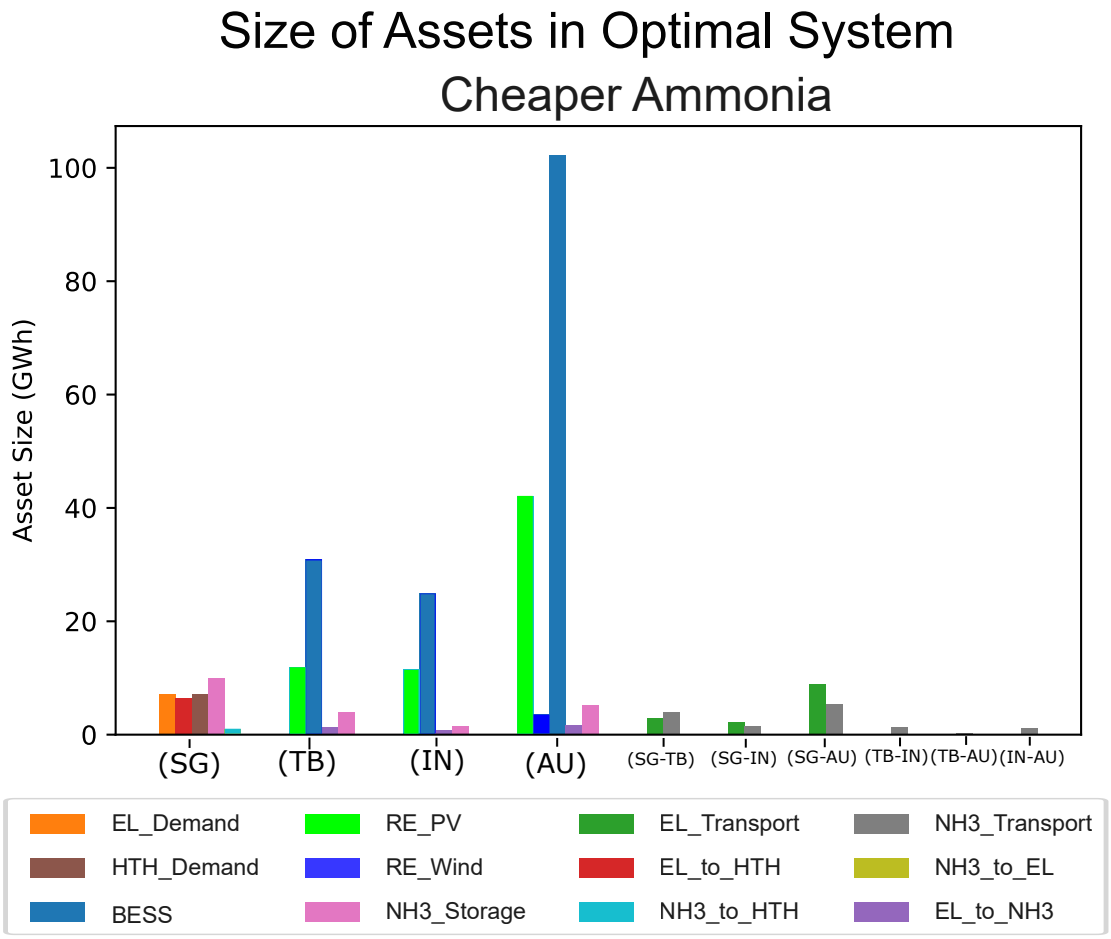

Figure 7.22: Size of Assets in Optimal System for Cheaper Ammonia Scenario. Columns with a pair of locations refer to assets that are place from the first to second location. E.g. (SG,TB) EL_Transport refers to an electricity line from Location SG (Singapore) to Location TB (Tibet). The brands of these scenarios are given in Table 7.10.

As expected, when ammonia storage and conversion technologies are cheaper, the optimal system consists of more ammonia storage and transport. In this scenario, there is slightly more wind and lower solar in Tibet and Australia.

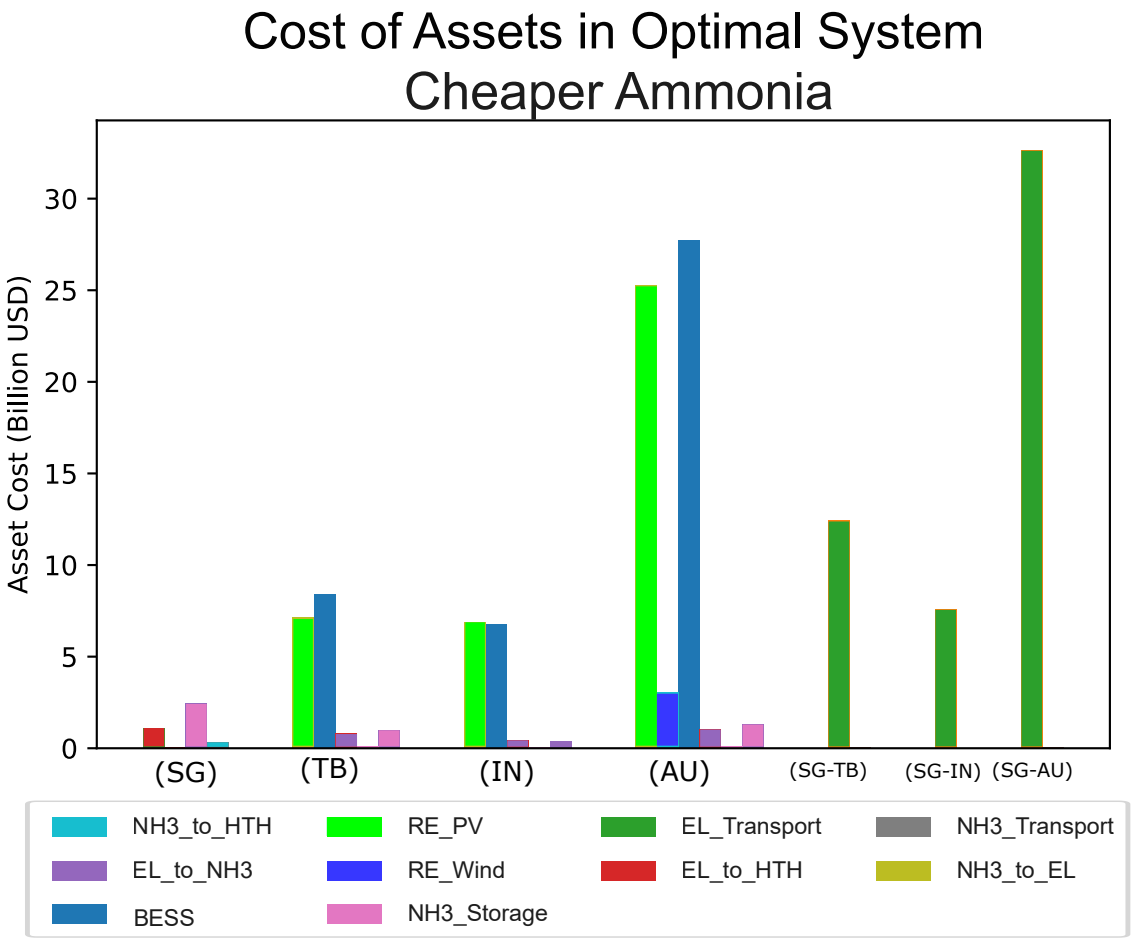

Figure 7.23: Cost of Assets in Optimal System for Cheaper Ammonia Scenario. This is the cost of assets in optimal systems at locations or between two locations. The brands of these scenarios are given in Table 7.10.

As seen in other scenarios, the size of wind farms and ammonia storage are correlated. This is also observed in the cheaper ammonia storage scenario. When ammonia storage is cheaper, the optimal system contains more ammonia storage. In this case, the optimal system also contains more wind. Note that while the optimal system contains more wind, it is still predominantly solar.

When ammonia storage is cheaper, ammonia storage tanks are also built in Tibet and India. Thus, when ammonia storage is cheaper, ammonia storage is also paired with solar PV.

When ammonia storage is cheaper, there is significant ammonia transport between Tibet and India, and between India and Australia. This shows that there are benefits to distributed storage of ammonia. The distributed storage tanks connected via ammonia transport seem to act together as a global ammonia storage system.

7.2.6 Efficient Ammonia

The current technologies to produce ammonia from electricity and convert it back to electricity are very inefficient. The high conversion losses of ammonia technologies leads to high implicit costs as RE generation farms need to be oversized to overcome higher losses. The cheaper ammonia scenario tests the impact of lowering the explicit cost of ammonia technologies. The efficient ammonia scenario tests the impact of lowering the implicit costs of ammonia technologies.

The fifth scenario considered in the case study is the efficient ammonia storage scenario. In this scenario, NH_3_to_EL and EL_to_NH_3 technologies are assumed to be more efficient than their respective BAU brands. Figures 7.24 and 7.25 show the size and cost of assets in the optimal system design for the efficient ammonia storage scenario, respectively.

Even when ammonia conversion technologies are assumed to be significantly more efficiency than the BAU scenario, the optimal system did not change significantly compared the BAU scenario. This is because the cost of generating energy is very small compared to the cost of moving energy in space, time, and type. Thus, the implicit costs of the high losses of ammonia storage are very small compared to the explicit costs of the ammonia storage and conversion technologies. Thus, it is more

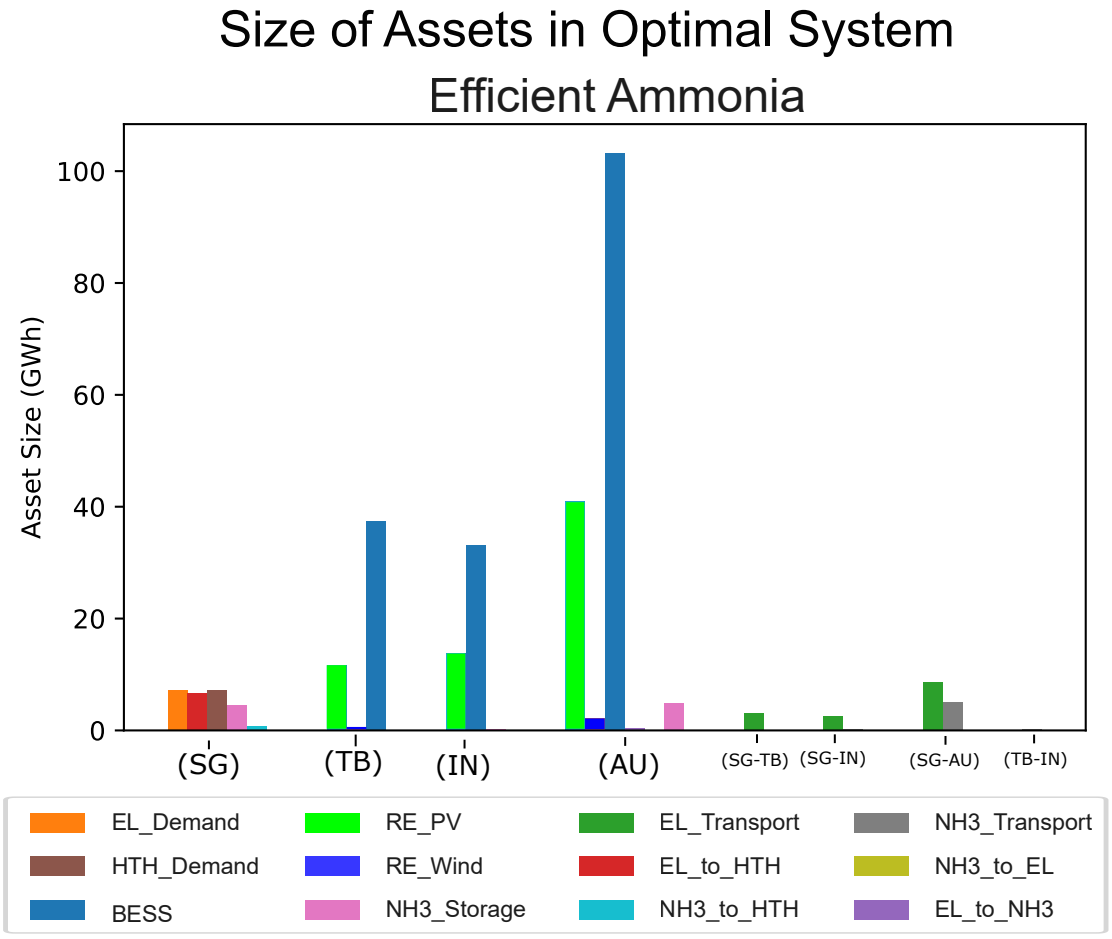

Figure 7.24: Size of Assets in Optimal System for Efficient Ammonia Scenario. Columns with a pair of locations refer to assets that are place from the first to second location. E.g. (SG,TB) EL_Transport refers to an electricity line from Location SG (Singapore) to Location TB (Tibet). The brands of these scenarios are given in Table 7.10.

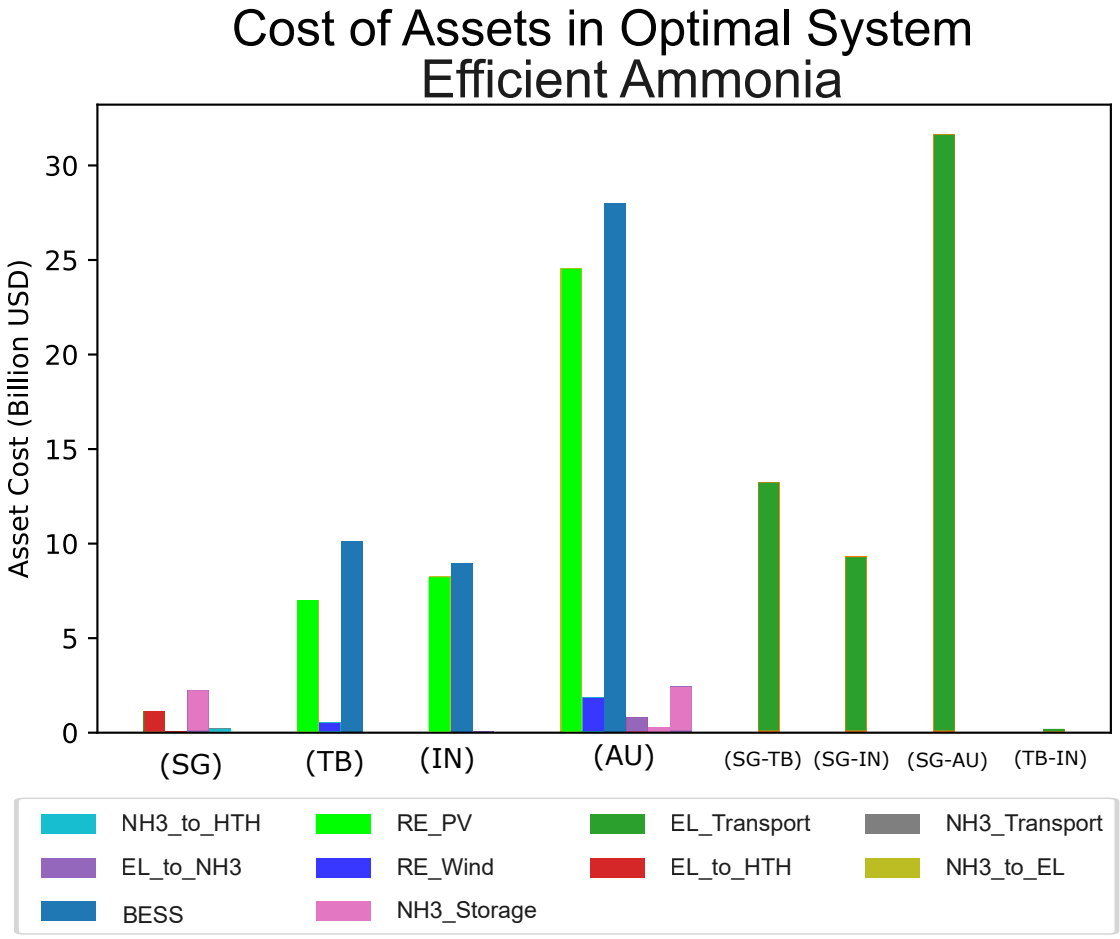

Figure 7.25: Cost of Assets in Optimal System for Efficient Ammonia Scenario. This is the cost of assets in optimal systems at locations or between two locations. The brands of these scenarios are given in Table 7.10.

important to reduce the explicit costs of ammonia storage and production technologies than it is to increase the efficiency of ammonia production technologies.

This highlights another important distinction between traditional fossil fuel-based energy systems and future RE-based energy systems. In traditional fossil fuel-based energy systems, the cost of generating energy is high but the cost of moving energy in space and time is low. In future RE-based energy systems, the cost of generating energy is low, but the cost of moving energy in space, time and type is high. Thus, the major challenge of future RE-based energy systems is to lower the cost of moving energy in space, time or type. If ammonia is used, the movement of energy is space and time is cheap, but the movement in type (conversion) is expensive. Thus, energy conversion is where efforts need to be concentrated for ammonia technology improvement.

7.2.7 Different Locations

The sixth and final scenario considered in the case study is the different locations scenario. In this scenario, the locations of the three RE farms were changed to Somalia, Sudan, and Mongolia. This was done to demonstrate that the STEVFNs tool can be used to easily change the location of assets allowing it to be used for the assessment of locations of assets in the design of an energy system. Figures 7.26 and 7.27 show the size and cost of assets in the optimal system design for the different locations scenario, respectively.

When the RE farm locations were changed, the optimal energy system only consisted of solar and wind farms at two RE locations, Somalia and Mongolia. The optimal energy system did not consists of any assets in Sudan. This is because even though Sudan would be give increased variation of profiles in longitude, it was much further away. Thus, the cost of moving energy in space was too high to justify any reductions in costs from lower movements of energy in time (storage).

The optimal energy system consisted of a higher fraction of wind power compared to the BAU scenario.

Ammonia storage was only built in Singapore and Somalia; it was not built in Mongolia. Thus, there was only ammonia transport between Somalia and Singapore.

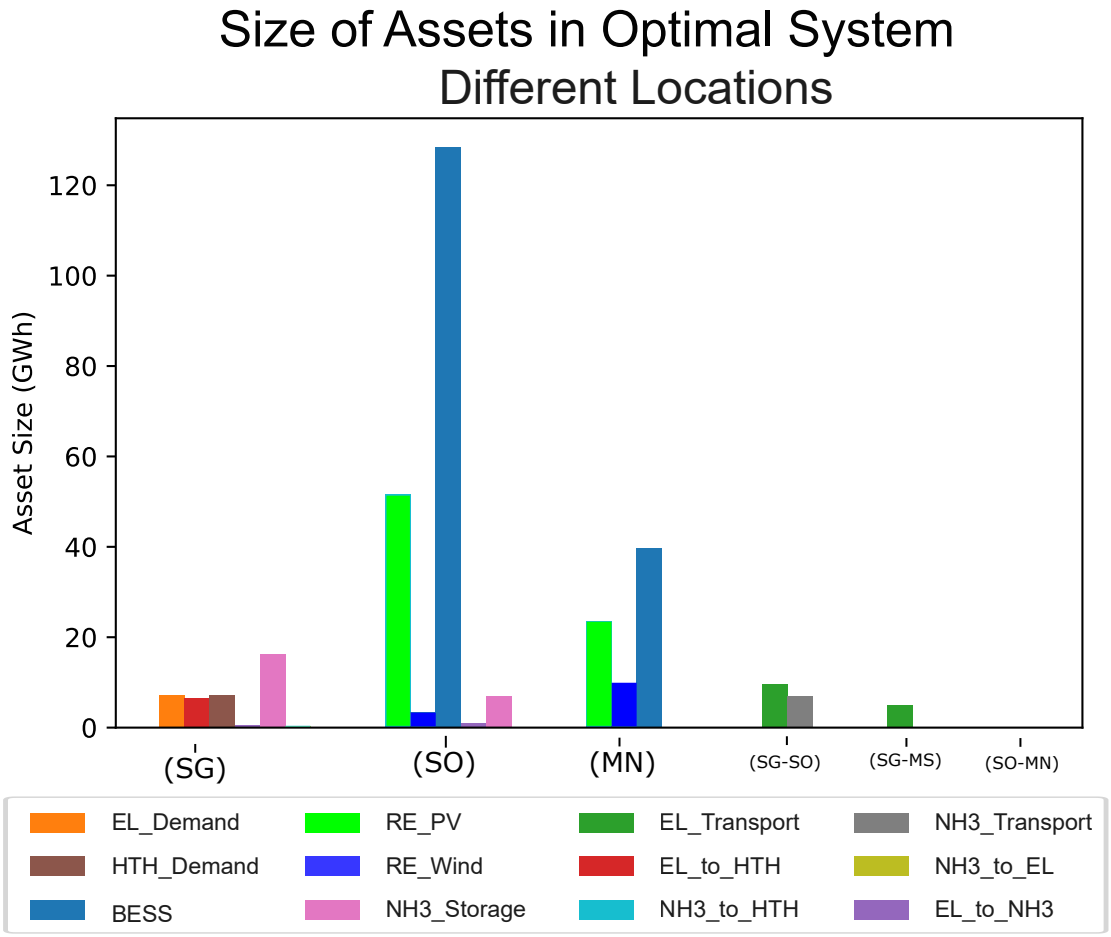

Figure 7.26: Size of Assets in Optimal System for Different Locations Scenario. Columns with a pair of locations refer to assets that are place from the first to second location. E.g. (SG,TB) EL_Transport refers to an electricity line from Location SG (Singapore) to Location TB (Tibet). The brands of these scenarios are given in Table 7.10.

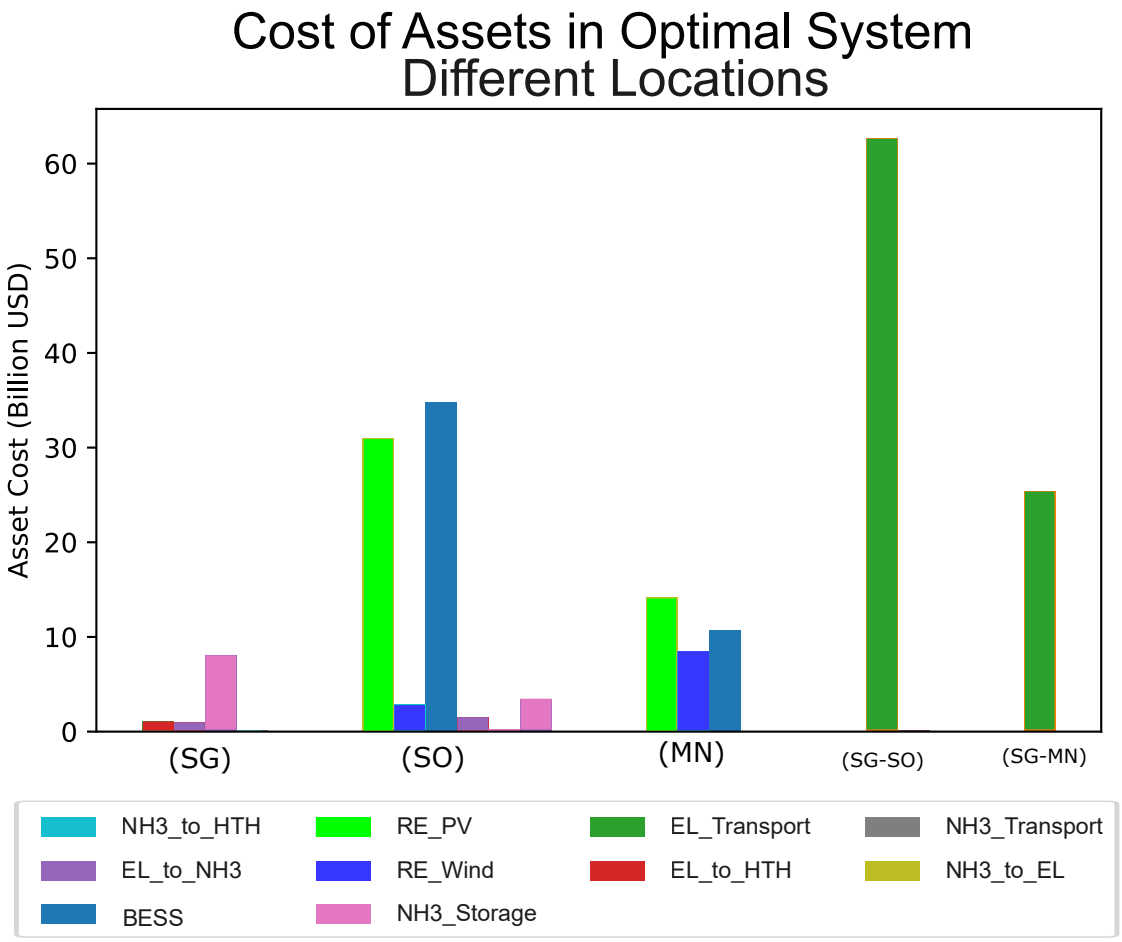

Figure 7.27: Cost of Assets in Optimal System for Different Locations Scenario. This is the cost of assets in optimal systems at locations or between two locations. The brands of these scenarios are given in Table 7.10.

7.3 Summary and Policy Recommendations

7.3.1 Policy Recommendations

The RE Singapore needs could come from one location, however, it may be beneficial for Singapore to potentially place multiple long-distance RE farms around the world. Singapore could also potentially bring the energy back to Singapore via multiple possible means, e.g. via electricity lines or via chemical energy vectors such as ammonia. There are both techno-economic and political benefits of having multiple RE farms and energy vectors. An example of the political advantages is increased energy security. If any country decides to block access to an RE farm or severs an electricity line that goes though that country, Singapore will still be able to get its energy from other locations or via other energy vectors. However, this is beyond the scope of the thesis and this assessment is a question for policy makers. This chapter uses the STEVFNs tool to assesses the techno-economic benefit of adding multiple RE farms and energy vectors. Policy makers may use the results from this study to decide if the political cost of future scenarios outweigh the techno-economic cost of building an energy system in a certain way.

Some techno-economic benefits of building multiple RE farms and energy vectors include being able to reduce the size of RE farms, or energy storage as energy can be moved in space and type, instead of being moved in time. It might be dark at one location in the world, but sunny in another. Thus, instead of using expensive batteries to move energy in time, we can use HVDC lines to move them in space instead. Furthermore, using ammonia could also provide an alternate means of moving energy in both space, time (via storage in tanks), and type (as we can burn ammonia for high temperature heating). Thus, we can qualitatively see the potential benefits of such a whole energy system.

The case study gave insights about optimal energy systems, as well as how they are affected by the costs and efficiencies of various technologies. These can be summarized as the following policy implications.

1. Solar PV is the dominant energy generation asset in future RE-based energy systems. This is true even when the cost of wind power is assumed to drop to

50% of BAU values. The cost of solar is predicted to fall, while the cost of wind is not expected to fall as quickly. Thus, global energy systems should consider predominantly solar PV.

2. Even though PV is the dominant energy generation type, a small amount of wind is still beneficial in a RE-based energy system. This is because it is uncorrelated with solar and drastically reduces the need to move energy in time (storage). This small amount of wind power should be used to balance the overall supply pattern rather than provide the bulk of energy supply.

3. Wind power pairs well with ammonia to move energy in time (storage). Similarly, solar PV pairs will with batteries to move energy in time (storage). Optimal energy systems with more ammonia storage will usually contain more wind.

4. Ammonia is useful in an energy system as it provides multiple energy system functions of movement in space, time, and type. Thus, a small amount of ammonia is useful in an energy system even when battery costs are half of BAU values. Future research assessing the viability of ammonia should consider the benefits of multiple functions of ammonia in an energy system, and not just one function independently.

5. Research should focus on reducing the costs of ammonia generation and storage technologies instead of improving their efficiencies. This is because the implicit cost of inefficiency losses are very low compared to explicit costs of sizing and using ammonia generation technologies. Reducing costs of ammonia generation and storage technologies increased their use. However, increasing the efficiency of ammonia generation technologies by 34% made no significant difference to the use of ammonia in an energy system.

6. Ammonia is used as a path, or energy vector, to satisfy HTH end-use demand. However, it is not useful to satisfy electricity end-use demand. This is because converting ammonia to electricity dramatically increases losses, and thus the energy production costs of over-sizing RE-farms. Using ammonia as an energy

vector to meet HTH demand only leads to 50% higher generation costs; however, using ammonia as an energy vector to meet electricity demand leads to 200% higher generation costs compared to using electricity and batteries as energy vectors.

7. In the existing fossil fuel-based energy system, the cost of generating energy is high, but the cost of moving energy in space and time is low. In the future RE-based energy system, the cost of generating energy will be low, but the combined cost of moving energy in space, time, and type will be high, accounting for approximately half of total system cost. Thus, research efforts should focus on reducing the costs of technologies that move energy.

It must be noted that the main purpose of the hypothetical case study is to perform as stress test to validate system dynamics of STEVFNs. The policy recommendations are still general and need to be further validated by testing more relevant and realistic scenarios.

7.3.2 Summary

This chapter answers the final thesis sub-question, thesis sub-question 5:"How do these model-generators and tool yield insights into real world energy system problems?" This chapter utilizes the open source STEVFNs tool to perform a case study of Singapore. This case study leads to insights on the design of long-distance DER farms and seven policy recommendations.

The case study is to optimize the sizing and operation of various assets to supply all of Singapore's hourly electricity and high temperature heating demand using long-distance DER farms at three potential locations around the world. The system could potentially have solar and/or wind farms at any of the three RE locations. The system could potentially have batteries, ammonia storage tanks, ammonia to electricity assets, and electricity to ammonia assets at any of the four locations. The system could potentially have HVDC electricity lines and/or ammonia transport between any pair of the four locations. This case study was performed for 100 scenarios to test the time taken for the optimizations to be done. Six interesting scenarios are discussed in this chapter.

The case study lead to insights of the value of ammonia in a whole energy system and various policy recommendations. There are various limitations to the case study. Firstly, HVDC lines were assumed to be laid using the shortest path, i.e. along great circles, or as the bird flies. This ignores the effect of terrain, and the ideal routing of HVDC lines may be different. Future work can include better HVDC routing algorithm, including those that use existing trade routes. The costs and efficiencies of HVDC lines and ammonia are still very uncertain. Thus, more work needs to be done to get more accurate estimates. This will allow newer and more certain insights. Lastly, hourly heating demand was assumed to follow the pattern of electricity demand. This is because hourly HTH demand data was not readily available. Future research, and regulatory work needs to be done to gather and make such data more readily available.

The main question of the thesis is to determine if a generalized spatio-temporal model of assets can be developed and utilized to optimize the sizing, operation and location of energy system assets. This chapter brings the thesis together by using the STEVFNs tool to perform a case study of optimal design of an energy system for Singapore. This lead to insights into emerging new energy systems. The next chapter concludes the thesis by summarizing the thesis contributions to knowledge and future research that this thesis enables.

Chapter 8

Conclusion

The core question the thesis addresses is:

"Can a generalized spatio-temporal asset model-generator be developed and utilized to optimize the sizing, operation, and location of energy system assets?"

This thesis develops a unified asset model-generator, and uses it to build a system design model-generator and tool for the optimal sizing, operation, and location of energy system assets with scenario assessment called the Space-Time Energy Vector Flow Networks (STEVFNs; pronounced "Stevens").

This thesis does so by answering the five thesis sub-questions. Before a system design model-generator can be developed, a unified generalized spatio-temporal asset model-generator needs to be developed, doing so requires answering the first thesis sub-question:

Sub-question 1: ***"What are the minimum and sufficient theoretical basis functions of all assets in an energy system, and can these functions be used to create a unified model-generator of assets?"*** **(Chapter 3)**

There are five basis functions of an energy system: energy demand, supply, transport, storage, and conversion. Any energy system function can be built from these basis functions. As demand response can be viewed as a generalization of energy storage, the five basis functions can model all combinations of the six types of energy

system assets. Chapter 3 develops a unified generalized spatio-temporal asset model-generator that describe any asset that can perform any combination of energy system functions.

With this unified asset model-generator, the second thesis sub-question is tackled:

Sub-question 2: ***"Can a model-generator of energy system design problems be developed, that utilizes the unified model-generator of assets, to co-optimize the sizing, operation, and location of real assets?" (Chapter 4)***

Chapter 4 develops the Space Time Energy Vector Flow Networks (STEVFN; pronounced like the name "Steven") system design model-generator to co-optimize the sizing, operation, and location of energy system assets with scenario assessment.

While Chapter 4 shows that there exists a solution to generate a model of any energy system asset using STEVFNs model-generators, the challenge of generating models for assets using the STEVFNs model-generators still needs to be tackled before STEVFNs can be utilized. To do this, this thesis answers the third thesis sub-question:

Sub-question 3: ***"How are models for real-world assets generated from traditional data using the model-generators?"*****(Chapter 5)**

Chapter 5 solves the problem and generates models for five simple and six complex real-world assets using the STEVFNs model-generators and manufacturer data or simple black-box measurements.

With real-world assets modelled in STEVFNs, the next step is to implement the STEVFNs model-generators and the models of assets generated using the STEVFNs model-generators as a tool. To do this, the thesis answers the fourth thesis sub-question:

Sub-question 4: ***"Can the model-generators be implemented as an easily accessible tool?"*****(Chapter 6)**

Chapter 6 implements the STEVFNs model-generators as an open-source tool for the co-optimization of sizing, operation, and location of energy system assets with scenario assessment. This tool is called the STEVFNs tool and is available on GitHub [1].

With the STEVFNs tool developed, the benefit of the tool can be demonstrated by answering the fifth, and final, thesis sub-question:

Sub-question 5: ***"How do these model-generators and tool yield insights into real world energy system problems?"*** **(Chapter 7)**

Chapter 7 utilizes the open source STEVFNs tool to perform a hypotherical case study of Singapore. The case study acts as a stress test to validate the system dynamics of the STEVFNs model-generators and tool. This case study also leads to insights on the design of long-distance DER farms and seven policy recommendations.

8.1 Contribution to Knowledge

This thesis generates the following five contributions to knowledge:

1. This thesis is the first to provide the fundamental basis functions of an energy system, and use them to develop a unified asset model-generator that can theoretically perform any combination of energy system functions.

2. Developed the STEVFNs system design model-generator for the co-optimization sizing, operation, and location of any type of energy system asset, with scenario assessment.

3. Generated models for five simple and six complex real assets using the STEVFNs model-generators and real-world data.

4. Implemented the STEVFNs model-generators as an easily accessible open-source tool in python, called the STEVFNs tool.

5. Performed a case study of Singapore to yield insights and seven policy recommendations about emerging energy systems with long-distance DER farms.

8.2 Future Work

Dissemination of Information

The results from this thesis will be published as a series of academic papers. There are currently four related papers at various stages in the publication pipeline.

Video tutorials are already available for system designer, however video tutorials need to be made available for two types of end-users: asset modellers and optimizers. These tutorials will also be combined as a course for the Open University. More detailed training courses will be made available for policy makers, industry, and academics in energy modelling summer schools such as the ICTP CCG joint summer school on modelling tools for sustainable development [188].

The STEVFNs tool is being verified against existing tools such as OSeMOSYS [8], and MARKAL/TIMES [10, 9].

Other Case Studies

The STEVFNs model-generators and tool developed in this thesis have already informed high level policy makers and high impact academics from at least six countries.

The STEVFNs model-generators and tool is being used to assess the case for building the first commercial fusion plants to be built in Singapore. This is because Fusion can provide flexible heating and electricity and can thus provide multiple functions and value in a whole energy system. A*STAR and NCCS-PMO are also in conversations to use the STEVFNs model-generator or tool to build an in-house national energy model that will be used by all ministries to align energy research efforts around the country. It is also being used by a consortium led by Climate Analytics to develop the Global Mitigation Potential Atlas that estimates how decarbonization costs can be reduced via international collaboration and renewable energy trade.

The STEVFNs tool is being used to guide Saudi Arabia's decarbonization strategies. The STEVFNs tool is being used to assess the ideal mix solar, wind, storage, and HVDC lines to meet Saudi Arabia's 50/50 target for 2030. It is also being used to assess the economic viability of early retirement of existing non-renewable energy infrastructure such as coal and oil power plants. The problem of stranding these assets may be outweighed by the economic benefits from cheaper DER generation.

The STEVFNs tool is also being used to make a case for a more ambitious energy decarbonization pathway for Saudi Arabia. This is being done by designing long term energy system decarbonization pathways for Saudi Arabia. It is also being used to study how the viability of hydrogen changes when it is used for multiple functions in Saudi Arabia, including for international trade.

The STEVFNs tool is being used in a collaboration between researchers from Oxford and Austria to build a tool to calculate and visualize the benefits of international HVDC links. It is also specifically being used to study the viability of a HVDC connection between South America and West Africa.

The STEVFNs tool is being used by researchers at the Energy and Power Group in Oxford to study the optimal bidding strategy of PV in the new Mexican energy market, with and without batteries.

Researchers from the Delta E-plus group at Simon Fraser University in Canada are also in conversations to use either the STEVFNs tool or model-generator as one of the building blocks for another energy system optimization framework. This new framework seeks to use STEVFNs to efficiently resolve the convex part of energy system design problems. It will then have an outer layer that will use machine learning and other heuristic optimization methods to solve the non-convex parts of energy system design.

Extensions of STEVFNs

The development of the STEVFNs model-generators was motivated to deal with energy systems. However, the physics of STEVFNs is not restricted to energy flows; this is already apparent in the hydrogen water heater asset in Section 5.1.5 which considers the flows of "hot water". Therefore, STEVFNs can be extended to model any type of general material flows, and thus assets. The immediate application is to extend STEVFNs to Climate, Land (Food), Energy, and Water strategies (CLEWs) [207]. Current research uses these other systems as constraints for the energy system design. STEVFNs can unify all usages and assets in CLEWs to not only uses land and water systems as constraints, but also co-optimize the design of land, water, and energy systems, together. Some integrated assessment models do optimize for

land and water use, but as they are federated models, studying their computational complexity is difficult, and their co-optimization becomes inefficient and sometimes contradictory if multiple modules attempt to optimize the same thing [208], [**?**].

Another extension of STEVFNs is to Industrial Symbiosis Networks (ISNs) [169]. These are systems of factories, etc, that are interconnected, e.g. the output of one factory is the input of another. The current state of the art methods of modelling ISNs require inversion of large sparse matrices just to simulate these systems. Modelling ISNs using STEVFNs can solve the following open problems in ISN modelling:

1. STEVFNs allows for much quicker simulation of large ISNs using parallelization allowed from the locality in STEVFNs as described in Section 4.4.6.

2. STEVFNs allows for more intuitive and automatic modelling of ISNs. Current methods require a lot of manual effort to "balance" and build matrices whose inverted forms represent the ISNs. The balancing of these matrices is non-trivial, and needs to be solved for each unique system[209].

3. STEVFNs allow for the simulation of multiple timesteps, and storage of materials that current ISN modelling methods struggle with (because they become computationally prohibitive).

4. STEVFNs allows for the optimization of the sizing and operation of ISNs; current methods require inversion of matrices to simulate ISNs. This means that the simulation of multiple timesteps becomes computationally intractable as it requires the inversion of an NxN matrix sparse matrix, where N is the number of timesteps. This representation makes it difficult to optimize ISN operation, let alone sizing. Some authors attempt to use linear programming to represent certain heat networks, this is very similar to the approach used by energy system models such as OSeMOSYS. They thus have similar limitations, and can benefit from similar computational improvements with STEVFNs.

Theoretical Implications

This thesis utilizes and develops various concepts from theoretical physics. There are various insights and implications that can be obtained from the work of the thesis. The conversion from snapshots in time to flows of generalized coordinates in time is linked to the conversion from the equations of motion of a system to the stationary-action principle. This may be viewed as converting a numerical integration problem to a numerical optimization problem. The study of the convexity of the optimization problem, and thus the computational complexity of the optimization problem can thus be linked to the computational complexity of solving the original equations of motion. This could allow us to find a new definition of chaos and a "good approximation". This could allow researchers to move from asking "is this a good approximation" to "does a good approximation exist". A good approximation exists if the mathematical optimization problem can be solved (or at least tested) in polynomial time. This would be equivalent to saying that the errors in the numerical integration can be bounded in polynomial time as the simulation time increases. A chaotic system may thus be a system for which no good approximation exists.

The visualization of flows in space, time, or type in a network may be mapped to classical field theories. Components or energy system functions can be mapped to physical forces. The costs of assets can be mapped to the action of a system. This may give us intuitive understanding of the origin of charge parity and time reversal (CPT) symmetry in classical field theories. This may further give insights into why some forces preserve subsets of CPT symmetry. The dependence of the costs of assets on local flows can also be mapped to the measure of "distance" and thus to curvature of spacetime in general relativity.

Bibliography

[1] A. Ahsan, "The Space-Time Energy Vector Flow Networks (STEVFNs) Tool." https://github.com/OmNomNomzzz/STEVFNs, 2022. Accessed: 29-09-2022.

[2] I. O. Adelekan, N. P. Simpson, E. Totin, and C. H. Trisos, "IPCC Sixth Assessment Report (AR6): Climate Change 2022-Impacts, Adaptation and Vulnerability: Regional Factsheet Africa," 2022.

[3] IPCC, " 2019 Refinement to the 2006 IPCC Guidelines for National Greenhouse Gas Inventories," tech. rep., Intergovernmental Panel on Climate Change (IPCC), 2019.

[4] C. Watch, "Climate Watch Historical GHG Emissions." https://www.climatewatchdata.org/ghg-emissions?breakBy=sector&chartType=area&end_year=2019&sectors=total-including-lucf&start_year=1990, 2022. Accessed: 08-08-2022.

[5] E. Data, "Global Solar Atlas." https://globalsolaratlas.info/support/about, 2022. Accessed: 29-09-2022.

[6] E. Data, "Global Wind Atlas." https://globalwindatlas.info/about/TermsOfUse, 2022. Accessed: 29-09-2022.

[7] L. Allington, C. Cannone, I. Pappis, K. C. Barron, W. Usher, S. Pye, E. Brown, M. Howells, M. Z. Walker, A. Ahsan, *et al.*, "Selected 'Starter kit'energy system modelling data for selected countries in Africa, East Asia, and South America (# CCG, 2021)," *Data in Brief*, vol. 42, p. 108021, 2022.

[8] M. Howells, H. Rogner, N. Strachan, C. Heaps, H. Huntington, S. Kypreos, A. Hughes, S. Silveira, J. DeCarolis, M. Bazillian, *et al.*, "OSeMOSYS: the open source energy modeling system: an introduction to its ethos, structure and development," *Energy Policy*, vol. 39, no. 10, pp. 5850–5870, 2011.

[9] R. Loulou, G. Goldstein, K. Noble, *et al.*, "Documentation for the MARKAL Family of Models," *Energy Technology Systems Analysis Programme*, pp. 65–73, 2004.

[10] R. Loulou, U. Remne, A. Kanudia, A. Lehtila, and G. Goldstein, "Documentation for the TIMES Model: PART I, 2005," *Energy Technology Systems Analysis Programme (ETSAP)*.

[11] T. Brown, J. Hörsch, and D. Schlachtberger, "PyPSA: Python for Power System Analysis," *Journal of Open Research Software*, vol. 6, no. 4, 2018.

[12] I. A. E. Agency, "Model for Analysis of Energy Demand (MAED-2)." `https://www.iaea.org/publications/7430/model-for-analysis-of-energy-demand-maed-2`, 2022. Accessed: 05-05-2022.

[13] I. I. for Applied Systems Analysis, "MESSAGE - IIASA." `https://previous.iiasa.ac.at/web/home/research/modelsData/MESSAGE/MESSAGE.en.html`, 2022. Accessed: 05-05-2022.

[14] OSeMOSYS, "OSeMOSYS - the Open Sourse Energy Modelling System." `https://github.com/OSeMOSYS/OSeMOSYS`, 2023. Accessed: 23-04-2023.

[15] OSeMOSYS, "Interfaces - OSeMOSYS clicSAND (Simple And Nearly Done)." `http://www.osemosys.org/interfaces.html`, 2023. Accessed: 23-04-2023.

[16] OSeMOSYS, "Interfaces - OSeMOSYS Model Management Infrastructure (MoManI)." `http://www.osemosys.org/interfaces.html`, 2023. Accessed: 23-04-2023.

[17] W. Usher, H. Henke, C. Muschner, and T. Barnes, "Welcome to the documentation of otoole." https://iea-etsap.org/index.php/etsap-tools/data-handling-shells/veda, 2023. Accessed: 23-04-2023.

[18] IEA-ETSAP, "Times model generator," Apr. 2023.

[19] I. E. Agency, "IEA-ESTAP — VEDA." https://iea-etsap.org/index.php/etsap-tools/data-handling-shells/veda, 2023. Accessed: 23-04-2023.

[20] Thomas Reindl, "Solar Photovoltaic (PV) Roadmap for Singapore," tech. rep., National Climate Change Secretariat, Singapore, 2020.

[21] "IEA Sankey Diagrams." https://www.iea.org/sankey/.

[22] K. A. Collett, A. Ahsan, C. Hollaran, A. Vijay, I. Berdellans, S. Hasanovic, A. Gritsevskyi, L. Stankeviciute, M. Tot, M. Welsch, and S. Hirmer, "Lecture 1: Course Introduction to EBS and MAED, Energy Balance Studio and MAED (demand projections)." https://www.open.edu/openlearncreate/course/view.php?id=6819, 2021. Release Version 1.0. [online presentation]. Climate Compatible Growth Programme and International Atomic Energy Agency.

[23] C. Heaps, "LEAP: The Low Emissions Analysis Platform. [Software version: 2020.1.61]." https://leap.sei.org, 2022. Accessed: 05-05-2022.

[24] A. Agrawal, B. Amos, S. Barratt, S. Boyd, S. Diamond, and J. Z. Kolter, "Differentiable convex optimization layers," in *Advances in Neural Information Processing Systems*, pp. 9558–9570, 2019.

[25] S. Diamond and S. Boyd, "CVXPY: A Python-embedded modeling language for convex optimization," *Journal of Machine Learning Research*, vol. 17, no. 83, pp. 1–5, 2016.

[26] A. Agrawal, R. Verschueren, S. Diamond, and S. Boyd, "A rewriting system for convex optimization problems," *Journal of Control and Decision*, vol. 5, no. 1, pp. 42–60, 2018.

[27] *Scalable spatial design of electricity access systems.* PhD thesis, University of Oxford, 2022.

[28] H.-K. Ringkjøb, P. M. Haugan, and I. M. Solbrekke, "A review of modelling tools for energy and electricity systems with large shares of variable renewables," *Renewable and Sustainable Energy Reviews*, vol. 96, pp. 440–459, 11 2018.

[29] A. B. Kennedy and H. R. Sankey, "THE THERMAL EFFICIENCY OF STEAM ENGINES. REPORT OF THE COMMITTEE APPOINTED TO THE COUNCIL UPON THE SUBJECT OF THE DEFINITION OF A STANDARD OR STANDARDS OF THERMAL EFFICIENCY FOR STEAM ENGINES: WITH AN INTRODUCTORY NOTE.(INCLUDING APPENDIXES AND PLATE AT BACK OF VOLUME).," in *Minutes of the Proceedings of the Institution of Civil Engineers*, vol. 134, pp. 278–312, Thomas Telford-ICE Virtual Library, 1898.

[30] M. Schmidt, "The Sankey diagram in energy and material flow management: part II: methodology and current applications," *Journal of industrial ecology*, vol. 12, no. 2, pp. 173–185, 2008.

[31] "IEA Data Tables-Data and Statistics." `https://www.iea.org/data-and-statistics/data-tables/?country=WORLD&energy=Balances/`.

[32] N. C. C. Secretariat, "Singapore's Fourth Biennial Update Report." `https://www.nccs.gov.sg/docs/default-source/default-document-library/2020-singapore-fourth-biennial-report.pdf`, 2020.

[33] "AURORAxmp." `https://www.energyexemplar.com/aurora/`.

[34] S. Carley, "Decarbonization of the US electricity sector: Are state energy policy portfolios the solution?," *Energy Economics*, vol. 33, no. 5, pp. 1004–1023, 2011.

[35] M. Z. Jacobson, M. A. Delucchi, M. A. Cameron, and B. A. Frew, "Low-cost solution to the grid reliability problem with 100% penetration of intermittent wind, water, and solar for all purposes," *Proceedings of the National Academy of Sciences*, vol. 112, no. 49, pp. 15060–15065, 2015.

[36] C. Bussar, P. Stöcker, Z. Cai, L. Moraes Jr, D. Magnor, P. Wiernes, N. van Bracht, A. Moser, and D. U. Sauer, "Large-scale integration of renewable energies and impact on storage demand in a European renewable power system of 2050—Sensitivity study," *Journal of Energy Storage*, vol. 6, pp. 1–10, 2016.

[37] M. Pereira, A. Monticelli, and L. Pinto, "Security-constrained dispatch with corrective rescheduling," *IFAC Proceedings Volumes*, vol. 18, no. 7, pp. 333–340, 1985.

[38] A. Monticelli, M. Pereira, and S. Granville, "Security-constrained optimal power flow with post-contingency corrective rescheduling," *IEEE Transactions on Power Systems*, vol. 2, no. 1, pp. 175–180, 1987.

[39] A. Soroudi, *Power system optimization modeling in GAMS*, vol. 78. Springer, 2017.

[40] Autodesk, "AutoCAD Software." `https://www.autodesk.co.uk/products/autocad/overview?term=1-YEAR&tab=subscription`, 2022. Accessed: 05-05-2022.

[41] Autodesk, "Revit: BIM Software." `https://www.autodesk.co.uk/products/revit/overview?term=1-YEAR&tab=subscription`, 2022. Accessed: 05-05-2022.

[42] "Monday.com — A new way of working." `https://monday.com/`, 2022. Accessed: 05-05-2022.

[43] bambooHR, "Bamboo HR Software." ://www.bamboohr.com/, 2022. Accessed: 05-05-2022.

[44] DIgSILENT, "PowerFactory - DIgSILENT." `https://www.digsilent.de/en/powerfactory.html`, 2022. Accessed: 05-05-2022.

[45] M. Wei, C. A. McMillan, *et al.*, "Electrification of industry: potential, challenges and outlook," *Current Sustainable/Renewable Energy Reports*, vol. 6, no. 4, pp. 140–148, 2019.

[46] J. Pospíšil, M. Špiláček, and L. Kudela, "Potential of predictive control for improvement of seasonal coefficient of performance of air source heat pump in Central European climate zone," *Energy*, vol. 154, pp. 415–423, 2018.

[47] O. Ruhnau, S. Bannik, S. Otten, A. Praktiknjo, and M. Robinius, "Direct or indirect electrification? A review of heat generation and road transport decarbonisation scenarios for Germany 2050," *Energy*, vol. 166, pp. 989–999, 2019.

[48] W. A. McEachern, *Economics: A contemporary introduction*. Cengage Learning, 2016.

[49] S. Pfenninger and B. Pickering, "Calliope: a multi-scale energy systems modelling framework," *Journal of Open Source Software*, vol. 3, no. 29, p. 825, 2018.

[50] DESSTINEE, "2050 DESSTINEE." `https://sites.google.com/site/2050desstinee/introduction`, 2022. Accessed: 05-05-2022.

[51] I. Staffell and S. Pfenninger, "The increasing impact of weather on electricity supply and demand," *Energy*, vol. 145, pp. 65–78, 2018.

[52] M. E. Burfisher, *Introduction to computable general equilibrium models*. Cambridge University Press, 2021.

[53] P. Capros, D. Van Regemorter, L. Paroussos, P. Karkatsoulis, C. Fragkiadakis, S. Tsani, I. Charalampidis, T. Revesz, M. Perry, and J. Abrell, "GEM-E3 model documentation," *JRC Scientific and Policy Reports*, vol. 26034, 2013.

[54] "GEM-E3 model." `https://joint-research-centre.ec.europa.eu/gem-e3/gem-e3-model_en`, 2022. Accessed: 05-05-2022.

[55] C. Böhringer, B. Bye, T. Fæhn, and K. E. Rosendahl, "Alternative designs for tariffs on embodied carbon: A global cost-effectiveness analysis," *Energy Economics*, vol. 34, pp. S143–S153, 2012.

[56] L. Hamilton, G. Goldstein, J. Lee, W. Marcuse, S. Morris, A. Manne, and C.-O. Wene, "MARKAL-MACRO: an overview," 1992.

[57] A. S. Manne and C.-O. Wene, "MARKAL-MACRO: A linked model for energy-economy analysis," tech. rep., Brookhaven National Lab., Upton, NY (United States), 1992.

[58] F. Charbonnier, T. Morstyn, and M. D. McCulloch, "Scalable multi-agent reinforcement learning for distributed control of residential energy flexibility," *Applied Energy*, vol. 314, p. 118825, 2022.

[59] F. Charbonnier, T. Morstyn, and M. McCulloch, "Coordination of resources at the edge of the electricity grid: systematic review and taxonomy," *arXiv preprint arXiv:2202.03786*, 2022.

[60] M. Khorasany, A. S. Gazafroudi, R. Razzaghi, T. Morstyn, and M. Shafie-khah, "A framework for participation of prosumers in peer-to-peer energy trading and flexibility markets," *Applied Energy*, vol. 314, p. 118907, 2022.

[61] M. Z. Jacobson, "The cost of grid stability with 100% clean, renewable energy for all purposes when countries are isolated versus interconnected," *Renewable Energy*, vol. 179, pp. 1065–1075, 2021.

[62] W. Klöpffer, "Life cycle assessment," *Environmental Science and Pollution Research*, vol. 4, no. 4, pp. 223–228, 1997.

[63] C. Hsien, K. Zi-Yu, E. Eisner, C. S. Ying, L. N. K. Yuan, J. Dönmez, M. Mennenga, C. Herrmann, and J. S. C. Low, "Self-Assessment and Improvement Tool for a Sustainability Excellence Framework in Singapore," *Procedia CIRP*, vol. 98, pp. 672–677, 2021.

[64] P. KERDLAP and J. S. C. LOW, "Advancements in Methods for Life Cycle Assessment of Industrial Symbiosis," in *Life Cycle Assessment: New Developments And Multi-disciplinary Applications*, pp. 233–243, World Scientific, 2022.

[65] A. Valente, D. Iribarren, and J. Dufour, "Life cycle assessment of hydrogen energy systems: a review of methodological choices," *The International Journal of Life Cycle Assessment*, vol. 22, no. 3, pp. 346–363, 2017.

[66] V. Muteri, M. Cellura, D. Curto, V. Franzitta, S. Longo, M. Mistretta, and M. L. Parisi, "Review on life cycle assessment of solar photovoltaic panels," *Energies*, vol. 13, no. 1, p. 252, 2020.

[67] J. Porzio and C. D. Scown, "Life-Cycle Assessment Considerations for Batteries and Battery Materials," *Advanced Energy Materials*, vol. 11, no. 33, p. 2100771, 2021.

[68] Y. Li, J. Song, and J. Yang, "A review on structure model and energy system design of lithium-ion battery in renewable energy vehicle," *Renewable and Sustainable Energy Reviews*, vol. 37, pp. 627–633, 2014.

[69] Y. Yang, S. Bremner, C. Menictas, and M. Kay, "Battery energy storage system size determination in renewable energy systems: A review," *Renewable and Sustainable Energy Reviews*, vol. 91, pp. 109–125, 2018.

[70] C. Crozier and K. Baker, "Optimal Sizing of an Energy Storage Portfolio Considering Multiple Timescales," in *2021 IEEE Power & Energy Society General Meeting (PESGM)*, pp. 01–05, IEEE, 2021.

[71] K. A. Baker, *Coordination of resources across areas for the integration of renewable generation: Operation, sizing, and siting of storage devices.* PhD thesis, Carnegie Mellon University, 2014.

[72] S. Tsushima and T. Suzuki, "Modeling and simulation of vanadium redox flow battery with interdigitated flow field for optimizing electrode architecture," *Journal of The Electrochemical Society*, vol. 167, no. 2, p. 020553, 2020.

[73] N. Salmon, R. Bañares-Alcántara, and R. Nayak-Luke, "Optimization of green ammonia distribution systems for intercontinental energy transport," *science*, vol. 24, no. 8, p. 102903, 2021.

[74] S. M. Alirahmi, A. R. Razmi, and A. Arabkoohsar, "Comprehensive assessment and multi-objective optimization of a green concept based on a combination of hydrogen and compressed air energy storage (CAES) systems," *Renewable and Sustainable Energy Reviews*, vol. 142, p. 110850, 2021.

[75] F. Faraji, A. Majazi, K. Al-Haddad, *et al.*, "A comprehensive review of flywheel energy storage system technology," *Renewable and Sustainable Energy Reviews*, vol. 67, pp. 477–490, 2017.

[76] M. E. Amiryar and K. R. Pullen, "A review of flywheel energy storage system technologies and their applications," *Applied Sciences*, vol. 7, no. 3, p. 286, 2017.

[77] D. A. Tziouvaras, P. McLaren, G. Alexander, D. Dawson, J. Esztergalyos, C. Fromen, M. Glinkowski, I. Hasenwinkle, M. Kezunovic, L. Kojovic, *et al.*, "Mathematical models for current, voltage, and coupling capacitor voltage transformers," *IEEE Transactions on Power Delivery*, vol. 15, no. 1, pp. 62–72, 2000.

[78] P. Davari, Y. Yang, F. Zare, and F. Blaabjerg, "A review of electronic inductor technique for power factor correction in three-phase adjustable speed drives," in *2016 IEEE Energy Conversion Congress and Exposition (ECCE)*, pp. 1–8, IEEE, 2016.

[79] M. Dreidy, H. Mokhlis, and S. Mekhilef, "Inertia response and frequency control techniques for renewable energy sources: A review," *Renewable and sustainable energy reviews*, vol. 69, pp. 144–155, 2017.

[80] "Velkess." `http://velkess.com/flywheel.html`, 2022. Accessed: 05-05-2022.

[81] L. Zhang, X. Hu, Z. Wang, F. Sun, and D. G. Dorrell, "A review of supercapacitor modeling, estimation, and applications: A control/management perspective," *Renewable and Sustainable Energy Reviews*, vol. 81, pp. 1868–1878, 2018.

[82] H. Peterson, N. Mohan, and R. Boom, "Superconductive energy storage inductor-converter units for power systems," *IEEE Transactions on Power Apparatus and Systems*, vol. 94, no. 4, pp. 1337–1348, 1975.

[83] S. Rehman, L. M. Al-Hadhrami, and M. M. Alam, "Pumped hydro energy storage system: A technological review," *Renewable and Sustainable Energy Reviews*, vol. 44, pp. 586–598, 2015.

[84] I. E. Agency, "How rapidly will the global electricity storage market grow by 2026? - Analysis - IEA." `https://www.iea.org/articles/how-rapidly-will-the-global-electricity-storage-market-grow-by-2026`, 2021. Accessed: 05-05-2022.

[85] G. I. Group, "DER-CAM — Grid Integration Group." `https://gridintegration.lbl.gov/der-cam`, 2022. Accessed: 05-05-2022.

[86] L. Hirth, "The european electricity market model EMMA model documentation," *Neon Neue Energieökonomik GmbH: Berlin, Germany*, pp. 1–17, 2017.

[87] C. Skar, G. Doorman, G. A. Pérez-Valdés, and A. Tomasgard, "A multi-horizon stochastic programming model for the European power system," *Trondheim: CenSES working paper*, vol. 2, p. 2016, 2016.

[88] SINTEF, "EMPS - multi area power-market simulator - SINTEF." `https://www.sintef.no/en/software/emps-multi-area-power-market-simulator/`, 2022. Accessed: 05-05-2022.

[89] L. Göransson, J. Goop, T. Unger, M. Odenberger, and F. Johnsson, "Linkages between demand-side management and congestion in the European electricity transmission system," *Energy*, vol. 69, pp. 860–872, 2014.

[90] A. Zerrahn and W.-P. Schill, "On the representation of demand-side management in power system models," *Energy*, vol. 84, pp. 840–845, 2015.

[91] R. E. Hedegaard, T. H. Pedersen, and S. Petersen, "Multi-market demand response using economic model predictive control of space heating in residential buildings," *Energy and Buildings*, vol. 150, pp. 253–261, 2017.

[92] J. Le Dréau and P. Heiselberg, "Energy flexibility of residential buildings using short term heat storage in the thermal mass," *Energy*, vol. 111, pp. 991–1002, 2016.

[93] F. Brahman, M. Honarmand, and S. Jadid, "Optimal electrical and thermal energy management of a residential energy hub, integrating demand response and energy storage system," *Energy and Buildings*, vol. 90, pp. 65–75, 2015.

[94] L. Zhang, J. Kuang, B. Sun, F. Li, and C. Zhang, "A two-stage operation optimization method of integrated energy systems with demand response and energy storage," *Energy*, vol. 208, p. 118423, 2020.

[95] P. Ahčin and M. Šikić, "Simulating demand response and energy storage in energy distribution systems," in *2010 International Conference on Power System Technology*, pp. 1–7, IEEE, 2010.

[96] W. Huang, N. Zhang, C. Kang, M. Li, and M. Huo, "From demand response to integrated demand response: Review and prospect of research and application," *Protection and Control of Modern Power Systems*, vol. 4, no. 1, pp. 1–13, 2019.

[97] A. Wierman, Z. Liu, I. Liu, and H. Mohsenian-Rad, "Opportunities and challenges for data center demand response," in *International Green Computing Conference*, pp. 1–10, IEEE, 2014.

[98] Y. Liu, J. Li, and L. Wu, "ACOPF for three-phase four-conductor distribution systems: semidefinite programming based relaxation with variable reduction and feasible solution recovery," *IET Generation, Transmission & Distribution*, vol. 13, no. 2, pp. 266–276, 2019.

[99] A. Castillo and R. P. O'Neill, "Computational performance of solution techniques applied to the ACOPF," *Federal Energy Regulatory Commission, Optimal Power Flow Paper*, vol. 5, 2013.

[100] C. Crozier, K. Baker, and B. Toomey, "Feasible region-based heuristics for optimal transmission switching," *Sustainable Energy, Grids and Networks*, vol. 30, p. 100628, 2022.

[101] T. Morstyn, K. A. Collett, A. Vijay, M. Deakin, S. Wheeler, S. M. Bhagavathy, F. Fele, and M. D. McCulloch, "OPEN: An open-source platform for developing smart local energy system applications," *Applied Energy*, vol. 275, p. 115397, 2020.

[102] Y. Xu, N. Myhrvold, D. Sivam, K. Mueller, D. J. Olsen, B. Xia, D. Livengood, V. Hunt, B. R. d'Orfeuil, D. Muldrew, *et al.*, "US test system with high spatial and temporal resolution for renewable integration studies," in *2020 IEEE Power & Energy Society General Meeting (PESGM)*, pp. 1–5, IEEE, 2020.

[103] B. Eldridge, R. O'Neill, and A. Castillo, "An improved method for the DCOPF with losses," *IEEE Transactions on Power Systems*, vol. 33, no. 4, pp. 3779–3788, 2017.

[104] S. Vaishya and V. Sarkar, "Accurate loss modelling in the DCOPF calculation for power markets via static piecewise linear loss approximation based upon line loading classification," *Electric power systems research*, vol. 170, pp. 150–157, 2019.

[105] C. W. Gellings, "A globe spanning super grid," *IEEE Spectrum*, vol. 52, no. 8, pp. 48–54, 2015.

[106] C. Wu, X.-p. Zhang, and M. J. Sterling, "Economic Analysis of Power Grid Interconnections Among Europe, North-East Asia, and North America With 100% Renewable Energy Generation," *IEEE Open Access Journal of Power and Energy*, vol. 8, pp. 268–280, 2021.

[107] F. ISE, "ENTIGRIS - Power System Model for expansion planning and unit-commitment - Fraunhofer ISE." `https://www.ise.fraunhofer.de/en/business-areas/power-electronics-grids-and-smart-systems/energy-system-analysis/energy-system-models-at-fraunhofer-ise/entigris.html`, 2022. Accessed: 05-05-2022.

[108] A. Ahsan, Q. Zhao, A. M. Khambadkone, and M. H. Chia, "Dynamic battery operational cost modeling for energy dispatch," in *2016 IEEE Energy Conversion Congress and Exposition (ECCE)*, pp. 1–5, IEEE, 2016.

[109] Z. Abdin, A. Zafaranloo, A. Rafiee, W. Mérida, W. Lipiński, and K. R. Khalilpour, "Hydrogen as an energy vector," *Renewable and sustainable energy reviews*, vol. 120, p. 109620, 2020.

[110] N. Salmon and R. Bañares-Alcántara, "Green ammonia as a spatial energy vector: a review," *Sustainable Energy & Fuels*, vol. 5, no. 11, pp. 2814–2839, 2021.

[111] A. Rafiee, K. R. Khalilpour, J. Prest, and I. Skryabin, "Biogas as an energy vector," *Biomass and Bioenergy*, vol. 144, p. 105935, 2021.

[112] D. Baeza, C. F. Ihle, and J. M. Ortiz, "A comparison between ACO and Dijkstra algorithms for optimal ore concentrate pipeline routing," *Journal of Cleaner Production*, vol. 144, pp. 149–160, 2017.

[113] E. Exemplar, "PLEXOS — Energy Market Simulation Software — Energy Exemplar." `https://www.energyexemplar.com/plexos`, 2022. Accessed: 05-05-2022.

[114] G. Luderer, M. Leimbach, N. Bauer, E. Kriegler, L. Baumstark, C. Bertram, A. Giannousakis, J. Hilaire, D. Klein, A. Levesque, *et al.*, "Description of the REMIND model (Version 1.6)," 2015.

[115] I. Zenginis, J. S. Vardakas, C. Echave, M. Morató, J. Abadal, and C. V. Verikoukis, "Cooperation in microgrids through power exchange: An optimal sizing and operation approach," *Applied Energy*, vol. 203, pp. 972–981, 2017.

[116] M. Saberi, S. A. Ahmadi, F. J. Ardakani, and G. H. Riahy, "Optimal sizing of hybrid PV and wind energy system with backup of redox flow battery to postpone grid expansion investments," *Journal of Renewable and Sustainable Energy*, vol. 10, no. 5, p. 055903, 2018.

[117] M. Z. Jacobson, M. A. Delucchi, M. A. Cameron, S. J. Coughlin, C. A. Hay, I. P. Manogaran, Y. Shu, and A. Krauland, "Impacts of Green New Deal Energy Plans on Grid Stability, Costs, Jobs, Health, and Climate in 143 Countries," *One Earth*, vol. 2, no. 1, p. 109, 2020.

[118] A. De Blaeij, R. J. Florax, P. Rietveld, and E. Verhoef, "The value of statistical life in road safety: a meta-analysis," *Accident Analysis & Prevention*, vol. 35, no. 6, pp. 973–986, 2003.

[119] C. R. Sunstein, "Lives, life-years, and willingness to pay," *Colum. L. Rev.*, vol. 104, p. 205, 2004.

[120] E. Triantaphyllou, "Multi-criteria decision making methods," in *Multi-criteria decision making methods: A comparative study*, pp. 5–21, Springer, 2000.

[121] M. Di Somma, B. Yan, N. Bianco, G. Graditi, P. Luh, L. Mongibello, and V. Naso, "Multi-objective design optimization of distributed energy systems through cost and exergy assessments," *Applied Energy*, vol. 204, pp. 1299–1316, 2017.

[122] M. Vasileiou, E. Loukogeorgaki, and D. G. Vagiona, "GIS-based multi-criteria decision analysis for site selection of hybrid offshore wind and wave energy systems in Greece," *Renewable and sustainable energy reviews*, vol. 73, pp. 745–757, 2017.

[123] X. Zhao, Y. Xu, and D. C. Hopkins, "Advanced multi-physics simulation for high performance power electronic packaging design," in *2016 International Symposium on 3D Power Electronics Integration and Manufacturing (3D-PEIM)*, pp. 1–5, IEEE, 2016.

[124] H. Liu, D. Liu, Q. Liu, *et al.*, "Modeling simulation technology research for distribution network planning," *Energy and Power Engineering*, vol. 5, no. 04, p. 980, 2013.

[125] S. Jaehnert, "Integration of regulating power markets in northern Europe," 2012.

[126] K. Van den Bergh, K. Bruninx, E. Delarue, and W. D'haeseleer, "LUSYM: a unit commitment model formulated as a mixed-integer linear program," *KU Leuven, TME Branch Working Paper*, vol. 7, 2014.

[127] J. Deane, G. Drayton, and B. Ó. Gallachóir, "The impact of sub-hourly modelling in power systems with significant levels of renewable generation," *Applied Energy*, vol. 113, pp. 152–158, 2014.

[128] S. Carrara and G. Marangoni, "Including system integration of variable renewable energies in a constant elasticity of substitution framework: the case of the WITCH model," *Energy Economics*, vol. 64, pp. 612–626, 2017.

[129] N. Blair, A. P. Dobos, J. Freeman, T. Neises, M. Wagner, T. Ferguson, P. Gilman, and S. Janzou, "System advisor model, sam 2014.1. 14: General description," tech. rep., National Renewable Energy Lab.(NREL), Golden, CO (United States), 2014.

[130] T. H. Y. Føyn, K. Karlsson, O. Balyk, and P. E. Grohnheit, "A global renewable energy system: a modelling exercise in ETSAP/TIAM," *Applied energy*, vol. 88, no. 2, pp. 526–534, 2011.

[131] S. Hilpert, S. Günther, C. Kaldemeyer, U. Krien, G. Pleßmann, F. Wiese, and C. Wingenbach, "Addressing energy system modelling challenges: The contribution of the Open Energy Modelling Framework (oemof)," 2017.

[132] A. Leonard, S. Wheeler, and M. McCulloch, "Power to the people: Applying citizen science and computer vision to home mapping for rural energy access," *International Journal of Applied Earth Observation and Geoinformation*, vol. 108, p. 102748, 2022.

[133] D. Bogdanov and C. Breyer, "North-East Asian Super Grid for 100% renewable energy supply: Optimal mix of energy technologies for electricity, gas and heat supply options," *Energy Conversion and Management*, vol. 112, pp. 176–190, 2016.

[134] H. E. Colak, T. Memisoglu, and Y. Gercek, "Optimal site selection for solar photovoltaic (PV) power plants using GIS and AHP: A case study of Malatya Province, Turkey," *Renewable energy*, vol. 149, pp. 565–576, 2020.

[135] S. W. Wallace and S.-E. Fleten, "Stochastic programming models in energy," *Handbooks in operations research and management science*, vol. 10, pp. 637–677, 2003.

[136] B. Zhao, H. Qiu, R. Qin, X. Zhang, W. Gu, and C. Wang, "Robust optimal dispatch of AC/DC hybrid microgrids considering generation and load uncertainties and energy storage loss," *IEEE Transactions on Power Systems*, vol. 33, no. 6, pp. 5945–5957, 2018.

[137] A. K. Sampathirao, P. Patrinos, A. Bemporad, and P. Sopasakis, "Massively parallelizable proximal algorithms for large-scale stochastic optimal control problems," *arXiv preprint arXiv:2107.01745*, 2021.

[138] S. Kutateladze, "Convex-programming," in *Soviet Math. Dokl*, vol. 20, pp. 391–393, 1979.

[139] M. Grant, S. Boyd, and Y. Ye, "Disciplined convex programming," in *Global optimization*, pp. 155–210, Springer, 2006.

[140] K. Baker, "Solutions of DC OPF are never AC feasible," in *Proceedings of the Twelfth ACM International Conference on Future Energy Systems*, pp. 264–268, 2021.

[141] J. Sun, Q. Qu, and J. Wright, "When are nonconvex problems not scary?," *arXiv preprint arXiv:1510.06096*, 2015.

[142] T. Joswig-Jones, A. S. Zamzam, and K. Baker, "OPF-Learn: An Open-Source Framework for Creating Representative AC Optimal Power Flow Datasets," *arXiv preprint arXiv:2111.01228*, 2021.

[143] M. H. Dinh, F. Fioretto, M. Mohammadian, and K. Baker, "Towards Understanding the Unreasonable Effectiveness of Learning AC-OPF Solutions," *arXiv preprint arXiv:2111.11168*, 2021.

[144] N. Kebir, A. Ahsan, M. McCulloch, and D. J. Rogers, "Modified Minimum Spanning Tree for Optimised DC Microgrid Cabling Design," *IEEE Transactions on Smart Grid*, 2022.

[145] S. H. Low, "Convex relaxation of optimal power flow—Part I: Formulations and equivalence," *IEEE Transactions on Control of Network Systems*, vol. 1, no. 1, pp. 15–27, 2014.

[146] K. V. Konneh, O. B. Adewuyi, M. E. Lotfy, Y. Sun, and T. Senjyu, "Application Strategies of Model Predictive Control for the Design and Operations of Renewable Energy-Based Microgrid: A Survey," *Electronics*, vol. 11, no. 4, p. 554, 2022.

[147] M. Dashtdar, A. Flah, S. M. S. Hosseinimoghadam, H. Kotb, E. Jasińska, R. Gono, Z. Leonowicz, and M. Jasiński, "Optimal Operation of Microgrids with Demand-Side Management Based on a Combination of Genetic Algorithm and Artificial Bee Colony," *Sustainability*, vol. 14, no. 11, p. 6759, 2022.

[148] "Optimal Operation of a Microgrid with Hydrogen Storage Based on Deep Reinforcement Learning, author=Zhu, Zhenshan and Weng, Zhimin and Zheng, Hailin," *Electronics*, vol. 11, no. 2, p. 196, 2022.

[149] A. Mobasseri, M. Tostado-Véliz, A. A. Ghadimi, M. R. Miveh, and F. Jurado, "Multi-energy microgrid optimal operation with integrated power to gas technology considering uncertainties," *Journal of Cleaner Production*, vol. 333, p. 130174, 2022.

[150] J. Yang and C. Su, "Robust optimization of microgrid based on renewable distributed power generation and load demand uncertainty," *Energy*, vol. 223, p. 120043, 2021.

[151] S. E. Institute, "NEMO: The Next Energy Modeling system for Optimization." `https://leap.sei.org/default.asp?action=NEMO`, 2017. Accessed: 18-04-2023.

[152] J.-W. Lee, M.-K. Kim, and H.-J. Kim, "A multi-agent based optimization model for microgrid operation with hybrid method using game theory strategy," *Energies*, vol. 14, no. 3, p. 603, 2021.

[153] M. Ma, H. Huang, X. Song, F. Peña-Mora, Z. Zhang, and J. Chen, "Optimal sizing and operations of shared energy storage systems in distribution networks: A bi-level programming approach," *Applied Energy*, vol. 307, p. 118170, 2022.

[154] B. Settou, N. Settou, A. Gouareh, B. Negrou, C. Mokhtara, and D. Messaoudi, "A high-resolution geographic information system-analytical hierarchy process-based method for solar PV power plant site selection: a case study Algeria," *Clean Technologies and Environmental Policy*, vol. 23, no. 1, pp. 219–234, 2021.

[155] T. L. Saaty *et al.*, "Decision making with the analytic hierarchy process," *International journal of services sciences*, vol. 1, no. 1, pp. 83–98, 2008.

[156] F.-z. Ouchani, O. Jbaihi, A. A. Merrouni, M. Maaroufi, and A. Ghennioui, "Yield analysis and economic assessment for GIS-mapping of large scale solar PV potential and integration in Morocco," *Sustainable Energy Technologies and Assessments*, vol. 47, p. 101540, 2021.

[157] D. Lavigne, "OSeMOSYS: Introducing Elasticity," *Universal Journal of Management*, vol. 5, pp. 254–260, 2017.

[158] L. Thurner, A. Scheidler, F. Schäfer, J.-H. Menke, J. Dollichon, F. Meier, S. Meinecke, and M. Braun, "pandapower—an open-source python tool for convenient modeling, analysis, and optimization of electric power systems," *IEEE Transactions on Power Systems*, vol. 33, no. 6, pp. 6510–6521, 2018.

[159] K. Baker, "Emulating AC OPF Solvers With Neural Networks," *IEEE Transactions on Power Systems*, 2022.

[160] D. Mentis, M. Howells, H. Rogner, A. Korkovelos, C. Arderne, E. Zepeda, S. Siyal, C. Taliotis, M. Bazilian, A. De Roo, *et al.*, "Lighting the World: the first application of an open source, spatial electrification tool (OnSSET) on

Sub-Saharan Africa," *Environmental Research Letters*, vol. 12, no. 8, p. 085003, 2017.

[161] N. Salmon and R. Bañares-Alcántara, "A global, spatially granular techno-economic analysis of offshore green ammonia production," *Journal of Cleaner Production*, vol. 367, p. 133045, 2022.

[162] T. Barnes, A. Shivakumar, M. Brinkerink, and T. Niet, "OSeMOSYS Global: An open-source, open data global electricity system model generator," 2022.

[163] J. Hoersch, F. Hofmann, D. Schlachtberger, and T. Brown, ""pypsa-eur: An open optimisation model of the european transmission system"," *Energy Strategy Reviews*, vol. 22, pp. 207 – 215, 2018.

[164] T. Brown, D. Schlachtberger, A. Kies, S. Schramm, and M. Greiner, "Synergies of sector coupling and transmission reinforcement in a cost-optimised, highly renewable European energy system," *Energy*, vol. 160, pp. 720–739, 2018.

[165] E. P. Ramos, V. Sridharan, T. Alfstad, T. Niet, A. Shivakumar, M. I. Howells, H. Rogner, and F. Gardumi, "Climate, Land, Energy and Water systems interactions–From key concepts to model implementation with OSeMOSYS," *Environmental Science & Policy*, vol. 136, pp. 696–716, 2022.

[166] D. Dreier and M. Howells, "OSeMOSYS-pulp: A stochastic modeling framework for long-term energy systems modeling," *Energies*, vol. 12, no. 7, p. 1382, 2019.

[167] K. Heussen, S. Koch, A. Ulbig, and G. Andersson, "Energy storage in power system operation: The power nodes modeling framework," in *2010 IEEE PES Innovative Smart Grid Technologies Conference Europe (ISGT Europe)*, pp. 1–8, IEEE, 2010.

[168] M. Mohammadi, Y. Noorollahi, B. Mohammadi-Ivatloo, and H. Yousefi, "Energy hub: From a model to a concept–A review," *Renewable and Sustainable Energy Reviews*, vol. 80, pp. 1512–1527, 2017.

[169] P. Kerdlap, *Life Cycle Environmental and Economic Performance Evaluation of Industrial Symbiosis Networks: A Methodology for Multi-Level Modeling and Analysis*. PhD thesis, National University of Singapore (Singapore), 2021.

[170] N. Moksnes, M. Howells, and W. Usher, "Increasing spatial and temporal resolution in energy system optimization model–the case of Kenya," 2022.

[171] S. von Breidenbach, "La signification du temps propre en mécanique ondulatoire," *Helvetica physica acta*, vol. 14, no. 5-6, pp. 322–323, 1941.

[172] R. P. Feynman, "Space-time approach to non-relativistic quantum mechanics," in *Feynman's Thesis—A New Approach To Quantum Theory*, pp. 71–109, World Scientific, 2005.

[173] S. Diamond, "CVXPY 1.2¶." `https://www.climatewatchdata.org/ghg-emissions?breakBy=sector&chartType=area&end_year=2019&sectors=total-including-lucf&start_year=1990`.

[174] P. E. Grohnheit, "Economic interpretation of the EFOM model," *Energy Economics*, vol. 13, no. 2, pp. 143–152, 1991.

[175] H. Xiaogang, "PREP-SHOT (Pathways for Renewable Energy Planning coupling Short-term Hydropower OperaTion)." `https://github.com/PREP-NexT/PREP-SHOT`, 2023. Accessed: 19-04-2023.

[176] M. Mohammadian, K. Baker, M. H. Dinh, and F. Fioretto, "Learning Solutions for Intertemporal Power Systems Optimization with Recurrent Neural Networks," in *2022 17th International Conference on Probabilistic Methods Applied to Power Systems (PMAPS)*, pp. 1–6, 2022.

[177] N. Strachan and R. Kannan, "Hybrid modelling of long-term carbon reduction scenarios for the UK," *Energy Economics*, vol. 30, no. 6, pp. 2947–2963, 2008.

[178] W. Moses and V. Churavy, "Instead of Rewriting Foreign Code for Machine Learning, Automatically Synthesize Fast Gradients," in *Advances in Neural Information Processing Systems* (H. Larochelle, M. Ranzato, R. Hadsell, M. F.

Balcan, and H. Lin, eds.), vol. 33, pp. 12472–12485, Curran Associates, Inc., 2020.

[179] W. S. Moses, V. Churavy, L. Paehler, J. Hückelheim, S. H. K. Narayanan, M. Schanen, and J. Doerfert, "Reverse-Mode Automatic Differentiation and Optimization of GPU Kernels via Enzyme," in *Proceedings of the International Conference for High Performance Computing, Networking, Storage and Analysis*, SC '21, (New York, NY, USA), Association for Computing Machinery, 2021.

[180] C. Crozier and K. Baker, "The effect of renewable electricity generation on the value of cross-border interconnection," *Applied Energy*, vol. 324, p. 119717, 2022.

[181] T. K. Vrana and P. Härtel, "Estimation of investment model cost parameters for VSC HVDC transmission infrastructure," *Electric Power Systems Research*, vol. 160, pp. 99–108, 2018.

[182] C. Wu, X.-P. Zhang, and M. J. Sterling, "Global Electricity Interconnection With 100% Renewable Energy Generation," *IEEE Access*, vol. 9, pp. 113169–113186, 2021.

[183] B. Xu, A. Oudalov, A. Ulbig, G. Andersson, and D. S. Kirschen, "Modeling of lithium-ion battery degradation for cell life assessment," *IEEE Transactions on Smart Grid*, vol. 9, no. 2, pp. 1131–1140, 2016.

[184] R. Dufo-López, T. Cortés-Arcos, J. S. Artal-Sevil, and J. L. Bernal-Agustín, "Comparison of lead-acid and Li-ion batteries lifetime prediction models in stand-alone photovoltaic systems," *Applied Sciences*, vol. 11, no. 3, p. 1099, 2021.

[185] A. Ahsan, "STEVFNs Tool Demo Seminar 09/11/2022." `https://www.youtube.com/watch?v=_n2w6Zzfofw`, 2022. Accessed: 16-04-2023.

[186] A. Ahsan, "STEVFNs Asset Model Seminar 16/11/2022." `https://www.youtube.com/watch?v=caSYzciVFKw`, 2022. Accessed: 16-04-2023.

[187] A. Ahsan, "STEVFNs Modelling Using Flows of Generalized Coordinates in Space-Time Type Seminar 18/11/2022." https://www.youtube.com/watch?v=GIrBYSPbma0, 2022. Accessed: 16-04-2023.

[188] C. C. Growth, "Joint Summer School and Energy Modelling Platform - Climate Compatible Growth." https://climatecompatiblegrowth.com/summer-school-and-teaching-materials/#Joint-summer-school, 2022. Accessed: 07-10-2022.

[189] A. Ahsan, S. Wheeler, and M. McCulloch, "The Interplay Between Electrification and Renewable Electricity Penetration Pathways on Energy System Decarbonization," 2022. In the publication pipeline.

[190] Joachim Luther, Thomas Reindl, "Solar Photovoltaic (PV) Roadmap for Singapore," tech. rep., National Climate Change Secretariat, Singapore, 2013.

[191] Energy Market Authority Singapore, "Singapore Energy Statistics," tech. rep., Energy Market Authority Singapore, Singapore, 2017.

[192] E. National Environment Agency Singapore, "INDUSTRY ENERGY EFFICIENCY Technology Roadmap," tech. rep., National Climate Change Secretariat, Singapore, 2015.

[193] Z. Cesaro, M. Ives, R. Nayak-Luke, M. Mason, and R. Bañares-Alcántara, "Ammonia to power: Forecasting the levelized cost of electricity from green ammonia in large-scale power plants," *Applied Energy*, vol. 282, p. 116009, 2021.

[194] E. M. Company, "Uniform Singapore Energy Price and Demand Forecast." https://www.emcsg.com/marketdata/priceinformation, 2019. Accessed: 01-05-2020.

[195] G. Modeling and A. O. (GMAO), "MERRA-2 $\mathrm{tavg1}_2 d_r a d_N x : 2d, 1 - Hourly, Time - Averaged, Single - Level, Assimilation, RadiationDiagnosticsV5.12.4,''$ 2015. *Accessed* : $01 - 05 - 2020$.

[196] G. Modeling and A. O. (GMAO), "MERRA-2 $\mathrm{tavg1}_2 d_s l v_N x$: $2d, 1 - Hourly, Time - Averaged, Single - Level, Assimilation, Single - LevelDiagnosticsV5.12.4,''$ 2015. $Accessed : 01 - 05 - 2020$.

[197] S. Pfenninger and I. Staffell, "Long-term patterns of European PV output using 30 years of validated hourly reanalysis and satellite data," *Energy*, vol. 114, pp. 1251–1265, 2016.

[198] I. Staffell and S. Pfenninger, "Using bias-corrected reanalysis to simulate current and future wind power output," *Energy*, vol. 114, pp. 1224–1239, 2016.

[199] S. Pfenninger and I. Staffell, "Renewables.ninja." `https://www.renewables.ninja/`. Accessed: 11-09-2022.

[200] A. Ahsan and M. Zachau Walker, "MERRA 2 Solar wind data gathering script." `https://bitbucket.org/epgoxford/solar_wind_data_gathering/src/master/`, 2022. Accessed: 29-09-2022.

[201] N. Salmon and R. Bañares-Alcántara, "Impact of grid connectivity on cost and location of green ammonia production: Australia as a case study," *Energy & Environmental Science*, vol. 14, no. 12, pp. 6655–6671, 2021.

[202] M. Taylor, P. Ralon, S. Al-Zoghoul, M. Jochum, and D. Gielen, "Renewable Power Generation Costs in 2021," tech. rep., International Renewable Energy Agency, 2022.

[203] P. Ralon, M. Taylor, A. Ilas, H. Diaz-Bone, and K.-P. Kairies, "Electricity Storage and Renewables: Costs and Markets to 2030," tech. rep., International Renewable Energy Agency, 2017.

[204] W. C. Leighty and J. H. Holbrook, "Alternatives to electricity for transmission, firming storage, and supply integration for diverse, stranded, renewable energy resources: Gaseous hydrogen and anhydrous ammonia fuels via underground pipelines," *Energy Procedia*, vol. 29, pp. 332–346, 2012.

[205] L. Luoyang Hongteng Electrical Equipment Co., "Alibaba.com Casting Foundry 200kg-5ton steel iron metal smelting furnace induction metling electric industrial furnace." https://www.alibaba.com/product-detail/Casting-foundry-200kg-5-ton-steel_60776536261.html?spm=a2700.galleryofferlist.normal_offer.d_title.24b6365d8ecdUb&s=p. Accessed: 14-09-2022.

[206] L. Luoyang Hongteng Electrical Equipment Co., "Alibaba.com 250 kg 500 kg 750 kg 1 ton 1.5 ton 2 ton 3 ton 4 ton 5 ton 15 ton 20 ton steel copper iron aluminum induction melting furnace." https://www.alibaba.com/product-detail/250-Kg-500-Kg-750-Kg_62536668429.html?spm=a2700.galleryofferlist.normal_offer.d_title.43a24b0fFQpZ9l&s=p. Accessed: 22-04-2023.

[207] E. Pereira Ramos, V. Sridharan, T. Alfstad, T. Niet, A. Shivakumar, H. Mark, H. Rogner, and F. Gardumi, "Climate, Land, Energy and Water systems interactions–from key concepts to model implementation with OSeMOSYS," 2022.

[208] E. A. Parson, Fisher-Vanden, and Karen, "Integrated assessment models of global climate change," *Annual Review of Energy and the Environment*, vol. 22, no. 1, pp. 589–628, 1997.

[209] P. Kerdlap, J. S. C. Low, D. Z. L. Tan, Z. Yeo, and S. Ramakrishna, "UM3-LCE3-ISN: a methodology for multi-level life cycle environmental and economic evaluation of industrial symbiosis networks," *The International Journal of Life Cycle Assessment*, pp. 1–21, 2022.